INSTITUTO DE GEORAFÍA
FACULTAD DE HISTORIA, GEOGRAFÍA Y CIENCIA POLÍTICA
PONTIFICIA UNIVERSIDAD CATÓLICA DE CHILE

ROL HIDROLÓGICO DE SUELOS CONGELADOS CERCA DE SANTIAGO DE CHILE

por

Sebastián Ruiz Pereira.

Tesis presentada al Instituto de Geografía, Facultad de Historia, Geografía y Ciencia Política de la Pontificia Universidad Católica de Chile para optar al grado académico de Doctor en Geografía.

Profesor Guía:

Dr. Fabrice Lambert, Instituto de Geografía, Pontificia Universidad Católica de Chile.

Comisión revisora:

Dr. Carlos Marquardt (co-tutor), Dr. Sarah Leray, Dr. Balázs Nagy

y Dr. Céline Lavergne.

Agosto de 2021.

Santiago de Chile,

©2021, Sebastián Ruiz Pereira

PONTIFICIA
UNIVERSIDAD
CATÓLICA
DE CHILE

GEOGRAPHY INSTITUTE

FACULTY OF HISTORY, GEOGRAPHY AND POLITICAL SCIENCE

PONTIFICAL CATHOLIC UNIVERSITY OF CHILE

HYDROLOGICAL ROLE OF MOUNTAIN FROZEN-GROUNDS NEAR SANTIAGO DE CHILE.

by

Sebastián Ruiz Pereira.

Thesis presented to the Geography Institute, Faculty of History, Geography and Political Science, Pontifical Catholic University of Chile, in completion of the academic degree of Doctor in Geography.

Thesis director:

Dr. Fabrice Lambert, Geography Institute, Pontifical Catholic University of Chile.

Commission:

Dr. Carlos Marquardt (co-director), Dr. Sarah Leray, Dr. Balázs Nagy

and Dr. Céline Lavergne

August 2021.

Santiago, Chile.

©2021, Sebastián Ruiz Pereira

DERECHOS DE AUTOR.

©2021, Sebastián Ruiz Pereira

Se autoriza la reproducción total o parcial, con fines académicos, por cualquier medio o procedimiento, incluyendo la cita bibliográfica que acredita al trabajo y a su autor.

COPYRIGHT.

© 2021, Sebastián Ruiz Pereira

The total or partial reproduction is authorized, for academic purposes, by any means or procedure, including the bibliographic citation that accredits the work and its author.

AGRADECIMIENTOS

El Autor agradece a la Dirección General de Agua (Ministerio de Obras Públicas, Chile), Parque Andino Juncal, y sus pares colaboradores.

El autor reconoce la financiación parcial de ANID / FONDAP 1511009 y ANID / FONDECYT 1191223.

ACKNOWLEDGEMENTS

The Author acknowledges the General Direction of Water (Ministry of Public Works, Chile), Parque Andino Juncal, and his colleagues.

The Author acknowledges partial funding from ANID/FONDAP 1511009, and ANID/FONDECYT 1191223.

CONTENIDOS / CONTENTS.

Portada	I
Cover	II
Derechos de Autor / Copyrights	III
Agradecimientos / Acknowledgements	III
Contenidos / Contents	IV
Lista de Tablas / List of Tables	VI
Lista de Figuras / List of Figures	VII
Resumen	VIII
Abstract	IX
1. Introducción /Introduction	
1.1 Marco Conceptual / Background	1
1.2 Hipótesis/Hypothesis	10
1.3 Objetivos / Objectives	11
2 Study site	12
3 Methodology	
3.1 Rationale for approach	14
3.2 System conceptualization	17
3.3 Permafrost mapping	18
3.4 Transit times	19
3.4.1 Hydraulic transit time distributions	19
3.4.2 Water transit time analysis	20
3.5 Seasonal thaw	22
3.6 Open or closed groundwater system	22
3.7 Environmental genetic analysis	23
4 Results	
4.1 Permafrost considerations	24
4.2 Flow system characterization	26
4.3 Metagenomic analysis	27
4.4 Transit time analysis	29
4.5 Volume implications at cryogenic conditions	30
5 Discussion	30

6 Outlook and future directions
6.1 Baseline considerations 32
6.2 Considerations for environmental assessments 34
7 Conclusions 35
8 Divulgación / Outreach. 36
Comic: "*Mountain research: the Andes cryosphere"* 37
9 References. 41
10 Supplementary material 52
11 Anexos / Annexes.
11.1 Mountain cryosphere and landscape legislation. 61
11.2 Assessment of landscape transformation in protected areas 82
11.3 Glacier decline in the Central Andes (33°S). 91
11.4 Permafrost evolution in the Central Andes. 101

LIST OF TABLES / LISTADO DE TABLAS.

Tabla / Table 1	Climate change and cryosphere legislations	3
Tabla / Table 2	Aspects for landscape description	5
Tabla / Table 3	Aspects for landscape analysis	5
Tabla / Table 4	Altitudinal zonation of a headwater catchment	7
Tabla / Table 5:	Water isotope analyses	26

Suplementarias / Additional

Tabla / Table 1	Lithological samples	52
Tabla / Table 2	Data for hydraulic parameterization	52
Tabla / Table 3	Water isotope analyses	53
Tabla / Table 4	Gas analyses	53
Tabla / Table 5	Groundwater spring microbial diversity	54
Tabla / Table 6	Isotope convolution equation outputs	54
Tabla / Table 7	Comparison of $\Delta^{18}O$	55

LIST OF FIGURES / LISTADO DE FIGURAS.

Figura / Figure 1	Palmer drought index in the Andes	1
Figura / Figure 2	Value appraisal intersection	8
Figura / Figure 3	Location of Monos de Agua catchment	13
Figura / Figure 4	Conceptual flow and transport model	17
Figura / Figure 5	Permafrost distribution at Monos de Agua	24
Figura / Figure 6	Evolution of permafrost distribution	25
Figura / Figure 7	Metagenomic analyses of 16S RNA	28
Figura / Figure 8	Convolution integral.	29
Figura / Figure 9	Mountain cryosphere baseline evolution.	33

Suplementarias / Additional

Figura / Figure 1	Lithological units at Monos de Agua catchment	56
Figura / Figure 2	Hydraulic parameters for transit times	57
Figura / Figure 3	Water isotope, anthropogenic gas levels	58
Figura / Figure 4	Histogram of turnover times	59

RESUMEN

La criosfera de montaña representa un sistema de almacenamiento de agua sólida en regiones semiáridas como los Andes centrales de Chile y Argentina. La cuenca del Aconcagua ha sido oficialmente declarada región con escasez de y, por lo tanto, es fundamental comprender la evolución de sus componentes hidrológicos ante futuros déficits de nieve y el calentamiento de la superficie.

Este trabajo evalúa el potencial rol de los suelos congelados (permafrost) en las cuencas glaciarizadas a gran altitud en los Andes centrales de Chile, 80 km al NE de Santiago. La primera tarea es comprender si existe permafrost y cómo se distribuye, en segundo lugar, si hay señales que se puedan utilizar como proxy para comprender la dinámica del subsuelo y, en consecuencia, las implicaciones de almacenamiento y flujo base. Los métodos incluyen análisis de isótopos de agua, resistividad eléctrica, parametrización de propiedades hidráulicas y el análisis de secuencias genéticas del agua en manantiales subterráneos.

Los resultados implican existencia de hielo en suelo a 3600m A.S.L. como límite inferior. Aproximadamente un 12% de la sub-cuenca sobre ése límite se encuentra en condiciones favorables de permafrost. El análisis hidrogeológico proporcionó tiempos de tránsito menores a una década para manantiales de agua, también asociados con firmas de diversidad microbiana fría. Los resultados implican un reservorio subterráneo de deshielo en Abril y, en consecuencia, fuente aportes estacionales desde permafrost. Esto representa un problema para evaluar la potencialidad hídrica (valor), ya que actualmente puede pasar por alto las reasignaciones de un elemento de la criosfera (superficie) a otro (relacionado con el agua subterránea) si la capacidad de suministro del sistema no se enmarca como una unidad completa y delimitada.

ABSTRACT.

Mountain cryosphere represents solid water storage system in semi-arid regions like the Central Andes of Chile and Argentina. For example, the Aconcagua basin has long been declared a water scarce region and therefore, it is critical to understand the evolution of its hydrological components considering future snow deficits and surface warming.

The current work assesses the potential role of frozen grounds (permafrost) at glacierized, high altitude headwater catchments in the Central Andes of Chile, 80 km NE from Santiago. The first task is to understand if there is permafrost and how it is distributed throughout the catchment, and secondly, if there are attestable signals which can be used as a proxy to understand subsurface dynamic and consequently storage and baseflow implications. The methods include analyzing water isotopes (stable and unstable), electrical resistivity survey, parameterizing the catchment in terms of hydraulic properties and the analysis of genetic sequences from water in groundwater springs.

Results show current ground ice present within the catchment at 3600m A.S.L., the lower boundary. And that about a 12% of the catchment above that boundary is under favorable permafrost conditions. The hydrogeological analysis delivered sub-decadal transit times for groundwater spring flows, also associated with cold microbial diversity signatures. The results imply a subsurface reservoir that gives a thawing input at least by April, and consequently show that within a permafrost affected catchment, permafrost should have a seasonal inputs to streamflow. This represents an issue for assessing hydric potentiality (value) as it currently may overlook reallocations from one cryosphere element (surface) to another (groundwater related) if the system supply capacity is not framed as a comprehensive, bounded unit.

1. Introducción / Introduction.

1.1 Marco Conceptual / Background.

Las montañas son torres de agua globales, que suplen demandas sustanciales de agua (Viviroli y Weingartner, 2008; Immerzeel et al., 2010) mediante suficiente escorrentía y capacidad de almacenamiento (Immerzeel et al., 2020). La criosfera de montaña (agua terrestre sólida) es capaz de re-congelar nieve / hielo fundido (Pfeffer et al., 1991; Stigter et al., 2021) y retrasar o acelerar la descarga subterránea en áreas de suelo congelado (Evans et al., 2015).

En América del Sur, millones de personas dependen de la criósfera de montaña para el suministro de agua dulce (Barnett et al., 2005; Naciones Unidas, 2013) y específicamente en los Andes del sur, el impacto climático reducirá la capa de nieve, glaciares y permafrost (Baraer et al., 2012), alterando la hidrogeología de tales regiones (Cheng & Jin, 2013; Oliva & Fritz, 2018). Las próximas décadas sufrirán una inseguridad sistemática en términos de recursos alimentarios (Wutich, 2020), sequedad relativa (Figura 1) y acceso al agua. Estas incertidumbres también cubren ambientes en retroceso glaciar como los Andes entre 10-56 ° S (Dussaillant et al., 2019), donde el permafrost también está sujeto a degradación (Ruiz Pereira et al., 2021b).

En este sentido, la preocupación por los estados de vida deseables implica jerarquías de responsabilidad partiendo de la toma de decisiones que recupera valor, lo asigna y prioriza preocupaciones.

Mountains are the water towers of the world, supplying global substantial water demands (Viviroli & Weingartner, 2008; Immerzeel et al., 2010) as they generate plentiful runoff downstream and by having storing and buffering capacity (Immerzeel et al., 2020). Mountain cryosphere (solid terrestrial water) is a buffering system able to refreeze molten snow/ice (Pfeffer et al., 1991; Stigter et al., 2021) but also delaying or speeding up groundwater discharge in frozen ground areas (Evans et al., 2015).

In South America, millions of people depend on the mountain cryosphere for freshwater supply (Barnett et al., 2005; United Nations, 2013) and specifically in the southern Andes, climate change-induced surface warming will reduce snow cover and accelerate glacier and permafrost retreat (Baraer et al., 2012), altering the hydrogeology of permafrost affected regions (Cheng & Jin, 2013; Oliva & Fritz, 2018). The next decades will endure systematic insecurity in terms of food resources (Wutich, 2020), relative dryness (Figure 1) and access to water. This uncertainties also cover environments with sustained glacier decline like the Andes mountains between 10-56°S (Dussaillant et al., 2019), where permafrost is also subject to degradation (Ruiz Pereira et al., 2021b).

In this sense, the concern for desirable states of life implies responsibility hierarchies starting out with decision making that retrieves value, allocates it, and prioritizes concerns.

Los recursos hídricos en áreas semiáridas de Sudamérica han sido abordados durante las últimas décadas por los Objetivos de Desarrollo Sostenible (Nino, 2015), legislaciones específicas (Tabla 1) y recomendaciones del IPCC (Hock et al., 2019, p. 157).

En los Andes chilenos alrededor de 33° S, un retroceso glacial consistente (Bown et al., 2008; Ruiz Pereira & Veettil, 2019) proyecta una disminución de la escorrentía de la cuenca en escenarios futuros (RCP45 & RCP85) a partir del año 2021 (Ragettli et al., 2016).

Inalienable resources like water in semi-arid areas of South America subject to climate forcing have been addressed during the last decades by *Sustainable Development Goals* (Nino, 2015), specific legislations (Table 1) and IPCC recommendations (Hock et al., 2019, p.157).

At the Chilean Andes around 33°S, a consistent glacial retreat (Bown et al., 2008; Ruiz Pereira & Veettil, 2019) projects catchment runoff decrease in future scenarios (RCP45 & RCP85) starting the year 2021 (Ragettli et al., 2016).

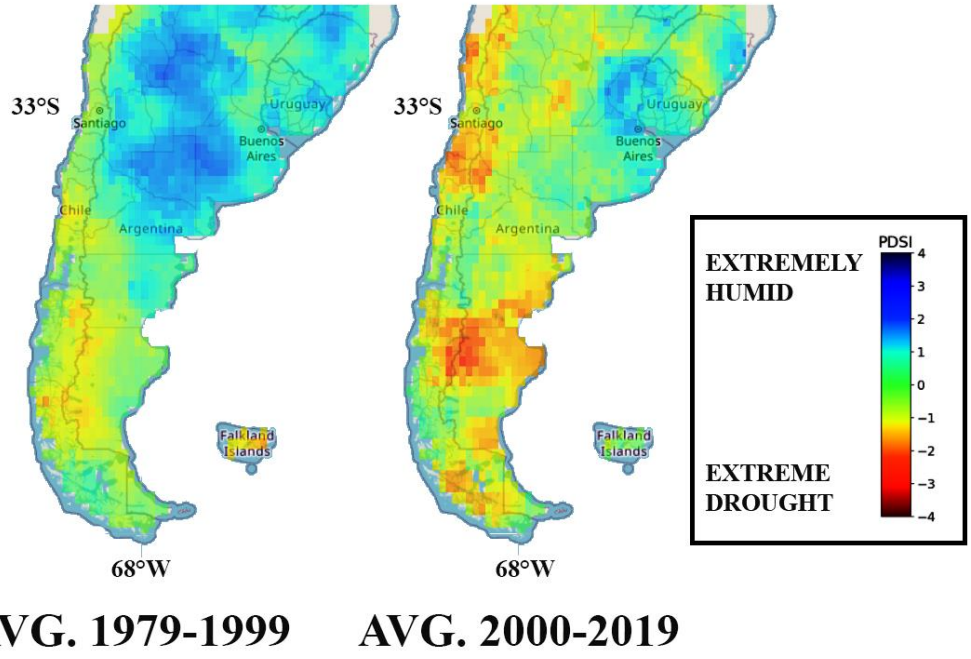

Figura 1. Índice de sequía de Palmer. Índice de severidad de sequía promedio de Palmer (PDSI) para períodos entre 1979-1999 y 2000-2019 desde; extremadamente húmedo (azul) hasta sequía extrema (rojo). Adaptado de *Explorador de sequías* (https://sada.cr2.cl) de Morales et al., 2020.

.

Figure 1. Palmer drought index. Average *Palmer Drought Severity Index* (PDSI) for periods between 1979-1999 and 2000-2019 ranging from extremely-wet (blue) to extreme drought (red). Adapted from *Drought explorer* (https://sada.cr2.cl) from Morales et al., 2020

Tabla 1. Regulaciones de cambio climático y criósfera (Fuente: Instituto de Investigación Grantham sobre Cambio Climático y Medio Ambiente, Observatorio de la Ley de Cambio Climático de Chile). Adaptado del manuscrito enviado en el Anexo 11.1.

Table 1. Climate change and cryosphere regulations (Source: Grantham Research Institute on Climate Change & the Environment, Observatory for the Climate Change Law in Chile). Adapted from submitted manuscript in Annex 11.1.

Country	Type	Cryosphere protection	Name
Peru	Law	Mountain environments and glaciers	Law N° 30754 on Climate Change, 2018
Argentina	Law	Glacial and periglacial environments	Law 27520, "Minimal budgets for Adaptation & Mitigation to Global Climate Change", 2019
Argentina	Law	Glacial and periglacial environments	Law 26639, “Minimal budgets for preservation of glaciers and periglacial environment”, 2010
Chile	Strategic plan	Included	National Climate Change Adaptation Plan, 2014
Chile	Law project	Not included	Climate change framework Law, 2020
Austria	Law	Not included	37th Federal Law for Climate & Energy funding, 2007
Austria	Law	Not included	106th Federal Law on Climate Protection, 2011
EU	Regulation in force	Not included	Regulation 842, 2018
EU	Strategic plan	Arctic and Boreal environments are mentioned	A Clean Planet for all, 2018
EU	Strategic plan	Indirectly mentioned through reference.	Forging a climate-resilient Europe - the new EU Strategy on Adaptation to Climate Change, 2021
Iceland	Passed	Not included	Act 70 on Climate Change, 2012
Iceland	Strategic plan	Glaciers mentioned	Iceland’s Climate Action Plan for 2018-2030

Todos estos procesos implican una valoración del potencial hídrico en evolución (Lepeška, 2010) de criósfera de montaña en regiones con escasez de agua, entrelazando perspectivas utilitarias de apropiación de recursos (Tabla 2) y valor intrínseco (Nordstrom, 1993), valor de no uso de paisaje (Bullock, 2017, p. 8-11). Sin embargo, esta preocupación considera líneas de base insuficientes o inadecuadas en áreas protegidas de montaña que descuidan transformaciones del paisaje (Ruiz Pereira et al., 2021a), que también son transformaciones hídricas y de uso de la tierra.

Por lo tanto, criósfera como ecosistema y unidades de almacenamiento de agua / hielo se asocia a problemas de valor (Tablas 2 y 3) en el contexto de la seguridad hídrica en regiones semiáridas. Este ha sido el enfoque legislativo (Tabla 1) que aborda los impactos potenciales en los ambientes glaciares / periglaciares (Art. 15, Ley No 26639, Argentina) y el predicamento detrás del Proyecto de Ley de Protección Glacial en Chile (Art. 1, Boletín No. 11.876-12).

Bajo estas preocupaciones estructurales, una gestión subóptima es impulsada por las legislaciones, sin perjuicio de conflictos de compatibilidad de escala entre las dimensiones del "paisaje" que amplifican incertidumbres bajo el forzamiento hidroclimático sostenido. En especial, cuando las legislaciones hablan de entornos sin descentralizar la urgencia sobre la heterogeneidad del forzamiento (impacto) en los Andes del Sur (Figura 1). Este es un problema de paisajes como “objetos” de análisis metaestables, latitudinales y altitudinales (Tabla 3 y 4).

All these processes imply an appraisal assessing the evolving hydric potential (Lepeška, 2010) of mountain cryosphere in water scarce regions, which entangles utilitarian perspectives of resource appropriation (Table 2) and intrinsic (Nordstrom, 1993), non-use value of landscape (Bullock, 2017, p. 8-11). Yet, this concern for resources is often assessed by either insufficient or inadequate baselines in mountain protected areas actually neglecting landscape transformations (Ruiz Pereira et al., 2021a), which are also a hydric and land use transformations.

Hence, cryosphere as ecosystem and water/ice storage units associates to value concerns (Table 2 & 3) as the potential of mountain cryosphere in the water security context at semi-arid regions. This has been the approach made by legislative framework (Table 1) addressing potential impacts on glacial/periglacial environments (Art. 15, Law no.26639, Argentina) and the predicament behind the Glacial protection Law Project in Chile (Art. 1, Bulletin No. 11.876-12).

Beneath these structural concerns, a sub-optimal management is enacted and propelled by legislations, nonwithstanding conflicts of scale compatibility between all dimensions of “landscape” which amplify uncertainties with sustained hydroclimatic forcing, especially when legislations talk about environments without descentralizing the objective concern on hydroclimatic forcing heterogeneity as in the Southern Andes (Figure 1). This is an issue of landscapes as metastable, latitudinal and altitudinal “objects” of analysis (Table 3 & 4).

Tabla 2. Aspectos para la descripción del paisaje. Adaptado de Sauer, 1963.

Table 2. Aspects for landscape description. Adapted from Sauer, 1963.

Aspects of landscape	**Description**
Comprehensive view of nature and culture	Interaction of natural and/or cultural factors
Internal vs. External perspective.	Area, as perceived by people.
Historical retrospection.	Land use transformations and appropiations.
Forms and processes.	Action and interaction
	Human factors.

Tabla 3. Aspectos para el análisis del paisaje. Adaptado de Bateman et al., 2010 y Ruiz et al., 2021a (Anexo 11.2).

Table 3. Aspects for landscape analysis. Adapted from Bateman et al., 2010 & Ruiz et al., 2021a (Annex 11.2).

Conceptual and legal background	Operative definitions	Ecosystem services
		Landscape transformation
		Impacts
		Value
Value transfer	Coercive measures Reference studies Benefit transfer	Appraisal of value transfer
Landscape value appraisal	Impacts	Physical impacts
	Landscape baseline	Landscape transformation
	Natural capital stocks	Natural insurance value
		Management
		Contingent valuation

Por lo tanto, criósfera como ecosistema y unidades de almacenamiento de agua / hielo se asocia a problemas de valor (Tablas 2 y 3) como su potencial en el contexto de la seguridad hídrica en regiones semiáridas. Este ha sido el enfoque adoptado por el marco legislativo (Tabla 1) que aborda los impactos potenciales en los ambientes glaciares / periglaciares (Art. 15, Ley No 26639, Argentina) y el predicamento detrás del Proyecto de Ley de Protección Glacial en Chile (Art. 1, Boletín No. 11.876-12).

Bajo estas preocupaciones estructurales, una gestión subóptima es impulsada por las legislaciones, sin perjuicio de conflictos de compatibilidad de escala entre las dimensiones del "paisaje" que amplifican incertidumbres bajo el forzamiento hidroclimático sostenido. En especial, cuando las legislaciones hablan de entornos sin descentralizar la urgencia sobre la heterogeneidad del forzamiento (impacto) en los Andes del Sur (Figura 1). Este es un problema de paisajes como “objetos” de análisis metaestables, latitudinales y altitudinales (Tabla 3 y 4).

Esta es una razón por la cual áreas montañosas protegidas enfrentan problemas de insuficiencia técnica, dada una inadecuada planificación de sostenibilidad. Este problema tiene radica en un "alejamiento" analítico desde líneas de base inadecuadas (estáticas) con el paisaje como simples cuenca visual dentro de las Evaluaciones de Impacto; evitando una adecuada diferenciación para transformaciones económicas y gestión de conservación, necesaria para comprender la evolución de su valor.

Hence, cryosphere as ecosystem and water/ice storage units associates to value concerns (Table 2 & 3) as the potential of mountain cryosphere in the water security context at semi-arid regions. This has been the approach made by legislative framework (Table 1) addressing potential impacts on glacial/periglacial environments (Art. 15, Law no.26639, Argentina) and the predicament behind the Glacial protection Law Project in Chile (Art. 1, Bulletin No. 11.876-12).

Beneath these structural concerns, a sub-optimal management is enacted and propelled by legislations, notwithstanding conflicts of scale compatibility between all dimensions of “landscape” which amplify uncertainties with sustained hydroclimatic forcing, especially when legislations talk about environments without decentralizing the objective concern on hydroclimatic forcing heterogeneity as in the Southern Andes (Figure 1). This is an issue of landscapes as metastable, latitudinal, and altitudinal “objects” of analysis (Table 3 & 4).

This is one plausible reason why protected mountainous areas faces problems of technical insufficiency, producing inadequate sustainability planning. This issue is rooted in a sort of analytical “estrangement” from inadequate (static) baselines under *landscape as a mere viewshed* guidelines within Environmental Impact Assessments; avoiding a proper differentiation for several types of economic transformations and conservation management which are necessary to understand the evolution of its value.

En Chile, la Ley No. 19300 presenta un principio de gradualidad y "susceptibilidad de alteración", entendido por la valoración procesal; relacionando magnitud del tiempo que incluye las transformaciones y la evolución imponderable de la potencialidad de los recursos.

Por un lado, el aval legislativo es para la prevención; por otro, podría estar relacionado con una medida de seguro y la reducción de un riesgo prima derivado del valor natural.

In Chile, the Law No. 19300 presents a principle of graduality and "susceptibility of alteration", understood for the procedural assessment; relating time magnitude which includes transformations and imponderable evolution of resource potentiality.

On one hand, the legislative endorsement is for prevention; on the other, it could be related to a measure of insurance and the reduction of a risk-prime derived from the natural value.

Tabla 4. Zonificación altitudinal de una cuenca hidrográfica, Monos de Agua / Alto del Plomo. Adaptado de Ruiz & Veetil, 2019 (Anexo 11.3).

Table 4. Altitudinal zonation of a headwater catchment, Monos de Agua/Alto del Plomo. Adapted from Ruiz & Veetil, 2019 (Annex 11.3).

Altitudinal segment (m)	**Preponderant feature**	**Area (km^2)**	**Area from total (%)**	**Average air temperature (1979–2016) range**	**Morphogenic paraglacial transition**	**Sediment cohesive deposit**
2775–3200	Alluvial Fans & Slopes	4.48	32.7	1.4 to (−4.7)	Lower Paraglacial sequence. Mature landscape Periglacial conditions	Fans/Slopes and Outwash plains
3200–3600	Rock Glacier associated landforms	1.48	13.5	−1.6 to (−4.7)	Paraglacial condition with secondary sediment reworking	Rock glaciers (both active/inactive) Moraines & relict ice in slopes.
3600–4000	Glaciers	3.62	21.7	−3.1 to (−4.7)	A proglacial condition with higher paraglacial sequence	Moraines and Taluses

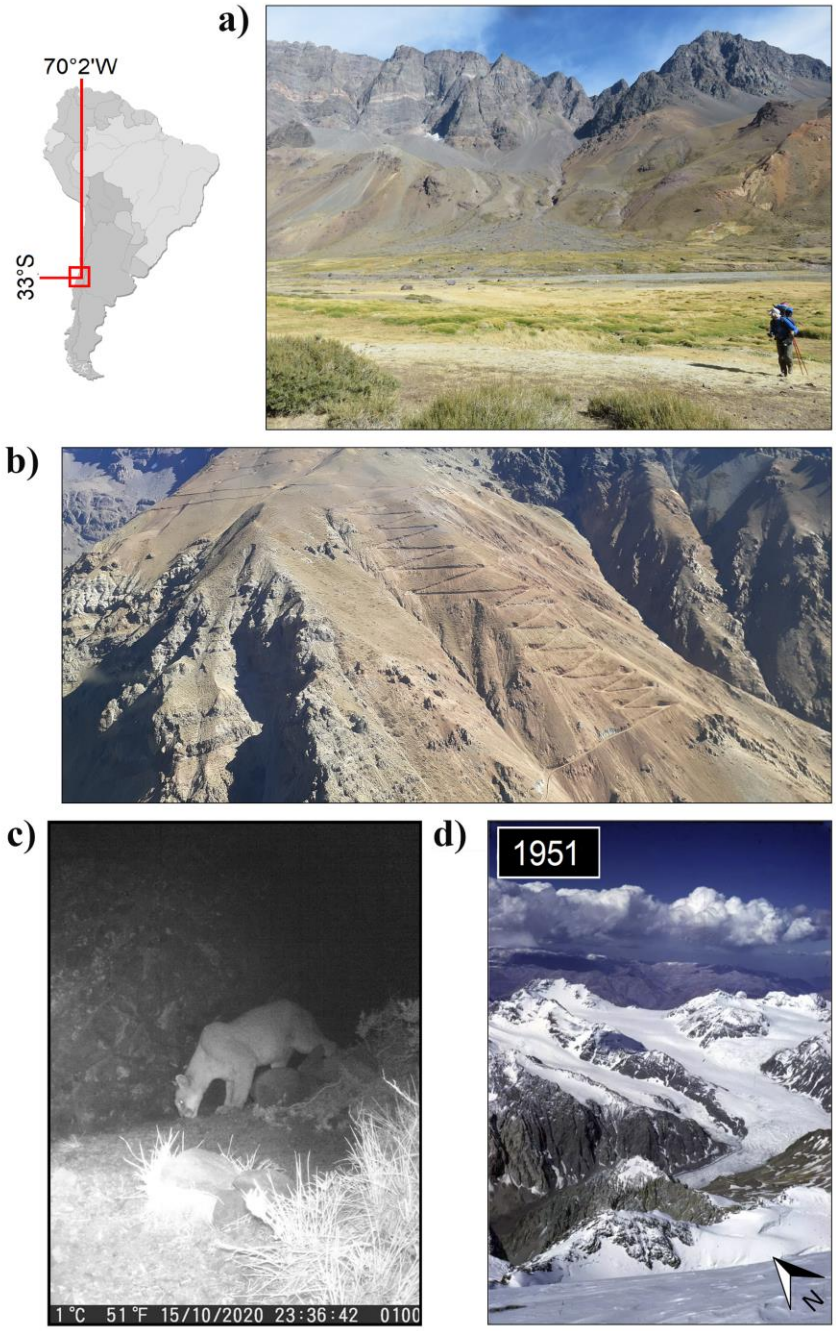

Figura 2. Intersección de valor a 33° S, Andes centrales de Chile. Dimensión cultural (a), explotación (b), biodiversidad (c) y potencial hídrico (d) del paisaje. Imágenes (c) y (d) son del personal de Parque Andino Juncal y Eberhard Meier (1951). Adaptado desde manuscrito enviado a la Política de uso del suelo, junio de 2021 (Anexo 11.1).

Figure 2. Value appraisal intersection at 33°S, Central Andes of Chile. The cultural (a), exploitative (b), biodiversity (c) and hydric potential (d) dimensions of landscape overlap. Pictures (c) and (d) are from Parque Andino Juncal staff and Eberhard Meier (1951). Adapted from submitted manuscript to *Land Use Policy*, June 2021 (Annex 11.1).

Todas estas prerrogativas pueden tener sus raíces en los planes integrados para la gestión de los recursos hídricos en la Convención Marco de las Naciones Unidas sobre el Cambio Climático (Naciones Unidas, 1997, p. 11), revitalizados a través del respaldo del Acuerdo de París para la responsabilidad futura. Sin embargo, cuando se analizan avales globales como los Objetivos de Desarrollo Sostenible (Griggs et al., 2013), es evidente que incluso conceptos como resiliencia y sostenibilidad se utilizan indistintamente (Elmqvist, 2017; Elmqvist et al., 2019), lo que en última instancia considera sistemas metaestables como estructuras epistemológicas estacionarias y no como una dinámica hidroclimática.

These prerogatives can all be rooted in integrated plans for water resource management in the *United Nations Framework Convention On Climate Change* (United Nations, 1997, p.11), revitalized through the *Paris Agreement* endorsement for future responsibility. Nevertheless, when analyzing global endorsements such as *Sustainable Development Goals* (Griggs et al., 2013), it is apparent that even concepts like resilience and sustainability are even used interchangeably (Elmqvist, 2017; Elmqvist et al., 2019), which would ultimately consider metastable systems as stationary epistemological structures, and not a hydroclimatic dynamic instead.

1.2 Hipótesis / Hypothesis.

Contexto:

Sin líneas de base sobre estructura del agua subterránea, desconocemos si un acuífero puede verse afectado en términos de sus procesos de recarga o descarga (Eckstein, 2007; Comisión de Derecho Internacional, 2008, Art. 1 y 6). Por lo tanto, el predicamento de la Comisión por el Derecho Internacional (CIR) incluye los sistemas acuíferos no confinados y confinados, siempre que presenten agua dulce, sin embargo, como destaca Bertazzo, 2019, la Resolución adoptada por la Asamblea General de la ONU (11 de diciembre de 2008). tiene una normativa ausente o poco clara sobre la interacción de la zona de recarga y los acuíferos como tales.

Context:

Without baselines understanding groundwater structure, we do not know how aquifer functioning can be affected in terms of either its recharge or discharge processes (Eckstein, 2007; International Law Commission, 2008, Art. 1 & 6). Therefore, the predicament of the Commission for International Right (CIR) includes unconfined and confined aquifer systems, as long as they present freshwater, yet as Bertazzo, 2019 highlights, the Resolution adopted by the General Assembly of the UN (11th December, 2008) has absent or unclear normative dealing with the interaction of the recharge zone and the aquifers as such.

Hipótesis general de trabajo:

"*Los suelos perennemente congelados tendrían un rol hidrológico atestiguable en áreas de alta montaña*".

La hipótesis específica de trabajo:

"Muestras de agua superficial y subterránea presentarían señales particulares, atribuibles a un rol hidrológico de suelo congelado en el área a 33°S".

General working hypothesis:

"Perennially frozen grounds would have an attestable hydrological role in high mountain areas".

The specific working hypothesis:

"Surface and groundwater water samples present particular signals, attributable to a hydrological role of frozen grounds in the area at 33°S.*"*

1.3 Objetivos / Objectives.

Primer objetivo:

Confirmar si el permafrost está presente en los Andes (33°S).

Tarea: Actualizar la estructura hidrológica de los suelos congelados dentro de una cabecera de captación en una región con escasez de agua.

Segundo objetivo: Determinar el papel hidrológico del permafrost en la cuenca de estudio (33°S).

Tarea: Establecer un papel para el permafrost al comprender el origen hidrológico y el tiempo de residencia dentro de la cuenca.

First objective:

To confirm whether permafrost is present the central Andes (33°S).

Task: To update the hydrological structure frozen-grounds within a headwater catchment in a water-scarce region.

Second objective: To determine the hydrological role of permafrost in the study catchment. (33°S).

Task: To establish a role for permafrost by understanding hydrological origin and residence time within the catchment.

2 Study site.

The Aconcagua river runs westwards between 32º40'-32º56'S starting from headwater catchments between 3000-5100m A.S.L.. In 2018 and 2019, the Chilean Public Works Ministry passed decrees to officially declare the Aconcagua basin a water-scarce region. This goes along a sustained regional glacier shrinkage (Figure 3) of over 30% between 1955-2016, equivalent to tens of square kilometers (Bodin et al., 2010; Monnier & Kinnard, 2017). Therein, the "Juncal River" sub-basin (Aconcagua basin) has an area of 342km^2. It is 75km north-east from Santiago de Chile, with a mean air temperature between 1979-2016 of (-3.1)°C at 3600m A.S.L. (Boisier et al., 2018), and a median annual precipitation of 581mm (Alvarez-Garreton et al., 2018). Here, the dominant input (>50% of peak) to mainstream during melt season (mid-October until April) is glacial melt rather than snowmelt; the latter being the dominant input only during spring (mid-October to mid-November) (Ohlanders et al., 2013).

Figure 3 shows a 1955 aerial photograph of the "Juncal River" sub-basin with two main valleys. This area is the current "Juncal Andean Park", a private biodiversity conservation project that regenerated the valley after XXth century cattle-raising and mining activities. The specific study-site lies within the headwater Monos de Agua (MA) catchment (red frame and insert in Figure 3), which is a transboundary catchment shared by Argentina and Chile. The MA catchment starts at the high peaks in Argentina and ends at the outwash plains in Chile and has had a consistent deglacierization above 3600m A.S.L. constituting areas with sediment resettling common in paraglacial environments (Ruiz Pereira & Veettil, 2019).

Rodriguez et al. (2016) described the eastern part of the "Juncal River" sub-basin presents mainly limestone, calcareous sandstone and coexist with igneous formations while at northeastern reaches (32°55'S;70°00'W), natural gypsum deposits exist and have been extracted commercially. Volcano-sedimentary strata dominate the local lithology in the central and western parts of the basin (32°58'S;70°07'W), with an important presence of dacitic, pyroclastic and basaltic rocks. Quaternary sequences consist of Pleistocene-Holocene alluvial and colluvial, in a lesser proportion fluvio-glacial deposits (Bown et al., 2008) and surface transports (Piquer et al., 2017). Lithological details are shown in Additional Figure 1.

Several debris covered/rock glaciers have been mapped since Lliboutry, 1956 (insert maps), followed by local Government inventories (Unidad de Glaciología, DGA, 2015). In general, frontal and lateral rock glacier slopes start appearing at 3600m A.S.L., indicating potential localized permafrost (Lambiel & Pieracci, 2008) which is in accordance with several permafrost distribution maps for the Central Andes.

Permafrost distribution maps deriving ground surface temperature from air temperatures at 1km resolution (Gruber, 2012) suggested "favorable" conditions in the Aconcagua basin above 4200m. Later downscaled models (1 arc-minute resolution) (Saito et al., 2016) for "Juncal River" sub-basin estimated discontinuous permafrost above 3000 m A.S.L. and above 4000 m

A.S.L. for continuous distribution. More recent mapping has shown a high uncertainty threshold between 3600-3900m A.S.L. (Bartsch et al., 2016). These results are in partial agreement with other available products (Obu et al., 2019; Tapia & Trombotto, 2019) determining mid and high-probability for permafrost above 3400m and 4200m A.S.L..

One last important factor is the differential timing of activation for groundwater springs, which implies that springs should have a differential thawing signal. Between 2019-2020, out of three available springs at 3600m A.S.L. (Figure 3b), one was always inactive and one (Spring-1) was active after freshet in December 2019, nevertheless Spring-2 was active only from February 2020. Volume implications will consider streamflow measurements during 2019-2020 at Spring-1 and Spring-2 accounting 0.143m^3/s and 0.141m^3/s respectively.

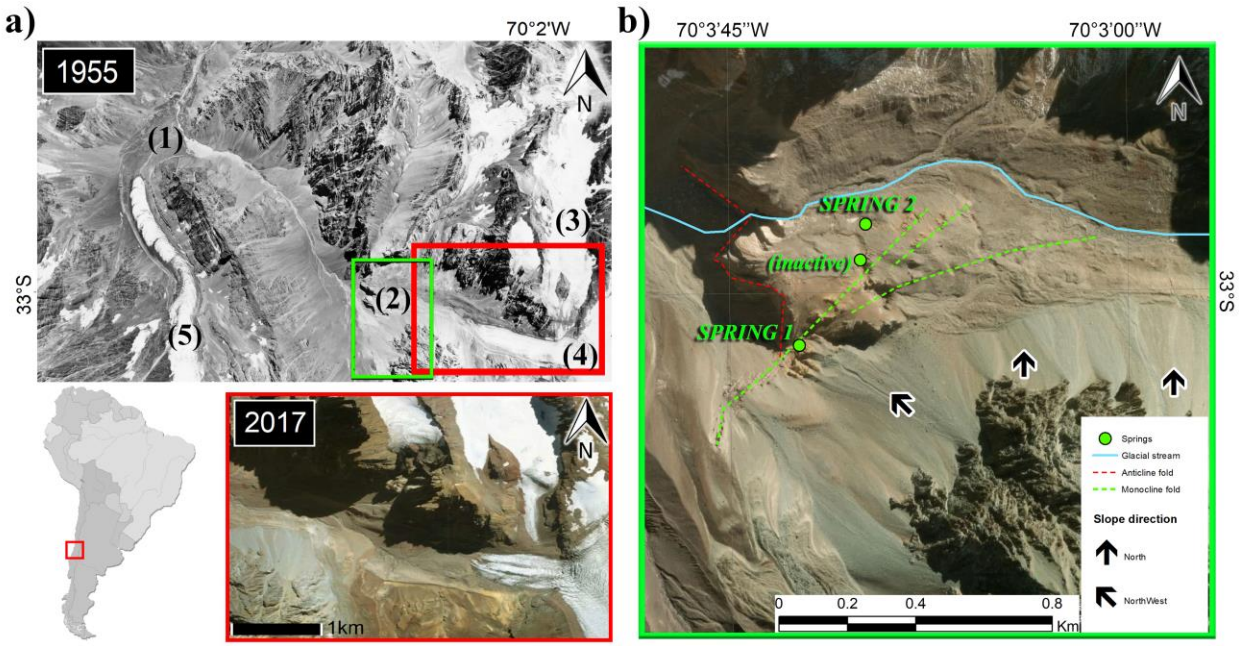

Figure 3 Location of **"**Monos de Agua" catchment in the Central Andes. (a) is a HYCON aerial image (1955) with local inserts in red and green squares (Landsat 8, 2017). In (a), (2) are ground surface thermal loggers at 3200-3600m A.S.L., (3-5) are "Monos de Agua" (local name "León Negro"), "Alto del Plomo" and "Juncal Norte" glaciers. (b) is the green insert in (a), showing groundwater spring sampling locations.

3 Methodology.

3.1 Rationale for the approach.

Knowledge on mountain groundwater processes in the Andes is scarce and often reduced to "Teflon® sub-basin" hydrological connectivity assumptions (Clow et al., 2003). Yet, coarse sediment alpine aquifers have fast discharge recession after recharge season (e.g., snowmelt) or rainfall events, followed by a slow recession that sustains discharge over a long period (Hayashi, 2020). For example, at the outlet of glacierized, permafrost-affected headwater, post-freshet baseflow (groundwater) has been identified to range between 32-52% in average at permafrost affected headwater catchments (Baraer et al., 2009; Evans et al., 2015; Liu et al., 2004; Rodriguez et al., 2014).

On recently ice-free areas, snowmelt partitioning between surface runoff and groundwater (Hammond et al., 2019) could alter flow timing, recharge magnitude (Green et al., 2011), contribution to streamflow (Evans et al., 2015) and ultimately increase water storage in the (seasonally thawing) thickening active-layer (Evans & Ge, 2017). Furthermore, with slower snowmelt rates (due to season contraction), hydrological connectivity could not exceed necessary wetness thresholds and lead to declines in runoff efficiency (Musselman et al., 2017). As a result, snowmelt-dominated watersheds may experience dry season water stresses (Evans et al., 2018) and lesser streamflow as infiltration fills previously depleted parts of the system (Alvarez-Garreton et al., 2021). Therefore, at discontinuous (more template) permafrost areas, baseflow could increase due to higher regional (horizontal and vertical) connectivity (rerouting) (Evans et al., 2020).

In specific, at mountainous areas dominated by sedimentary disturbance (paraglacial environment) (Slaymaker, 2009), coarse grained units like proglacial taluses and moraine complexes (permafrost features) buffer snowmelt transmission (Kurylyk & Hayashi, 2017) and constitute conduits for high mountain groundwater (Somers & McKenzie, 2020). Consequently, groundwater could recharge via coarse slope deposits and moraines, delayed by finer grained sediments and then discharged (Glas et al., 2018). Therefore, permafrost degradation therein could potentially impact surface and subsurface hydrologic conditions, soil strength properties (Kurylyk et al., 2014), water quality (Szopińska et al., 2016; Toohey et al., 2016) and enhance chemical weathering (Colombo et al., 2019).

The methodological aim is understanding how putative confined/unconfined aquifers have "old water" (inter-annual storage) without an assumed recharge, hence not exploitable in a sustainable manner and therefore categorized as "fossil waters" (Barberis, 1986, p.4; Eckstein & Eckstein, 2003, p.215-216). The approach is to interpret the hydrological structure of a headwater catchment, assuming recharge/discharge processes as subsurface soil differentiation as also a differentiation of hydraulic properties of aquifer systems.

First, the premise for permafrost presence in the Central Andes considered previous mappings. For example, using global elevation data and air temperatures from reanalysis at 1 km resolution, Gruber (2012) suggested "favorable" conditions for permafrost in the Aconcagua basin above 4200 m. Later, Saito et al., (2016) used downscaled models (1 arc-minute resolution) and showed the "Juncal River" (Figure 3) sub-basin to be affected by discontinuous and continuous permafrost above 3000 m a.s.l. and 4000m a.s.l., respectively. Later, Bartsch et al., 2016, estimated a high probability for permafrost occurrence above 3600 m a.s.l. They considered Mean Annual Ground Temperatures (MAGT) inputs between -2 to -4°C (Gisnås et al., 2013; Westermann et al., 2015; Obu et al., 2019). More recently, Tapia-Baldis & Trombotto-Liaudat (2019a) estimated mid and high-probability above 3400 m and 4200 m a.s.l., respectively.

Nevertheless, permafrost as an element is often associated solely with the sub-type of rock glaciers. These cryoforms often appear on (less sun exposed) slopes as surface flows and then mapped as rock-glacier type features (Rodriguez et al., 2016) coinciding with historical analyses Lliboutry, 1956 and current glacier-inventories from the *General Directory of Waters* (Unidad de Glaciología, 2015). Even though these studies are well-suited for estimating large-scale permafrost distribution, they lack the resolution for excessively rugged terrain. The minimal conditions for permafrost occurrence and its distribution in high-mountain areas as well as magnitudes for permafrost aggradation and future degradation are necessary baselines involved in groundwater structure and functions.

Secondly, to determine the hydrological role of permafrost in the study catchment it is necessary to understand hydrological origin and transit times (travel time magnitude within the catchment) as an inter-annual confinement under permafrost conditions. This would imply that, at ground ice affected areas (O'Neill et al., 2019), isotope signals can be significantly distinct than for areas without ground ice influence (Gibson et al., 2021), but also that by sequencing microbial communities (Ramírez et al., 2020) there could be taxonomical composition differences (Bochet et al., 2020) of psychrophiles in alpine environments (Frey et al., 2016).

Hence, sampling specific locations (streams and springs) would find biological (representative of niche conditions) and isotopic/gas signatures different to current atmospheric background levels (snow). For example, isotope enrichment (stable ones) constitutes a hydrological-source proxy while as decaying tritium (^{3}H) allows time-related interpretations for permafrost affected environments. Tritium, deuterium and ^{18}O, have been used for decades to analyze snow runoff mountain environments (Dinçer et al., 1970) and lowlands (Burn and Michel, 1988), but do require more local atmospheric background levels for the Andes (Houston, 2007).

The methodology considers conjoint work by the Author and co-authors on an ongoing manuscript. The credited contributions are as follows:

Title:

Permafrost signals in mountain groundwater: Chilean Andes (33°s)

First Author:

[1,2]Ruiz Pereira, S.

Co-Authors:

[2,3,4]Díez, B., [3]Cifuentes-Anticevic, J., [5]Leray, S., [6]Fernandoy, F., [7]Marquardt, C., [1,2]Lambert, F.

Affiliations:

[1]Instituto de Geografía, Pontificia Universidad Católica de Chile, Santiago, Chile.
[2]Center for Climate and Resilience Research, Universidad de Chile, Santiago, Chile.
[3]Dep. de Genética Molecular y Microbiología, Pontificia Universidad Católica de Chile, Santiago, Chile.
[4] Center for Genome Regulation (CRG), Santiago, Chile.
[5]Dep. Ing. Hidráulica y Ambiental, Pontificia Universidad Católica de Chile, Santiago, Chile
[6]Laboratorio de Análisis Isotópico, Universidad Andrés Bello, Viña del Mar, Chile
[7]DIEM/DIEG, Pontificia Universidad Católica de Chile, Santiago, Chile

Authorship distribution:

S. Ruiz Pereira is the main manuscript writer, data analyst and fieldwork organizer. Field sampling and sample analysis by C. Marquardt. Research conceptualization by Ruiz Pereira, F. Lambert and S. Leray. Amplicon sequencing and processing of 16S rRNA V4-V5 region by B. Díez and J. Cifuentes-Anticevic. Stable isotope analyses by F. Fernandoy. Integrative data analyses by Ruiz Pereira, Lambert, Díez, Leray and Marquardt.

3.2 System conceptualization.

The studied system is circumscribed to north facing slopes of the upper MA catchment (Figure 3), whereby travelling water has distinct signature distributions defined by hydrological origin and transit times. The system assumption considered steady-state influx of multiyear, multi-entry points for surface infiltrations from an upper reservoir (roughly analogous to the vadose zone) with either a surface runoff outflux (stream) or base flow from a lower reservoir (saturated zone) to groundwater springs.

Hence, the recharge considers infiltration of glacial/snow water (above 3600 m a.s.l.) and discharge from snowmelt, rock glacier and/or interstitial water from permafrost thaw through groundwater springs at ~3600 m a.s.l. (Figure 3). This needs to account on soil responsiveness (Hrachowitz et al., 2009) related to interstitial or massive ground-ice as aquitards (transmissivity lag) or aquicludes (impervious barrier) as discontinuous layers supporting perched groundwater (Hayashi, 2020) coupled to multi-entry proglacial (ice-cored) moraines (Langston et al., 2011).

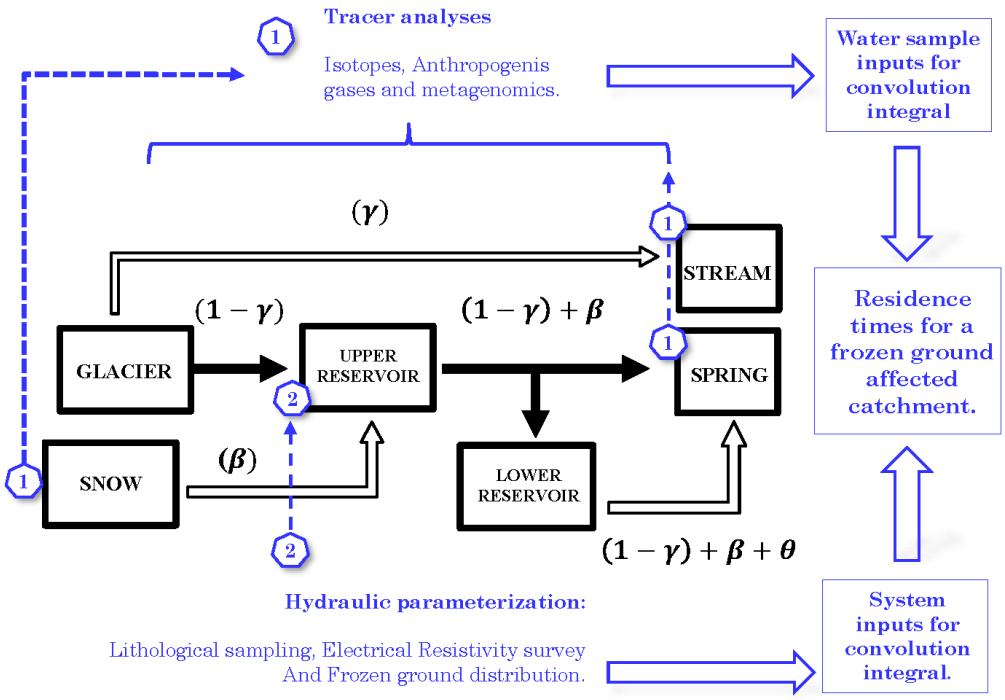

Figure 4. Conceptual hydrological flow and transport model for the study catchment. The flowchart shows the assumed hydrological pathways within the catchment. Snow is **ß**, surface signal is **γ** with a complementary previously stored fractional (1-**γ**).and the assumed inter-annually stored subsurface signal is **θ**.

We consider that subsurface sources feeding groundwater springs contain a thawing fraction (θ) accounting a signal for an inter-annual storages and a significant distinction from surface signalsh in isotope and genetic makeup composition. Therefore, by using linear steady-state mixing models we can differentiate isotope background concentrations as snow precipitation signals (ß) from surface (γ) fractions flowing through reservoirs in the catchment (Figure 4).

This follows a conceptualization by Rose (2007), where fractions (γ) of the total volume of the ground water reservoir are released to base flow while the remaining fractions (1- γ) completely mix with new inputs from the upper precipitation mixing reservoir. The time water spends travelling subsurface describes the storage, flow pathway heterogeneity and sources of water in a catchment (McDonnell et al., 2010) where to distinguish a mean transit time distribution as representative for a lower reservoir sub-system assuming a completely mixed reservoir under steady-state flow conditions.

Hence, the proposition is to couple a measure for system response for a magnitude of time, which can be associated to an expression integrating (isotope) tracer values and account range of system response the (flow regime). We first require a hydraulic parameterization of the catchment's lower reservoir and then to parametrize all tracer inputs and outputs by a "lumped parameter" approach (Maloszewski & Zuber, 1996; Stewart et al., 2017). The attestment of subsurface and inter-annual storage in groundwater should also contain a biological signature (16S rRNA metabarcoding) which if associated to subsurface from thawing niches.

3.3 Permafrost mapping.

For complex rugged terrain, permafrost distribution maps over 1 km pixels are inadequate to spot restricted areas. For example, in a narrow setting, within one kilometer pixel (Bartsch et al., 2016; Tapia Baldis & Trombotto Liaudat, 2019) one slope can be totally exposed to incoming radiation while the another is perennially covered. Therefore, to include hydraulic properties considering "aquitard" behavior considered a downscaled mapping in the catchment considering previous work by the Author.

In the MA catchment, Ruiz Pereira et al. (2021b) considered Mean Annual Ground Surface Temperature (MAGST) and incoming radiation as the main factors involved in "cold spots" for permafrost occurrence. The radiation magnitudes considered Area Solar Radiation (Niu et al., 2018) derived from 12.5 m Digital Elevation Model and calibrated with local measurements. The ratio between these variables delivers a surface energy output magnitude conditioned by aspect (Duguay et al., 2005; Smith, 1975). Afterwards, the output grid was clustered using partitional k-means (Arthur & Vassilvitskii, 2007; Gulbrandsen et al., 2016; Nitze et al., 2018) and hierarchical (agglomerative) clustering methods (Azócar et al., 2017; Carvalho et al., 2016; Zeng et al., 2020) evaluated by Calinski-Harabasz criterion (Caliński & Harabasz, 1974; Arbelaitz et al., 2013; Lamirel et al., 2016), the Silhouette approach (Rousseeuw, 1987), and the Davis-Bouldin (Davies & Bouldin, 1979; Casteleiro-Roca et al., 2020) indices. The output from this distribution approach also considered atmospheric of + 1.2° C (RCP2.6) and +3.5° C (RCP8.5) (Bozkurt et al., 2018) for

the Central Andes of Chile, accounting on the future evolution of hydraulic properties in the MA catchment. Their uncertainty considered error propagation considering Altitudinal Lapse Rate deviation of ±0.15°/ 100m, also accounting logger accuracy, pyranometer error, and statistical deviation for each input variable. These details are inserted in Annex 11.4.

3.4 Transit times.

3.4.1 Hydraulic transit time distributions

The interpretation of a lower reservoir connected to groundwater springs is requires considering ‘‘piston’’ to “exponential” flow model assumptions (Małoszewski & Zuber, 1982) under limited steady-state interpretation from confinement and unaltered travelling tracer concentrations (Leray et al., 2012). For example, turnover time (t_d) (McGuire & McDonnell, 2006) corresponds to a “hydraulic” time magnitude (hydraulic residence time) approached by assuming different spatial combinations for the system and integrating them with hydraulic parameters determined from field samples:

$$t_d = n_e \frac{(\Delta l)^2}{k \Delta h} \qquad \text{(Equation 1)}$$

n_e → effective porosity.
k → mean hydraulic conductivity.
Δl → distance from recharge to discharge.
Δh → height difference of the hydraulic head.

In terms of catchment geometry, both flow path length and gradient distribution reflect the hydraulic driving force of catchment-scale transport, i.e. *Darcy's* law (McGuire et al., 2005), but also soil-type constraints (Rodgers et al., 2005). For example, in sedimentary aquifers, permeability can takes a wide range of values (1×10^{-5} to 1×10^{-2} m/s) (Sakata & Ikeda, 2013) with unconsolidated deposits (gravel, sands) with porosity ranges between 0.25-0.5 (Yu et al., 2015).

Therefore, hydraulic coefficients (Additional Table 1 and 2) considered lithological samples and hydraulic property values from literature (Morris & Johnson, 1967; Domenico & Schwartz, 1998; Heath, 2004). Additionally, considering the sites as under paraglacial conditions (current sedimentary reworking due to deglacierization, quaternary deposits (Additional Figure 1 and 2) are assumed to have an approximate alluvium thickness between 1-11 m, with a median of seven meters (Mashburn et al., 2003, p.9). We also considered a top of permafrost depth of 8 m, considering estimations for period 2008-2014 at equivalent latitude (~33° S) and altitude (~3600 m a.s.l.)(Trombotto & Borzotta, 2009; Trombotto & Bottegal, 2020).

The hydraulic conductivities and porosities were iterated in Equation 1 considering values starting from semipervious to impervious sedimentary rock ($k = 10^{-6}$ to10^{-5} m/s) (Bear, 1988, p.4), combinations for hydraulic head (Δh between 90-900 m) and path length (Δl between 1.5-3.0 km). Each parameter (hydraulic head, length, porosity, and conductivity) (Additional Tables 1-2 and

Additional Figures 1-2) had a hundred linearly spaced values combined over 10^8 iterations. This process delivered a turnover time distribution from which median was determined.

3.4.2 **Water transit time analysis.**

Catchments receive tracer (^{18}O, ^{2}H, ^{3}H, CFCs) inputs after transport through diverse pathways, resulting in a distribution of transit times at sampling zones. The differentiation of hydrological fractions by hydrochemical analysis obeys two main criteria:

(i) Origin within the hydrological cycle (snow, glacier, permafrost).
(ii) Reservoir location.

Limitations using water stable isotopes may include that they are indicative of turnover-times <5 years (McGuire et al., 2005; Stewart et al., 2010a) as detectible variation in ^{18}O is smaller than the measurement error (Stewart et al., 2010). This can be explained due to the attenuation of the variation after convolution beyond four years, masking the stable isotope variation with analytical error, for example, by delivering no significant deuterium variation (Małoszewski et al., 1983) under certain flow-model assumption.

In change, ^{3}H gradient presents the advantage of radioactive decay, a temporal difference easily attestable by regional calibration curves, especially in the Southern Hemisphere where anthropogenic peak (Cauquoin et al., 2016) did not exert such an ambiguity as in Canada, Russia and China (Gibson et al., 2016; Makarov, 2016; Yi et al., 2018). Tritium is an unstable hydrogen isotope (2 neutrons and 1 proton), with a half-life of 12.3 years and is measured in TU (tritium units, 1 atom of ^{3}H in 10^{18} atoms of protium ^{1}H).

This study obtained water isotope concentrations from snow composite, surface glacial stream and groundwater springs. The sampling took place between 3550-3590 m a.s.l. and between September-November 2018.

The water samples to be analyzed from specific locations are:

(a) Snow: background signal, ‘youngest’ surface water.

(b) Glacial stream: surface water mix with inter-annual storage signal.

(c) Groundwater spring: subsurface water mix with inter-annual storage signal.

Water isotopes concentrations can be the input for calibrating value ranges to fit measured tracer (sampling) output concentration (Maloszewski & Zuber, 1996) resulting in transit time distributions. Therefore, it is necessary to parametrize all inputs and outputs by a “lumped parameter” approach which estimates system’s dynamic (piston to exponential system response ratio) and describes integrated tracer transport through a catchment by discretizing physical constraints.

Lumped parameter may be explained by the following convolution integral (Dinçer et al., 1970; Zuber et al., 1986);

$$\boldsymbol{C_{out} = \int_0^{\infty} C_{in}(t-\tau)e^{\lambda\tau}g(\tau)d\tau} \qquad \text{(Equation. 2.0)}$$

$C(t)$ & $C_{in}(\tau)$ → output and input concentrations.
V(t) → total volume in the system.
Q_{in} → volumetric inflow rate.
C_I(z) → (dimensionless) concentration from instant injection.
$g(\tau)$ → system response function from assumed model.

For the present case, we assumed a proglacial moraine system consisting of quaternary coarse sedimentary areas with internal thickness dependent structures affecting flows. We looked for the lowest number of fitting parameters and avoided the a great number of cells, since it is not justified by the number of sampling sites (Małoszewski and Zuber, 1993). The idea was to go through all the system response type values, so for example, the $\boldsymbol{g(\tau)}$ considered a *flow model* for water isotopes as in Equations 2.1 and 2.2:

$$\boldsymbol{g(\tau) = 0}$$

$$for\ \tau < \tau_m(1-\frac{1}{n})$$

$$\boldsymbol{g(\tau) = \left(\frac{n}{\tau_m}\right)^{\left(-\frac{\tau n}{\tau_m}+n-1\right)}}$$

$$for\ \tau \geq \tau_m(1-\frac{1}{n})$$

Here, $\boldsymbol{\tau_m}$ is Mean Transit Time (MTT) and $\boldsymbol{\tau}$ time, the integration variable representing the entry time of tracer (Chattarjee et al., 2019) and $\boldsymbol{n}$ is the ratio of the piston to exponential flow (EPM) aquifer area ranging from (+1) to (+6). The *EPM* is ratio of the piston to exponential flow aquifer area and the piston flow component can represent young groundwater that travelled vertically within the recharge zone.

The mean transit time (residence time) is integrated throughout different flow regime assumptions contained in Equations 2. Values considered the lowest measured tritium uncertainty and a wider range considering two half-lives back and forth from the snow background level. The possible value tails for the given system range between 1-60 years (Hiyama et al., 2013; Kralik, 2015) as $\boldsymbol{\tau_m}$ inputs.

The complex distribution of catchment flow paths is represented by a distribution of transit times describing tracer transport through the catchment. This assumption obeys the condition that an annual hydrological flush promotes seasonal and inter-annual isotopic stability for a steady-state isotope balance model (Gibson et al., 2015) and no concentration gradient throughout the catchment, or at least from the lower reservoir to the sampling output. For example, average

residence time estimates for ground water between 14-18 years at an aquifer with 10-20m thick regolith, 20-30% regolith/bedrock porosity and hydraulic conductivity between 1.0e-08 to 1.16e-05 m/s (Rose, 2007).

In the present case, we estimate time-related distributions from water isotope measurements (^{2}H and ^{18}O and ^{3}H). Water stable isotopes were analyzed in collaboration with the *Stable Isotope Laboratory* (UNAB, Viña del Mar). The tritium analysis at GNS Science (New Zealand) used radiometric detection; first processed by electrolytic enrichment and later measured by scintillation detectors with a resolution of 0.02TU.

Snow samples as background tritium values is normalized (Equation 3) to the sampling time (Yi et al., 2018) of other samples (Houston, 2007). In the Southern Hemisphere, the tritium peak due to atomic energy testing is neglected and assumed stabilized (Cauquoin et al., 2016).

$$Nr = Ni * e^{-T/17.93} \qquad \text{Equation 3}$$

N_i = Initial Tritium Concentration of given waterbody.

N_r = Residual Tritium concentration after time-defined radioactive decay.

Residence time distributions using tritium values considered a range using both the uncertainty (0.02TU) and two half-lives back from the snow background level (0.02-18TU).

3.5 **Seasonal thaw.**

Besides the point source differentiation, seasonal differences are also expected. To account any stable isotope enrichment coming from e.g. a frozen ground, an *isotopic separation* between river water and precipitation ($\Delta^{18}O$) will depend on both elevation and Mean Annual Air Temperature (MAAT).

$$\Delta^{18}O = \delta_{PRECIPITATION} - \delta_{SOURCE} \qquad \text{Equation 4}$$

The estimation reflects runoff augmentation by water sources such as permafrost thaw or glacial melt with $\Delta^{18}O \geq 0$. For example, in Yukon (Canada), Gibson et al. (2020) screened stable isotopes throughout permafrost affected areas and found enrichment in streams from thawing grounds.

3.6 **Open or closed groundwater system**

Groundwater springs may constitute outputs from a closed system, for example the thawing of interstitial ice or a rock glacier, but also a mixed recharge from snow, permafrost, and glacial water. Human emitted gas (CFC's and SF6's) concentrations aid the interpretation of surface/subsurface connection. Groundwater spring samples were analyzed at GNS Science in

New Zealand by method of Gas Chromatography with Electron Capture. Uncertainty for CFC and SF_6 was 1.2% and 3% respectively.

If the system is closed, the gas concentrations will be theoretically higher than current atmospheric levels but if the system is partially open, levels will be equivalent to the current atmospheric ones.

3.7 **Environmental genetic analyses.**

In this study, the diversity, abundance, and composition of the prokaryotic community was analyzed from two spring sources where water was collected in April 2019. Briefly, one hundred liters of water from Spring-1 and Spring-2 (Figure 3) were pumped up through a 50 µm polyester net to exclude large organisms and particles and transported in darkness to the laboratory in Santiago. In the laboratory, sample serial filtration used a peristaltic pump (6-600 rpm; pressure up to 2 bar), through 3 µm polycarbonate filters and 0.22 µm Sterivex filters (Millipore). Filters were maintained at -80°C until nucleic acids extraction. DNA extraction of both 0.2µm and 3µm utilized a commercial DNeasy PowerSoil (Qiagen) kit.

DNA quantification used a Qubit® 2.0 Fluorometer (Thermo Fisher Scientific, USA). Quality assessment utilized spectrophotometry (A260/A280 ratio) and integrity by standard agarose gel electrophoresis. Subsequently, PCR amplifications and mass sequencing of the 16S rRNA genes used primers 515f and 926r amplifying the V4-V5 region (~376bp) (Parada et al., 2016) (Illumina MiSeq platform; Argonne National Laboratory, Illinois, USA).

Raw sequences of the 16S rRNA gene were imported to the QIIME2 platform (v2019.7) (Caporaso et al., 2010; Bokulich et al., 2018; Bolyen et al., 2019) and demultiplexed (q2-demux plugin). Then, the paired-end sequences were trimmed and merged using DADA2 (Callahan et al., 2016) to obtain the Amplicon Sequencing Variants (ASVs).

ASVs taxonomy was assigned with the q2-feature-classifier (classify-consensus-vsearch) (Rognes et al., 2016) using the SILVA132 database (Quast et al., 2012). ASVs classified as "Mithocondria", or "Chloroplast" were filtered out for the analysis of the Bacteria and Archaea community. Sequences from 3 and 0.2 µm fractions were mixed for each source (JS1 and JS2).

Finally, to remove singletons and rare taxa, ASVs were filtered by frequency (ASVs with >2 counts) and by taxonomy (Phyla with >2 ASVs) in the R package *phyloseq* (McMurdie & Holmes, 2013; Team, 2020). Alpha diversity analysis was performed on the clean reads with phyloseq and Vegan packages (Oksanen et al., 2019) considering observed diversity from *Shannon* and *Simpson* indexes (Wagner et al., 2018).

4 Results.

4.1 Permafrost considerations.

The analysis of permafrost distribution maps suggests that at least 15% of the "Monos de Agua" catchment area is currently under permafrost conditions, predominantly above 4200 m a.s.l.. The lower boundary for permafrost occurrence is at 3900 m a.s.l. (Figure 5), with only a patchy distribution consistent with negative mean annual ground surface temperatures below -2.25° C and >4500m a.s.l. discontinuous distribution up to the mountain tops. The *Incoming Solar Radiation* inputs captured the rugged topography down to 12.5 m of a pixel. Permafrost affected areas consistently have a southward orientation with large favorable areas within the glacial foreland (red contour, Figure 5).

Overall, MA catchment showed 22.18 ± 7% under favorable conditions for permafrost occurrence and some of these areas within the 50-year old ice-retreat margins. Additionally, projected warmings over Andean basins in Central Chile represent a potential decrease of permafrost affected areas of at least 13% for RCP 2.6 and 87% for RCP 8.5, implying that permafrost affected areas below 5000 m a.s.l. would disappear (Figure 6).

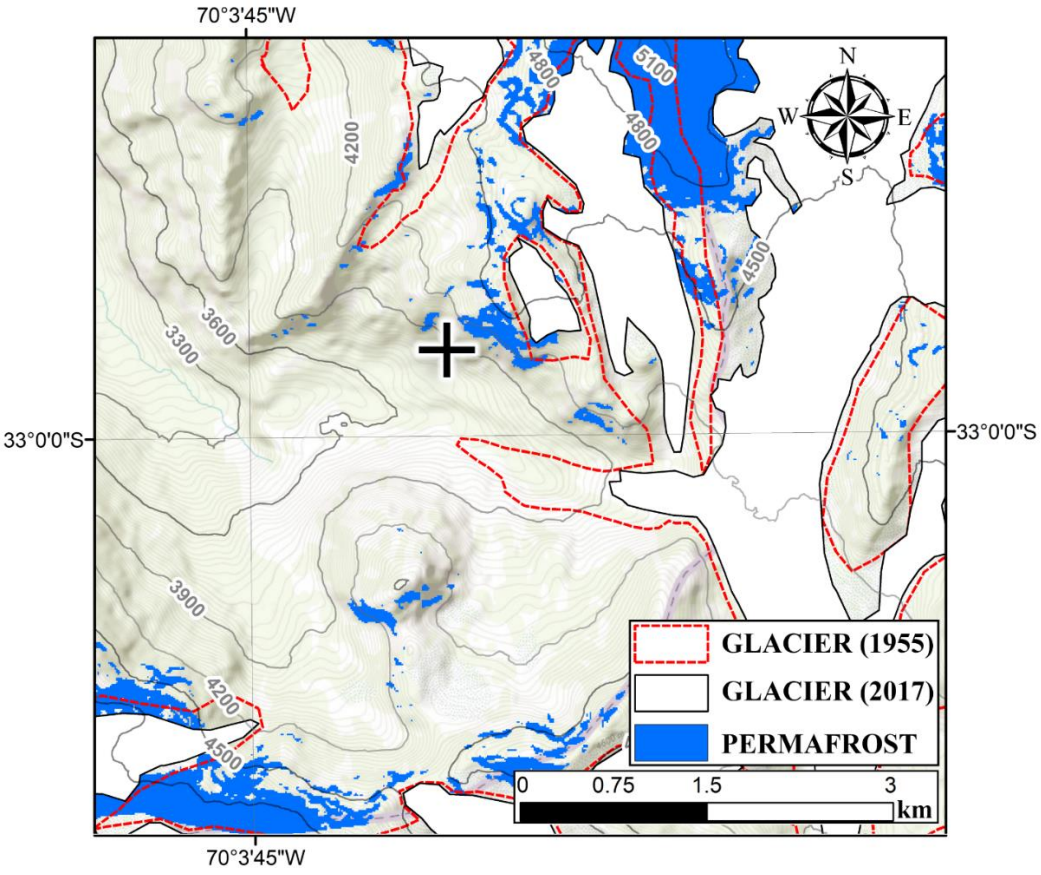

Figure 5. Permafrost distribution at the "Monos de Agua" catchment (taken from Ruiz Pereira et al., 2021b).

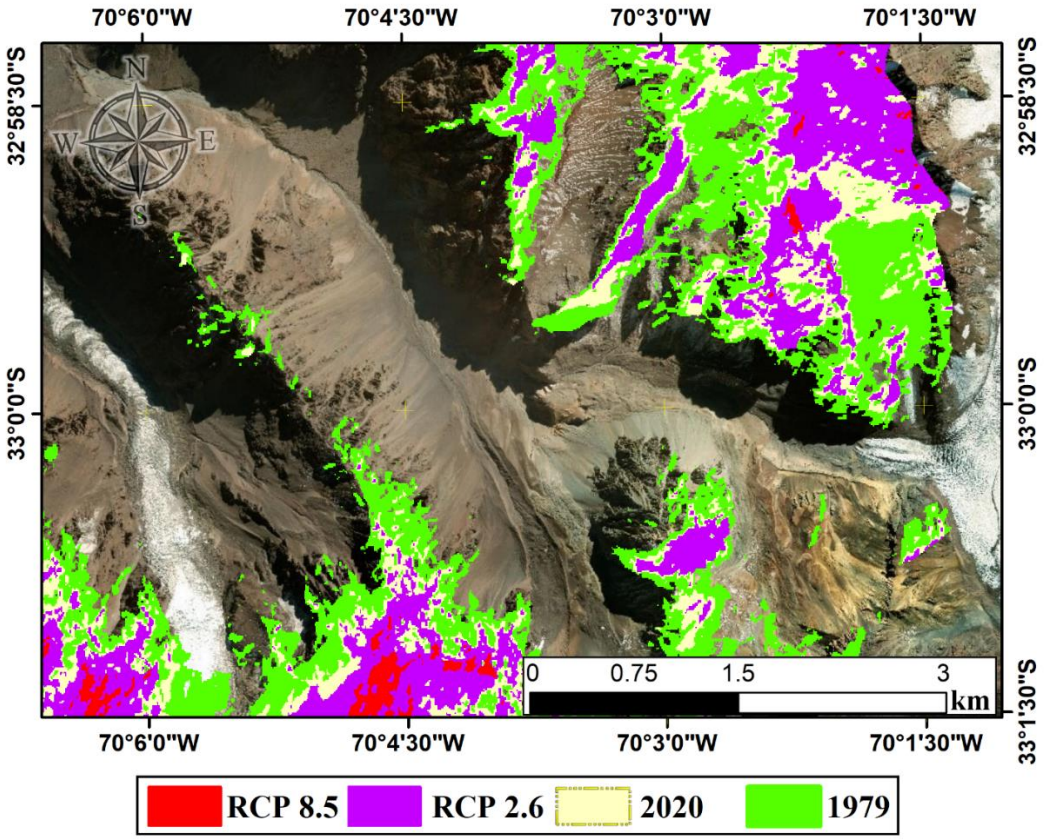

Figure 6. Evolution of permafrost distribution in a headwater catchment at the Central Andes of Chile/Argentina. (taken from Ruiz et al., 2021b).

4.2 Flow system characterization from water sample analyses

The isotopic signal (D and ^{18}O) of groundwater spring and glacial streams between 2019-2020 showed distinct concentrations for hydrological sources (Table 5 & Additional Figure 3a) and a statistically significant seasonality between the post-freshet samples (December) and early autumn. In brief, the stable isotope levels measured for Spring 1 and glacial stream showed that the signal was enriched for both sources; deuterium level was more similar for both sources in December but very different in April samples (Additional Table 3). The ^{18}O concentration also changed significantly with differences between sources diverging 2.1-fold in December to 2.7-fold in April.

Table 5. Water isotope analyses for groundwater springs and surface streams at 3600m A.S.L.. Bi-annual measurements from April 2019-2020.

Site ID	**δD ‰ VSMOW ± 0.8**	**±**	**$\delta^{18}O$ ‰ VSMOW ± 0.1**	**±**	**D-excess**	**Tritium (TU)**	**±**
Snow	-140.01	44.53	-18.39	5.73	7.11	6.39	2.66
Stream	-143.11	8.08	-19.22	0.87	10.63	2.13	1.04
Spring 1	-137.00	9.09	-18.37	1.05	9.99	2.03	0.68
Spring 2	-139.11	10.37	-18.65	1.17	10.08	2.72	0.19

The snow composite (September-November 2019 to April 2020) as background had a tritium level of 6.39±2.66 TU. Early autumn ^{3}H groundwater spring (Spring-1 and 2) average between 2019-2020 was 2.38±0.44 TU, and the glacial stream 2.13±1.04 TU (Table 5 and Additional Figure 3c). Between 2019-2020, Spring-2 changed its tritium signal 9% and Spring-1 60% (Additional Table 3). Overall, stable isotopes between 2019-2020 changed virtually the same proportion for both springs but the tritium for Spring 1 changed eight-fold more than for Spring 2.

Concentration ratios (Table 5 & Additional Table 3) between stable isotopes and tritium showed that groundwater springs are lighter than surface signals and have more depleted tritium signal than background (snow) yet presenting differences between springs and the glacial stream. This difference leaves Spring-2 as a more differentiated source, which is consistent with its late-summer activation.

Whether the groundwater spring system is closed or open was interpreted from the anthropogenic gas concentrations and genetic analysis of two groundwater springs. Anthropogenic gas levels (CFCs, SF_6) resulted equivalent to atmospheric levels (Additional Table 4 & Additional Figure 3b) for same variables; therefore, they cannot be used in the "lumped parameter" approach to time residences but offer a partial confirmation of the opening of the aquifer.

4.3 Metagenomic analysis.

The 16S rRNA gene sequence taxonomic composition attested the presence and abundance of (low temperature adapted) psychrophiles obtained from groundwater spring samples. The estimated diversity values for (150-0.2 µm size fraction) prokaryotic communities was similar between springs for ASVs and Shannon index, however, there were differences in presence and relative abundance of some populations between springs (Figure 7). Details for each spring are shown in Additional Table 5.

The taxonomic identity (Figure 7a) showed the highest relative abundance for phylum Proteobacteria mainly represented by Betaproteobacteriales, seconded by phyla Bacteroidetes with Flavobacteriales dominating the phylum. Figure 7b shows genera representing >1% of prokaryotic (Bacteria and Archaea) communities per spring. Minor and rare genera in Figure 7c shows 30 most abundant <1%.

Venn plots show shared and unique taxa (represented by ASVs) for springs at phylum (Figure 7d), genera >1% (Figure 7e) and genera <1% or "uncultured taxa" (Figure 7f) levels. At phylum level, there were 522 shared ASVs, but only 66 ASVs assigned to the >1% genera communities.

Most abundant and exclusive Spring-1 ASVs from >1% genera were *Thalassospira* (2.9%) *Flavobacterium* (1.9%) and *Halomonas* (1.5%). For Spring-2 they were *Flavobacterium* (1.3%) and *Polaromonas* (2.6%). The most abundant ASVs in common for both springs were from genera representing >1%, affiliated to *Gallionella*, *Sideroxydans*, *Thiobacillus*, *Flavobacterium*, *Rhodoferax*, and *Polaromonas*. Each of these ASVs was similarly abundant for both springs (representing 1-5% of the community) but the ASVs assigned to *Polaromonas* and *Rhodoferax* were solidly more abundant in Spring-2 (Figure 3b). The high number of unique ASVs observed between springs denotes the differences in bacterial community composition.

In specific, *Polaromonas* is a known psychrophile. Some species of *Rhodoferax* could also be considered "psychrotolerant" and grow near 0 °C like *R. antarcticus*, recovered from glacial habitats (Madigan et al., 2000), or R. *ferrireducens* isolated from anaerobic subsurface aquifer sediments (Finneran et al., 2003). The other shared genera (Thiobacillus, Gallionella, Syderoxidans) are (chemolithotrophic) nitrifying Betaproteobacteriales commonly associated with iron oxidation and found in dark and iced environments, likely as primary producers, fixing carbon and weathering minerals, thus explaining how such microbial ecosystem can be sustained in ice (Toubes-Rodrigo et al., 2017).

Additionally, other nitrifiers and Fe redox bacterial genera were present within the “minor and rare” (<1%) group. Spring-1 differed by showing higher relative abundance of Bacteroidetes (Flavobacteriales and Sphingobacteriales orders) and twice as many Cyanobacteria (Figure 3a,b).

Dominant bacterial members of Spring-2 (*Polaromonas* and *Rhodoferax*), together with other taxa also shared with Spring-1, are associated to a biogeochemical role in C cycling as primary producers, mainly as nitrifiers in N cycling in this environment. Results imply that sequences from groundwater spring samples potentially come from a putative subsurface habitat with freezing-thawing conditions.

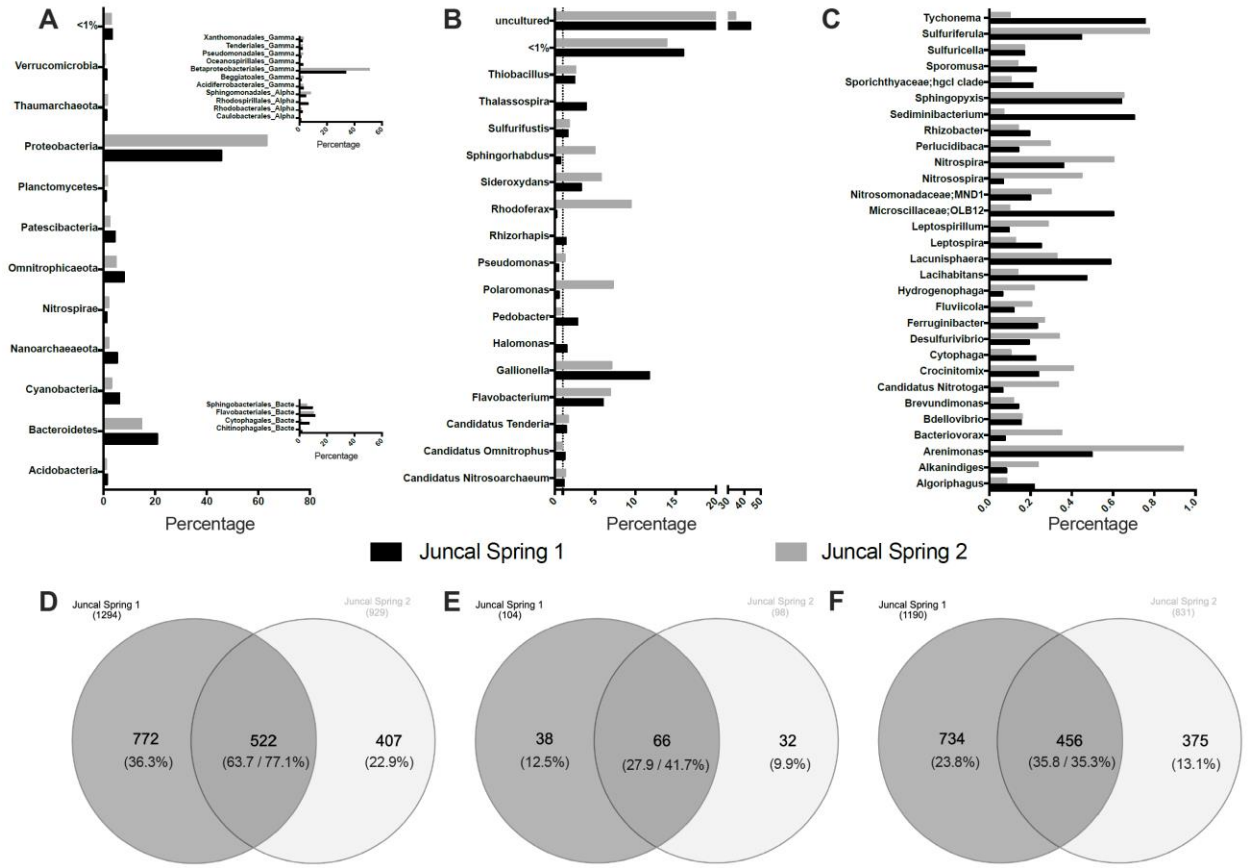

Figure 7. Metagenomic analysis of 16S rRNA from groundwater springs. (A) shows relative abundance for phylum, (B) for prokaryotic >1% genera and (C) for <1% abundant genera. Venn diagrams show shared ASVs per phylum (D), (E) for >1% abundant genera and (F) the <1% abundant genera.

4.4 Transit time analysis.

Isotope derived transit time ($^{3}H/^{18}O/D$) estimation (Additional Table 6) resulted in 4.77 ± 2.05 years. In specific, the "lumped parameter" approach had a system response **G(*t*)** with a ***n*** ratio (EPM) value (4.17 ± 1.17) for catchment geometry. The convolution outputs in Figure 8 show a predominant peak around 5 years of mean transit time with decreasing tales towards >10 years. This implies that the system conceptualization would have the largest outflux fraction belonging to mixtures rendering recent, young (Kazemi et al. 2006, p.123 & 171) modern (Gleeson et al., 2016) groundwater yet of an inter-annual storage.

On the other hand, the hydraulic transit time (turnover time) was 13.67 ± 20.09 years, only varying a 0.01% between 10^{6} and 10^{8} iterations (Additional Figure 4). Considering isotope derived transit times within hydraulic turnover-time expressions for transit times, results imply a wide range of variability but in average, transit times over two years for a lower reservoir.

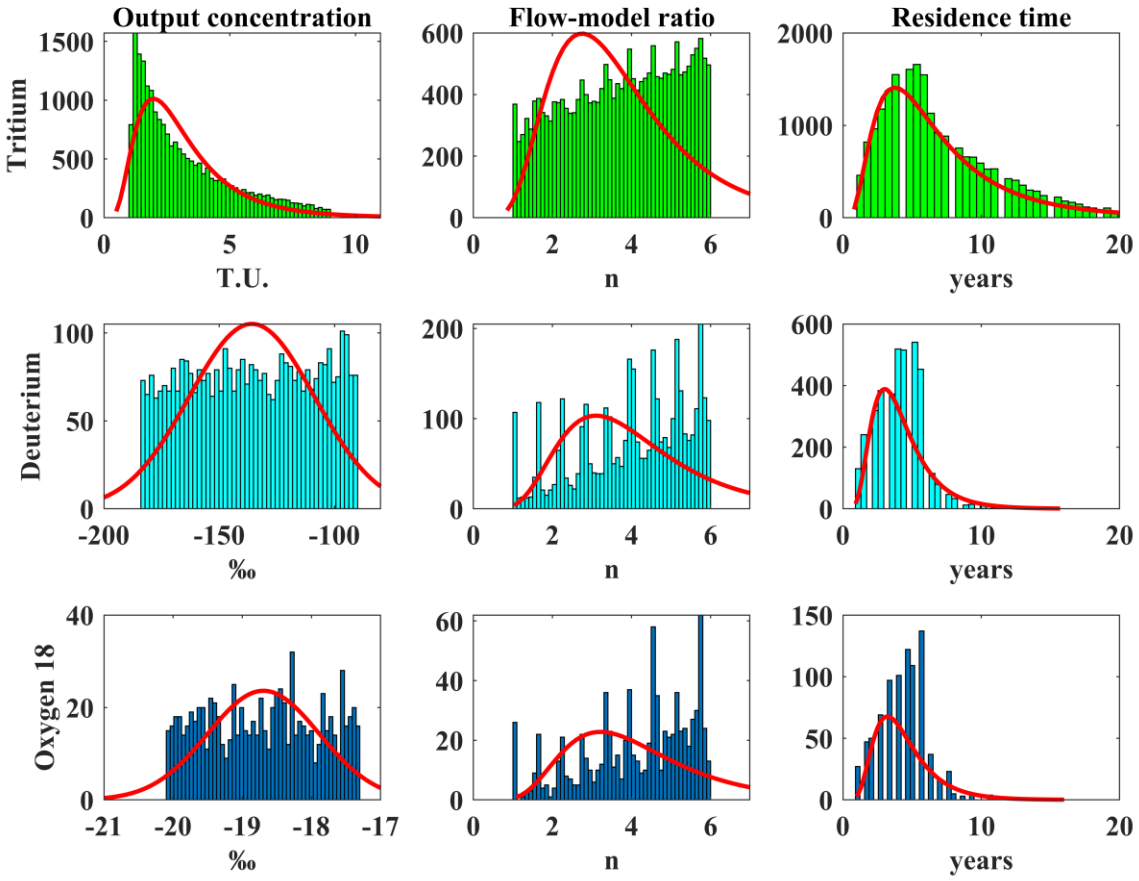

Figure 8 Convolution integral with rows for tritium, deuterium and ^{18}O. The "Flow model" column shows Exponential to Piston Flow ratio (*n*) and residence time shows all transit time outputs.

4.5 Volume implications at cryogenic conditions.

Volume estimations considered streamflow measurements (fieldworks 2017-2019) and available volume storage capacity (Additional Figure 2) of the assumed aquifers. We consider a ninety-day period per year as Spring-2 was only seen active during February-April and is allegedly the strongest candidate of a cryogenic source.

From spring streamflow only (mean 0.141 m^3/s), the estimated annual volume per a minimal ninety-day thawing season is at least 0.004 km^3 assuming the average travel time taking around 4 years in average with no additional recharge.

The catchment's parameterized volume (the whole north-facing mountain above 3600 m A.S.L.) corresponds to 2.52 km^3 with one spring accounting 0.004 km^3 associated to groundwater "reservoir" volume representing less than a 0.2% of the total vadose volume.

5 Discussion

First, considering that Spring-1 was active since December-2019 and Spring-2 only after February-2020, we argued that groundwater springs have different origins (different reservoir, Figure 4), and that Spring-1 is less likely related to thawing sources than Spring-2.

Stable isotopes between 2019-2020 showed seasonality in groundwater spring and stream samples between late-spring (December, 2019) and early-autumn (April, 2020), which could be explained by the loss of a snow-predominant signal from strong flow path convergence resulting in a high proportion of young water (Leray et al., 2016). The stable isotope composition of groundwater springs is consistent with results from Rodríguez et al., 2016, who sampled the "Monos de Agua" watershed's outlet (2750 m a.s.l.) in April 2012. In terms of tritium content, both (our) groundwater springs seem to be a mixture of two endpoints (glacier and snow) when considering their average value of 2.34 ± 0.11 TU. Nevertheless, a seasonal glacial origin for groundwater springs could not be attained by linear mix but only explained by differences in storage time and/or hydrological origin.

If groundwater springs are glacial water going underground and coming out in late summer, then tritium content should not differ from that of the glacial stream. If in change, springs are a mixture of snow and thawing ice only, that ice tritium content should be (more than twice) higher than the current background (Additional Figure 3b) which is unlikely in terms of the current global tritium levels (Cauquoin et al., 2016; Lázslo et al., 2020) and natural background for the Andes (Houston, 2007). In change, tritium from Spring 2 was less depleted than surface runoff signal (stream) and had a "lighter" $D/^{18}O$ content, implying an intermediate mixture. Therefore, we consider that the groundwater (Spring 2) in late summer does not have a main glacial source from that same season.

Secondly, water from the glacial stream was found to be equal to, or more enriched than snow precipitation ($\Delta^{18}O > 0$), which is consistent with water balance processes modifying initial precipitation isotope signatures (Gibson et al., 2020) and a feature of permafrost thawing

environments (Wan et al., 2019; Yi et al., 2018). Between December-2019 and April-2020, the $\Delta^{18}O$ almost doubled for all sources (groundwater springs and glacial stream) over snow, which is consistent with Crespo et al., 2017.& Crespo et al., 2020 results in the region, although stable isotopic values between hydrological sources were consistently different between themselves (Additional Table 7).

Additionally, our snow samples presented a low (≤8.04) D-excess value (Dansgaard, 1964) shown in Table 1, which represents the evaporation before sampling. D-excess has shown to increase towards winter months but to be lower in less enriched sources (Froehlich et al., 2008) such as our summer snow samples. Spring-1 turned a 5% higher D-excess from December to April (2019-2020), with both Spring-1 and 2 having virtually the same D-excess. This is contrary to the seasonal increase (into warm season) in D-excess mentioned by Froehlich et al., 2008. Hence, also indicative of a thaw enrichment rather than a product of evaporation.

In third place, the nature of the reservoirs (Figure 4) relates to possibilities of glacial infiltration and/or thawing of subsurface, interstitial water from a previous season. Metagenomic analyses of 16S rRNA allowed identification and comparison between springs, showing differences in the presence and abundance of both major (>1% of the total community) and minor/rare (<1%) taxa between springs, reinforcing the idea that Spring-2 may represent a seasonal thawing niche. The finding is coherent with analyses from Alaska, where *Rhodoferax ferrireducens* was abundant (metaproteome to metagenome) in permafrost (Hultman et al., 2015) and in the Swiss Alps, Betaproteobacteria such as *Polaromonas* and *Rhodoferax* associated to the 12 ky. radiocarbon dated) permafrost layer (Frey et al., 2016) and also 15000 year old ice cores from the Tibetan Plateau (Zhong et al., 2021).

The isotopic analyses indicated short inter-annual groundwater transit time (>1–10 year) coherent with low-conductivity zones (Hayashi, 2020) and the biological interpretation of Spring-2 as from a “lower reservoir” sustaining psychrophile diversity. Transit times derived from hydraulic and isotopic analyses of a year or less (Cochand et al., 2020) are assumed predominantly from the “upper reservoir” fractions (Figure 4) while long tails (Figure 8) are most likely associated with our hypothesis of a “lower reservoir”. These results imply that Spring-1 is less related to thawing sources (θ in Figure 4) than Spring-2 as revealed by taxonomic identity, but also its “late summer” activation. Spring-2 is ultimately recognized as potentially coming from frozen ground thawing in late-summer but of recent recharge, meaning it is a mix from snow and glacial water with inter-annual storage.

The groundwater spring connectivity is assumed to have a seasonal evolution, as suggested by tritium and metagenomic identity between groundwater springs. This interpretation resembles spring water analyses in Siberia, showing bipartite composition containing an main older precipitation recharge and water partly sourced from thawing permafrost (Hiyama et al., 2013).

In summary, with less snowfall and earlier snowmelt events (season contraction), seasonal recharge will be affected and potentially cause the disruption of hydrological connectivity as

infiltration might not exceed necessary wetness thresholds (Musselman et al., 2017). This could compromise post-freshet contribution to groundwater reservoirs, and as consequence of permafrost degradation (Evans & Ge, 2017), change timing and magnitude of groundwater recharge and discharge (Green et al., 2011).

Consequently, upon future warming, snowmelt partitioning could increase storage within newly available subsurface pathways depending on the altitude (permafrost zonation). This has also the implication that as connectivity increases, microbial habitats will also be affected, for example, increasing temperature in old permafrost soils could increase the relative abundance of Proteobacteria and Bacteroidetes taxa (Luláková et al., 2019).

Understanding permafrost distribution at 33◦S, an officially declared water scarce region since 2008 is crucial for interpreting subsurface hydrology. In high mountain catchments, groundwater flows are a concealed element of these natural mountain towers. Therefore, to understand the future evolution of the mountain cryosphere is vital for resource baselines, planning, and future water security policies. These cold spots are consistent with negative mean annual ground surface temperatures predominantly around 4000 m a.s.l..

The relevance is framed as the hydraulic parameters assume discontinuous aquitards supporting perched groundwater (Hayashi, 2020)**,** coupled to multi-entry proglacial (ice-cored) moraine system (Langston et al., 2011) and soil responsiveness (Hrachowitz et al., 2009). Nevertheless, the buffering of transit time through the catchment under discontinuous permafrost distribution could be of even less than a year (Cochand et al., 2020).

In this sense, they contemplate the issue that different transit time waters can have the same ^{3}H concentrations since initial concentrations compensate in time for the radioactive decay in waters already in the catchment (Stewart et al., 2010). Additionally, since catchments under discontinuous permafrost distribution can even have mean transit times of less than a year (Cochand et al., 2020), hydraulic parameterization is necessary to adjust isotope-derived timescales within realistic ranges.

6 Outlook and future directions.

6.1 Baseline considerations.

Understanding these processes becomes more relevant as mountain isotherm 0° C rises alongside with snowmelt season contraction ultimately affecting aquifer hydraulic properties. These imminent changes demand weighing future hydraulic conductivity shifts at high mountain catchments considering feedbacks between ice-retreat, permafrost degradation, and (surface/subsurface) hydraulic properties (Figure 9).

The thermal structure of a headwater catchment with limited field data (ground surface temperature and incoming radiation magnitudes) and delivered inputs for hydrological parameterization. The frozen-ground mapping did not consider rock glaciers as response variables

as the aim was to establish a representative permafrost zonation and because specific conditions for permafrost-related cryoforms are acknowledged as different from interstitial water storage.

Understanding a regional hydrological role of frozen grounds could be attained by upscaling the methods described onto larger ungauged catchments. This would first require local temperature and incoming radiation datasets to either downscale reanalysis data or available permafrost distribution maps or following the catchment-scale resampling method. These analyses will only show favorable conditions for hydraulic changes without delivering insights on the connectivity behind "black box" mechanistic assumptions at those catchments. Secondly, it would be necessary to assess water transit-time analysis, aiming at the conceptualization of the system, and look for "candidate" sources (springs, seepage faces, streams), to group them by seasonal activity and prioritize their sampling accordingly.

Choosing groundwater springs as outflow signals conveys uncertainties due to seasonality and asynchronous flow activation and the constraint of imminent depletion/rerouting. Andean headwater catchments are predominantly young landscapes in terms of sedimentary redistribution (paraglacial environments) and bear high variability. Because of the high seasonality within every catchment, the recommendation is to increase catchment resolution within representative, contrasting sub-units of one or two adjacent catchments rather than choosing a lesser resolution and covering larger areas with a larger number of watersheds.

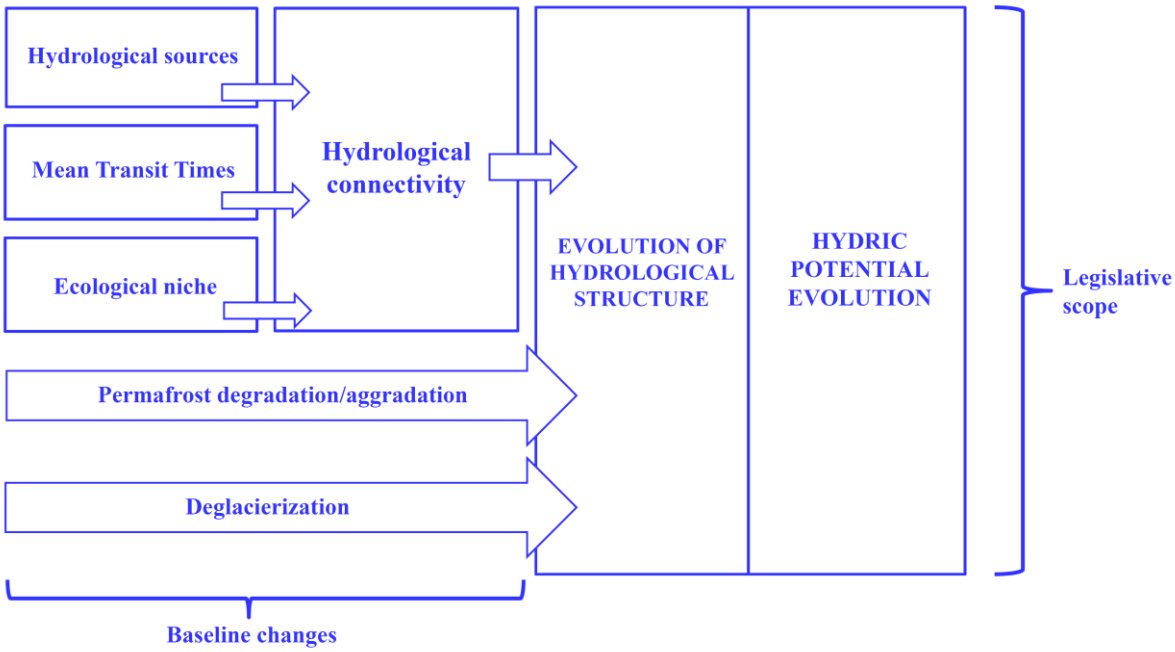

Figure 9. Mountain cryosphere baseline evolution. Conceptual dynamic for Andean, glacierized catchments under permafrost conditions.

6.2 Considerations for environmental assessments.

The present work also highlights the divergence of hydric potentiality (resource value) within a catchment under permafrost conditions (Figure 9), implying reallocation of value from one item (surface) to another (subsurface). In other words, climate/cryosphere changes could modify the distribution of the water-bearing capacity of a catchment, challenging the scope of current legislation (Figure 9). Seasonal groundwater as freshwater represents an underestimated fraction, partially due to the complexity of understanding its magnitude and because most gauging stations and analyses occur at catchment outlets.

In a broader sense, the main policy issue is that hydrological restructuring of mountain environments requires understanding how hydric potential will evolve in the following decades, opening the door for a specific concern on headwater catchments and legislation. This issue is relevant in the Andes as it has different hydroclimatic regions with distinct groundwater resilience to atmospheric warming. This issue might even include transboundary aquifers in desertic areas of Northern Chile and Argentina.

For example, the preventive approach of scarcity in dry Andean areas does not account for groundwater recharge and storage evolution. Consequently, hydric values could reallocate to another item (cryosphere element) upon gradual transformations within the hydrological network. These value changes also relate to biodiversity and biogeochemical niches therein; for example, preservation dimensions in protected areas require a hypothetical baseline that often neglects the frozen diversity underlying the glacial landscape. Moreover, in terms of hydrological connectivity, this biodiversity has also served as a proxy for attesting connectivity between cryosphere elements, representing a value as unaccounted, partially isolated fragments of genetic identity.

Furthermore, from the conservation point of view, value transactions of high hydric potential areas cannot be reduced to mere satisfaction (the present day) as their natural value also possesses undesirable outcomes. This context for the mountain cryosphere represents a rapidly evolving domain incompatible with other analytical baselines for legislation. Hence, water legislation should visualize a common ground for different land uses as potential water pollution or streamflow alteration (non-potable) may not only be due to anthropogenic influences and overlap (or be overlapped by) industrial impacts.

7 Conclusions.

The current analysis determined a seasonal signal in groundwater springs at a permafrost affected catchment in the Andes at 33°S and 3600 m a.s.l.. At warm-seasons of 2019-2020, springs presented a positive $\Delta^{18}O$ and D-excess, stable isotope enrichment, and depleted tritium content. One spring (Spring-2) activated at late warm-season implying a thawing source, representative of a non-surface, non-seasonal source, implying inter-annual storage. Metagenomic results also showed taxa (*Polaromonas* and *Rhodoferax*) common in mountain glaciers and lowland permafrost environments, coinciding with the interpretation of Spring-2 as a potential thawing source, a "lower reservoir", sustaining psychrophile diversity.

The hydraulic parameterization and isotope derived convolution equation mean transit times, suggest a catchment structure with short inter-annual subsurface storage (lower reservoir). Upon incoming warming, snowmelt partitioning could increase storage within these newly available subsurface pathways depending on the altitude. Therefore, water volumes assumed to be stored inter-annually in the subsurface and delivered upon thawing through groundwater spring systems has would imply that as connectivity increases, microbial habitats (with several unique sequences) will also be affected, highlighting a preponderant role of the frozen ground seasonal contribution but also the subsurface biochemical evolution.

These results acknowledge a structural and water-contributing role to groundwater potentially associated with frozen grounds at a semi-arid catchment in the central Andes of Chile, which is a conveyed element of biodiversity and hydric potential in rapidly evolving periglacial landscapes in water scarce regions. The approach developed in this work is a process-based reference for mountain cryosphere and biodiversity baselines.

In a high mountain area, results showed hydrological connections between glaciers and groundwater springs, representing a microbiological link for colonization/expansion at the ice/soil interface. This connectivity implies hydric potential, as groundwater spring signals showed an inter-annual storage. Additionally, results delivered seasonal outflow drift magnitudes useful for understanding the evolution of the hydrological network (snow, ice, springs, and seepage faces).

Upcoming negative mass balances in mountain cryosphere derive in short-term concerns for water-scarcity, yet permafrost/glacier feedback is neglected in the interpretation of evolving proglacial settings. Consequently, upon deglacierization, the hydraulic parameterization lacks mechanistic estimates of flow buffering capacity of the catchment.

8 Outreach: Comic "*Mountain research: the Andes cryosphere".*

Non-expert audiences need to be informed about issues on climate impact on hydric resources in water-scarce regions.

The following material is product of cooperation between the Author and the painter Sebastián Martinez Fadic, attempting to show how a graphic interface can be used to demonstrate the spatial dimension of landscape inserted in mountain research.

This kind of material has been previously produced by groups like the Permafrost Young Researchers Network (PYRN), demonstrating how a simple format can be translated to many languages to reach out different audiences.

Mountain research: the Andes cryosphere

This is a short watercolor comic. The cover is an adaptation from E. Meier's photograph at the "Andino Juncal" Park during 1951.

concept by Sebastian Ruiz Pereira

illustrations by Sebastian Martinez Fadic

The Andes mountains are
“Water Towers for millions of people.

Nevertheless, how these water reservoirs
will evolve is an important question
yet to be answered .

In Central Chile,
our researcher friends try to
understand how water is stored
in the mountains.

The Andino Juncal park is a
protected area, where
glaciers and wildlife coexist.

Here’s where our
researchers go to work.

A park with a
wonderful landscape

Hello
friends!

We need to
do our sampling
near the glacier.

sure! leave no
trace & call if
you need help

Climbers ahead.
let’s ask how
conditions are

so, all good up
there by the
glacier ?

yeah, all safe.
we saw some
friendly pumas!

And so, the researchers approach the glaciers...

Find shelter in the natural setting...

And get ready for their second day of work up in the mountains!

today we collect water samples and get our logger data!

Look! the Park ranger is coming from the glacier

Nice day huh? Hey, please tell the Goverment chopper to NOT fly low!

we don't want to scare the animals!

Safe travel back to base!

Then, the researchers sample water for chemical and biological analyses.

With those results, they will interpret the groundwater network inside the mountain.

Suddenly, the team from the Government Water Directory flies over our researchers

and lands on a safe area
to meet our researchers

The Government and independent researchers
sometimes work together in understanding
mountain hydric resources.

thanks for taking these samples back to the city!

no problem! safe travels

Finally, after retrieveing
annual data from
ground temperature loggers...

The researchers head back home
to analyze their data...

...and figure out
what is going on
with water inside
the mountains.

yet, some
will stay up there...

forever...

9 **References**.

Alvarez-Garreton, C., Mendoza, P. A., Boisier, J. P., Addor, N., Galleguillos, M., Zambrano-Bigiarini, M., Lara, A., Cortes, G., Garreaud, R., & McPhee, J. (2018). The CAMELS-CL dataset: catchment attributes and meteorology for large sample studies-Chile dataset. *Hydrology and Earth System Sciences*, *22*(11), 5817–5846.

Arbelaitz, O., Gurrutxaga, I., Muguerza, J., PéRez, J. M., & Perona, I. (2013). An extensive comparative study of cluster validity indices. *Pattern Recognition*, *46*(1), 243–256.

Arthur, D., & Vassilvitskii, S. (2007). k-means++: The advantages of careful seeding. *Proceedings of the Eighteenth Annual ACM-SIAM Symposium on Discrete Algorithms*, 1027–1035.

Baraer, M., Mark, B. G., McKenzie, J. M., Condom, T., Bury, J., Huh, K.-I., Portocarrero, C., Gómez, J., & Rathay, S. (2012). Glacier recession and water resources in Peru's Cordillera Blanca. *Journal of Glaciology*, *58*(207), 134–150.

Baraer, M., McKenzie, J. M., Mark, B. G., Bury, J., & Knox, S. (2009). Characterizing contributions of glacier melt and groundwater during the dry season in a poorly gauged catchment of the Cordillera Blanca (Peru). *Advances in Geosciences*, *22*, 41–49.

Barberis, J. A. (1986). *International groundwater resources law* (Issue 40). Food & Agriculture Org.

Barnett, T. P., Adam, J. C., & Lettenmaier, D. P. (2005). Potential impacts of a warming climate on water availability in snow-dominated regions. *Nature*, *438*(7066), 303–309.

Bartsch, A., Grosse, G., Kääb, A., Westermann, S., Strozzi, T., Wiesmann, A., Duguay, C., Seifert, F. M., Obu, J., & Goler, R. (2016). GlobPermafrost—How Space-BasedEarth Observation Supports Understanding of Permafrost. *Living Planet Symp*, *740*, 332.

Bateman, I. J., Brouwer, R., Cranford, M., Hime, S., Ozdemiroglu, E., Phang, Z., & Provins, A. (2010). Valuing environmental impacts: Practical guidelines for the use of value transfer in policy and project appraisal. *Main Report to the Department for Environment, Food and Rural Affairs, Economics for the Environment Consultancy (Eftec), London*.

Bear, J. (1988). *Dynamics of Fluids in Porous Media*. Courier Corporation.

Bertazzo, S. (2019). Los acuíferos y las aguas subterráneas en el Derecho internacional público. *Revista de Derecho Administrativo Económico*, *27*, 41–66.

Bochet, O., Bethencourt, L., Dufresne, A., Farasin, J., Pédrot, M., Labasque, T., Chatton, E., Lavenant, N., Petton, C., & Abbott, B. W. (2020). Iron-oxidizer hotspots formed by intermittent oxic–anoxic fluid mixing in fractured rocks. *Nature Geoscience*, *13*(2), 149–155.

Bodin, X., Rojas, F., & Brenning, A. (2010). Status and evolution of the cryosphere in the Andes of Santiago (Chile, 33.5 S.). *Geomorphology*, *118*(3–4), 453–464.

Boisier, J. P., Alvarez-Garretón, C., Cordero, R. R., Damiani, A., Gallardo, L., Garreaud, R. D., Lambert, F., Ramallo, C., Rojas, M., & Rondanelli, R. (2018). Anthropogenic drying in

central-southern Chile evidenced by long-term observations and climate model simulations. *Elem Sci Anth*, *6*(1).

Bokulich, N. A., Kaehler, B. D., Rideout, J. R., Dillon, M., Bolyen, E., Knight, R., Huttley, G. A., & Caporaso, J. G. (2018). Optimizing taxonomic classification of marker-gene amplicon sequences with QIIME 2's q2-feature-classifier plugin. *Microbiome*, *6*(1), 1–17.

Bolyen, E., Rideout, J. R., Dillon, M. R., Bokulich, N. A., Abnet, C. C., Al-Ghalith, G. A., Alexander, H., Alm, E. J., Arumugam, M., & Asnicar, F. (2019). Reproducible, interactive, scalable and extensible microbiome data science using QIIME 2. *Nature Biotechnology*, *37*(8), 852–857.

Bown, F., Rivera, A., & Acuña, C. (2008). Recent glacier variations at the Aconcagua basin, central Chilean Andes. *Annals of Glaciology*. https://doi.org/10.3189/172756408784700572

Bullock, C. (2017). *Nature's Values: From Intrinsic to Instrumental* (NESC (ed.)). National Economic and Social Council.

Burn, C. R., & Michel, F. A. (1988). Evidence for recent temperature-induced water migration into permafrost from the tritium content of ground ice near Mayo, Yukon Territory, Canada. *Canadian Journal of Earth Sciences*, *25*(6), 909–915. https://doi.org/10.1139/e88-087

Caliński, T., & Harabasz, J. (1974). A dendrite method for cluster analysis. *Communications in Statistics-Theory and Methods*, *3*(1), 1–27.

Callahan, B. J., McMurdie, P. J., Rosen, M. J., Han, A. W., Johnson, A. J. A., & Holmes, S. P. (2016). DADA2: High-resolution sample inference from Illumina amplicon data. *Nature Methods*, *13*(7), 581–583. https://doi.org/10.1038/nmeth.3869

Caporaso, J. G., Kuczynski, J., Stombaugh, J., Bittinger, K., Bushman, F. D., Costello, E. K., Fierer, N., Pena, A. G., Goodrich, J. K., & Gordon, J. I. (2010). QIIME allows analysis of high-throughput community sequencing data. *Nature Methods*, *7*(5), 335–336.

Casteleiro-Roca, J.-L., García-Ordás, M. T., Jove, E., Zayas-Gato, F., Quintián, H., Alaiz-Moretón, H., & Calvo-Rolle, J. L. (2020). A Solar Thermal System Temperature Prediction of a Smart Building for Data Recovery and Security Purposes. *International Conference on Intelligent Data Engineering and Automated Learning*, 468–476.

Cauquoin, A., Jean-Baptiste, P., Risi, C., Fourré, E., Stenni, B., & Landais, A. (2015). The global distribution of natural tritium in precipitation simulated with an Atmospheric General Circulation Model and comparison with observations. *Earth and Planetary Science Letters*. https://doi.org/10.1016/j.epsl.2015.06.043

Cheng, G. D., & Jin, H. J. (2013). Groundwater in the permafrost regions on the Qinghai-Tibet Plateau and it changes. *Hydrogeology & Engineering Geology*, *40*(1), 1–10.

Clow, D. W., Schrott, L., Webb, R., Campbell, D. H., Torizzo, A., & Dornblaser, M. (2003). Ground water occurrence and contributions to streamflow in an alpine catchment, Colorado Front Range. *Groundwater*, *41*(7), 937–950.

Cochand, M., Molson, J., Barth, J. A. C., van Geldern, R., Lemieux, J. M., Fortier, R., & Therrien, R. (2020). Rapid groundwater recharge dynamics determined from

hydrogeochemical and isotope data in a small permafrost watershed near Umiujaq (Nunavik, Canada). *Hydrogeology Journal*, *28*(3). https://doi.org/10.1007/s10040-020-02109-x

Colombo, N., Salerno, F., Martin, M., Malandrino, M., Giardino, M., Serra, E., Godone, D., Said-Pullicino, D., Fratianni, S., Paro, L., Tartari, G., & Freppaz, M. (2019). Influence of permafrost, rock and ice glaciers on chemistry of high-elevation ponds (NW Italian Alps). *Science of The Total Environment*, *685*, 886–901. https://doi.org/https://doi.org/10.1016/j.scitotenv.2019.06.233

Crespo, S. A., Fernandoy, F., Cara, L., Klarian, S., & Lavergne, C. (2020). First snow, glacier and groundwater contribution quantification in the upper Mendoza River basin using stable water isotopes. *Isotopes in Environmental and Health Studies*, 1–20. https://doi.org/10.1080/10256016.2020.1797713

Crespo, S., Aranibar, J., Gomez, L., Schwikowski, M., Bruetsch, S., Cara, L., & Villalba, R. (2017). Ionic and stable isotope chemistry as indicators of water sources to the Upper Mendoza River basin, Central Andes of Argentina. *Hydrological Sciences Journal*, *62*(4), 588–605.

Dansgaard, W. (1964). Stable isotopes in precipitation. *Tellus*, *16*(4), 436–468.

Davies, D. L., & Bouldin, D. W. (1979). A cluster separation measure. *IEEE Transactions on Pattern Analysis and Machine Intelligence*, *2*, 224–227.

DeSA, U. N. (2013). World population prospects: the 2012 revision. *Population Division of the Department of Economic and Social Affairs of the United Nations Secretariat, New York*, *18*.

Dinçer, T., Payne, B. R., Florkowski, T., Martinec, J., & Tongiorgi, E. (1970). Snowmelt runoff from measurements of tritium and oxygen-18. *Water Resources Research*, *6*(1), 110–124. https://doi.org/10.1029/WR006i001p00110

Domenico, P. A., & Schwartz, F. W. (1998). *Physical and chemical hydrogeology* (Vol. 506). Wiley New York.

Dussaillant, I., Berthier, E., Brun, F., Masiokas, M., Hugonnet, R., Favier, V., Rabatel, A., Pitte, P., & Ruiz, L. (2019). Two decades of glacier mass loss along the Andes. *Nature Geoscience*, 1–7.

Eckstein, G. E. (2007). Commentary on the UN International Law Commission's draft articles on the law of transboundary aquifers. *Colo. J. Int'l Envtl. L. & Pol'y*, *18*, 537.

Eckstein, G. E., & Eckstein, Y. (2003). A hydrogeological approach to transboundary ground water resources and international law. *Am. U. Int'l L. Rev.*, *19*, 201.

Elmqvist, T. (2017). Development: Sustainability and resilience differ. *Nature*, *546*(7658), 352.

Elmqvist, T., Andersson, E., Frantzeskaki, N., McPhearson, T., Olsson, P., Gaffney, O., Takeuchi, K., & Folke, C. (2019). Sustainability and resilience for transformation in the urban century. *Nature Sustainability*, *2*(4), 267–273.

Evans, S. G., & Ge, S. (2017). Contrasting hydrogeologic responses to warming in permafrost and seasonally frozen ground hillslopes. *Geophysical Research Letters*, *44*(4). https://doi.org/10.1002/2016GL072009

Evans, S. G., Ge, S., & Liang, S. (2015). Analysis of groundwater flow in mountainous, headwater catchments with permafrost. *Water Resources Research*, *51*(12), 9564–9576.

Evans, S. G., Ge, S., Voss, C. I., & Molotch, N. P. (2018). The role of frozen soil in groundwater discharge predictions for warming alpine watersheds. *Water Resources Research*, *54*(3), 1599–1615.

Evans, S. G., Yokeley, B., Stephens, C., & Brewer, B. (2020). Potential mechanistic causes of increased baseflow across northern Eurasia catchments underlain by permafrost. *Hydrological Processes*, *34*(11), 2676–2690.

Finneran, K. T., Johnsen, C. V, & Lovley, D. R. (2003). Rhodoferax ferrireducens sp. nov., a psychrotolerant, facultatively anaerobic bacterium that oxidizes acetate with the reduction of Fe (III). *International Journal of Systematic and Evolutionary Microbiology*, *53*(3), 669–673.

Frans, C., Istanbulluoglu, E., Lettenmaier, D. P., Naz, B. S., Clarke, G. K. C., Condom, T., Burns, P., & Nolin, A. W. (2015). Predicting glacio-hydrologic change in the headwaters of the Z ongo R iver, C ordillera R eal, B olivia. *Water Resources Research*, *51*(11), 9029–9052.

Frey, B., Rime, T., Phillips, M., Stierli, B., Hajdas, I., Widmer, F., & Hartmann, M. (2016). Microbial diversity in European alpine permafrost and active layers. *FEMS Microbiology Ecology*, *92*(3). https://doi.org/10.1093/femsec/fiw018

Froehlich, K., Kralik, M., Papesch, W., Rank, D., Scheifinger, H., & Stichler, W. (2008). Deuterium excess in precipitation of Alpine regions–moisture recycling. *Isotopes in Environmental and Health Studies*, *44*(1), 61–70.

Gibson, J. J., Birks, S. J., Yi, Y., & Vitt, D. H. (2015). Runoff to boreal lakes linked to land cover, watershed morphology and permafrost thaw: a 9-year isotope mass balance assessment. *Hydrological Processes*, *29*(18), 3848–3861. https://doi.org/10.1002/hyp.10502

Gibson, J. J., Eby, P., Stadnyk, T. A., Holmes, T., Birks, S. J., & Pietroniro, A. (2021). Dataset of 18O and 2H in streamflow across Canada: A national resource for tracing water sources, water balance and predictive modelling. *Data in Brief*, *34*, 106723.

Gibson, J. J., Holmes, T., Stadnyk, T. A., Birks, S. J., Eby, P., & Pietroniro, A. (2020). 18O and 2H in streamflow across Canada. *Journal of Hydrology: Regional Studies*, *32*, 100754. https://doi.org/https://doi.org/10.1016/j.ejrh.2020.100754

Gisnås, K., Etzelmüller, B., Farbrot, H., Schuler, T. V, & Westermann, S. (2013). CryoGRID 1.0: Permafrost distribution in Norway estimated by a spatial numerical model. *Permafrost and Periglacial Processes*, *24*(1), 2–19.

Glas, R., Lautz, L., McKenzie, J., Mark, B., Baraer, M., Chavez, D., & Maharaj, L. (2018). A review of the current state of knowledge of proglacial hydrogeology in the Cordillera Blanca, Peru. *Wiley Interdisciplinary Reviews: Water*, *5*(5), e1299.

Gleeson, T., Befus, K. M., Jasechko, S., Luijendijk, E., & Cardenas, M. B. (2016). The global volume and distribution of modern groundwater. *Nature Geoscience*, *9*(2), 161–167.

Green, T. R., Taniguchi, M., Kooi, H., Gurdak, J. J., Allen, D. M., Hiscock, K. M., Treidel, H., & Aureli, A. (2011). Beneath the surface of global change: Impacts of climate change on groundwater. *Journal of Hydrology*, *405*(3–4), 532–560.

Griggs, D., Stafford-Smith, M., Gaffney, O., Rockström, J., Öhman, M. C., Shyamsundar, P., Steffen, W., Glaser, G., Kanie, N., & Noble, I. (2013). Sustainable development goals for people and planet. *Nature*, *495*(7441), 305–307.

Gruber, S. (2012). Derivation and analysis of a high-resolution estimate of global permafrost zonation. *Cryosphere*. https://doi.org/10.5194/tc-6-221-2012

Gulbrandsen, M. L., Minsley, B. J., Ball, L. B., & Hansen, T. M. (2016). Semiautomatic mapping of permafrost in the Yukon Flats, Alaska. *Geophysical Research Letters*, *43*(23), 12–131.

Hammond, J. C., Harpold, A. A., Weiss, S., & Kampf, S. K. (2019). Partitioning snowmelt and rainfall in the critical zone: effects of climate type and soil properties. *Hydrol. Earth Syst. Sci.*, *23*(9), 3553–3570. https://doi.org/10.5194/hess-23-3553-2019

Hayashi, M. (2020). Alpine hydrogeology: The critical role of groundwater in sourcing the headwaters of the world. *Groundwater*, *58*(4), 498–510.

Heath, R. C. (2004). *Basic ground-water hydrology*. US Geological Survey Reston, VA.

Hiyama, T., Asai, K., Kolesnikov, A. B., Gagarin, L. A., & Shepelev, V. V. (2013). Estimation of the residence time of permafrost groundwater in the middle of the Lena River basin, eastern Siberia. *Environmental Research Letters*, *8*(3), 35040.

Hock, R., Rasul, G., Adler, C., Cáceres, B., Gruber, S., Hirabayashi, Y., Jackson, M., Kääb, A., Kang, S., & Kutuzov, S. (2019). *High Mountain Areas: In: IPCC Special Report on the Ocean and Cryosphere in a Changing Climate*.

Houston, J. (2007). Recharge to groundwater in the Turi Basin, northern Chile: An evaluation based on tritium and chloride mass balance techniques. *Journal of Hydrology*, *334*(3–4), 534–544.

Hrachowitz, M., Soulsby, C., Tetzlaff, D., Dawson, J. J. C., & Malcolm, I. A. (2009). Regionalization of transit time estimates in montane catchments by integrating landscape controls. *Water Resources Research*, *45*(5). https://doi.org/10.1029/2008WR007496

Hultman, J., Waldrop, M. P., Mackelprang, R., David, M. M., McFarland, J., Blazewicz, S. J., Harden, J., Turetsky, M. R., McGuire, A. D., & Shah, M. B. (2015). Multi-omics of permafrost, active layer and thermokarst bog soil microbiomes. *Nature*, *521*(7551), 208–212.

Immerzeel, W. W., Lutz, A. F., Andrade, M., Bahl, A., Biemans, H., Bolch, T., Hyde, S., Brumby, S., Davies, B. J., & Elmore, A. C. (2020). Importance and vulnerability of the world's water towers. *Nature*, *577*(7790), 364–369.

Immerzeel, W. W., Van Beek, L. P. H., & Bierkens, M. F. P. (2010). Climate change will affect the Asian water towers. *Science*, *328*(5984), 1382–1385.

International_Law_Commission. (2008). Draft articles on the Law of Transboundary Aquifers, with commentaries. In *Yearbook of the International Law Commission, V2, 2*. (pp. 21–43). United Nations. https://legal.un.org/ilc/texts/instruments/english/commentaries/8_5_2008.pdf

Kazemi, G. A., Lehr, J. H., & Perrochet, P. (2006). *Groundwater age*. John Wiley & Sons.

Kralik, M. (2015). How to estimate mean residence times of groundwater. *Procedia Earth and Planetary Science*, *13*, 301–306.

Kurylyk, B. L., & Hayashi, M. (2017). Inferring hydraulic properties of alpine aquifers from the propagation of diurnal snowmelt signals. *Water Resources Research*, *53*(5), 4271–4285.

Kurylyk, B. L., MacQuarrie, K. T. B., & McKenzie, J. M. (2014). Climate change impacts on groundwater and soil temperatures in cold and temperate regions: Implications, mathematical theory, and emerging simulation tools. *Earth-Science Reviews*, *138*, 313–334.

Lambiel, C., & Pieracci, K. (2008). Permafrost distribution in talus slopes located within the alpine periglacial belt, Swiss Alps. *Permafrost and Periglacial Processes*, *19*(3), 293–304.

Lamirel, J.-C., Dugué, N., & Cuxac, P. (2016). New efficient clustering quality indexes. *2016 International Joint Conference on Neural Networks (IJCNN)*, 3649–3657.

Langston, G., Bentley, L. R., Hayashi, M., McClymont, A., & Pidlisecky, A. (2011). Internal structure and hydrological functions of an alpine proglacial moraine. *Hydrological Processes*, n/a-n/a. https://doi.org/10.1002/hyp.8144

Lepeška, T. (2010). Hydric potential of landscape and integrated river basin management in mountain and submontane regions. *Ecohydrology & Hydrobiology*, *10*(1), 13–24. https://doi.org/https://doi.org/10.2478/v10104-010-0017-9

Leray, S., De Dreuzy, J.-R., Bour, O., Labasque, T., & Aquilina, L. (2012). Contribution of age data to the characterization of complex aquifers. *Journal of Hydrology*, *464*, 54–68.

Leray, S., Engdahl, N. B., Massoudieh, A., Bresciani, E., & McCallum, J. (2016). Residence time distributions for hydrologic systems: Mechanistic foundations and steady-state analytical solutions. *Journal of Hydrology*. https://doi.org/10.1016/j.jhydrol.2016.01.068

Liaudat, D. T., & Bottegal, E. (2020). Recent evolution of the active layer in the Morenas Coloradas rock glacier, Central Andes, Mendoza, Argentina and its relation with kinematics. *Cuadernos de Investigación Geográfica/Geographical Research Letters*, *46*, 159–185.

Liu, F., Williams, M. W., & Caine, N. (2004). Source waters and flow paths in an alpine catchment, Colorado Front Range, United States. *Water Resources Research*, *40*(9). https://doi.org/10.1029/2004WR003076

Lliboutry, L. (1956). Nieves y glaciares de Chile. Fundamentos de Glaciología. Ediciones de la Universidad de Chile. *Santiago*, *1957*, 18–25.

Luláková, P., Perez-Mon, C., Šantrůčková, H., Ruethi, J., & Frey, B. (2019). High-Alpine Permafrost and Active-Layer Soil Microbiomes Differ in Their Response to Elevated Temperatures . In *Frontiers in Microbiology* (Vol. 10, p. 668). https://www.frontiersin.org/article/10.3389/fmicb.2019.00668

Madigan, M. T., Jung, D. O., Woese, C. R., & Achenbach, L. A. (2000). Rhodoferax antarcticus sp. nov., a moderately psychrophilic purple nonsulfur bacterium isolated from an Antarctic microbial mat. *Archives of Microbiology*, *173*(4), 269–277.

Małoszewski, P., Rauert, W., Stichler, W., Herrmann, A. (1983). Application of flow models in an alpine catchment area using tritium and deuterium data. *Journal of Hydrology*, *66*(1–4), 319–330. https://www.sciencedirect.com/science/article/pii/0022169483901932

Maloszewski, P., & Zuber, A. (1993). Principles and practice of calibration and validation of mathematical models for the interpretation of environmental tracer data in aquifers. *Advances in Water Resources*, *16*(3), 173–190.

Maloszewski, P., & Zuber, A. (1996). *Lumped parameter models for the interpretation of environmental tracer data*. https://inis.iaea.org/search/search.aspx?orig_q=RN:28020904

Małoszewski, P., & Zuber, A. (1982). Determining the turnover time of groundwater systems with the aid of environmental tracers. 1. Models and their applicability. *Journal of Hydrology*. https://doi.org/10.1016/0022-1694(82)90147-0

Mashburn, S. L., Cope, C. C., & Abbott, M. M. (2003). *Aquifer characteristics, water availability, and water quality of the Quaternary aquifer, Osage County, northeastern Oklahoma, 2001-2002* (Vol. 3, Issue 4235). US Department of the Interior, US Geological Survey.

McDonnell, J. J., McGuire, K., Aggarwal, P., Beven, K. J., Biondi, D., Destouni, G., Dunn, S., James, A., Kirchner, J., & Kraft, P. (2010). How old is streamwater? Open questions in catchment transit time conceptualization, modeling and analysis. *Hydrological Processes. 24: 1745-1754*, *24*, 1745–1754.

McGuire, KJ, McDonnell, J. (2006). A review and evaluation of catchment transit time modeling. *Journal of Hydrology*, *330*(3–4), 543–563. https://www.sciencedirect.com/science/article/pii/S0022169406002150

McGuire, K. J., McDonnell, J. J., Weiler, M., Kendall, C., McGlynn, B. L., Welker, J. M., & Seibert, J. (2005). The role of topography on catchment-scale water residence time. *Water Resources Research*, *41*(5). https://doi.org/10.1029/2004WR003657

McMurdie, P. J., & Holmes, S. (2013). phyloseq: an R package for reproducible interactive analysis and graphics of microbiome census data. *PloS One*, *8*(4), e61217.

Monnier, S., & Kinnard, C. (2017). Pluri-decadal (1955-2014) evolution of glacier-rock glacier transitional landforms in the central Andes of Chile (30-33° S). *Earth Surface Dynamics*, *5*(3).

Morales, M. S., Cook, E. R., Barichivich, J., Christie, D. A., Villalba, R., LeQuesne, C., Srur, A. M., Ferrero, M. E., González-Reyes, Á., Couvreux, F., Matskovsky, V., Aravena, J. C., Lara, A., Mundo, I. A., Rojas, F., Prieto, M. R., Smerdon, J. E., Bianchi, L. O., Masiokas,

M. H., … Boninsegna, J. A. (2020). Six hundred years of South American tree rings reveal an increase in severe hydroclimatic events since mid-20th century. *Proceedings of the National Academy of Sciences*, *117*(29), 16816 LP – 16823. https://doi.org/10.1073/pnas.2002411117

Morris, D. A., & Johnson, A. I. (1967). *Summary of hydrologic and physical properties of rock and soil materials, as analyzed by the hydrologic laboratory of the US Geological Survey, 1948-60*. US Government Printing Office.

Musselman, K. N., Clark, M. P., Liu, C., Ikeda, K., & Rasmussen, R. (2017). Slower snowmelt in a warmer world. *Nature Climate Change*, *7*(3), 214–219.

Nino, F. S. (2015). Sustainable Development Goals—United Nations. *United Nations Sustainable Development*.

Nitze, I., Grosse, G., Jones, B. M., Romanovsky, V. E., & Boike, J. (2018). Remote sensing quantifies widespread abundance of permafrost region disturbances across the Arctic and Subarctic. *Nature Communications*, *9*(1), 5423. https://doi.org/10.1038/s41467-018-07663-3

Niu, F., Yin, G., Luo, J., Lin, Z., & Liu, M. (2018). Permafrost distribution along the Qinghai-Tibet Engineering Corridor, China using high-resolution statistical mapping and modeling integrated with remote sensing and GIS. *Remote Sensing*, *10*(2), 215.

Nordstrom, K. F. (1993). Intrinsic value and landscape evaluation. *Geographical Review*, *83*(4), 473–476.

O'Neill, H. B., Wolfe, S. A., & Duchesne, C. (2019). New ground ice maps for Canada using a paleogeographic modelling approach. *The Cryosphere*, *13*(3), 753–773.

Obu, J., Westermann, S., Kaab, A., & Bartsch, A. (2019). Ground Temperature Map, 2000-2016, Andes, New Zealand and East African Plateau Permafrost. In *University of Oslo*. PANGAEA. https://doi.org/10.1594/PANGAEA.905512

Ohlanders, N., Rodriguez, M., & Mc Phee Torres, J. (2013). *Stable water isotope variation in a Central Andean watershed dominated by glacier and snowmelt*.

Oksanen, J., Blanchet, F. G., Friendly, M., Kindt, R., Legendre, P., McGlinn, D., Minchin, P. R., O'Hara, R. B., Simpson, G. L., & Solymos, P. (2019). *vegan: Community Ecology Package. R package version 2.5–6. 2019*.

Oliva, M., & Fritz, M. (2018). Permafrost degradation on a warmer Earth: Challenges and perspectives. *Current Opinion in Environmental Science & Health*, *5*, 14–18.

Parada, A. E., Needham, D. M., & Fuhrman, J. A. (2016). Every base matters: assessing small subunit rRNA primers for marine microbiomes with mock communities, time series and global field samples. *Environmental Microbiology*, *18*(5), 1403–1414.

Pereira, S. R., Fernández, J., Herrera, J., & Olea, J. (2021). Assessment of landscape transformation in protected areas. *Environmental Impact Assessment Review*, *86*, 106472. https://doi.org/https://doi.org/10.1016/j.eiar.2020.106472

Pfeffer, W. T., Meier, M. F., & Illangasekare, T. H. (1991). Retention of Greenland runoff by refreezing: implications for projected future sea level change. *Journal of Geophysical Research: Oceans*, *96*(C12), 22117–22124.

Piquer, J., Hollings, P., Rivera, O., Cooke, D. R., Baker, M., & Testa, F. (2017). Along-strike segmentation of the Abanico Basin, central Chile: New chronological, geochemical and structural constraints. *Lithos*, *268*, 174–197.

Polk, M. H., Young, K. R., Baraer, M., Mark, B. G., McKenzie, J. M., Bury, J., & Carey, M. (2017). Exploring hydrologic connections between tropical mountain wetlands and glacier recession in Peru's Cordillera Blanca. *Applied Geography*, *78*, 94–103.

Quast, C., Pruesse, E., Yilmaz, P., Gerken, J., Schweer, T., Yarza, P., Peplies, J., & Glöckner, F. O. (2012). The SILVA ribosomal RNA gene database project: improved data processing and web-based tools. *Nucleic Acids Research*, *41*(D1), D590–D596.

Ragettli, S., Immerzeel, W. W., & Pellicciotti, F. (2016). Contrasting climate change impact on river flows from high-altitude catchments in the Himalayan and Andes Mountains. *Proceedings of the National Academy of Sciences*, *113*(33), 9222–9227.

Ramírez, P. B., Fuentes-Alburquenque, S., Díez, B., Vargas, I., & Bonilla, C. A. (2020). Soil microbial community responses to labile organic carbon fractions in relation to soil type and land use along a climate gradient. *Soil Biology and Biochemistry*, *141*, 107692.

Rodgers, P., Soulsby, C., & Waldron, S. (2005). Stable isotope tracers as diagnostic tools in upscaling flow path understanding and residence time estimates in a mountainous mesoscale catchment. *Hydrological Processes: An International Journal*, *19*(11), 2291–2307.

Rodriguez, M, Ohlanders, N., & McPhee, J. (2014). Estimating glacier and snowmelt contributions to stream flow in a Central Andes catchment in Chile using natural tracers. *Hydrology and Earth System Sciences Discussions*, *11*(7), 8949–8994.

Rodriguez, Maximiliano, Ohlanders, N., Pellicciotti, F., Williams, M. W., & McPhee, J. (2016). Estimating runoff from a glacierized catchment using natural tracers in the semi-arid Andes cordillera. *Hydrological Processes*, *30*(20), 3609–3626. https://doi.org/10.1002/hyp.10973

Rognes, T., Flouri, T., Nichols, B., Quince, C., & Mahé, F. (2016). VSEARCH: a versatile open source tool for metagenomics. *PeerJ*, *4*, e2584.

Rose, S. (2007). Utilization of decadal tritium variation for assessing the residence time of base flow. *Groundwater*, *45*(3), 309–317.

Ruiz Pereira, S, Marquardt, C., Beriain, E., & Lambert, F. (2021). Permafrost evolution in a mountain catchment near Santiago de Chile. *Journal of South American Earth Sciences*, 103293.

Ruiz Pereira, Sebastian, & Veettil, B. K. (2019). Glacier decline in the Central Andes (33° S): Context and magnitude from satellite and historical data. *Journal of South American Earth Sciences*, 102249.

Saito, K., Trombotto Liaudat, D., Yoshikawa, K., Mori, J., Sone, T., Marchenko, S.,

Romanovsky, V., Walsh, J., Hendricks, A., & Bottegal, E. (2016). Late Quaternary Permafrost Distributions Downscaled for South America: Examinations of GCM-based Maps with Observations. *Permafrost and Periglacial Processes*, *27*(1), 43–55.

Sakata, Y., & Ikeda, R. (2013). Depth dependence and exponential models of permeability in alluvial-fan gravel deposits. *Hydrogeology Journal*, *21*(4), 773–786.

Sauer, C. (1963). The morphology of landscape. *University of California Publications in Geography*, *2*(2), 19–54.

Slaymaker, O. (2009). Proglacial, periglacial or paraglacial? *Geological Society, London, Special Publications*, *320*(1), 71–84.

Somers, L. D., & McKenzie, J. M. (2020). A review of groundwater in high mountain environments. *Wiley Interdisciplinary Reviews: Water*, *7*(6), e1475.

Stewart, M. K., Morgenstern, U., Gusyev, M. A., & Małoszewski, P. (2017). Aggregation effects on tritium-based mean transit times and young water fractions in spatially heterogeneous catchments and groundwater systems. *Hydrology and Earth System Sciences*, *21*(9), 4615–4627. https://doi.org/10.5194/hess-21-4615-2017

Stewart, M. K., Morgenstern, U., & McDonnell, J. J. (2010). Truncation of stream residence time: how the use of stable isotopes has skewed our concept of streamwater age and origin. *Hydrological Processes*, *24*(12), 1646–1659. https://doi.org/10.1002/hyp.7576

Stigter, E. E., Steiner, J. F., Koch, I., Saloranta, T. M., Kirkham, J. D., & Immerzeel, W. W. (2021). Energy and mass balance dynamics of the seasonal snowpack at two high-altitude sites in the Himalaya. *Cold Regions Science and Technology*, *183*, 103233. https://doi.org/https://doi.org/10.1016/j.coldregions.2021.103233

Szopińska, M., Szumińska, D., Polkowska, Ż., Machowiak, K., Lehmann, S., & Chmiel, S. (2016). The chemistry of river–lake systems in the context of permafrost occurrence (Mongolia, Valley of the Lakes). Part I. Analysis of ion and trace metal concentrations. *Sedimentary Geology*, *340*, 74–83.

Tapia-Baldis, C., & Trombotto-Liaudat, D. (2019). Permafrost model in coarse-blocky deposits for the Dry Andes, Argentina (28°-33° S). *Cuadernos de Investigación Geográfica*.

Tapia Baldis, C., & Trombotto Liaudat, D. (2019). Rockslides and rock avalanches in the Central Andes of Argentina and their possible association with permafrost degradation. *Permafrost and Periglacial Processes*, *30*(4), 330–347.

Team, R. C. (2020). *R: a language and environment for statistical computing. R Foundation for Statistical Computing website*.

Toohey, R. C., Herman-Mercer, N. M., Schuster, P. F., Mutter, E. A., & Koch, J. C. (2016). Multidecadal increases in the Yukon River Basin of chemical fluxes as indicators of changing flowpaths, groundwater, and permafrost. *Geophysical Research Letters*, *43*(23).

Toubes-Rodrigo, M., Potgieter-Vermaak, S., Sen, R., Elliott, D. R., & Cook, S. J. (2017). Geomicrobiology of basal ice in a temperate glacier: implications for primary microbial production and export, elemental cycling and soil formation. *EGU General Assembly*

Conference Abstracts, 519.

Trombotto, D., & Borzotta, E. (2009). Indicators of present global warming through changes in active layer-thickness, estimation of thermal diffusivity and geomorphological observations in the Morenas Coloradas rockglacier, Central Andes of Mendoza, Argentina. *Cold Regions Science and Technology*. https://doi.org/10.1016/j.coldregions.2008.08.009

Unidad de Glaciología, D. (2015). *Inventario de Glaciares DGA v2015*.

United Nations. (1997). United Nations framework convention on climate change. *Kyoto Protocol, Kyoto*, *19*, 497.

Viviroli, D., & Weingartner, R. (2008). "Water towers"—A global view of the hydrological importance of mountains. In *Mountains: Sources of water, sources of knowledge* (pp. 15–20). Springer.

Wagner, B. D., Grunwald, G. K., Zerbe, G. O., Mikulich-Gilbertson, S. K., Robertson, C. E., Zemanick, E. T., & Harris, J. K. (2018). On the Use of Diversity Measures in Longitudinal Sequencing Studies of Microbial Communities . In *Frontiers in Microbiology* (Vol. 9, p. 1037). https://www.frontiersin.org/article/10.3389/fmicb.2018.01037

Wan, C., Gibson, J. J., Shen, S., Yi, Y., Yi, P., & Yu, Z. (2019). Using stable isotopes paired with tritium analysis to assess thermokarst lake water balances in the Source Area of the Yellow River, northeastern Qinghai-Tibet Plateau, China. *Science of the Total Environment*, *689*, 1276–1292.

Westermann, S., Østby, T. I., Gisnås, K., Schuler, T. V, & Etzelmüller, B. (2015). A ground temperature map of the North Atlantic permafrost region based on remote sensing and reanalysis data. *The Cryosphere*, *9*(3), 1303–1319.

Wutich, A. (2020). Water insecurity: An agenda for research and call to action for human biology. *American Journal of Human Biology*, *32*(1), e23345.

Yi, P., Wan, C., Jin, H., Luo, D., Yang, Y., Wang, Q., Yu, Z., & Aldahan, A. (2018). Hydrological insights from hydrogen and oxygen isotopes in Source Area of the Yellow River, east-northern part of Qinghai–Tibet Plateau. *Journal of Radioanalytical and Nuclear Chemistry*, *317*(1), 131–144. https://doi.org/10.1007/s10967-018-5864-7

Yu, C., Kamboj, S., Wang, C., & Cheng, J.-J. (2015). *Data collection handbook to support modeling impacts of radioactive material in soil and building structures*. Argonne National Lab.(ANL), Argonne, IL (United States).

Zhong, Z.-P., Tian, F., Roux, S., Gazitúa, M. C., Solonenko, N. E., Li, Y.-F., Davis, M. E., Van Etten, J. L., Mosley-Thompson, E., Rich, V. I., Sullivan, M. B., & Thompson, L. G. (2021). Glacier ice archives nearly 15,000-year-old microbes and phages. *Microbiome*, *9*(1), 160. https://doi.org/10.1186/s40168-021-01106-w

Zuber, A., Maloszewski, P., Stichler, W., & Herrmann, A. (1986). Tracer relations in variable flow. *5th International Symposium on Underground Water Tracing. Institute of Geology and Mineral Exploration (IGME), Athens*, 355–360.

10 Supplementary material.

Additional Table 1. Lithological samples.

ID.	LAT	LON	ROCK	TYPE
RX1 / SED.	-33.00145	-70.060317	sedimentary	gypsum
RX2	-32.995583	-70.060483	sedimentary	limestone
RX3	-32.995083	-70.056683	sedimentary	limestone
RX4.1	-32.9954	-70.052017	sedimentary	gypsum
RX4.2	-32.995317	-70.050583	sedimentary	limestone
RX5 / SED.	-33.00125	-70.05499	sedimentary	shale

Additional Table 2. Data for the hydraulic parameterization of the Monos de Agua catchment.

Litholog y	Type	Porosity (%)		Hydraulic conductivity (m/s)		Saturation (m) thickness		Code
		from	*to*	*from*	*to*	*from*	*to*	
Qg (Jr.s)	Rock glaciers	0.1	0.46	0.000006	0.03	1	7	510
Qc	Fans	0.18	0.46	0.00005	0.02	7	12	625
Jk1	Rock outcrop (mountain)	0.1	0.3	6E-05	0.00006	0.1	1	654
Jr.s	Rock outcrop (mountain)	0.1	0.3	3E-05	0.00003	0.1	1	677
Qa	Glacio-fluvial	0.25	0.5	0.0003	0.01	7	12	700

Additional Table 3. Water isotope analysis of groundwater springs and surface streams at 3600m a.s.l..

Source	Date	DeltaO18	DeltaD	D-excess	Tritium (T.U.)	dev
Spring-1	14-Dec-18	-17.29	-129.22	9.092	n-a	
Snow composite	19-Sep-18	-12.93	-97.99	5.426	4.51	0.08
	6-Nov-18	-15.75	-119.06	6.956		
Stream	14-Dec-19	-17.57	-130.42	10.172	n-a	
Stream	14-Dec-19	-17.71	-131.44	10.232	n-a	
Stream	6-Apr-19	-19.83	-148.82	9.844	2.86	0.05
Spring-1	6-Apr-19	-19.11	-143.42	9.484	2.51	0.05
Spring-2	6-Apr-19	-19.48	-146.44	9.384	2.59	0.05
Stream	14-Apr-20	-18.60	-137.40	11.416	1.33	0.15
Spring-1	14-Apr-20	-17.63	-130.57	10.494	1.48	0.16
Spring-2	14-Apr-20	-17.82	-131.77	10.782	2.79	0.17
Snow	14-Apr-20	-22.44	-171.50	8.036	8.21	0.27

Additional Table 4. Gas analysis of groundwater springs and surface streams at 3600m a.s.l.

Site ID	**CFC 11**	**CFC 12**	**CFC 113**	**Ar**	**N2**	**SF6**	**H1301**
Spring-1	3.69±0.05	2.74±0.09	0.42±0.02	0.293±0.006	10.98±0.21	3.32±0.09	9.08±0.17
Spring-2	3.63±0.05	2.8±0.09	0.44±0.02	0.292±0.006	10.74±0.21	3.44±0.09	9.47±0.18

Additional Table 5. Groundwater spring microbial diversity from ASV analysis.

		Spring-1	**Spring-2**
ASVs		1294	929
Unique ASVs		772	407
Shannon index		5.8	5.3
Proteobacteria	Relative abundance %	45.7	63.3
Betaproteobacteriales		33.8	55.1
Bacteroidetes		20.8	14.7
Bacteria and Archaea community		40.4	51.5
Minor/Rare genera <1%		15.9	13.8
Polaromonas		0.2	4.1
Rhodoferax		0.1	9.2
per Phylum	Shared ASV %	63.7	77.1
per '>1% genera'		27.9	41.7

Additional Table 6. Isotope convolution equation outputs. Output concentrations (C_{out}), Exponential to Piston ratio (n) and time range ($\mathbf{t_m}$).

	Concentration	±	Exponential to Piston flow model ratio (n)	±	Mean transit time (years)	±
Deuterium	-135.73	23.54	4.18	1.15	3.98	1.36
Oxygen-18	-18.68	0.70	4.51	1.13	4.58	1.35
Tritium	2.62	1.58	3.83	1.23	5.77	3.45

Additional Table 7. Comparison of $\Delta^{18}O$ with other studies in the area.

	$\Delta^{18}O$ precipitation and surface runoff		
Rodríguez et al., 2016 (springs)	Early	1.070	enrichment
	Late	3.29	
Crespo et al., 2016	Early	-6.42	no enrichment
	Late	-4.00	
Crespo et al., 2020	Early	1.90	enrichment
	Late	3.50	
This study	Early	4.65	enrichment
	Late	4.08	

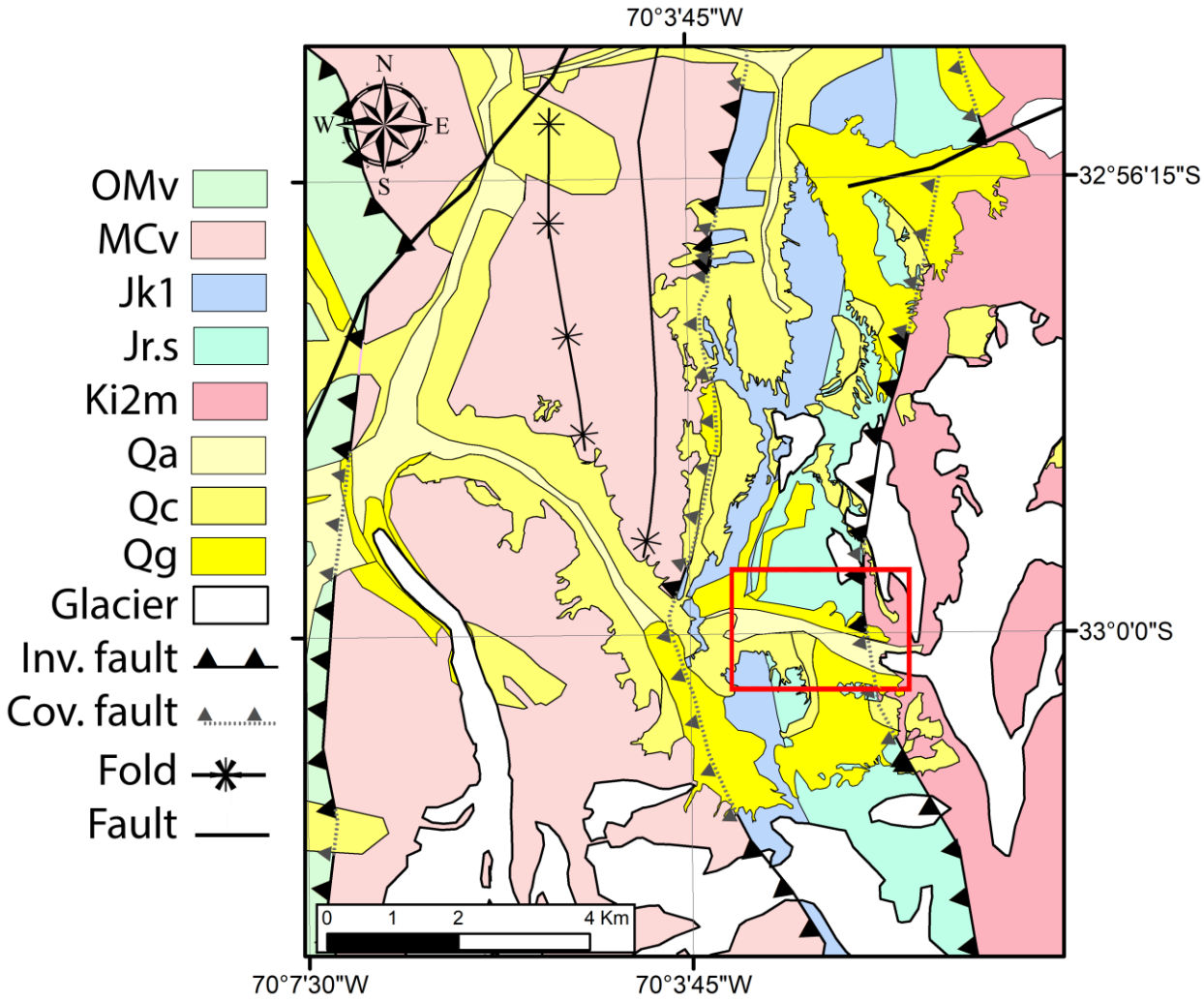

Additional Figure 1. Lithological units at the Monos de Agua catchment. Red square is the upper catchment, study area. OMv is Oligocene-Miocene volcano-sedimentary, MCv is a Lower Cretacic volcano continental with scarce sedimentary intrusions, Jk1.s (blue) is upper Jurassic, Lower Cretacic, marine sedimentary sequences (limestones, lutites, calcic sandstones), Jr.s is Upper Jurassic with gypsum, breccias and red sandstones, Ki2m is Lower Cretacic volcanic and marine sedimentary (Andesitic and basaltic lavas, volcanic breccias, tuff, sedimentary limestones, and sandstones). Quaternary sequences consist of Qa, a Pleistocene-Holocene alluvial and colluvial and lesser fluvio-glacial deposit. Qc represents colluvial quaternary surface transports and Qg consists of Pleistocene-Holocene morainic fluvio-glacial deposits with silt/clay, gravel, and sands.

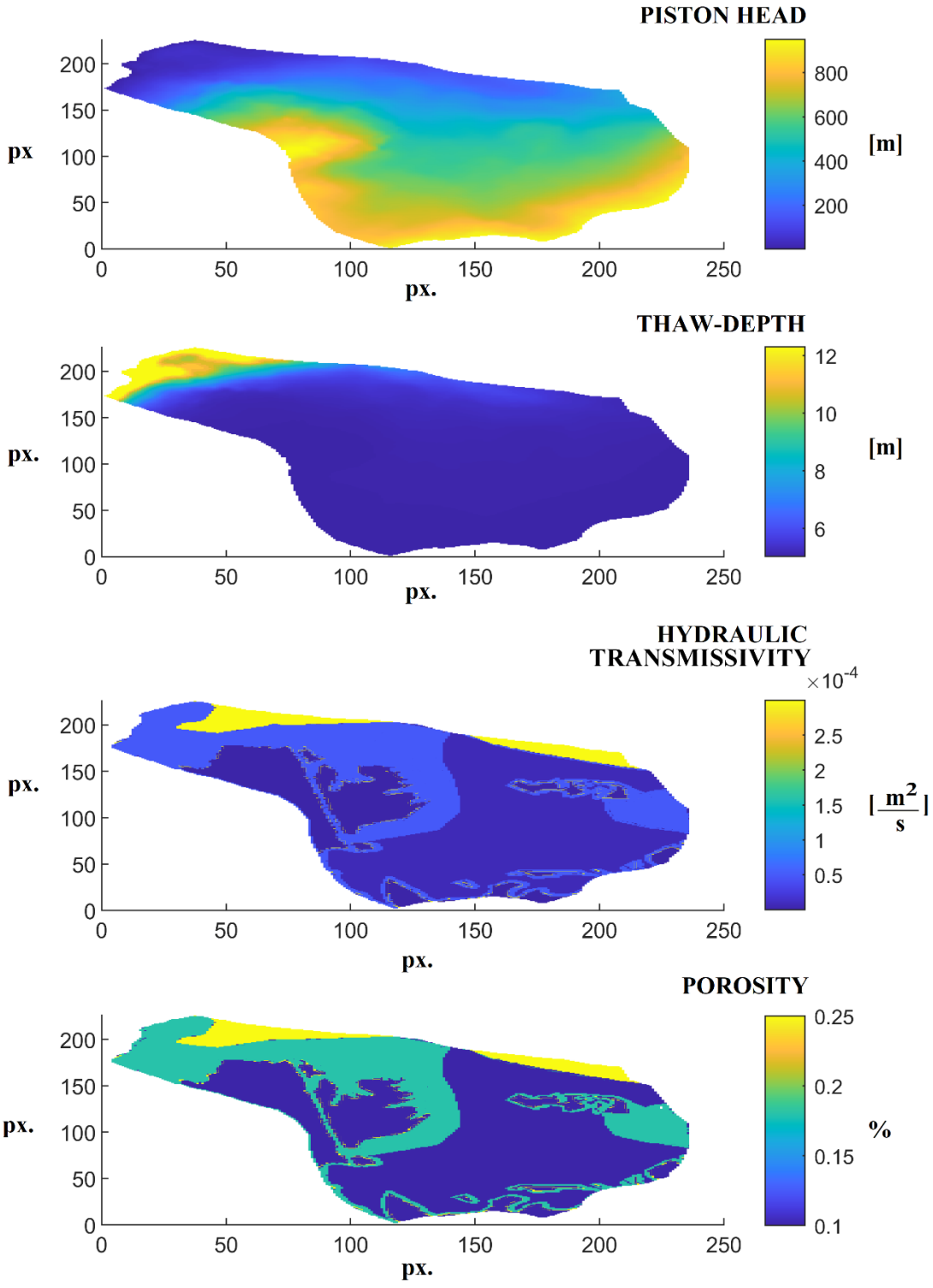

Additional Figure 2. Hydraulic parameters for transit time estimations in the Monos de Agua catchment.

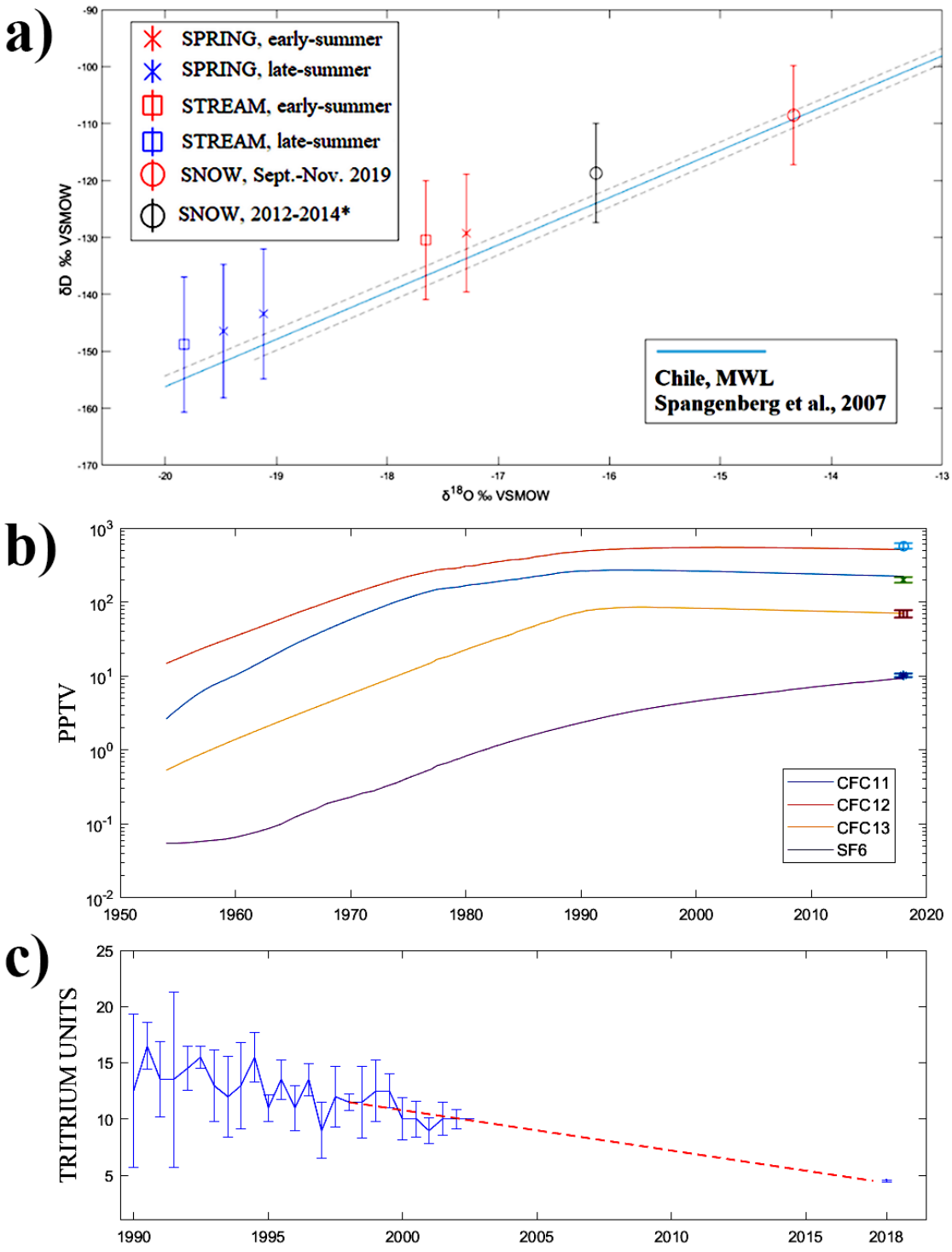

Additional Figure 3. Water isotopes from 'Monos de Agua' catchment and anthropogenic gas levels for Chile. (a) are D and ^{18}O values (2018-2019), (b) are measured samples (marks) for each gas curve time series and (c) is tritium time-series for Santiago, Chile. The red dotted line in (c) represents the theoretical tritium decay level, the last data point is the tritium background level measured in snow samples.

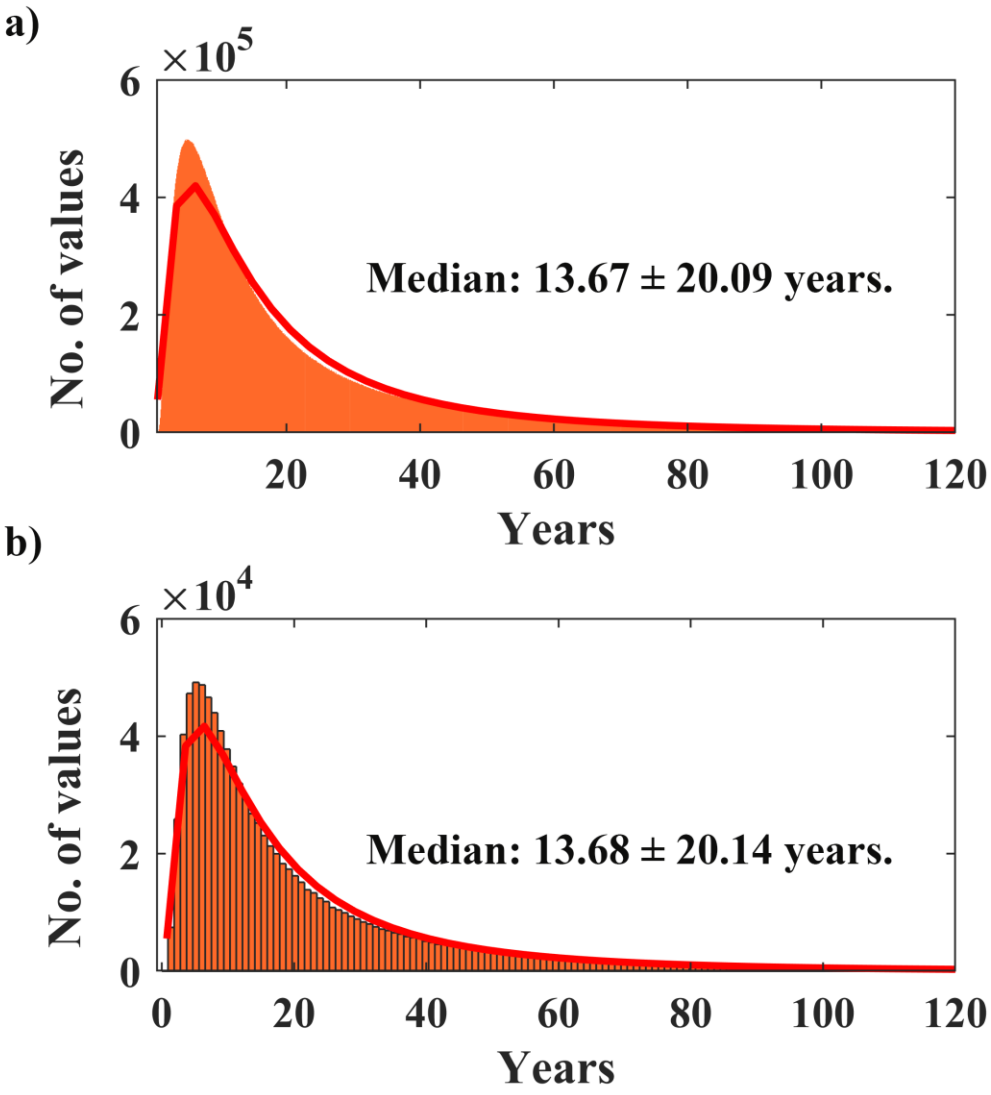

Additional Figure 4. Histogram of turnover times from piston-flow parameterization. Using Equation 1 (a) 1.0e+08 and (b) 1.0e+06 iterations were performed through all parameters within the studied catchment. Values with a transit time above three months are shown since that is the fastest runoff (seasonal flush).

11 Annexes.

	11.1	11.2	11.3	11.4
Type	Scientific article	Scientific article	Scientific article	Scientific article
Status	Submitted	Published	Published	Published
Running title	Mountain cryosphere landscape legislation	Assessment of landscape transformation in protected areas	Glacier decline in the Central Andes (33°S)	Permafrost evolution in a mountain catchment near Santiago de Chile
Journal title	Land Use Policy	Environmental impact assessment reviews	Journal of South American Earth Sciences	Journal of South American Earth Sciences
Year	2021*	2021	2019	2021
Authors	Ruiz Pereira, Alvarado Peterson, Trombotto Liaudat	Ruiz Pereira, Fernández, Herrera, Olea	Ruiz Pereira & Veetil	Ruiz Pereira, Marquard, Beriain, Lambert
Index	WoS	WoS	WoS	WoS
Impact Factor	5.3	4.5	2	2
DOI	-	10.1016/j.eiar.2020.106472	10.1016/j.jsames.2019.102249	10.1016/j.jsames.2021.103293

Land Use Policy

MOUNTAIN CRYOSPHERE AND LANDSCAPE LEGISLATION

--Manuscript Draft--

Manuscript Number:	
Article Type:	Full Length Article
Keywords:	Mountain cryosphere; Landscape assessment; Hydric potential; Central Andes
Corresponding Author:	Sebastian Ruiz Pereira Pontificia Universidad Católica de Chile: Pontificia Universidad Catolica de Chile CHILE
First Author:	Sebastian Ruiz-Pereira
Order of Authors:	Sebastian Ruiz-Pereira
	Voltaire Alvarado-Peterson
	Darío Trombotto-Liaudat
Abstract:	Mountain landscapes bear hydric and biodiversity potential conveyed behind a myriad of land use perspectives. For protected areas, the focal point justifying land use is often the ethical endorsement of legislations. In this sense, if overlapping scales of contingency converge without a common legal ground, we visualize the protection of hydric potential to be problematic. Mountain cryosphere landscapes can be considered both ecosystem and water/ice storage units associated to value transactions and concerns. Hereby, we focused on prerogatives for the legislation of mountain protected areas and examine moral dissonances on the assessment of natural assets. This contingency is framed in the balance between hydric potential and water security of mountain cryosphere at semi-arid regions in the Dry Andes. The land use prerogative was found to be a clash between instrumental/non-instrumental value affecting transaction costs but most importantly neglecting the temporal dimension of landscape evolution. In concrete, as scales of analysis for ecosystem-services (non-use values) and hydrological connectivity (quantities and mechanisms) diverge, protection of landscape cannot be allocated. We therefore recommend a framework solving landscape units apart but under the most inclusive scale to which transaction costs and insurance value estimation remains feasible. This univocal endorsement for a unifying value scale for the protection of landscape potential is pivotal if it remains transposable and adaptable to land use contingencies.
Suggested Reviewers:	Gunnar Þór Jóhannesson Haskoli Islands gtj@hi.is Experience in planning and policy.
	Áslaug Geirsdóttir Háskóli Islands: Haskoli Islands age@hi.is Experience in Quaternary environments and climate change.
	Pål Ringkjøb Nielsen Bergen University: Universitetet i Bergen Pal.R.Nielsen@uib.no Experience in Terrestrial Climate and Environmental Changes
	Helga Ögmundardottir Háskóli Islands: Haskoli Islands helgaog@hi.is Experience in environmental anthropology.
	Aino Kulonen City of Lahti: Lahden kaupunki aino.kulonen@giub.unibe.ch Environmental coordinator, sustainable planning experience.

Powered by Editorial Manager® and ProduXion Manager® from Aries Systems Corporation

Manuscript (without Author Details)
Click here to view linked References

MOUNTAIN CRYOSPHERE AND LANDSCAPE LEGISLATION

[1,2]Ruiz Pereira, S., [3]Alvarado Peterson, V, [4]Trombotto Liaudat, D.

[1]*Instituto de Geografía, Pontificia Universidad Católica de Chile, Santiago, Chile.*
[2]*Center for Climate and Resilience Research, Universidad de Chile, Santiago, Chile.*
[3]*Departamento de Geografía, Universidad de Concepción, Concepción, Chile.*
[4]*Geocryology, Instituto Argentino de Nivología, Glaciología y Ciencias Ambientales, CCT CONICET, Mendoza, Argentina.*

ABSTRACT

Mountain landscapes bear hydric and biodiversity potential conveyed behind a myriad of land use perspectives. For protected areas, the focal point justifying land use is often the ethical endorsement of legislations. In this sense, if overlapping scales of contingency converge without a common legal ground, we visualize the protection of hydric potential to be problematic.

Mountain cryosphere landscapes can be considered both ecosystem and water/ice storage units associated to value transactions and concerns. Hereby, we focused on prerogatives for the legislation of mountain protected areas and examine moral dissonances on the assessment of natural assets. This contingency is framed in the balance between hydric potential and water security of mountain cryosphere at semi-arid regions in the Dry Andes.

The land use prerogative was found to be a clash between instrumental/non-instrumental value affecting transaction costs but most importantly neglecting the temporal dimension of landscape evolution. In concrete, as scales of analysis for ecosystem-services (non-use values) and hydrological connectivity (quantities and mechanisms) diverge, protection of landscape cannot be allocated. We therefore recommend a framework solving landscape units apart but under the most inclusive scale to which transaction costs and insurance value estimation remains feasible. This univocal endorsement for a unifying value scale for the protection of landscape potential is pivotal if it remains transposable and adaptable to land use contingencies.

KEYWORDS: Mountain cryosphere, Landscape assessment, Hydric potential, Central Andes.

1. INTRODUCTION (<700 words).

Desirable states of life imply responsibility hierarchies starting out with decision making that retrieves value, allocates it, and prioritizes concerns on inalienable resources like water. Due to imminent water-scarcity under climate forcing, the security issue has been addressed by *Sustainable Development Goals* (Nino, 2015), specific legislations (Table 1) and IPCC recommendations (Hock et al., 2019, p.157).

Mountainous environments are hence important, as they often constitute water towers (amidst dry regions) that currently supply global substantial water demands (Viviroli & Weingartner, 2008; Immerzeel et al., 2010) by generating runoff downstream and having storing/buffering capacity (Pfeffer et al., 1991; Immerzeel et al., 2020; Stigter et al., 2021). In specific, mountains may delay or speed up stream (Trombotto et al., 1999) groundwater discharge in frozen ground areas (Evans et al., 2015) even dominating dry season streamflow by contributing from fractured bedrock aquifers (Somers et al., 2019).

It is in this sense, mountain cryosphere (solid water structure) represents landscapes with hydric potential (Lepeška, 2010) entangling utilitarian perspectives (of land use) with their intrinsic value dimension (Nordstrom, 1993), comprising biodiversity and non-use value (Bullock, 2017, p. 8-11) predominantly representing protected areas worldwide (Kollmair et al., 2005). Hence, if we address protection of natural assets as an optimal management in land-use, we also refer to their potentiality, which may increase their future value upon widespread scarcity.

Nevertheless, conceptual disagreements persist in protective endorsements as, on one hand, resource use-value is inherently tied to the ecosystem functioning itself (Therme, 2014) and on the other, the exchange-value reflects underlying social relations (Sweezy, 1968) and "social arrangements" (Mill, 1994, p.54) which lie beyond "value-in-use" (Von Wieser, 1893, p.3) and then relate to subjective valuation. The problem is when certain object increases or decreases its value (potential of use) without defining valorization timescales and a decision-value to be addressed within a present-day legislation.

In this sense, whether mountain cryosphere's potential changes lie beyond the scope of present-day legislative efforts (Table 1), could be a matter of scale compatibility between landscape dimensions (Table 2) under atmospheric forcing, shaping objects of analysis and rendering scaling procedures sub-optimal (Adler, 1997).

The aim of this study is to highlight the importance of mountain cryosphere impacts and procedural shortcomings in their protective/management framework. The discussion deals with particularities of glacial/periglacial environments affected by the presence of ice-rich frozen ground, decadal groundwater regime? flows and hence relevant for protection and the consideration mountain landscapes as areas with strategic water supplies often overlapping both conservation and mining interests.

We first examine the context for transformation processes in mountain cryosphere landscapes observing different value regimes, and secondly, look at the inherent complexity of their value evolution. In specific, discuss on the hydric potential a region, and then discuss key processes for its mountain cryosphere protection under sustained atmospheric forcing.

Table 1. Climate change and cryosphere regulations (Source: Grantham Research Institute on Climate Change & the Environment, Observatory for the Climate Change Law in Chile).

Country	Type	Cryosphere protection	Name	Year of appearance
Austria	Law	Not included	37th Federal Law for Climate & Energy funding	2007
Argentina	Law	Glacial and periglacial environments	Law 26639, "Minimal budgets for preservation of glaciers and periglacial environment"	2010
Austria	Law	Not included	106th Federal Law on Climate Protection	2011
Iceland	Passed	Not included	Act 70 on Climate Change	2012
Chile	Strategic plan	Included	National Climate Change Adaptation Plan,	2014
Peru	Law	Mountain environments and glaciers	Law N° 30754 on Climate Change	2018
Iceland	Strategic plan	Glaciers mentioned	Iceland's Climate Action Plan for 2018-2030	2018
EU	Regulation in force	Not included	Regulation 842	2018
EU	Strategic plan	Arctic and Boreal environments are mentioned	A Clean Planet for all	2018
Argentina	Law	Glacial and periglacial environments	Law 27520, "Minimal budgets for Adaptation & Mitigation to Global Climate Change"	2019
Chile	Law project	Not included	Climate change framework Law	2020
EU	Strategic plan	Indirectly mentioned through reference.	Forging a climate-resilient Europe - the new EU Strategy on Adaptation to Climate Change	2021

Table 2. Summary of landscape analysis. Adapted from Sauer, 1963.

Aspects of landscape	Description
Comprehensive view of nature and culture.	Interaction of natural and/or cultural factors.
Internal vs. External perspective.	Area, as perceived by people.
Historical retrospection.	Balance loss, fragmentation destruction, or transformation of landscape units.
Forms and processes.	Action and interaction, Human factors.

2. METHODS (300 words)

First, we downscale our concern for mountain cryosphere hydric potential in the Andes at important basins in Chile above 2300m ASL (altitudinal median plus deviation of all catchments) representing periglacial and/or glacial environments. A rough estimation for instrumental potentiality of a considered annual peak discharge and catchment area as inputs for *Landscape Hydric Potential* (Lepeška, 2010; Wałęga et al., 2020) is made. Using databases for catchment runoff and attribute information (Alvarez-Garreton et al., 2018), and clustering by k-means (Carvalho et al., 2016; Zeng et al., 2020) and PCA (Ballabio, 2015) processes, we obtained estimates of altitudinal hydric potential per area are covering over 4000 km from north to south in the Chilean Andes.

Secondly, we analyze overlapping dimensions in environmental protection for land use. We use a perspective of value and utility, intending to unravel the timescale complexity for environmental protection purposes both for instrumental and non-instrumental uses on mountain cryosphere. This considers the fact that headwater catchments generally coexist with protected areas. Therefore, land use of protected areas ranges from conservation prerogatives rescuing the intrinsic value and marginal utility of biodiversity as well as the hydric (landscape) potential of glaciers and permafrost related features under climate variability affecting ice as a future resource.

We propose that the problem deals with analytical incommensurability, as management options (transforming value) (i) cannot be compared (ii) lack a particular scale and/or (iii) the scaling procedure is sub-optimal (Adler, 1997). This issue also coincides with the fact that expectations cannot be adequately expressed as a single end, but only as a hierarchy of ends (Hayek, 2001, p.60).

Finally, examples on hydrological relevance of headwater catchments and mountain cryosphere are interpreted to deliver insights on the evolution of landscape environmental protection in Argentina and Chile. The areas covered the “Mendoza River” in Argentina and the “Juncal Park” within the “Juncal River” sub-basin, around 33°S at Mendoza (Argentina) and Aconcagua (Chile) river basins. We also discuss about protected areas around 42°S in Argentina.

3. Changing mountain cryosphere environments.

Millions of people depend on freshwater provided by mountain cryosphere along the Andean mountain range (Barnett et al., 2005; United Nations, 2013), prone to systematic insecurity in terms of food resources (Wutich, 2020) and physical/economical water scarcity (Mancosu et al., 2015). This uncertainties cover environments under sustained glacier decline like the Andes mountains between 10-56°S (Dussaillant et al., 2019), where permafrost (perennially frozen ground) is also subject to degradation in some regions (Liaudat & Bottegal, 2020; S Ruiz Pereira et al., 2021; Trombotto & Borzotta, 2009).

Additionally, at glacierized catchments in the low-latitude Andes of Bolivia (Frans et al., 2015) and Peru (Polk et al., 2017), peak water has been reached for 82-95 % of the glacier area before 2019. In contrast, at the Chilean Andes around 33°S, a consistent glacial retreat (Bown et al., 2008; Ruiz Pereira & Veettil, 2019) projects catchment runoff decrease in future scenarios (RCP45 & RCP85) starting the year 2021 (Ragettli et al., 2016).

Furthermore, the Central-Southern Andean region (30-48°S) presented a declining precipitation trend over 1960–2016 (Boisier et al., 2018) and expects a snowpack loss of up to 75–85% by the year 2100 (Bozkurt et al., 2018). This becomes relevant as snow-dominated catchments over the Western Andean Front (30–35°S) may have a larger groundwater contribution to streamflow than pluvial basins (Alvarez-Garreton et al., 2021) with a surface warming expected to reduce snow cover hence increasing glacier and permafrost retreat (Baraer et al., 2012). An earlier snowmelt (seasonal contraction under lower available energy) would substantially vary depending on regional climate, elevation and soil properties (Musselman et al., 2017), affecting hydrological connectivity in snow dominated catchments. Another important factor in a warming climate is increased evapotranspiration, which may shift the precipitation fraction that runs off as surface water or infiltrates to the subsurface as recharge (Condon et al., 2020).

Consequently, at higher altitudes there would likely be a more preponderant role of frozen surfaces involved in infiltration processes (formation of aquicludes and aquitards), which are elements often outside impact assessment baselines. However, periglacial environments in the Chilean Andes are still neglected of legislation acknowledging them a role in the hydrological cycle, thus simply reducing the contingency to overall runoff (Table 3) and omitting the mechanistic complexities occurring at different timescales. For example, long-term resilience implies coping with precipitation deficits (Keys et al., 2019) which requires considering precipitation–recharge relationships essential for reliable predictions of impacts and adaptation strategies(Cuthbert et al., 2019a *global resilience*).

Table 3. Hydric potential of high-altitude catchments in the Andes (> 2303m ASL). The median streamflow (Qmed) and mean absolute deviation (m.a.d.) are shown after k-means and PCA clustering processes.

	Q_{med}	m.a.d.	Area	m.a.d.	Mean elevation	m.a.d.
K-MEANS	50.84	15.00	2112.50	1253.90	2865.42	373.46
	5.24	2.26	1874.11	2092.42	3105.33	353.14
	22.20	4.43	1249.14	455.53	3184.07	257.40
	0.61	0.69	981.57	3725.22	3631.83	569.96
PCA	2.17	7.48	1111.60	2492.04	3169.48	378.50
	0.36	0.32	1202.22	4521.04	4300.32	408.45

Nevertheless, groundwater partitioning is still unknown in arid basins (Gleeson et al., 2016; Cuthbert et al., 2019b) as groundwater in (currently) hyper-arid regions may have been recharged when a wetter climatic regime prevailed in the past (paleo recharge) (Cuthbert, *et al.*, 2019a) in contrast to settings with more recent recharge. Hence, we deem that groundwater flow balances in water scarce regions do not account groundwater recharge and storage (water table) long-term evolution and consequently the resilience to depletion is uncertain.

Therefore, robust assessments of the impact of climate change on hydrological drought aiming at estimating "groundwater responsiveness" (Van Lanen et al., 2012) are obviously necessary for long-term planning but also for understanding the current trends. Consequently, we recognize temporality as an overlooked dimension within the complexity of hydrological potentiality inherent in mountainous, snow-dominated landscapes of the Andes.

4. Hydric potential.

Environmental protection is bounded to mechanistic gaps of hydrological connectivity, unequivocally inherent to the hydric potential of headwater catchments (Table 3). For example, even though atmospheric forcing is attested in semi-arid, snow dependent areas, groundwater thermal evolution is neglected in a temporal dimension for protection, even though many areas of the Andes represent coexisting volcanic and cryosphere settings accounting high altitude marshlands in extremely arid areas. Andean countries often meet mountain borders with transboundary aquifers therein; raising the issue of asymmetrical assessments as one country monitors and understands the aquifer evolution while the other border neglects that concern, or the concern is under private assessment such as mining.

Nevertheless, the first appraisal of natural areas is as landscape, ensembles of mostly visual (surface) information. Therefore, we talk about landscape, since it is overall an "average citizen" appraisal and value retrieval of mountain cryosphere settings, not a hydrogeological or technical in ecosystem service perspective in the first place. Then, after a value has been proposed (following a hierarchical, reference-based prioritization), efforts are made to understand multi-dimensional impacts – e.g., hydrogeological, geophysical assessments/surveys integrated to impact assessments. The technical constraints for assessing (and perceiving) periglacial environments are that sometimes cryosphere elements lie outside legal definitions (Water Code of Law or specific laws) or remain as off-surface elements (interstitial or ground ice) (Trombotto Liaudat et al., 2014), slope-dependent hydric bodies (protalus ramparts) with a restricted, isolated distribution and attestable only by fieldwork.

This is one plausible reason why protected mountainous areas faces problems of technical insufficiency, producing inadequate sustainability planning. This issue is rooted in a sort of analytical "estrangement" from inadequate (static) baselines under "landscape as a mere viewshed" guidelines within Environmental Impact Assessments; avoiding a proper differentiation for several types of economic transformations and conservation management (Ruiz Pereira et al., 2021a) which are necessary to understand the evolution of its value. In specific, protecting mountain environments entails different (value) dimensions of concern: water resource protection (consumption, utilitarian, human right), biodiversity (intrinsic value) and landscape protection (non-use values, intrinsic value). Nevertheless, if *water-security* implies inter-scale analysis (Bakker, 2012) and additionally, as a concept does not have a univocal moral philosophy procedural framework as discussed by (Cook & Bakker, 2012), it might fail to optimally cover the optimal scope of protection.

Attempts to overcome this issue in the New Zealand Resource Management Act of 1991 defined intrinsic value in relation to ecosystems and their constituent parts, including their biological and genetic diversity and the essential characteristics that determine an ecosystem's integrity, form, functioning, and resilience (Nordstrom, 1993). This dimensionality considers that profit can emerge from value transactions of hydric potential but also the biodiversity and non-instrumental potential for a given landscape unit. Nevertheless, the scale convergence is what we assume here as a latent (quiescent) constraint affecting landscape value allocation.

5. Landscape protection

The prerogative for protections can be rooted in integrated plans for water resource management in the United Nations Framework Convention On Climate Change (United Nations, 1997, p.11), revitalized through the Paris Agreement endorsement for future responsibility. Nevertheless, when analyzing global endorsements such as *Sustainable Development Goals* (Griggs et al., 2013), it is apparent that even concepts like resilience and sustainability are even used interchangeably (Elmqvist, 2017; Elmqvist et al., 2019), which would ultimately consider metastable systems as stationary, and not a hydroclimatic dynamic instead.

Landscape appreciation in protected regions often relates to perception-based valuations of aesthetic value (Schirpke et al., 2016), remaining relatively detached from the temporary changes in society (valuation timescale) as symbolic representations of non-artificiality or non-interference (Figure 1 & 2). Hence, it is the government predicament to guarantee this sort of idealized "permanence" of unspoiled nature. Nevertheless, intrinsic characteristics of many nonliving objects, as well as living objects, are inextricably linked to their mobility and growth, requiring an understanding of the boundaries of complex systems and the linkages and flows into and from these systems (Nordstrom, 1993).

Nowadays, the complexity of scale incompatibility for a future legislation of land use in protected areas with hydric potential is rooted in the framing of scales describing the structure of concerns, which later require technical closure for further apprehension of correct baselines. In contrast, until the beginning of the 20th century most of the (alpine) mountain peaks did not have names it was common to describe the borders of alpine pastures with neighbors, cardinal points or mountain peaks (Bütler, 2007).

Additional repercussions on the protected landscape/individual interaction may even consider physical, artistic, and psychological attributes of the landscape (Albrecht et al., 2007; Otero Pastor et al., 2007) but as we mentioned also the buffering capacity of the hydrological systems in many watersheds that may increase impacts and risks on urban areas (Breuste, 1985; Breuste et al., 2013). In this sense, the concept of *landscape balance* (Landschaftshaushalt), if implemented for any order of magnitude (Volk & Steinhardt, 2001), requires scale compatibility to be the leading thread in assessing landscape as a unit.

On the one hand, aesthetic landscape character, within the cultural historical enclave that is currently lived, and consequently, water resource protection considering the benefit (potential) of headwater catchments as recharge zones. This is a premise behind the "water tower" concept (Viviroli & Weingartner, 2008) of mountain cryosphere that stresses the inalienable necessity for certain resources.

Examples for such protected areas are Nahuel Huapi (created in 1922, 41°′S; 71°30′W) and Los Alerces (created in 1937, 42°48′S 71°53′W) national parks in Argentina, that currently endure unsupervised impacts as consequence of unplanned (human) occupation. Further north, near the city of Mendoza (Argentina, around one million hab.), the creation of the "Provincial Park Cordón del Plata" ensured the protection of

mountain permafrost and rock glaciers, which are cryogenic indicators of underground ice, little known for their hydrological importance. The park also protects water recharge areas, glaciers *sensu stricto*, flora and fauna of the Andean tundra (File No. 8372 / C / 9930091,Trombotto et al., 1999). Here, one prerogative is not only about protecting cryoforms such as rock glaciers, protalus ramparts or cryogenic sedimentary slopes, but the entire periglacial environment of the upper hydrographic basin that is being transformed by environmental changes and the climatic variability.

In Chile, the "Andino Juncal" park (33°S; 70°5'W) is a private property since 1911, used between 1970-2000 for cattle raising and decreasingly mining. It currently constitutes a conservation project facing transformative pressure (Figure 1 and Figure 2-b) due to current surrounding (within the Park's viewshed) mining activities as cement private companies have extraction rights and built roads to sites. By the year 2003, the park's owners decided to prohibit any exploitative activity in their property and by 2010 a RAMSAR site (Number 1909 at 32°55'S 70°03'W) within the park was designated.

Resources in this protected area are hydric resources (glacierized, permafrost affected catchments) and mountain biodiversity (mountain lions, guanacos, foxes, and marshlands) (Figure 2). The Park's management stated in the Environmental Impact Assessment declaration (2006-2007) a useful-life span of twenty years for the "sustainable tourism" project.

In cases of National and private parks, underestimated impacts deal with notions of protection and insurance, as parties benefiting from natural value loss as exogeneity and endogeneity of risks link governance to insurance value and its provision (Paavola & Primmer, 2019). For example, biodiversity providing natural insurance to risk averse users of ecosystem services or financial insurance to hedge their income risk (Quaas & Baumgärtner, 2008).

6. Landscape transformations.

In the Central Andes of Argentina-Chile, we addressed that high altitude catchments associated to mountain cryosphere do represent an important input for dry regions. In them, rock glaciers reach upper valleys influencing downstream flows and potentially constituting excellent aquifers (Trombotto-Liaudat et al., 2020). Nevertheless, regional atmospheric warming is deepening the permafrost table, altitudinally shifting the air isotherm 0° C, enhancing ice-rich permafrost degradation (Trombotto & Borzotta, 2009; Liaudat & Bottegal, 2020).

Such transformations pose challenges for mountain landscape assessment in a value perspective. For example, production in terms of use/exchange values assume any process of technological transformation under nominal value (Lefebvre, 1991, p.120). However, some dimensions of landscape (experiential) could establish productive scheme countervalues from dilemmas of collective heritage or common goods in terms of property right allocation at mountain landscapes, when one value dimension overshadows other land use possibilities (e.g., conservation). Furthermore, if sustainable development discourses become increasingly chimerical, the concreteness of a society-nature relationship will end up with the fabrication of value with imponderable degree of uncertainty.

For the case presented, as mountain cryosphere gradually becomes scarce, it (nominally) increases its natural value. Yet, if resources are valued in terms of an "unspoiled character" (conservation), as Krutilla, (1967) noted, the depletion problem of providing present and future amenities faces the inadequacy (market failure) to account on provision itself. For example, as scarcity is a pervasive aspect of human life and is a fundamental precondition of economic behavior (Lynn, 1991), its source could be framed as the capacity of an ecosystem to sustain the flow of a (hydrological) service (Batabyal et al., 2003).

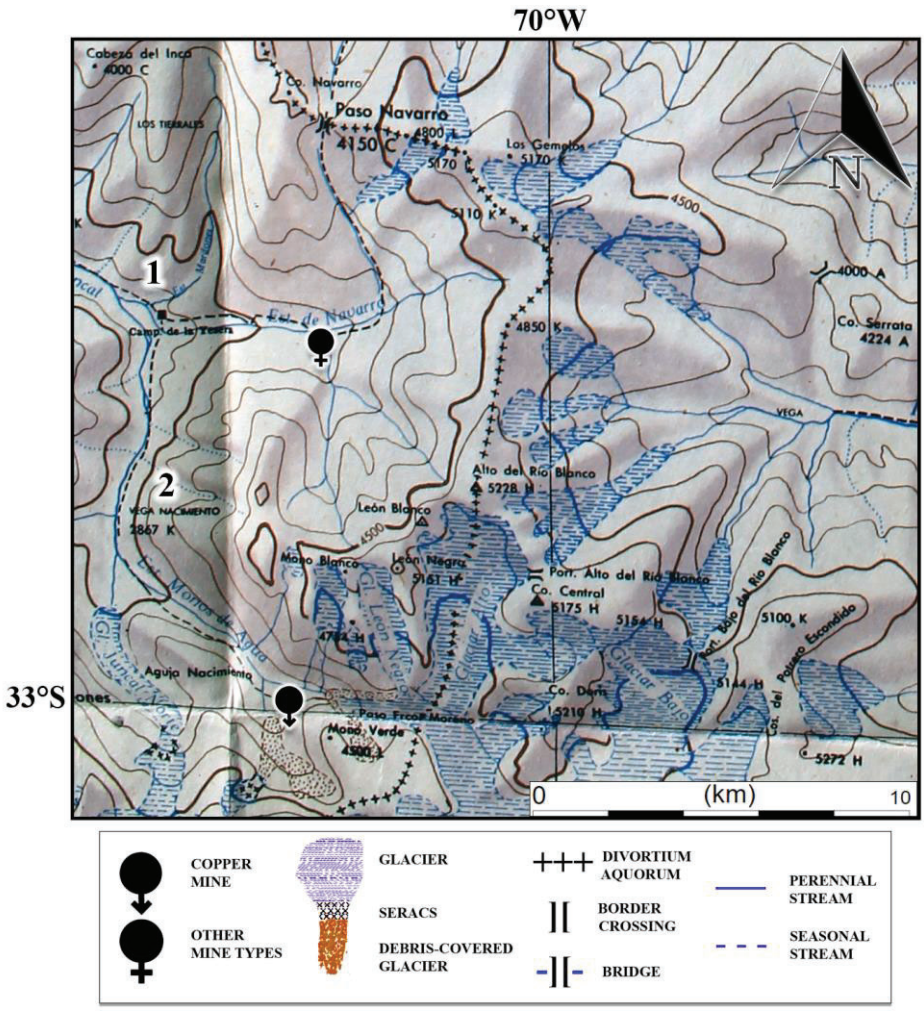

Figure 1. Mountain protected area in the Chilean central Andes. Adapted from Lliboutry, 1956. (1) is the "Juncal Andean" Park's entry point and (2) is the RAMSAR site (No. 1909, 2010).

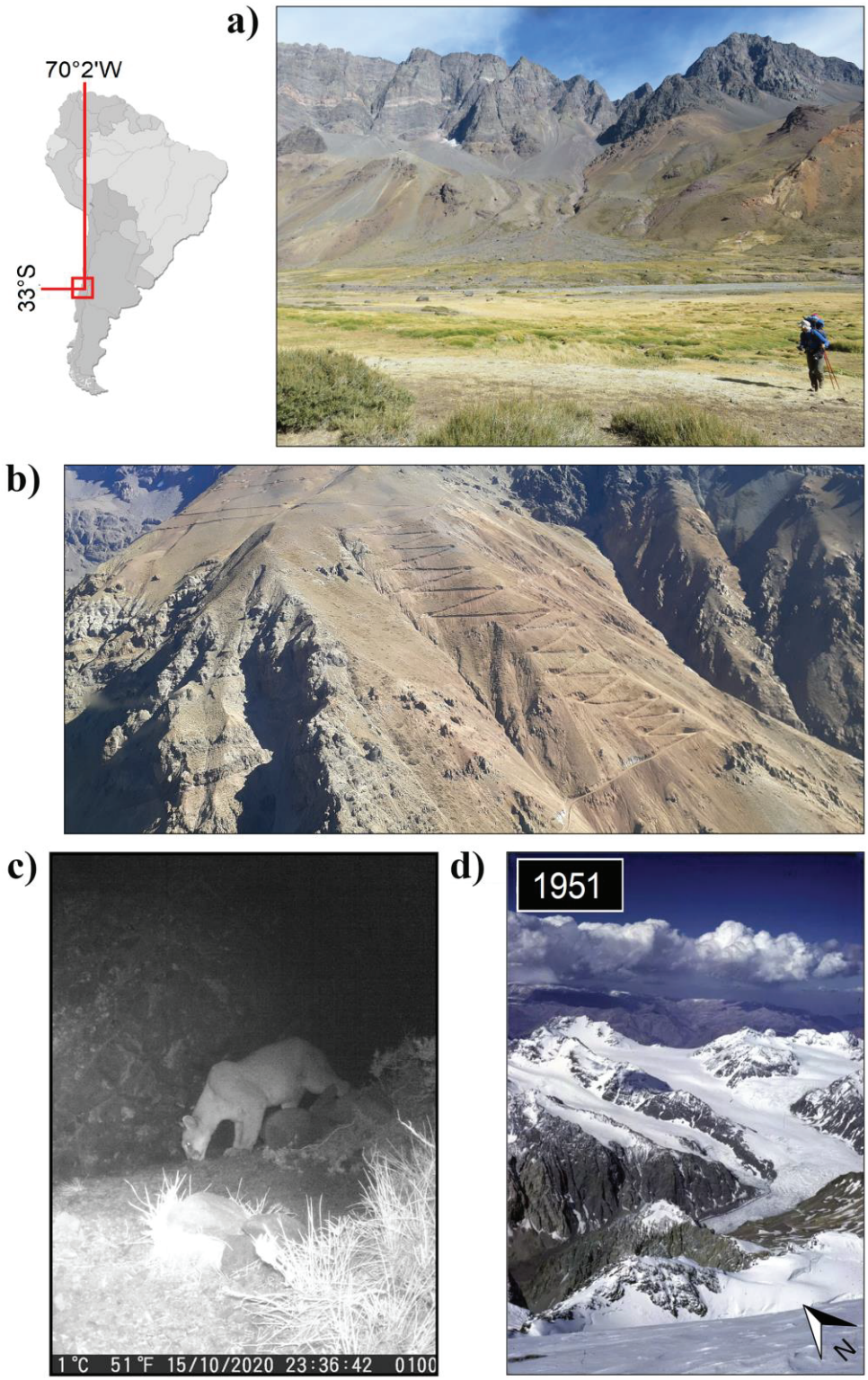

Figure 2. Intersected dimensions of landscape appraisal in the Central Andes of Argentina/Chile. (a) is RAMSAR site (b) is aerial photograph of mining activity within the viewshed at "Juncal Park" (33°S). (c) is a *Puma concolor* image from trap-cameras within the park and (d) is a 1951 photograph (aiming at North-East) of the Chile/Argentina border at 33°S taken by E. Meier

But the problem is that some resources (framed as ecosystem services) have a latent potential, for example groundwater baseflow, it may become preponderant at a given time soon due to the same forcing agent rendering hydric provision scarce and scarcer. Additionally, one problem in central legislative outlooks is that impacts will not exert the same effect at equal spatiotemporal scales, hence centralized normative apparatuses do have this challenge as well.

In specific, upon statistically consistent drought trends in the Central Andes, available groundwater systems responsiveness can or cannot be enough to sustain a provision capacity at different scales. The object under protection then constitutes a dynamic (metastable) configuration, surpassing a reduced definition of landscape content as well as the synthetic aggregation of its results, which, if subdivided into partial systems, can be investigated with sufficient accuracy (Haase & Richter, 1983).

Additionally, if hydric potentiality (value) evolves and is reallocated to another item (cryosphere element), then this prioritization issue should aim at the hydric capacity for provision instead of aiming at a fixed, static element. Also, by reallocating value, a risk reallocation also occurs, and the issue engages the insurance value of natural assets and "integrate it into the disaster risk management agenda" (Bauduceau et al., 2015). Upon transformations, any idea of "insurance" fundamentally refers to (i) objective risks in terms of different possible states of nature, (ii) the decision maker's subjective risk preferences over these states, and (iii) a mechanism that allows mitigation (Baumgärtner & Strunz, 2014) relating to the idea of a future water insecurity (Wutich, 2020).

The problem with a subjective valuation of hydric potential is due to its condition of an inalienable resource, which should in fact, be more connected to a distribution of concerns, a range of value estimates spanning from sub-systems rather than a univocal non-instrumental estimate. Furthermore, the issue with privileged (government or private) information allocating marginal utility to inalienable assets is also a focal point of ethical discussions that ultimately befall on property rights. Simply put, the depletion of hydric potential is irrevocably a driver of utility and therefore a forcing agent of its present-day protection. The issue encircling such transformation of concerns is in our opinion, a problem of conceptual gaps connecting value appraisal in terms of a functioning process, a service, within the limits of a certain area from where the notion of landscape emerged.

7. **Epistemological inadequacy**.

The "reality" of nature deals with the challenge of being knowable through culturally coded concepts (Benediktsson & Waage, 2020). Hence, it is always sustained on debatable grounds of ontological and epistemological realism as analytical scales are often inadequate, absent, or incompatible.

We mentioned that analyses modifying natural value, usually face scale incompatibility when assessing water security (hydric resource related risks), falling short when assessing overlapping dimensions in one object. This can be distinguished from methodological incommensurability, according to which there is no common measure between (types of) accumulative knowledge as (theory) comparisons are sometimes a matter of weighing historically developing values, not following fixed, definitive rules (Sankey & Hoyningen-Huene, 2001, vii-xv). This may not be a problem of equivalence as long as relevant goods meet (scale) particular standards (Anderson, 1995, p.55) and relate to the ordinary use of a unitary scale and the claim of commensurability (Sunstein, 1994, p.834-835), even though nothing but partial scales of value exist under a hierarchy of ends as a comprehensive scale of values (Hayek, 2001, p.60).

These inconsistencies can be explained by noticing that some approaches require an increase in "verisimilitude" and may reject characterizations by emphasizing changes in ontology (Oberheim &

Hoyningen-Huene, 2009) refining the older ontology instead. This is a complex challenge as legal objects have an identity in bulk epistemological ensembles whose conceptual analogs can either fail to preserve the conditions of application or to reproduce inferential relations, leaving the adequacy of potential translations unidentified (Carrier, 2001). It is in this regard that a scale divergence may cause equivocal endorsement of legislation undermining cumulative knowledge as scientific theories, and other cultural artifacts are incommensurable - i.e., (as a first approximation) and can only be evaluated from within particular (and temporary) paradigms (Siegel, 2001).

Then, one option is guiding decision-making processes through a cross-scale approach serving the best interests of all those in the river basin terms of transaction costs (Perry & Easter, 2004) in a hydrological-scale focus. Additionally, incorporating transaction costs, as well as abatement costs, will bring in normally ignored issues by basing policy instruments on practices or some other easily observable factor (McCann, 2013). However, the problem is that empirical analyses for baselines and impacts often misvalue such transactions, for example, within Austrian value theory, value is strictly understood as a term that reflects a subject's ranking of particular goods and can only be depicted as an ordinal scale (Olbrich et al., 2015). Importantly, value theory concerns dispositions of the individual as the economic subject earnings conform to a certain permissible level of needs (Morgenstern, 1934, p.437). In this sense, we deal with a non-static baseline which requires the inclusion of a "permissible" timescale of appreciation and utilization within the temporal grasp of utility and containment of value.

8. Land use and metastable resources

For impact assessments and decision-making, the temporal scale issue is evident when considering that system evolution is an evolution of its use. To maintain mountain landscapes as aesthetically attractive, land managers and policy makers have to cope with both present landscape transformations and the effects of former land-use changes (Schirpke et al., 2016). Hence, when addressing preservation, we often refer to an ideal (optimal) management), detached from undesired, land use.

The problem is then how current legislations include the valuation of components, as well as their organization and perceptions of permanence and change (Green, 1995), necessary to surpass the uncritical acceptance of landscape stability and understand realities (Bailey, 1997) modified to obtain natural resources (Sauer, 1925). Stability is often brought by the naivety of impermanence and not including internal processes (and depletion) of hydric potential within landscape if the regular normative is abided. Nevertheless, indirect measures approaching environmental protection require a determined fixed moment to occur. For example, the expansion of risk assessment scope may determine that it is "necessary to adopt an appropriate landscape scale ecological paradigm" (Landis, 2003) to address the legislative urgency. In this sense, the problem may well not be the actual scale of the issue but the scale of decision-making process as it depends on transaction costs and moral hazard as well.

Such problems emerge from a equivocal predicament of landscape in the sense of *omne ignotum pro magnifico*, it is to say the importance or difficulty of the unknown is exaggerated, an ontologizing overestimation of the object sphere of reality (landscape as an "entity") and a grossly overdrawn pretension of totality (Haase & Richter, 1983). Hence, a common thread piercing through the ontological disparity could be merging interactions and dynamics of ecological systems at temporal and spatial scales (Landis, 2003) but only as far as contingencies are limited by the feasibility of concrete solutions.

The issue of concern, protection, is finally nested causalities (of all overlapping dimensions) embedded in a metastable organization. For example, a RAMSAR marshland life span includes several generational cycles of biological renewal which could be genetically tied to a same original biodiversity bloom. At the same time, the whole marshland ecosystem within a viewshed coinciding with a hydrological watershed, includes a perpetual prerogative for the protection of its hydric potential. Therefore, a functional hierarchy appears, guiding the observation and characterization of the system subject to a theoretical depreciation, and extrapolation towards its null potential.

9. Unifying landscape values.

The temporal dimension of landscape changes is approached by guidelines and legislations (Table 1) but in concrete, it does not engage an objective measure (scale) of change. One possibility is addressing hydric potential (Table 3) as a hydrological capacity of a system, which encloses sub-dimensions of complexity (Table 2) as overlapping concerns but also subject to the reallocation of value (potential) as exogeneous forcing sets in and rearranges elements of modifies the current dynamic. For the case presented, mountain cryosphere elements have a hydric potentiality (value) at certain catchments which can be modified (reallocated) from one item to another (cryosphere element) throughout a myriad of baseflow components.

This initial value appraisal for analyzing future changes assumes a value triangulation (hydric potential, biodiversity, non-use value) (Figure 2) intersected by legislative premises (technical concern) altering transaction costs and marginal value in protected areas according to priorities of land use. This relates to framing environmental protection concerns within the scope of familiarity, "going toward" the phenomena, alluding a proximity of thinking in the process to surpass the methodological insufficiency. Here, familiarity is not only an experiential proxy of epistemological retrieval, but a way of dealing with commensurable precaution, which by affecting natural value will affect the urgency of (water) security in our case.

This link for convergence needs to reside within predictable thresholds, however, this reductionism obeys a logical necessity to find a timescale of critical concern which could be related to ecological thresholds not only assessing shifts in system variables but also its parameters (Horan et al., 2011). The issue is that thresholds of water scarcity may or not be equalized with subjective value transactions for local or non-local users. Hence, for example, to operationalize the insurance value concept in ecosystem management/restoration, the rights and obligations of ecosystem service users and providers need to be clearly defined and transaction costs must be low (Unterberger & Olschewski, 2021). Then, the problem is that the shareholder value focuses on market value equity as the central measure of management purposes and therefore requires a method to value equity (Olbrich et al., 2015).

An additional issue arises from the monistic theory of value, with hedonist approaches to transactions of subjectivity as experiences cannot be reduced to mere satisfaction (the present day) because natural value also possesses undesirable potentiality (Anderson, 1995, p.127), resource depletion. As we said, a hydric potential does require including the "risk potential" of natural disasters as well and justifies the notion of "insurance". This affordable-risk situation of humans in a landscape necessarily calls for revisiting a natural-anthropogenic compatibility principle, identifying characteristics of succession prediction (Milkow, 1973). This is a revision (for the prediction) of desirable states which are inexorably bound to management options.

For example, changes in streamflow, baseflow and hydrochemical components affecting mountain water quality (Trombotto-Liaudat et al., 2020; Sileo et al., 2020) require hydrochemical mapping, not only

necessary in protected areas, but also for areas with mining potential to know and guarantee the potability of regional water supply. Downstream, water consumers can be affected by their land uses as they both either, add up mineral content (mining operation) or do not purify a natural inadequate solute composition. Then, both dimensions of land use affect operational costs of water supply as the inalienable resource engages shared decision-value and transaction costs in a coinciding hydrological boundary (e.g. sub-basin).The scale compatibility for resource use and consequently protection should finally be questioned priorly in order to avoid legislative contradictions (conservation/exploitation) regarding land use.

The full overview of the problems arising from the inclusion of time in economic theory and the ways to solve them, also requires a separate treatment of the time dispositions of the entrepreneur (Morgenstern, 1934, p.458). on the one hand, neo-classical equilibrium properties explain pricing on idealized capital markets if all market participants have homogenous expectations, are rational and risk-averse and cannot influence prices (Quaas et al., 2019). In contrast, approaches like Future Earnings Method are framed in decision-making rather than "market price" and additionally, assesses risk within the decision field of risk analysis instead of the "risk prime" as in insurance value assessments (Olbrich et al., 2015). Hence a combined perspective of natural insurance value (Augeraud-Véron et al., 2019) that frames management in terms of optimal needs and is complimented by subjective valuation theory, could unveil risks affecting value and hence the transactions for its preservation.

Overall, cryosphere as ecosystem and water/ice storage units associates to value concerns (Table 3) as the potential of mountain cryosphere in the water security context. This has been the approach made by legislative framework (Table 1) addressing potential impacts on glacial/periglacial environments (Art. 15, Law no.26639) in Argentina and the predicament behind the Glacial protection Law Project in Chile (Art. 1, Bulletin No. 11.876-12). Beneath these structural concerns, a sub-optimal management is propelled by legislations, notwithstanding conflicts of scale compatibility between all dimensions of "landscape". Under future hydroclimatic forcing, the legislative prerogative should never neglect the concern on hydric potential heterogeneity as in the Southern Andes (Figure 1) when looking at landscapes as metastable, latitudinal, and altitudinal "objects" of analysis (Table 3 & 4).

10. Conclusions and recommendations.

Mountain cryosphere represents hydric landscapes conveying a multi-dimensional potentiality. The apparently static landscapes reflect different levels of human appropriation and value production, rendering them dynamic and sensitive to value loss. This calls for the endorsement for desirable states of value, inexorably bound to management options, framing management as optimal needs to be complimented by subjective valuation theory to unveil risks affecting value and hence the necessary transactions for its preservation.

Nevertheless, cryosphere legislations try to protect land use of environmental elements using inappropriate or inconclusive scales of analysis as their potential is often challenged by a methodological and epistemological incommensurability overdrawn by the pretension of totality in assessments. Hence, legislation of the long-term evolution of mountain cryosphere is conceptually insufficient and consequently, its interpretation of resilience to depletion is equivocal.

Therefore, landscapes are often under a baseline paradox lacking a common scale rescuing adequate "decision values" in all landscape dimensions of concern. The assessment scale should operate as a recognition of objectives, regardless of the paradigm of valuation (biocentric, anthropocentric). In this sense, land-use as protection, non-exploitation and isolation is a measure of value creation contrary to the

predicament of current cryosphere legislations in the Andes range, highlighting the premise of strategic future exploitation as the rationale for conservation.

Additionally, if hydric potentiality (value) is reallocated to another item (cryosphere element) then the prioritization of value should address a dimension including the capacity for provision of a resource instead of a fixed element. The recommendation is to address the legislative concern for protection to the enclosing unit of analysis and potentiality, a hydrological scale within a timeframe of connectivity between nested processes.

Overall, we recognize temporality as an overlooked dimension within the complexity of hydrological potentiality inherent in mountain cryosphere landscapes of the Andes. If sustainable development discourses fail to solve the methodological insufficiency of quiescent hydrological structure and potential, the concreteness of a society-nature relationship will end up with the fabrication of value with imponderable degree of uncertainty for such assets.

The land use recommendation is to assess landscape by inserting the landscape-entity into the most inclusive dimension of analysis, which can then be divided into units with specific timescales and objectives to which transaction costs and insurance value estimation are still possible to obtain.

11. Acknowledgements.

The Authors acknowledge the work of Parque Andino Juncal staff and in particular the help provided by T. Dinges.

12. Funding.

This study has been partially funded by the Geography Institute (Pontificia Universidad Católica de Chile), ANID/FONDAP 1511009, and ANID/FONDECYT 1191223.

13. References.

Adler, M. (1997). Law and Imcommensurability: Introduction. *U. Pa. L. Rev.*, *146*, 1169.

Alvarez-Garreton, C., Boisier, J. P., Garreaud, R., Seibert, J., & Vis, M. (2021). Progressive water deficits during multiyear droughts in basins with long hydrological memory in Chile. *Hydrology and Earth System Sciences*, *25*(1), 429–446.

Alvarez-Garreton, C., Mendoza, P. A., Boisier, J. P., Addor, N., Galleguillos, M., Zambrano-Bigiarini, M., Lara, A., Cortes, G., Garreaud, R., & McPhee, J. (2018). The CAMELS-CL dataset: catchment attributes and meteorology for large sample studies-Chile dataset. *Hydrology and Earth System Sciences*, *22*(11), 5817–5846.

Anderson, E. (1995). *Value in ethics and economics*. Harvard University Press.

Augeraud-Véron, E., Fabbri, G., & Schubert, K. (2019). The value of biodiversity as an insurance device. *American Journal of Agricultural Economics*, *101*(4), 1068–1081.

Bailey, D. W. (1997). *Impermanence and flux in the landscape of early agricultural south eastern Europe*. na.

Bakker, K. (2012). Water security: research challenges and opportunities. *Science*, *337*(6097), 914–915.

Ballabio, D. (2015). A MATLAB toolbox for Principal Component Analysis and unsupervised exploration of data structure. *Chemometrics and Intelligent Laboratory Systems*, *149*, 1–9.

Baraer, M., Mark, B. G., McKENZIE, J. M., Condom, T., Bury, J., Huh, K.-I., Portocarrero, C., Gómez, J., & Rathay, S. (2012). Glacier recession and water resources in Peru's Cordillera Blanca. *Journal of Glaciology*, *58*(207), 134–150.

Barnett, T. P., Adam, J. C., & Lettenmaier, D. P. (2005). Potential impacts of a warming climate on water availability in snow-dominated regions. *Nature*, *438*(7066), 303–309.

Batabyal, A. A., Kahn, J. R., & O'Neill, R. V. (2003). On the scarcity value of ecosystem services. *Journal of Environmental Economics and Management*, *46*(2), 334–352.

Bauduceau, N., Berry, P., Cecchi, C., Elmqvist, T., Fernandez, M., Hartig, T., Krull, W., Mayerhofer, E., Sandra, N., & Noring, L. (2015). Towards an EU research and innovation policy agenda for nature-based solutions & re-naturing cities: final report of the Horizon 2020 expert group on 'nature-based solutions and re-naturing cities.' *Publications Office of the European Union: Brussels, Belgium*.

Baumgärtner, S., & Strunz, S. (2014). The economic insurance value of ecosystem resilience. *Ecological Economics*, *101*, 21–32.

Benediktsson, K., & Waage, E. R. H. (2020). Power without politics? Nature, landscape and renewable energy in Iceland. *Annales de Geographie*, *6*, 107–130.

Boisier, J. P., Alvarez-Garretón, C., Cordero, R. R., Damiani, A., Gallardo, L., Garreaud, R. D., Lambert, F., Ramallo, C., Rojas, M., & Rondanelli, R. (2018). Anthropogenic drying in central-southern Chile evidenced by long-term observations and climate model simulations. *Elem Sci Anth*, *6*(1).

Bown, F., Rivera, A., & Acuña, C. (2008). Recent glacier variations at the Aconcagua basin, central Chilean Andes. *Annals of Glaciology*. https://doi.org/10.3189/172756408784700572

Bozkurt, D., Rojas, M., Boisier, J. P., & Valdivieso, J. (2018). Projected hydroclimate changes over Andean basins in central Chile from downscaled CMIP5 models under the low and high emission scenarios. *Climatic Change*, *150*(3–4), 131–147. https://doi.org/10.1007/s10584-018-2246-7

Breuste, J. (1985). Zur Anwendung der Landschaftselement-Konzeption bei der Analyse der urbanen Landschaf. In *Geographische Landschaftsforschung in Agrarräumen und urbanen Räumen: methodische Ansätze und Ergebnisse* (pp. 64–79). Halle.

Breuste, J., Haase, D., & Elmqvist, T. (2013). Urban landscapes and ecosystem services. *Ecosystem Services in Agricultural and Urban Landscapes*, 83–104.

Bullock, C. (2017). *Nature's Values: From Intrinsic to Instrumental* (NESC (ed.)). National Economic and Social Council.

Bütler, M. (2007). Glaciers–objects of law and international treaties. In *Alpine space - man & environment* (pp. 19–31). Innsbruck University press.

Carrier, M. (2001). Changing laws and shifting concepts. In *Incommensurability and related matters* (pp. 65–90). Springer.

Carvalho, M. J., Melo-Gonçalves, P., Teixeira, J. C., & Rocha, A. (2016). Regionalization of Europe based on a K-Means Cluster Analysis of the climate change of temperatures and precipitation. *Physics and Chemistry of the Earth, Parts A/B/C*, *94*, 22–28. https://doi.org/https://doi.org/10.1016/j.pce.2016.05.001

Condon, L. E., Atchley, A. L., & Maxwell, R. M. (2020). Evapotranspiration depletes groundwater under warming over the contiguous United States. *Nature Communications*, *11*(1), 1–8.

Cook, C., & Bakker, K. (2012). Water security: Debating an emerging paradigm. *Global Environmental*

519 *Change*, *22*(1), 94–102.

520 Cuthbert, M O, Gleeson, T., Moosdorf, N., Befus, K. M., Schneider, A., Hartmann, J., & Lehner, B.
521 (2019). Global patterns and dynamics of climate–groundwater interactions. *Nature Climate Change*,
522 *9*(2), 137–141.

523 Cuthbert, Mark O, Taylor, R. G., Favreau, G., Todd, M. C., Shamsudduha, M., Villholth, K. G.,
524 MacDonald, A. M., Scanlon, B. R., Kotchoni, D. O. V., & Vouillamoz, J.-M. (2019). Observed
525 controls on resilience of groundwater to climate variability in sub-Saharan Africa. *Nature*,
526 *572*(7768), 230–234.

527 DeSA, U. N. (2013). World population prospects: the 2012 revision. *Population Division of the*
528 *Department of Economic and Social Affairs of the United Nations Secretariat, New York*, *18*.

529 Dussaillant, I., Berthier, E., Brun, F., Masiokas, M., Hugonnet, R., Favier, V., Rabatel, A., Pitte, P., &
530 Ruiz, L. (2019). Two decades of glacier mass loss along the Andes. *Nature Geoscience*, 1–7.

531 Elmqvist, T. (2017). Development: Sustainability and resilience differ. *Nature*, *546*(7658), 352.

532 Elmqvist, T., Andersson, E., Frantzeskaki, N., McPhearson, T., Olsson, P., Gaffney, O., Takeuchi, K., &
533 Folke, C. (2019). Sustainability and resilience for transformation in the urban century. *Nature*
534 *Sustainability*, *2*(4), 267–273.

535 Evans, S. G., Ge, S., & Liang, S. (2015). Analysis of groundwater flow in mountainous, headwater
536 catchments with permafrost. *Water Resources Research*, *51*(12), 9564–9576.

537 Frans, C., Istanbulluoglu, E., Lettenmaier, D. P., Naz, B. S., Clarke, G. K. C., Condom, T., Burns, P., &
538 Nolin, A. W. (2015). Predicting glacio- hydrologic change in the headwaters of the Z ongo R iver,
539 C ordillera R eal, B olivia. *Water Resources Research*, *51*(11), 9029–9052.

540 Gleeson, T., Befus, K. M., Jasechko, S., Luijendijk, E., & Cardenas, M. B. (2016). The global volume and
541 distribution of modern groundwater. *Nature Geoscience*, *9*(2), 161–167.

542 Green, N. (1995). Looking at the Landscape: Class Formation and the Visual. In E. Hirsch & M.
543 O'Hanlon (Eds.), *The Anthropology of Landscape. Perspective on Place and Space* (pp. 31–42).
544 Clarendon Press.

545 Griggs, D., Stafford-Smith, M., Gaffney, O., Rockström, J., Öhman, M. C., Shyamsundar, P., Steffen, W.,
546 Glaser, G., Kanie, N., & Noble, I. (2013). Sustainable development goals for people and planet.
547 *Nature*, *495*(7441), 305–307.

548 Haase, G., & Richter, H. (1983). Current trends in landscape research. *GeoJournal*, *7*(2), 107–119.

549 Hayek, F. A. (2001). *The Road to Serfdom* (2nd ed.). Routledge.

550 Hock, R., Rasul, G., Adler, C., Cáceres, B., Gruber, S., Hirabayashi, Y., Jackson, M., Kääb, A., Kang, S.,
551 & Kutuzov, S. (2019). *High Mountain Areas: In: IPCC Special Report on the Ocean and*
552 *Cryosphere in a Changing Climate*.

553 Horan, R. D., Fenichel, E. P., Drury, K. L. S., & Lodge, D. M. (2011). Managing ecological thresholds in
554 coupled environmental-human systems. *Proceedings of the National Academy of Sciences of the*
555 *United States of America*, *108*(18), 7333–7338. https://doi.org/10.1073/pnas.1005431108

556 Immerzeel, W. W., Lutz, A. F., Andrade, M., Bahl, A., Biemans, H., Bolch, T., Hyde, S., Brumby, S.,
557 Davies, B. J., & Elmore, A. C. (2020). Importance and vulnerability of the world's water towers.
558 *Nature*, *577*(7790), 364–369.

559 Immerzeel, W. W., Van Beek, L. P. H., & Bierkens, M. F. P. (2010). Climate change will affect the Asian
560 water towers. *Science*, *328*(5984), 1382–1385.

561 Keys, P. W., Porkka, M., Wang-Erlandsson, L., Fetzer, I., Gleeson, T., & Gordon, L. J. (2019). Invisible
562 water security: moisture recycling and water resilience. *Water Security*, *8*, 100046.

563 Kollmair, M., Gurung, G. S., Hurni, K., & Maselli, D. (2005). Mountains: special places to be protected?
564 An analysis of worldwide nature conservation efforts in mountains. *The International Journal of*
565 *Biodiversity Science and Management*, *1*(4), 181–189.

566 Krutilla, J. V. (1967). Conservation reconsidered. *The American Economic Review*, *57*(4), 777–786.

567 Landis, W. G. (2003). The Frontiers in Ecological Risk Assessment at Expanding Spatial and Temporal
568 Scales. *Human and Ecological Risk Assessment: An International Journal*, *9*(6), 1415–1424.
569 https://doi.org/10.1080/10807030390250912

570 Lefebvre, H. (1991). *The production of space*. 454.

571 Lepeška, T. (2010). Hydric potential of landscape and integrated river basin management in mountain and
572 submontane regions. *Ecohydrology & Hydrobiology*, *10*(1), 13–24.
573 https://doi.org/https://doi.org/10.2478/v10104-010-0017-9

574 Liaudat, D. T., & Bottegal, E. (2020). Recent evolution of the active layer in the Morenas Coloradas rock
575 glacier, Central Andes, Mendoza, Argentina and its relation with kinematics. *Cuadernos de*
576 *Investigación Geográfica/Geographical Research Letters*, *46*, 159–185.

577 Lynn, M. (1991). Scarcity effects on value: A quantitative review of the commodity theory literature.
578 *Psychology & Marketing*, *8*(1), 43–57.

579 Mancosu, N., Snyder, R. L., Kyriakakis, G., & Spano, D. (2015). Water Scarcity and Future Challenges
580 for Food Production. In *Water* (Vol. 7, Issue 3). https://doi.org/10.3390/w7030975

581 McCann, L. (2013). Transaction costs and environmental policy design. *Ecological Economics*, *88*, 253–
582 262.

583 Mill, J. S. (1994). *Principles of Political Economy. edited by Jonathan Riley*. New York: Oxford
584 University Press.

585 Morgenstern, O. (1934). Das Zeitmoment in der wertlehre. *Zeitschrift Für Nationalökonomie*, *5*(4), 433–
586 458.

587 Musselman, K. N., Clark, M. P., Liu, C., Ikeda, K., & Rasmussen, R. (2017). Slower snowmelt in a
588 warmer world. *Nature Climate Change*, *7*(3), 214–219.

589 Nino, F. S. (2015). Sustainable Development Goals—United Nations. *United Nations Sustainable*
590 *Development*.

591 Nordstrom, K. F. (1993). Intrinsic value and landscape evaluation. *Geographical Review*, *83*(4), 473–476.

592 Oberheim, E., & Hoyningen-Huene, P. (2009). *The incommensurability of scientific theories*.

593 Olbrich, M., Quill, T., & Rapp, D. J. (2015). Business valuation inspired by the Austrian school. *Journal*
594 *of Business Valuation and Economic Loss Analysis*, *10*(1), 1–43.

595 Otero Pastor, I., Martínez, M. A. C., Canalejoa, A. E., & Mariño, P. E. (2007). Landscape evaluation:
596 comparison of evaluation methods in a region of Spain. *Journal of Environmental Management*,
597 *85*(1), 204–214.

598 Paavola, J., & Primmer, E. (2019). Governing the provision of insurance value from ecosystems.
599 *Ecological Economics*, *164*, 106346.

600 Pereira, S. R., Fernández, J., Herrera, J., & Olea, J. (2021). Assessment of landscape transformation in
601 protected areas. *Environmental Impact Assessment Review*, *86*, 106472.
602 https://doi.org/https://doi.org/10.1016/j.eiar.2020.106472

603 Perry, J., & Easter, K. W. (2004). Resolving the scale incompatibility dilemma in river basin
604 management. *Water Resources Research*, *40*(8).

605 Pfeffer, W. T., Meier, M. F., & Illangasekare, T. H. (1991). Retention of Greenland runoff by refreezing:
606 implications for projected future sea level change. *Journal of Geophysical Research: Oceans*,
607 *96*(C12), 22117–22124.

608 Polk, M. H., Young, K. R., Baraer, M., Mark, B. G., McKenzie, J. M., Bury, J., & Carey, M. (2017).
609 Exploring hydrologic connections between tropical mountain wetlands and glacier recession in
610 Peru's Cordillera Blanca. *Applied Geography*, *78*, 94–103.

611 Quaas, M., Baumgärtner, S., & De Lara, M. (2019). Insurance value of natural capital. *Ecological*
612 *Economics*, *165*, 106388.

613 Quaas, M. F., & Baumgärtner, S. (2008). Natural vs. financial insurance in the management of public-
614 good ecosystems. *Ecological Economics*, *65*(2), 397–406.

615 Ragettli, S., Immerzeel, W. W., & Pellicciotti, F. (2016). Contrasting climate change impact on river
616 flows from high-altitude catchments in the Himalayan and Andes Mountains. *Proceedings of the*
617 *National Academy of Sciences*, *113*(33), 9222–9227.

618 Ruiz Pereira, S, Marquardt, C., Beriain, E., & Lambert, F. (2021). Permafrost evolution in a mountain
619 catchment near Santiago de Chile. *Journal of South American Earth Sciences*, 103293.

620 Ruiz Pereira, Sebastian, & Veettil, B. K. (2019). Glacier decline in the Central Andes (33° S): Context
621 and magnitude from satellite and historical data. *Journal of South American Earth Sciences*, 102249.

622 Sankey, H., & Hoyningen-Huene, P. (2001). Introduction: Incommensurability and related matters.
623 *Boston Studies in the Philosophy of Science*, *216*, 7–34.

624 Sauer, C. (1925). The morphology of landscape. *University of California Publications in Geography*,
625 *2*(2), 19–54.

626 Sauer, C. (1963). The morphology of landscape. *University of California Publications in Geography*,
627 *2*(2), 19–54.

628 Schirpke, U., Timmermann, F., Tappeiner, U., & Tasser, E. (2016). Cultural ecosystem services of
629 mountain regions: Modelling the aesthetic value. *Ecological Indicators*, *69*, 78–90.
630 https://doi.org/https://doi.org/10.1016/j.ecolind.2016.04.001

631 Siegel, H. (2001). Incommensurability, rationality and relativism: in science, culture and science
632 education. In *Incommensurability and related matters* (pp. 207–224). Springer.

633 Sileo, N. R., Dapeña, C., & Trombotto Liaudat, D. (2020). Isotopic composition and hydrogeochemistry
634 of a periglacial Andean catchment and its relevance in the knowledge of water resources in
635 mountainous areas. *Isotopes in Environmental and Health Studies*, *56*(5–6), 480–494.

636 Somers, L. D., McKenzie, J. M., Mark, B. G., Lagos, P., Ng, G. C., Wickert, A. D., Yarleque, C., Baraër,
637 M., & Silva, Y. (2019). Groundwater buffers decreasing glacier melt in an Andean watershed—But
638 not forever. *Geophysical Research Letters*, *46*(22), 13016–13026.

Stigter, E. E., Steiner, J. F., Koch, I., Saloranta, T. M., Kirkham, J. D., & Immerzeel, W. W. (2021). Energy and mass balance dynamics of the seasonal snowpack at two high-altitude sites in the Himalaya. *Cold Regions Science and Technology*, *183*, 103233. https://doi.org/https://doi.org/10.1016/j.coldregions.2021.103233

Sunstein, C. R. (1994). Incommensurability and valuation in law. *Michigan Law Review*, *92*(4), 779–861.

Sweezy, P. (1968). *Theory of capitalist development, the: Principles of Marxian political Economy.*

Therme, T. (2014). Les services d'usage indirect fournis par les écosystèmes marins et côtiers: l'exemple de la Guadeloupe. *Études Caribéennes*, *27–28*.

Trombotto-Liaudat, D., Sileo, N., & Dapeña, C. (2020). Periglacial water paths within a rock glacier-dominated catchment in the Stepanek area, Central Andes, Mendoza, Argentina. *Permafrost and Periglacial Processes*, *31*(2), 311–323.

Trombotto, D., & Borzotta, E. (2009). Indicators of present global warming through changes in active layer-thickness, estimation of thermal diffusivity and geomorphological observations in the Morenas Coloradas rockglacier, Central Andes of Mendoza, Argentina. *Cold Regions Science and Technology*. https://doi.org/10.1016/j.coldregions.2008.08.009

Trombotto, D., Buk, E., & Hernández, J. (1999). Rock glaciers in the southern central Andes (approx. 33–34 S), Cordillera Frontal, Mendoza, Argentina. *Bamberger Geographische Schriften*, *19*, 145–173.

United Nations. (1997). United Nations framework convention on climate change. *Kyoto Protocol, Kyoto*, *19*, 497.

Unterberger, C., & Olschewski, R. (2021). Determining the insurance value of ecosystems: A discrete choice study on natural hazard protection by forests. *Ecological Economics*, *180*, 106866. https://doi.org/https://doi.org/10.1016/j.ecolecon.2020.106866

Van Lanen, H. A. J., Wanders, N., Tallaksen, L. M., & Van Loon, A. F. (2012). Hydrological drought across the world: impact of climate and physical catchment structure. *Hydrology & Earth System Sciences Discussions*, *9*(10).

Viviroli, D., & Weingartner, R. (2008). "Water towers"—A global view of the hydrological importance of mountains. In *Mountains: Sources of water, sources of knowledge* (pp. 15–20). Springer.

Volk, M., & Steinhardt, U. (2001). Landscape balance. In *Landscape balance and landscape assessment* (pp. 163–202). Springer.

Von Wieser, F. F. (1893). *Natural value*. Macmillan and Company.

Wałęga, A., Młyński, D., Wojkowski, J., Radecki-Pawlik, A., & Lepeška, T. (2020). New Empirical Model Using Landscape Hydric Potential Method to Estimate Median Peak Discharges in Mountain Ungauged Catchments. *Water*, *12*(4), 983.

Wutich, A. (2020). Water insecurity: An agenda for research and call to action for human biology. *American Journal of Human Biology*, *32*(1), e23345.

Zeng, W., Jiang, Y., Huo, Z., & Hu, K. (2020). Clustering Analysis of Extreme Temperature Based on K-means Algorithm. *International Conference on Artificial Intelligence and Security*, 523–533.

Milkow, F.H. (1973). Human and Landscape (*Человек и ландшафты: очерки антропогенного ландшафтоведения*). Мысль.

Environmental Impact Assessment Review 86 (2021) 106472

Contents lists available at ScienceDirect

Environmental Impact Assessment Review

journal homepage: www.elsevier.com/locate/eiar

Assessment of landscape transformation in protected areas

Sebastian Ruiz Pereira[a,b,*], José Fernández[c], José Herrera[d], Jorge Olea[a,e,f]

[a] Instituto de Geografía, Pontificia Universidad Católica de Chile, Chile
[b] Center for Climate and Resilience Research, Universidad de Chile, Chile
[c] University of Bonn, Germany
[d] Universidad Autónoma de Chile, Temuco, Chile
[e] Facultad de Recursos Naturales, Universidad Católica de Temuco, Chile
[f] Laboratório História e Natureza, UFRJ, Brazil

ARTICLE INFO

Keywords:
Landscape value
Mountain protected areas
Commercial concession
Economical transformation
EIA

ABSTRACT

Mountain protected landscapes continuously endure conflicts of appropriation that bear inherent transformations. One type of direct intervention is by Commercial Concessions within these areas, affecting their landscape value. The aim is to determine conceptual gaps in Environmental Impact Studies regarding landscape assessment and propose a way to improve them in this sense.

Shortcomings regarding landscape are checked in different normative frameworks and tensions are analyzed through the case of a Commercial Concession grant within a Mountain Protected area in the South-Central Andes of Chile (38°22′S;71°35′W).

Weak or absent definitions of landscape are found in normative frames and Environmental Impact guidelines. A reductionism of landscape as mere viewshed units avoids a proper differentiation for several types of economic transformations and conservation management purposes therein. Hence, transformations affecting the inherent value of landscape are latent under monitoring and legislation abiding practices.

Tensions between protected areas and commercial concessions depend on landscape management strategies which are associated to capital gain uncertainties by risking the nonuse-value of landscape. This uncertainty as a natural insurance value can be integrated to conceptual analyses assessing landscape transformations and report their depreciation.

These transformations of landscape value are deemed necessary to be implemented in Environmental Impact Assessment without having to discretize bipartite purposes in protected areas by assessing landscape value through conceptual and economic analyses.

1. Introduction

In brief, the present work aims at highlighting that landscape value loss deals with a way of being of the transforming agents, which ultimately may disrupt or preserve the relation between the landscape object and landscape subjects. A framework is proposed to solve these challenges in Environmental Impact Assessments (EIA).

The experience of nature is not a static nor a defined one, it changes as does the perception of an unspoiled wilderness (Müller and Job, 2009). As wilderness may be dynamic, so too is the wilderness debate and the wider role of law in protecting such areas (Bastmeijer, 2016).

Natural landscapes represent a myriad of 'epistemical' fragments built upon interactions between the subject and space. The building blocks of these epistemic standpoints emerges from both a historical and complex interplay of subject and object and their corresponding ontological determinations. The European Landscape Convention considered it an area as perceived by people whose character results of the action and interaction of natural and/or human factors (Council of Europe, 2000).

Landscapes analysis synthesizes space trajectories and components configuring them. Within each one there are 'other' landscapes and smaller dimensions through hierarchies (Farina, 2011, p. 44) and properties (Gaddis, 2002) because as an arbitrary 'condensation' of space (Gomes, 2017), they intersect memories, meanings, histories and spaces composing human existence (Tuan, 1974; Schama, 1996; Cresswell, 2008).

Visually, landscapes are regarded as social documents in which symbols must be decoded to interpret the actions of various social groups (Cosgrove et al., 1988, p.1–10). This relational perspective implies the subjective assignation of 'value' to landscape (Table 1). In

* Corresponding author at: Instituto de Geografía, P.U.C., Vicuña Mackenna 4860, Macul, Santiago de, Chile.
E-mail address: spruiz@uc.cl (S.R. Pereira).

https://doi.org/10.1016/j.eiar.2020.106472
Received 13 March 2020; Received in revised form 7 September 2020; Accepted 8 September 2020
0195-9255/ © 2020 Elsevier Inc. All rights reserved.

Table 1
Summary of landscape analysis. Adapted from Sauer, 1963.

Aspects of landscape	Description
Comprehensive view of nature and culture.	Interaction of natural and/or cultural factors.
Internal vs. External perspective.	Area, as perceived by people.
Historical retrospection.	"Result of..."
Forms and processes.	Action and interaction, Human factors.

general, the conceptual structure of landscape includes visual and aesthetic services (Cosgrove et al., 1988), relational services (Relph, 1976, p.17; Tuan, 1977, p.6) and physical as land (Sauer, 1925; Hart, 1998, p.276). Therefore, landscapes bear a rugged topology with overlapping ontologies often used indistinctively.

Understood as part of Cultural Ecosystem Services (CES), mapping assessments should be pushed ahead as indispensable elements in the management and protection of cultural landscapes (Plieninger et al., 2013). Economically, ecosystem services are classified by a utilitarian perspective. On one hand, their 'use-value' is that inherently tied to the ecosystem functioning itself (Therme, 2014) and on the other, the exchange-value reflects underlying social relations (Sweezy, 1968) not "from the nature of things" but from "social arrangements" (Mill, 1994, p.54).

The landscape's paradox of value relates to its 'intrinsic value', when the 'exchange-value' is negligible (or beyond methodological grasp) but has an incommensurable 'use-value'. Briefly put, things with the greatest value in use have frequently little or no value in exchange; and on the contrary, those with the greatest value in exchange have frequently little or no value in use (Smith, 1989).

Therefore, difficulties to assess value on certain elements are also difficulties to ponder their depreciation and eventual loss as an asset. Examples are shown through guidelines from the *Scottish Natural* Heritage (2017) and in Chile the *Servicio de Evaluación de Impacto Ambiental* (SEIA) in 2013 and 2019, where visual impact creates artificiality and undermines the overall quality of the natural object. In this sense, impact assessments may fall short when evaluating natural sites, for example, sites under threats of cultural changes and habitat degradation (Dudley et al., 2009) but also contradictory conservation objectives when commercial and protected areas coexist (Gutiérrez and López, 2017).

Here, 'natural capital' refers to natural resources as factors in the production function along with human and social capital (Bullock, 2017, p.3) whose value estimation comes from evaluations of production costs and their monetary translation or its replacement costs (Failler et al., 2011). In this sense, assessing landscapes implies understanding the dynamics of appropriation, for example a commercial activity within a protected area. Here, landscape as materiality or an ontological question determines tensions of a dispute between physical elements in conflict with appropriation and control against competing meanings in representations influencing space-framing-processes (Tuan, 2013).

The European Landscape Convention (2000) recommended to analyze landscape characteristics and transforming forces aiming at protecting, managing, and planning interventions to seek specific quality objectives. It all obeys the spirit to 'harmonically' develop, enhance, restore, or create landscapes.

This 'harmony' is often never defined in normative frameworks yet endorsed as a constant condition in theoretical guidelines. We argue that it deals with a contradiction between ontological (bipartite) purposes; conservation/protection and exploitation. Landscape management can have commercial purposes gradually undermining landscape value. Since the bipartite purpose is to protect landscape as well, it is a sub-optimal and contradictory management.

This idea has also been expressed by the distinction between interface and deface (Reynolds, 1990): while interfacing is the coexistence of two systems, for the one hand the system of human life, and on the other hand the ecosystem, which mutually cooperate and foster the existence of each other. Opposite circumstances are those of defacing, in which these two systems are in no cooperating correlation to each other, and one is destructing the other as it profits from it and abuses it.

The problem is how EIAs can assess such processes since they can only be considered prognosis tools for interventions carrying conceptual tensions. First, impacts imply transformations, hence when landing any assessment on interventions particular selections will imply the valuation of components, as well as their organization and perceptions of permanence and change (Green, 1995). These are necessary to surpass the uncritical acceptance of landscape stability and understand realities (Bailey, 1997) modified to obtain natural resources (Sauer, 1925). Stability is often brought by the biased notion that landscape does not depreciate if the regular normative is abided yet the stress we intend to set is on detrimental changes on the use-value of the landscape.

For example, when we talk about value and time, or value and use, we are already talking about depreciation. Landscape transformations set on objects with undetermined use-value and no exchange-value like protected biodiversity areas, deals then with a depreciation of their 'intrinsic value' by denaturalization, a loss of its inherent quality of not being an artificial creation. Therefore, in EIAs problems will emerge because of reducing landscapes into purely visual and aesthetic qualities, mere viewsheds with quantifiable elements therein.

EIAs are not only linked to descriptions or representations but also to conflicts of appropriation and plundering (Walker, 2018) where involved parties are not always compatible in terms of their 'fates'. This is the multi-dimensional scheme where EIAs should aim at when assessing landscapes.

In protected areas, integration of legal frameworks and sanctions constitutes the protection which assumes the potential violation of 'purity' contained within the null-agency object 'nature'. This violation is derived from a certain *modus* regarding technic as a domain of affairs and a historic-ontological fate (Sloterdijk, 2000, p.76). These are ways of being which may converge in normative operations focused on solving the generational asymmetry by intergenerational justice (Rawls, 2005; Gosseries, 2008) which is why areas are protected, or simply disrupt that possibility by erasing the identity or by making artificial something that is natural.

For example, a normative framework assesses impacts of a Commercial Concession within a protected area but does not assess if its management will be conservative and will not derive in economical transformations diminishing landscape value. Hence, we deem that transformations are integrated by fragmentary units of potential change, impacts sometimes sharing causalities but not outcomes.

Therefore, an economic analysis of landscape-value and its loss in time can be specified through user preferences and constraints, termed as benefit estimations with specific connections to preference functions (Smith et al., 2002). The issue emerges with assets interpreted as invaluable where only a depreciation magnitude of their value could represent them in an evaluation.

Investments in protected areas are still economic systems having devices for shifting risks which are imperfect and one would expect an underinvestment in risky activities. Nevertheless, the potential of these devices is limited by moral factors (Arrow, 1962, p.614). This is why environmental and development policies in regions where users face high environmental uncertainty can rely natural insurances to diminish uncertainty (Lukomska et al., 2014).

An insurance value is poorly captured in the risk and cost-benefit calculations because the risk buffering capacity of ecosystems is typically a public good (Paavola and Primmer, 2019). Insurance values for natural assets are an increasing function of the intrinsic volatility of landscape (trading price change over time) in face of undesirable states

of its productivity (deterioration) and of risk aversion (decrease of uncertainty). Uncertainties as risks can then be linked to optimum management strategies and represent a parallel measure to observe while assessing future commercial interventions.

The study aims to analyze the implementation of landscape transformation within EIAs, stressing the attention in cases of protected areas with potential commercial concessions therein. In specific, landscape transformations are analyzed in the context of commercial concessions within a protected area in a touristic mountain environment in the South-Central Andes of Chile.

The first part will work concepts on landscape transformations and explore conceptual gaps in current normative approaches in different countries. The second part will propose how landscape transformation processes should be implemented in EIAs after the analysis of a commercial concession in a mountain protected area.

2. Methods

The first task is to specify the uncertainty problem of landscape transformations in protected areas as changes in value. Then, to find how landscape has been approached in certain legislations and finally a proposition for improving the conceptual reach of EIAs.

Landscape transformations are here interpreted as economical transformations performed by agents who seek profit from tourism derived activities, which inside protected areas are legally commercial concessions. The analysis takes a conceptual categorization of processes done by Terkenli (2002) and later used for studying mountain landscape evolution in the context of tourism development (Chrenka and Ira, 2011).

Briefly, transformations of a new cultural economy of space can occur through *transworldment* processes that will interconnect worlds, transfer experience and standardize the notion of place. *Enworldments*, represent the onset of cosmopolization as a fusion of distinctiveness between nature and culture. *Unworldment* processes would represent the dissolution of geographical particularity and landscape identity, as a local-to-global cosmopolization. Finally, *deworldment* processes stand as commodification; anesthetization and 'Disneyfication'.

Next, it is necessary to work on causes before being able to act on their consequences by first acknowledging the criteria capable to evaluate and separate technologies (Neyrat, 2017, p.115). This part takes concepts drawn from Sloterdijk (2000), establishing distinct 'ways of being' for a given intervention.

The *allotechnologies* imply the 'violation of the earth' by deep interventions that disable primary materials (Sloterdijk, 2000, p.90). They are exogenous in nature and imply the agency of a subject that "contribute[s] to the erosion of [their] resilience" (Neyrat, 2017, p.115). In contrary, *homeotechnologies*, emerging from the thought of complexity and ecology as they entail a strategy of cooperation of dialogue with nature (Neyrat, 2017, p.116). Hence, they cannot (by essence) "*want something different than what those things themselves are for themselves or become for themselves*" (Sloterdijk, 2000, p.91).

After identifying interventions in mountain protected settings, it is necessary to establish if their management is sub-optimal in terms of conservation practices and affect landscape value beyond the grasp of EIAs. This is an issue to be put in the long-term perspective for EIA since landscape value will depreciate in time, in terms of CES for example.

A proposed example will analyze transformations and ways of being in terms of management, considering the ongoing expansion impacts of touristic infrastructure (Additional Table 1) in areas surrounding National Reserves at 38°S in the Andes. We downscaled the conceptual assessment to a critical example intersecting Commercial Concession within borders of protected areas. There, current and future landscape dynamics were approached by using available field and remote data.

In parallel, insights on value changes were put in the context of economic devices so as to relate them to management. A baseline from benefit transfer is considered a viable approach for estimating the value of environmental goods and services uses economic information captured at one place and time to make inferences about the economic value of environmental goods and services at another place and time (Wilson and Hoehn, 2006).

Since landscape value can be understood as a nonuse-value, is necessary to indirectly measure its existence-value loss (Freeman, 1993, p.266) on a scale compatible to the intervening agent. The purpose is to find an optimum management in an evaluation, as one preserving baselines and thereby protecting its capital gain by doing so.

One option is to apply contingent valuations for inventoried benefits by considering the bottom-up structure (Torquati et al., 2015) of relevant actors and to report their Willingness To Pay (WTP) for different options to that changing scenario, but also to consider Willingness To Accept (WTA) compensations (Bateman, 1996) upon imminent damages. The assumption could be that a WTP can cover the uniqueness and changes in character of a site (Santos, 2007). Other options like Natural Resource Damage Assessment (NRDA) evaluate the liability for environmental damages (Sanders et al., 2016) and consider compensation payments for natural resource injuries from e.g. pollution accidents (Navrud and Ready, 2007, p.283).

Upon impact, the nonuse-value can be addressed through perspectives of Replacement Cost, Mitigation or Avoided cost method (Pascual et al., 2010, p.200) but also through the influence on pricing that an ecosystem has, which relates to the Willingness to Pay (WTP) that a certain public has for assets ina Protected Ecosystem. Therefore, an indirect measure of the nonuse-value of a non-consumptive benefit from landscapes inserted in ecosystem as the capital gain and risk reduction Commercial Concessions granted by the nonuse-value of landscape at baseline condition.

Insurance (landscape) value of natural capital depends on properties of the ecosystem dynamic and ecosystem user preferences. The insurance value is associated to a conservative use of the ecosystem and precautionary investment of capital stock, in terms of self-insurance as size of loss and self-protection as probability of loss (Ehrlich and Becker, 1972). Here, moral factors (moral-hazard) limit the possibilities of insurance as effects of market insurance on self-protection increase probabilities of hazardous decisions (Arrow, 1962, p.612) as undesirable impacts.

Insurance values provides an additional rationale for the rehabilitation, restoration and conservation of intact natural ecosystems (Dallimer et al., 2020) and can be positive or negative when related to their conservative use and precautionary investments in the natural capital stock (Quaas et al., 2019), specifically as the optimal conversion/conservation of total value in terms of the welfare gain from conservation and the marginal value in terms of risk premium reduction (Augeraud-Véron et al., 2019).

3. Theory

3.1. Landscape transformation

Landscapes are very often reduced to an interchangeable viewshed-unit of territory and any additional readings are tied to limitations or simplifications. For example, in Iceland, visual impacts on landscape viewsheds as documented by in a Summary for the National Planning Agency for the formulation of national landscape planning policy named *Landslag og vindorka* (ALTA Consulting, 2019). Here, the impact was measured in terms of how turbines become noticeable and dominate the landscape, consequently changing landscape 'appearance'. In Chile, 'landscape' is not legally defined within the Constitution. The Law 19,300 (1994) and 20,417 (2010) on the *General Guidelines for the Environment*, only defines landscapes as elements of the environment. Landscape is set as value and there is only differentiation between landscape and cityscape, but there lacks any comprehensive structure on landscape understanding.

We could argue these guidelines only deal with the aesthetic-value

of the area's viewshed when the landscape character implies a recognizable identity that can change in its experienced essential characteristics by a given transformation.

The EIA and consequently EIS (Environmental Impact Study) intend to foresee and prevent undesirable changes from a certain baseline, the protected object in a relative stage zero of intervention. Here, impacts are categorized and thus not blocked but regulated. This opens the door for private commercial interests, assuming that both conservation and commercial usage can coexist and goes along the rejection of an ecology of separation, which conceives the degree of conservation to be inversely proportional to the degree of human contact with the territory: an insulation.

This artificiality includes an increase of the exchange-value of the determined area, but the landscape value contained in the area has changed its nonuse-value. This happened since epistemological shifts from resources to services entail issues on Man and Ecosystem interdependence. The issue is whether subjects can profit from ecosystem services and adopt an interaction equivalent to optimal conservation management.

3.2. EIAs and commercial concessions

In Chile, the *Law of the Environment* (19,300, Art. 11-e) points out which interventions require EIS by having '*significantly affected (by magnitude or length) the landscape and touristic value of a given zone*'. An area with 'landscape value' is that which by being perceived visually possesses natural attributes that make it unique and representative (SEIA, 2013, p.14).

Once it is determined that a Project significantly alters landscape value in magnitude and duration, an EIS is enacted, and should include mitigation measures to match the impacts.

Nevertheless, mitigations have a point of no return and for protected areas with no exchange-value but a nonuse-value, retroactive mitigations are undetermined with no other recipient of any compensation than the Central Government, who does not engage in the formal recognition of landscape value but only censors this dynamic.

The impact evaluation stage implies perceptions of magnitude and singularity yet, most guidelines are offered only regarding visual dissonance from a certain baseline but also artificiality due to human presence (SEIA, 2013). Here, a detachment from the intrinsic property of landscape as being natural is implied.

Nevertheless, Commercial Concessions are widely allowed in different countries. As interventions, they are widely allowed without the examination of the gradual transformations they may exert on landscape value if only abiding certain conditions. In the case of the USA, National Park Services (NPS) require Commercial Use Authorizations (CUA) present in the Code of Federal Regulation (CFR). Then, the Commercial Visitor Services states that a decision to authorize or expand a park concession will consider effects and needs for additional infrastructure if it is consistent with enabling legislation and complementary to a Park's Mission and visitor-service objectives.

The Mission includes appropriate principles and practices, environmental goals, and the avoidance of unacceptable impacts. So Federal Law mandates the NPS to issue CUAs only for commercial activities that go along a certain Park's purpose and regulations. Landscape concepts are missing.

The 4th of August 2020, the *Great American Outdoors Act* was passed establishing the *National Parks and Public Land Legacy Restoration Fund* to support deferred maintenance projects on federal lands, and making funding for the *Land and Water Conservation Fund* (LWCF) permanent. Again, landscape concepts are missing in the bill's definition.

In the case of Iceland, the Mission are rules of conduct that are considered as in Paragraph 2, Art. 12 of the Conservation Law no.44/1999, which states that *"everyone is obliged to take care of the country's nature and show extreme caution so that it is not spoiled"* (Óskarsdóttir, 2011, p.311). Further, the *Act on Environmental Impact Assessment* (2000, no. 106 May 25th) stated that the EIA should identify, describe and evaluate significant direct/indirect effects on land, landscape, wilderness, geological formations, soil, water, air and climate but also material values, cultural monuments.

Here, the protecting interests of the rule are first and foremost Nature itself, then the interests of the public and individuals. For example, the National Park at "Þingvellir" was protected by special laws in 1930 and Act no.47/2004 and "Vatnajökull" in spring 2007 (Law no.60/2007) and June 2008. On them, this land must be protected in order to preserve as much as possible of its original natural habitat and additionally to protect the landscape, biosphere, geological formations and cultural heritage of the area, hence allowing to enjoy its nature (Óskarsdóttir, 2011, p.215–216). Here, the sense of non-artificiality is implied by addressing the protection of the 'original' value, but also to preserve the circumstances in which relations emerge.

For the Scottish case (Scottish Natural Heritage, 2017), landscape impact upon the installation of eolic turbines tries to avoid the potential land use based on categories of areas with differentiated values. A priority land-use exclusion is set through three area categories intended for their protection as being or containing vulnerable objects (see Additional Tables 1 and 2); Category 1 implies no acceptance of infrastructure; Category 2 has significant protection after proven impacts and potential mitigation measures are set. The criteria for Category 2 include cultural reasons for protection and visual impact. Category 3, potential areas for the installation of structures demand a detailed assessment as well.

In continental Europe, the central aim of Natura 2000 (Bastmeijer, 2016) and other imperatives of the Habitats Directive is 'to maintain or restore, at favorable conservation status, natural habitats and species of wild fauna and flora of Community interest Special Areas of Conservation. The European Court of Justice (ECJ) legally manages Natura 2000 sites and requires in Article 6(1) that Member States 'establish the necessary conservation measures' to achieve the conservation objectives that must be set for each site. Also, the Article 6(2) obliges Member States to avoid the deterioration of natural habitats.

In April 2019, objectives and justification for touristic concessions in 'Wild Protected Areas' aimed at protecting biodiversity and cultural wellbeing but also improving the visitor's experience by diversifying existing offers and promoting the active participation of neighbor communities/residents (Ord. N°252, Apr. 2019, CONAF, Chile). Landscape itself has escaped the objectives but still appears undefined in the evaluation charts.

A commercial concession, called the 'Corralco' complex, was located within the mountain protected area of the 'Malalcahuello' National Reserve (38°S). It has been inspected by the Ministry of the Environment and CONAF resulting in reports (Superintendence of the Environment, 2013). The audit covered landscape as a component to be evaluated but never defined it and only addressed mitigation of the visual impact by "*using natural materials as wood and stone… using*

Table 2
Classification of landscape economical transformations occurring at 'Malalcahuello' area, Andes at 38°S.

Landscape transformation	Outcome	Main agent
Transwordlment	Interconnect worlds	Private investor
	Transfer experience	National Tourism Service
	Standardize the 'place' notion	Middle-upper class users
Enworldment	Onset of cosmopolization	Private sector
	Standardization	
Unworldment	Change of identity (local to global)	Local investors
	Cosmopolization	Foreign investors
Deworldment	Commodification	Big investors

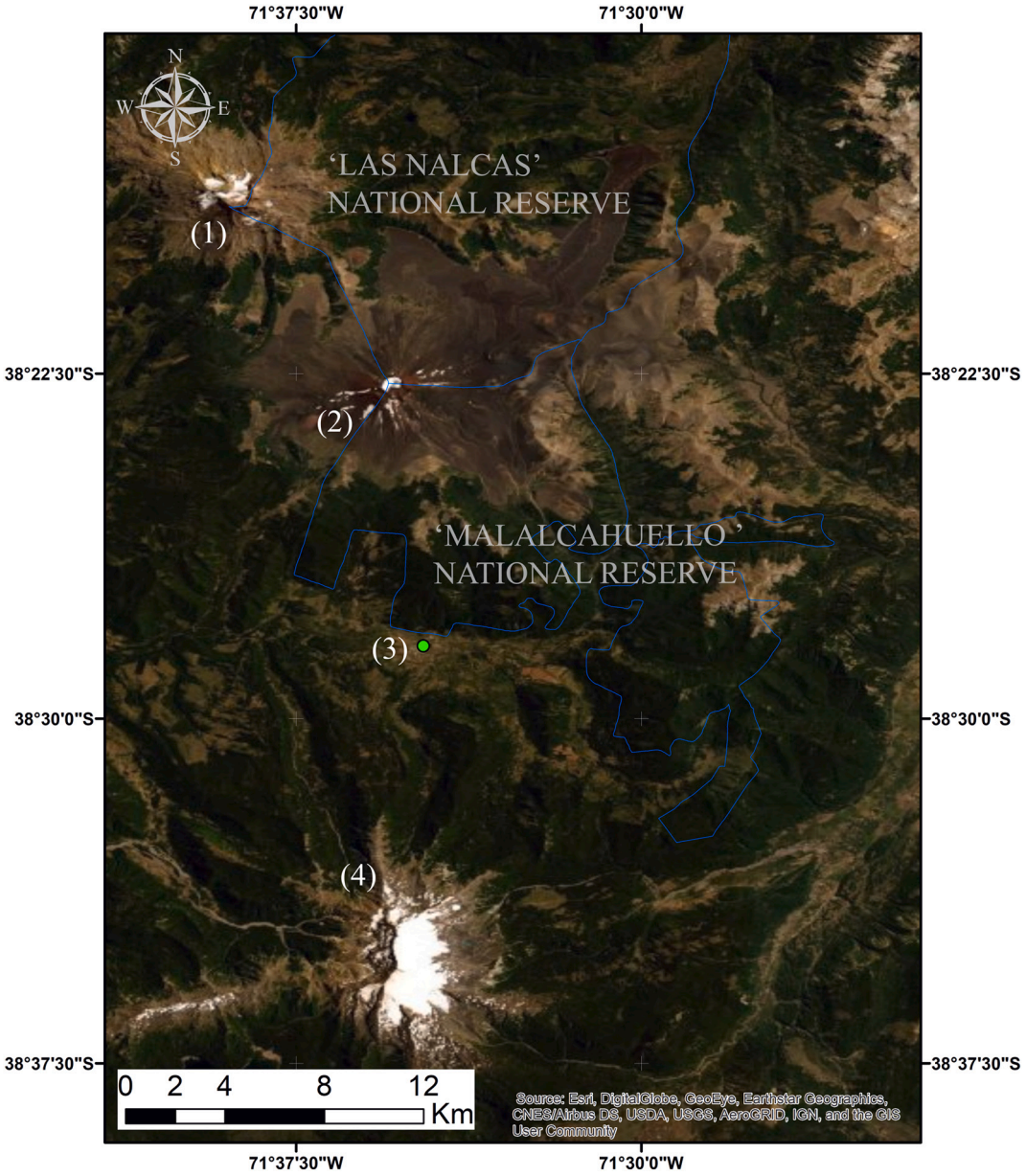

Fig. 1. Mountain protected areas in the South-Central Andes of Chile (38°S). Protected forest areas (blue borders). As shown; 'Tolhuaca' (1) and 'Lonquimay' (2) volcanos. The town of 'Malalcahuello' is the green point in (3) and the short glacierized range of 'Sierra Nevada' is on number (4). (For interpretation of the references to colour in this figure legend, the reader is referred to the web version of this article.)

natural colors". After the inspection, the agencies declared on the environmental qualification resolution RCA no.23/2003 that the 'Corralco' complex had mitigated the visual impact and only failed to plant enough trees around the sewage dependencies. A dynamic oscillating between desirable limits for the viewshed as threshold only.

The 'Malalcahuello' National Reserve represents an asset for present and future generations (conservation) in terms of biodiversity and autochthonous vegetational floors (Fig. 2 a-d) but also as a cultural and recreational object, winter sports. It has commercial concessions granted by the State and therefore is considered a transformed landscape due to commercial land use bordering the natural reservation limits, which affects the valuation of the National Reserve itself by the way of depreciation.

4. Results

4.1. Transformation of a protected area

The Natural Reserve 'Malalcahuello' (Figs. 1 and 2) is located within the Araucanía region in South-Central Chile (38°S;71°W). It was created on the 31st of March 1931 by Decree (n°1670) of the Ministry of Austral Property. The Decree stated the need to constitute a Forest Reserve in lands that belonged to an ex-concession with the objective of protecting the forests therein. These are composed of *Araucaria araucana*, *Nothofagus alpina*, *Nothofagus obliqua* and others (see Fig. 2). This operation destined almost thirty thousand hectares. Later, in October 1953, the Article-1, Law-11,304 (Ministry of the Interior) destined 50has to the creation of the Malalcahuello town itself, within the Natural Reserve back then.

In July 1956, Decree 4363 stated that to profit better from National

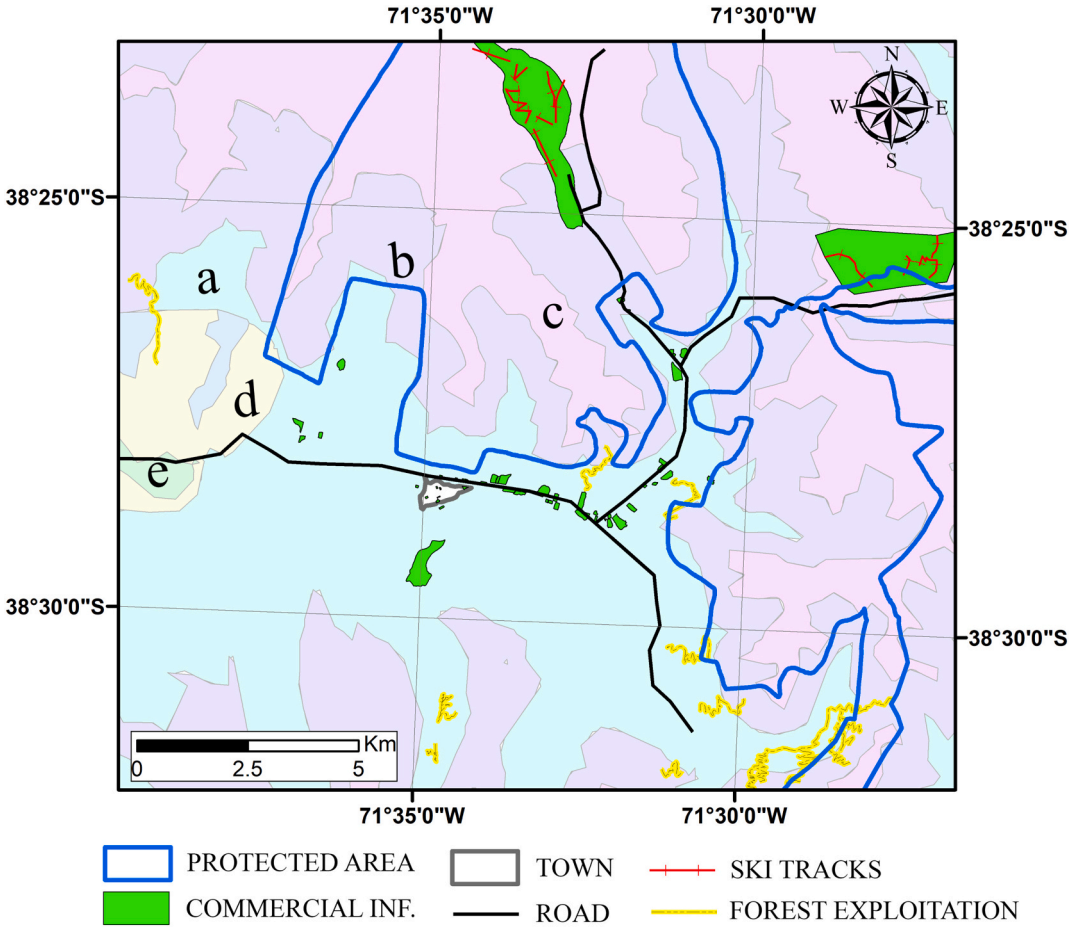

Fig. 2. Coexistence of commercial infrastructure and protected areas in the Araucanian Andes. Protected forest areas (blue borders), urban areas (white polygons) and tourism infrastructure (electric green polygons) are shown. Autochthonous vegetational floors (a-d) are described in the text. The wood extraction routes are mapped (yellow/black lines). The ski center tracks (red lines) are visibly within the margins of the protected areas. (For interpretation of the references to colour in this figure legend, the reader is referred to the web version of this article.)

Parks and Forestry Reservations, Corporación Nacional Forestal (CONAF) could enact all sorts of contracts and execute necessary acts to attain the purpose. In 1984, the National System for Wild Areas was created in Chile with the objective of preserving and improving the representative natural diversity and resources of the country, also including scenic 'resources' and related cultural elements including landscapes and geological sites in order to promote education, research and natural processes of the ecosystem.

There was an area expansion rate between 1950 and 2014 of 0.025 km^2/y and 0.13 km^2/y between 2014 and 2019 around and within mountain protected Areas in the 'Andean Araucanía' at about 38°S of latitude (Additional Table 3).

4.2. Management and EIA

The EIA is not driven by the assumption of different management outcomes apart from that of individuals partaking (both customers and vendors) in the business they regulate. Nevertheless, the pre-

Table 3
General framework for the analysis for landscape value in EIA. (Adapted from Bateman et al., 2010).

Conceptual and legal background	Operative definitions	Ecosystem services Landscape transformation Impacts Value Conservation objectives		Conceptual shortcomings	Limitations of value estimates
	Coercive measures	Appraisal of value	Infringement fines	Value reference	Total value
Value transfer	Reference studies Benefit transfer	transfer	Data quality Normalization and scaling		
Landscape value appraisal	Impacts	Physical impacts	*Natural Resource Damage Assessment* Scale and duration	Value uncertainty	
		Subjective impacts	Significance		
	Landscape baseline	Landscape transformation	Value change		
	Natural capital stocks	Natural insurance value	Changes in the risk premium		
		Management	Moral hazard		
		Contingent valuation	Willingness to pay Willingness to accept compensation	User value	

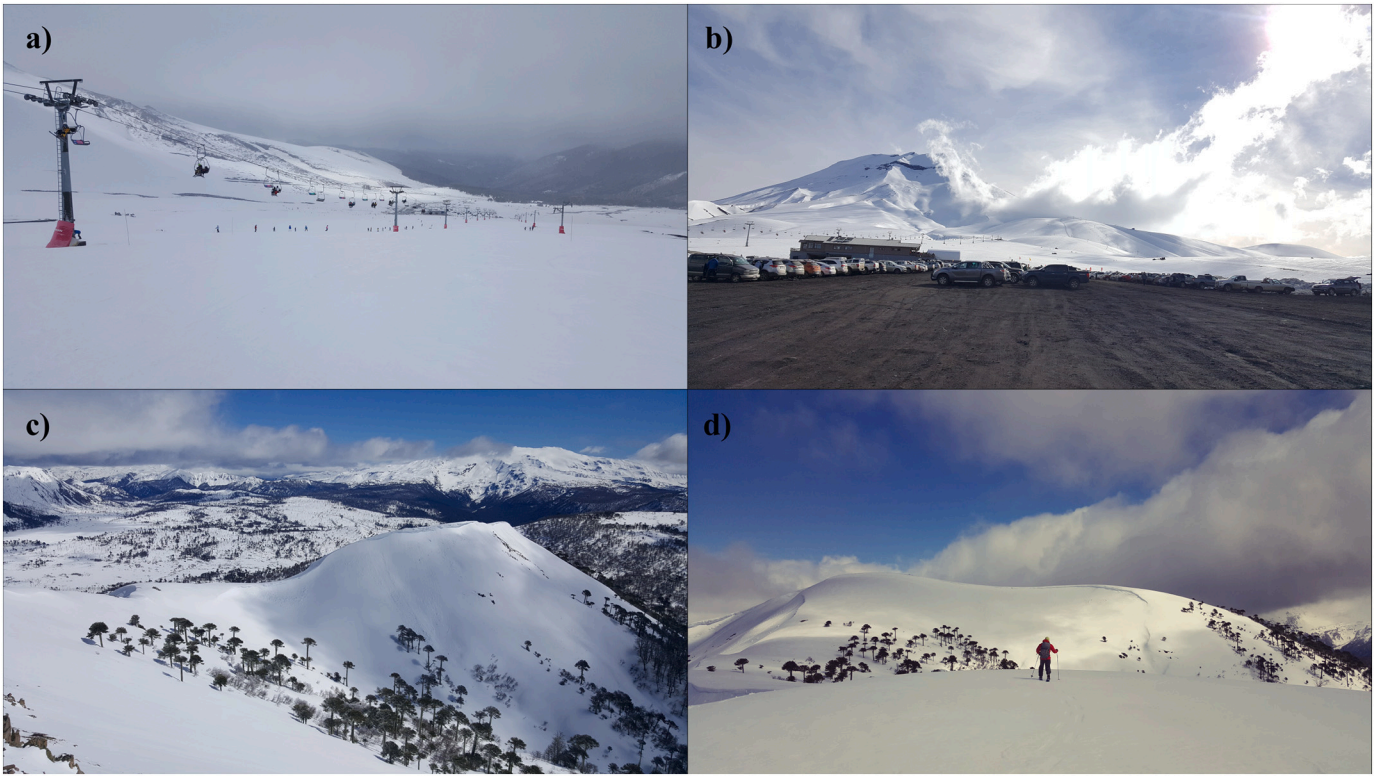

Fig. 3. Transformations of landscape value. Contrasts between commercial concession within a protected mountain area and a private-owned (non-protected) area in the same region. (a) and (b) are the 'Corralco' commercial concession within the 'Malalcahuello' National Reserve for ski activities. Below, (c) and (d) represent unexploited areas in the Andes of the Araucania region.

ascertainment of those possibilities should avoid sub-optimal managements by enforcing that law. In short: the law abiding verbatim, which in the original context is perfectly in harmony with its spirits, goes in the new context against the very spirit of the law.

Once a general baseline is set, it is necessary to analyze which transformations are in process, so it is possible to determine if they are related to a structural neglect by protection framework and hence deemed irrelevant. One task to accomplish is to determine which are the emerging transformations in mountain areas by either State agencies or Commercial agents.

A clear aesthetic dichotomy emerges when contrasting landscapes within the same areas. As seen in Figs. 2 and 3, commercial concessions within mountain protected areas change dramatically the perception of 'where we locate ourselves' as *enworldment* standarizations executed by a private operator happen (Table 2). Also, residents have faced *unworldment* processes with consequent change of identity as investors have commodified the landscape.

Consequently, audiences using Commercial Concessions overlap audiences sightseeing the preexistent landscape. Indirect impacts from increasing audiences to certain landscapes are also important to highlight as small rural roads are not prepared to sustain the high load of trucks and buses carrying hundreds of people within one day.

The agents for economic transformation processes of a protected landscape are Private investors, State agencies, Residents and Foreign/Seasonal residents. Transformations by processes outlined in Table 2 represented consequences of standardization, *cosmopolization* and commodification of mountain protected areas assessed and are attributed to the actions of Private investors, State Tourism and Conservation Agencies in general. Consequences are for example, the identity change of from 'local to global' which may also represent processes valuable for citizens in terms of experience transfer and access to new jobs in the area.

In many cases, both State and Private agencies engage in a dynamic that configures a new touristic landscape without a previous value baseline to compare with. For example, the ecosystem value transfer as benefits was not partaken.

Abrupt expansion of touristic infrastructure (Additional Table 1) usually occurs after the commercial concessions are granted because of capital gain. For example, the Fig. 3 (a and b) shows that clear visual impacts are inherent to concessions, yet inspections only address secondary aspects of the whole transformation as we have explained. In contrast, private-owned areas nearby the National Reserve in Fig. 3 (c and d), still represent the pristine or unspoiled aspect addressed as the object of concern written in Park legislations. Hence, upon the commodification of a protected area, processes of standardization affect the purpose itself of the conservation framework, landscape as a CES. Therefore, results point out that economical transformations derive in the loss of their value, unless an optimal management guarantees the intervention to lie under a conservation threshold compatible with the conservation and landscape value purposes visualized from a baseline.

Cases solving tensions of interest and management in EIAs for USA, Scotland, Iceland, and Chile showed many similarities, for example the selective insulation of land-use according to subjective priorities set by central agencies (Additional Tables 2, 3). Nevertheless, definitions of landscape were sometimes ambiguous or inexistent, allowing us to understand the challenge of grasping its complex dimensionality. The management mission for safeguarding landscape existence-value and integrity is found in the Scottish and Icelandic legislation was valuable because it looked for an integrity (unspoiled character) but ultimately fell short as the rest in our consideration on how does that value evolve and depreciate which is in our opinion a next step for EIAs to take.

Following the example of a Commercial Concession within a mountain protected area, in stage zero, the investment will gain value due to the influence of Ecosystem Services upon it. In brief, snow allows winter sports and the audience uses their facilities but requires a minimum of unspoiled character to remain an appealing experience.

Consequently, the degree of conservation that landscape has, is associated to the experience and therefore to a risk reduction of the commercial operation, since the integrity of the natural asset acts as an insurance value decreasing the uncertainty of business and hence the risk prime.

Environmental valuation should then include compensation devices for 'natural resource injuries' affecting the perceived unspoiled character as an overall value. By transferring available information from previous studies, a door is opened to understand magnitudes of value loss upon granting commercial concessions in protected areas.

In this sense, economic devices like insurance values can be utilized to understand how landscapes will lose value. Natural insurance value stands as the reduction of the risk premium of risky income from ecosystem services when protected areas are managed optimally.

In specific, an ecosystem's natural capital stocks have a natural insurance function if an increase of such stocks decreases the risk premium of benefits from natural capital. Therefore, changes in the natural insurance value are connected to ecosystem management strategies, which indirectly imply moral hazards and uncertainty.

An integration of value transformation processeses is summarized in Table 3. Landscape value appraisal first defines and recognizes values through different tools which are later put in the context transformation/depreciation. These changes are ultimately deductions and uncertainty of revenues and/or fluctuation of capital gain.

In sum, at protected areas the utility of Commercial Concessions could be constrained by the inverse magnitude of landscape value (expressed as an ecosystem service) reducing risk and uncertainty (insurance).

5. Discussion

The present analysis acknowledged the representation of the social-world developed by space organizing agents through cultural-economical operations. Such operations generate their own ecosystem in order to reproduce themselves (Harvey, 2007; Brenner, 2014) often overlooking the changes in the ontological fate of the objects modified, the management outcome. When a Commercial Concession appears within a protected area, it becomes a hybrid category as classified by the Scottish normative (see Additional Tables 1 and 2), meaning it has a dual nature obeying the protection of an area but also embodying the need for a commercial gain.

Current international policies can regulate Concessions in protected areas but fail to consider CESs since they fail to grasp their complexity as it happens at different scales and (epistemological) moments as ambivalent relations between the political aims for preservation and the social reality in protected areas emerge (Frazão-Moreira et al., 2009).

Therefore, the relationship between commercial agencies and protected landscapes may become counterproductive due to inherent transformations rendering depreciation. Landscape value lies in the paradox of no exchange-value and incommensurable nonuse-value or existence value.

Transformations constitute operations changing the value of protected natural assets and consequently human property. Thus, landscape-value as natural capital can go through commodification which is a consequence of *deworldment* processes (Terkenli, 2002), a depreciation due to the disruption of a protected landscape's insulation. Hence, depreciation constitutes a consequence of an artificial appropriation under a valid management.

The direct consequence is that objects under EIA are irrevocably modified and will not be withheld by the same impact thresholds anymore. If audiences are attracted by this transformation, then that landscape baseline is one apart from the one used for granting the Commercial Concession in the first. The shift in value due to transformations is neglected.

The management conflict in Commercial Concession is partially explained as they simply act as a common business and intend to maximize profit in the short-term regardless of the long-term transformation of the asset, a moral hazard. Therefore, there is a commercial relationship with the protected area that presents a conflict between different outcomes through different management strategies.

This sort of "estrangement" from the initial baseline persists under *landscape as a mere viewshed* guideline in EIAs. Tensions between insulation and artificiality parallel the technical (management) dichotomy proposed by Sloterdijk (2000) where a sub-optimal management decreases landscape-value by not exerting adequate protection.

Here we proposed an integrated assessment option for EIAs (Table 3) as a framework coupling legislative and conceptual tools along with economic devices such as natural insurance value. Insurance of landscape-value as incentives for landscape conservation can hedge against the volatility of touristic productivity and convey a combined environment-and-development perspective supplying users with adequate means of financial insurance against their environmentally induced income risk (Lukomska et al., 2014), in our case a Commercial Concession inside protected areas. The examination of the insurance magnitude is the indicator of a certain type of management in the planwork for a given Concession in protected areas. For landscapes, a total current or future use-value has 'non-consumptive' (e.g. recreational activities) direct and indirect use-values with key ecosystem services (Bateman et al., 2010). They are deemed as having insurance-value but also option-value is associated with retaining the option to use a resource in the future.

The notion that landscape's existence-value as an intrinsic value is an object to weigh in the whole intervention, since it is a latent subject of detriment and depreciation of its nonuse-value which nevertheless offers a magnitude of risk reduction by offering capital gain. Such analyses should be present in EIAs to coherently grasp the particularities of landscape and related CES upon the onset and duration of transformations.

The current work reflected on the clash between diverging landscape perceptions and their protection as a matter of discussion. The question is whether conservation is indeed the end itself, or if bipartite goals are detrimental between themselves. As stressed by Frazão-Moreira et al. (2009), the conceptualization of traditional ecological knowledge in administrative policies is different from the local perception of knowledge, and so their convergence should have a common ground.

A conceptual framework of Ecosystem Services in protected areas must be agreed among concerned actors to be sustained in time. If Governments fail to account the transformations behind commercial interventions and protected areas, it is then impossible for effective policies to emerge from that intersection without sacrificing the landscape-value and consequently, capital gain and conservation goals. In this sense, defining landscape in connection to conceptual and economic devices may aid EIAs to understand transformations as transitional impacts.

6. Conclusions

Landscapes undergo transformations beyond the grasp of normative EIA frameworks. These legislations allow Commercial Concessions to intervene protected landscapes under the bipartite purpose of conservation and the engagement of the public with that ecosystem.

Impacted areas show that EIAs do not assess transformations as commodification of landscapes performed by economic agents, resulting in the disruption of landscape character and consequent value loss. A loss in landscape-value is also a loss of capital gain for the Concession.

In this sense, a precautionary management of the ecosystem can be linked to economical devices related to natural insurance value of landscapes.

The type of management is the driver of potential impacts and a

sub-optimal one decreases landscape-value by not exerting adequate protection. Hence, the examination of the insurance value magnitude indicates a type of management uncertainty to be noticed.

In sum, EIAs failing to account landscape transformations behind commercial interventions in protected areas are unable to determine management consequences on landscape-value and its conservation.

Funding

First author received partial funding from FONDAP 1511009 (Fund for Research Centers in Priority Areas, Ministerio de Educación, Gobierno de Chile).

Declaration of Competing Interest

The authors declare that they have no known competing financial interests or personal relationships that could have appeared to influence the work reported in this paper.

Acknowledgements

The Authors acknowledge CONAF, the Malalcahuello Town and Curacautin Townhall and Santiago Rodríguez.

Appendix A. Supplementary data

Supplementary data to this article can be found online at https://doi.org/10.1016/j.eiar.2020.106472.

References

ALTA Consulting, 2019. Landslag og Vindorka. In: Summary for the National Planning Agency, pp. 26–27.
Arrow, K.J., 1962. Economic Welfare and the Allocation of Resources for Invention.
Augeraud-Véron, E., Fabbri, G., Schubert, K., 2019. The value of biodiversity as an insurance device. Am. J. Agric. Econ. 101, 1068–1081.
Bailey, D.W., 1997. Impermanence and flux in the landscape of early agricultural south eastern Europe. na.
Bastmeijer, K., 2016. Natura 2000 and the Protection of Wilderness in Europe.
Bateman, I.J., 1996. Household willingness to pay and farmers' willingness to accept compensation for establishing a recreational woodland. J. Environ. Plan. Manag. 39, 21–44.
Bateman, I.J., Brouwer, R., Cranford, M., Hime, S., Ozdemiroglu, E., Phang, Z., Provins, A., 2010. Valuing environmental impacts: Practical guidelines for the use of value transfer in policy and project appraisal. In: Main Rep. to Dep. Environ. Food Rural Aff. Econ. Environ. Consult. (eftec), London.
Brenner, N. (Ed.), 2014. Implosions/Explosions. Towards a Study of Planetary Urbanization. Verlag GmbH, Berlin.
Bullock, C., 2017. Nature's Values: From Intrinsic to Instrumental. National Economic and Social Council.
Chrenka, B., Ira, V., 2011. Transformation of tourist landscapes in mountain areas: case studies from Slovakia. Hum. Geogr. Stud. Res. Hum. Geogr. 5, 13–20.
Cosgrove, D., Daniels, S., Baker, A.R.H., 1988. The Iconography of Landscape: Essays on the Symbolic Representation, Design and Use of Past Environments. Cambridge University Press.
Cresswell, T., 2008. Place: A Short Introduction. Blackwell Publishing, Malden.
Dallimer, M., Martin-Ortega, J., Rendon, O., Afionis, S., Bark, R., Gordon, I.J., Paavola, J., 2020. Taking stock of the empirical evidence on the insurance value of ecosystems. Ecol. Econ. 167, 106451.
Dudley, N., Higgins-Zogib, L., Mansourian, S., 2009. The links between protected areas, faiths, and sacred natural sites. Conserv. Biol. 23. https://doi.org/10.1111/j.1523-1739.2009.01201.x.
Ehrlich, I., Becker, G.S., 1972. Market insurance, self-insurance, and self-protection. J. Polit. Econ. 80, 623–648.
Europe, C.O., 2000. European landscape convention. In: Report and Convention.
Failler, P., Binet, T., de Battisti, A.B., 2011. Création de la réserve marine régionale du Prêcheur: Diagnostic socio-économique des écosystèmes marins et côtiers. Prêcheur, Rapp. pour le Cons. Régional la Martinique, Fort-de-France (Martinique 1).
Farina, A., 2011. Ecología del Paisaje. Publicaciones de la Universidad de Alicante, Alicante.
Frazão-Moreira, A., Carvalho, A.M., Martins, E., 2009. Local ecological knowledge also 'comes from books': cultural change, landscape transformation and conservation of biodiversity in two protected areas in Portugal. Anthropol 15 Notebooks 27–36.
Freeman, A.M., 1993. Nonuse values in natural resource damage assessment. Valuing Nat. Assets Econ. Nat. Resour. Damage Assess. 264–303.
Gaddis, J.L., 2002. The Landscape of History. How Historians Map the Past. Oxford University Press, Oxford.
Gomes, P.C. da C., 2017. Quadros Geograficos. Uma forma de ver, uma forma de pensar. Bertrand Brasil, Rio de Janeiro.
Gosseries, A., 2008. Theories of intergenerational justice: a synopsis. SAPI EN. S. Surv. Perspect. Integr. Environ. Soc. Vol.1 / n°1.
Green, N., 1995. Looking at the landscape: Class formation and the visual. In: Hirsch, E., O'Hanlon, M. (Eds.), The Anthropology of Landscape. Perspective on Place and Space. Clarendon Press, Oxford, pp. 31–42.
Gutiérrez, I.G., López, Á.L., 2017. Cuatrociénegas: Conflictos asociados al turismo en un área natural protegida. Cuad. Tur. https://doi.org/10.6018/turismo.40.309711.
Hart, J.F., 1988. The rural landscape. JHU Press, pp. 276.
Harvey, D., 2007. Espacios del capital: hacia una geografía crítica. Akal, Madrid.
Heritage, S.N., 2017. Siting and Designing Wind Farms in the Landscape.
Lukomska, N., Quaas, M.F., Baumgärtner, S., 2014. Bush encroachment control and risk management in semi-arid rangelands. J. Environ. Manag. 145, 24–34.
Mill, J.S., 1994. In: Riley, Jonathan (Ed.), Principles of Political Economy.
Müller, M., Job, H., 2009. Managing natural disturbance in protected areas: Tourists' attitude towards the bark beetle in a German national park. Biol. Conserv. 142, 375–383. https://doi.org/10.1016/j.biocon.2008.10.037.
Navrud, S., Ready, R.C., 2007. Environmental Value Transfer: Issues and Methods. Springer.
Neyrat, F., 2017. Elements for an ecology of separation. Gen. Ecol. New Ecol. Paradig. 101.
Óskarsdóttir, A.V., 2011. Náttúruvernd, hvítbók um löggjöf til verndar náttúru Íslands. Reykjavík, Icel, Umhverfisráðuneytið.
Paavola, J., Primmer, E., 2019. Governing the provision of insurance value from ecosystems. Ecol. Econ. 164, 106346.
Pascual, U., Muradian, R., Brander, L., Gómez-Baggethun, E., Martín-López, B., Verma, M., Armsworth, P., Christie, M., Cornelissen, H., Eppink, F., 2010. The economics of valuing ecosystem services and biodiversity. Econ. Ecosyst. Biodivers. Ecol. Econ. Found. 183–256.
Plieninger, T., Dijks, S., Oteros-Rozas, E., Bieling, C., 2013. Assessing, mapping, and quantifying cultural ecosystem services at community level. Land Use Policy 33, 118–129.
Quaas, M., Baumgärtner, S., De Lara, M., 2019. Insurance value of natural capital. Ecol. Econ. 165, 106388.
Rawls, J., 2005. A theory of justice (Original ed.). Cambridge Belkn.
Relph, E., 1976. Place and placelessness. Pion, London, pp. 17.
Reynolds, M.E., 1990. Earthship: How to Build your Own. Earthship Biotecture.
Sanders, B., Ammann, M., Hoff, R., Huston, M., Jenkins, K., Palagyi, T., Pelto, K., Rettig, T., Wagner, A., 2016. Coordinating ecological risk assessment with natural resource damage assessment: a panel discussion. Integr. Environ. Assess. Manag. 12, 616–621.
Santos, J.M.L., 2007. Transferring Landscape Values: How and how Accurately?, in: Environmental Value Transfer: Issues and Methods. Springer, Dordrecht, pp. 45–75. https://doi.org/10.1007/1-4020-5405-x_4.
Sauer, C., 1925. The morphology of landscape. Univ. Calif. Publ. Geogr. 2, 19–54.
Sauer, C., 1963. The morphology of landscape. Univ. Calif. Publ. Geogr. 2, 19–54.
Schama, S., 1996. Landscape and Memory. Vintage, New York.
Servicio de Evaluación de Impacto Ambiental, 2013. Guía para la Evaluación de Impacto Ambiental del Valor Paisajístico, 1st ed. .
Sloterdijk, P., 2000. La domestication de l'être: pour un éclaircissement de la clairière. Editions Mille et une nuits.
Smith, A., 1989. Of the origin and use of money. In: General Equilibrium Models of Monetary Economies. Elsevier, pp. 47–53.
Smith, V.K., Van Houtven, G., Pattanayak, S.K., 2002. Benefit transfer via preference calibration:"Prudential algebra" for policy. Land Econ. 78, 132–152.
Sweezy, P., 1968. Theory of Capitalist Development, the: Principles of Marxian Political Economy.
Terkenli, T.S., 2002. Landscapes of tourism: towards a global cultural economy of space? Tour. Geogr. 4, 227–254.
Therme, T., 2014. Les services d'usage indirect fournis par les écosystèmes marins et côtiers: l'exemple de la Guadeloupe. Études Caribéennes. 27–28.
Torquati, B., Giacchè, G., Venanzi, S., 2015.. Economic analysis of the traditional cultural vineyard landscapes in Italy. J. Rural. Stud. 39, 122–132.
Tuan, Y.F., 1974. Topophilia: A Study of Envi Ronmental Perception, Attitudes, and Values. University of Minnesota Press, Madison.
Tuan, Y.F., 1977. Space and place: The perspective of experience. University of Minnesota Press, pp. 6.
Tuan, Y.F., 2013. Romantic geography. In: Search of the Sublime Landscape. The University of Wisconsin Press, Madison.
Walker, J., 2018. From landscape to ontology in Amazonia. In: Barber, S., Joyce, A. (Eds.), Religion and Politics in the Ancient Americas. New York.
Wilson, M.A., Hoehn, J.P., 2006. Valuing environmental goods and services using benefit transfer: the state-of-the art and science.

Journal of South American Earth Sciences 94 (2019) 102249

Contents lists available at ScienceDirect

Journal of South American Earth Sciences

journal homepage: www.elsevier.com/locate/jsames

Glacier decline in the Central Andes (33°S): Context and magnitude from satellite and historical data

Sebastian Felipe Ruiz Pereira[a,b], Bijeesh Kozhikkodan Veettil[c,d,*]

[a] Instituto de Geografía, Pontificia Universidad Católica de Chile, Santiago, Chile
[b] Center for Climate and Resilience Research (CR2), Universidad de Chile, Santiago, Chile
[c] Department for Management of Science and Technology Development, Ton Duc Thang University, Ho Chi Minh City, Vietnam
[d] Faculty of Environment and Labour Safety, Ton Duc Thang University, Ho Chi Minh City, Vietnam

ARTICLE INFO

Keywords:
Central Andes
Mountain cryosphere
Historical maps
Sentinel-2
Deglacierization

ABSTRACT

Central Andes (33°S) represent a water-scarce region. During arid years, glacier runoff may constitute the main hydrological input at warm season and hence a steadfast deglacierization may represent a decrease in the regional water-budget. Ice-retreat enables landscape transitions from proglacial towards a paraglacial environment, allowing the formation of newly formed cryogenic deposits. Ice-surface changes in the Central Andes (33°S), including the high-mountain areas from Aconcagua, Mendoza and Maipo basins (Argentina and Chile), were studied using digitalized maps, aerial photographs, Landsat (1–8) and Sentinel-2A data for the period between 1956 and 2015. Band ratio and Normalized Difference Snow Index (NDSI) methods were tested using Landsat 8 and Sentinel-2A data for comparison. Geomorphological changes were assessed at Monos de Agua catchment (2750–4000 m a.s.l.) in the Aconcagua basin (Chile) as a regionally representative landscape transition case. Regional glacier shrinkage of 46 ± 5% between 1956 and 2016 was observed for the Central Andean sub-basins in both Argentina and Chile at 33°S. Overall, 107.1 ± 5 km^2 of newly exposed surfaces are subject to permafrost conditions. Such insights raise concern in terms of current and future environmental assessments for newly formed cryospheric elements in water scarce regions.

1. Introduction

Glaciers around the world are losing mass at an unprecedented pace in the early 21st century (Zemp et al., 2015); South American Andes are not exception (Davies and Glasser, 2012; Veettil et al., 2017a, 2017b). Andes Mountains in Chile and Argentina have more than 4000 km in length from 17°30′S to 49°S, most of them are glacierized and the type of glacier, climate, and topography vary latitudinally along the Andes (Lliboutry and Corte, 1998).

Andean Glaciers can either belong to Dry Andes (17°30′S to 35°S) or Wet Andes (35°S to 49°S). Central Andes (between 31°S and 35°S), which is a part of the Dry Andes in Chile and Argentina, had a glacierized area of nearly 2200 km^2 (Lliboutry and Corte, 1998). Rock-glaciers, protalus and gelifluction lobes are predominant cryoforms between 31°S and 33°S and white glaciers are predominant features between 33°S and 49°S (García et al., 2017). The Andes Mountain Range at 33°S has neoglacial and glacial limits oscillating between 3000 and 3300 m a.s.l. for Chile and between and 3400–3650 m a.s.l. for Argentina, respectively (Espizua, 1993), despite the fact that these mountain ranges belongs to similar climatic conditions.

Photogrammetry and remote sensing have been a complementary and sometimes alternative for traditional glaciological observations at high altitudes (Paul et al., 2016; Veettil and de Souza, 2017). Recently, Veettil and Kamp (2017) discussed the suitability of various remote sensing data and methods for long-term monitoring of snow and ice in the tropical Andes, mentioning the potential of high spatial resolution satellite data for delineating glacier boundaries. Medium resolution Landsat series satellite data were mostly used since mid-1970s and the latest of this series – Landsat 8 Operational Land Imager (OLI) – has better geometric stability and radiometric performance (Kääb et al., 2016). Recently, images from the multispectral instrument (MSI) of the Sentinel-2A satellite launched by the European Space Agency (ESA) are available at no cost from the United States Geological Survey (USGS). These data have been predicted to enhance worldwide glacier monitoring (Kääb et al., 2016) and have a spatial resolution of 10 m in four and 20 m in six visible and infrared channels, instead of 15–30 m for Landsat 8. Further improvement is the higher temporal resolution (10 days for Sentinel 2A instead of 16 days for Landsat 8 and better swath

* Corresponding author. Ton Duc Thang University, Ho Chi Minh City, Vietnam.
E-mail address: bijeesh.veettil@tdtu.edu.vn (B.K. Veettil).

https://doi.org/10.1016/j.jsames.2019.102249
Received 13 March 2019; Received in revised form 6 June 2019; Accepted 24 June 2019
Available online 27 June 2019
0895-9811/ © 2019 Elsevier Ltd. All rights reserved.

width (290 km instead of 185 km). However, Sentinel-2A has no thermal channel compared to Landsat 8. In this study, we investigated the possibility of using both Landsat and Sentinel-2A data for glacier observations in Central Argentina and Chile.

The main objective is to assess the context and magnitude regional deglacierization at the climatic border 33°S in the Andes, emphasizing sub-basin scale analysis at Tupungato (Río Mendoza basin, Argentina) and Blanco, Juncal and Olivares Rivers (Chile) using historical maps, aerial photography and satellite imagery. These assessments are relevant considering the sustained regional water scarcity at biodiversity conservation areas (a 13,796 ha Ramsar mountain wetland) (United Nations, 1983) within Juncal Park (Juncal sub-basin, Aconcagua basin, Chile) and sub-basins with ongoing mining prospections (Blanco and Olivares sub-basins) in glacierized areas.

2. Study area and its climatic conditions

The studied glaciers reside within 32°57′27″S; 69°55′04″W, 32°56′43″S; 70°15′37″W, 33°18′48″S; 70°16′26″W; 33°18′32″S; 69°56′00″W and include Juncal Norte, Mono Blanco, Monos de Agua, Colgante Juncal Norte, Juncal Sur, Escondido, Olivares group (Alfa, Beta and Gamma), Esmeralda, La Paloma, Risopatrón and other glaciers on the Chilean side (Fig. 1). Argentinean glaciers included Glaciar Alto and Bajo del Plomo, Río del Plomo, Juncal 1st East, Juncal 2nd East (units alpha, beta and gamma) and other unnamed glaciers (see Appendix 1). This whole region is known for high altitude mountains, including those above 6,000 m a.s.l. Snowline altitudes can be observed below 4500 m a.s.l. in most of the areas (Azócar and Brenning, 2010) and may reach down to an elevation of about 2800 m a.s.l. in the south (Nogami, 1972). Deglacierization and subsequent zonation at sub-catchment scale included Monos de Agua catchment, within Juncal River sub-basin, Aconcagua basin, Chile (33°00′S; 70°06′W). Glaciers in the semi-arid Juncal region belong to the northernmost mid-latitudes (extending from 31°S to 38°S), rather than subtropics, based on the recent classification of glacierized region in the Andes suggested by Sagredo and Lowell (2012) and Sagredo et al. (2014), and so, the present study locates in a region between the Subtropics and Northern Patagonia.

The study region is under the influence of Pacific/westerly (Garreaud et al., 2009) and shows mild wet climate in the winter and a dry climate during the summer (Bown et al., 2008). Westerly winds are responsible for the four months long wet winter (December–March) (Garreaud et al., 2009) and the air temperature near glaciers may vary from −5.3 °C in the winter to 5.5 °C in the summer (Sagredo and Lowell, 2012). Total annual precipitation is less than 750 mm with mean annual humidity slightly above 50%. However, there has been an uninterrupted sequence of dry years in central Chile with a reduction in precipitation ranging from 25% to 45% since 2010 (Garreaud et al., 2017). Using historical (1980–2015) data explorer (http://explorador.cr2.cl) from the Center for Climate and Resilience Research (CR2, University of Chile), 30 stations both north and south of 33°S in Chile showed that the mean annual precipitation ranged from 255.5 ± 46.2 to 474.5 ± 97.3 mm from the north to the south of the study area. Hence, chosen latitude for study partially represents a precipitation gradient.

Since the 1975, snowline elevation has increased by 122 m in the winter and 200 m in the summer and mid-tropospheric warming has been considered as one of the main reasons for glacier retreat in Chile (Carrasco et al., 2005). Glaciers at Central Chile have receded in recent decades in response to changes in the 0 °C isotherm, resulting a 20% reduction in glacier area has observed in the Aconcagua Basin between 1955 and 2006 using Aerial photographs and satellite imagery (Bown et al., 2008). Le Quesne et al. (2009) studied glaciers between 34°31′21″ and 34°42′51″ and established a net retreat (between 1955 and 2007) with mean frontal rates of −22 m/year and −15 m/year in the Chilean and Argentinean sides of the Andes, respectively. Later, Malmros et al. (2016) determined glacier area retreat for the Olivares sub-basin (Maipo River basin, Chile) as 30 ± 3% since 1955–2013. This underlines the importance of a continuous glacier monitoring in this region, particularly under a warming climate. Despite the regional importance of glaciers, this region still remains as data scarce in terms of glaciological records (Pellicciotti et al., 2014).

Glaciers are one of the key factors controlling late-summer runoff in many catchments of the region (Bown et al., 2008; Janke et al., 2015) where mass balance maybe dependent on El Niño–Southern Oscillation (ENSO) occurrence (Waylen and Caviedes, 1990). Further, at Juncal basin's outlet, historical monthly flow range between 1.0 and 30.0 m^3/s (with an annual mean flow of 6.2 m^3/s) (Rodriguez et al., 2016) while Juncal gauging station at Juncal River (32.8625°S; 70.1675°W, 1800 m a.s.l.) (General Directory of Waters, Ministry of Public Works, Government of Chile) showed a decrease in the monthly mean streamflow (in summer) of about 2.5 m^3/s for period 1970–2018 (Data from CR2 explorer) (Source: http://explorador.cr2.cl).

3. Data and methods

This work used Sentinel-2A data for glacier mapping in the South American Andes. Sentinel-2A MSI images are available since 2014 from USGS Earth-Explorer (https://earthexplorer.usgs.gov). For understanding the glacier surface changes between 1956 and 2015, we used historical maps (Lliboutry, 1956), aerial photographs in 1956 (Hycon, scale 1:70,000 and focal length 153.62 mm) and Landsat image series (Thematic Mapper - TM and Enhanced Thematic Mapper Plus - ETM + and OLI) with 30 m resolution. Furthermore, we compared glacier areas estimated from OLI and MSI data acquired on the same date (26th January 2017) near Monos de Agua/Alto del Plomo termini at Monos de Agua catchment (Fig. 2). We used ALOS PALSAR digital elevation model (DEM) with a 12.5 m spatial resolution for understanding topographical features of the study site. Details of the remote sensing data used for this study is summarized in Table 1. Image acquisition dates were restricted to the austral summer since this season is characterized by dry conditions thus reducing potential errors related to seasonal snow cover (Veettil and Kamp, 2017).

For estimating glacier surface in 1956, historical maps (Lliboutry, 1956) with glacier outlines were carefully scanned and later georeferenced using the Hycon (taken in 1955) aerial imagery. The drawn limits in such maps strikingly matched current day moraine limits and photographs taken during expeditions in the same book (Lliboutry, 1956) and the German Andean Club expedition in 1951. Fieldworks done in 2017–2018 also attested the current state of glaciers at Juncal and Monos de Agua sub-catchments for comparison.

Sentinel-2A data has proven to be effective in glacier mapping, such as in the Himalayas and the European Alps, due to its spatial as well as spectral resolution (Kääb et al., 2016; Naegeli et al., 2017; Paul et al., 2016). This research tested these data in the Central Andes.

Normalized difference snow index (NDSI = [Green – SWIR]/[Green + SWIR]) method was used for mapping debris-free glaciers from Landsat images. Two methods (NDSI and band-ratio) were applied to Sentinel-2 data as suggested in Paul et al. (2016). NDSI method has been widely used in the Andes in previous studies (e.g. Silverio and Jaquet, 2005; Veettil and de Souza, 2017; Racoviteanu et al., 2008). For a comparative study, besides NDSI, two band-ratios (Red/SWIR and NIR/SWIR) were tested using MSI and OLI data (MSI4/MSI11 and MSI8/MSI11, which are equivalent to OLI4/OLI6 and OLI5/OLI6 for Landsat 8 and TM3/TM5 and TM4/TM5 for Landsat TM, respectively). The latest Randolph Glacier Inventory (RGI-v6) from the Global Land Ice Measurements from Space (GLIMS) data (https://www.glims.org/) was used to compare the latest glacier boundaries with polygons.

Accuracy of delineated glacier boundary from satellite image can be dependent on the segmentation threshold – too small and too high threshold values may cause overestimation and underestimation of glacier area, respectively (Kamp and Pan, 2015; Paul et al., 2009). To

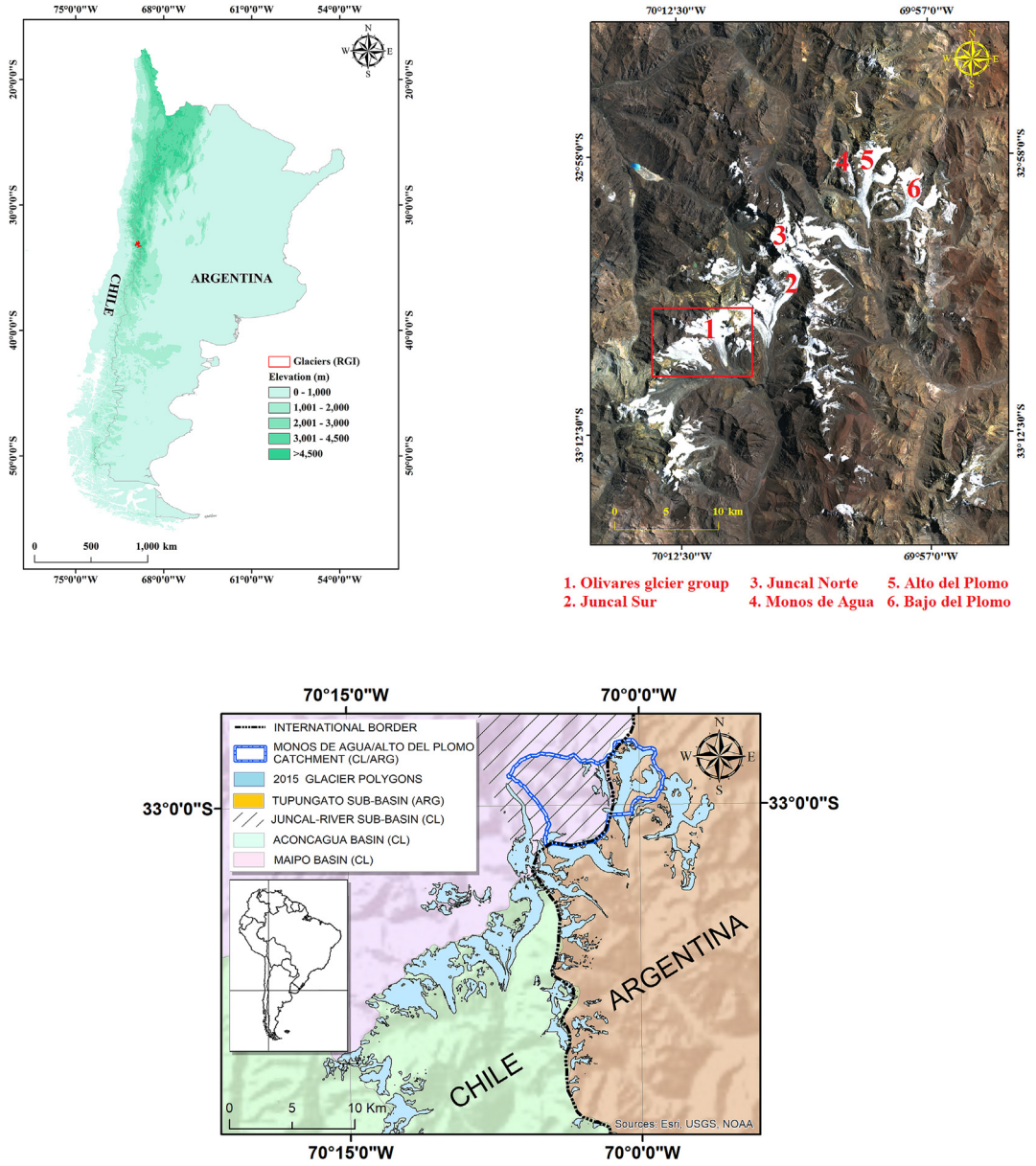

Fig. 1. (a) Geographical location of study area; (b) Satellite image subset showing the glacierized peaks studied; (c) Glacier distribution map in the study area.

estimate the accuracy of glacier polygons derived from satellite data in 1986, 2000 and 2015, Frey et al. (2012) method has been followed; a ± 1-pixel error (A_{er} = ± 100. (f_s.n.m)/A_{gl}) was assumed for glaciers with areas > 0.1 km^2. Here, A_{er} is the error associated with glacier area, A_{gl} is the estimated glacier area, n is the number of pixels defining the perimeter of the glacier, m is the spatial resolution of satellite data expressed as area of a pixel (100 m^2 for a Sentinel-2A image with 10 m pixel size), and f_s is the systematic fractional pixel error that has been taken as 1. For estimating the accuracy of glacier areas in 2015, Bolch et al. (2010) method was followed by comparing the glacier polygons with high resolution images (from Google Earth) for additional errors, if present. Errors due to debris cover and frozen lakes were minimized by manual editing.

Ice retreat has regionally exposed surfaces, which have entered a paraglacial transition (from a proglacial environment), persisting as many ice-rich sedimentary deposits like ice-cored moraines. Monos de Agua/Alto del Plomo sub-catchment was classified by altitudinal zonation (for understanding the thermal conditions of surfaces at different elevation) using 1980–2016 air-surface temperature trends from 5 km reanalysis grids (CR2met – Boisier et al., 2018). Slope characteristics of the areas with recent ice-retreat in the Monos de Agua/Alto del Plomo catchments were estimated from the ALOS PALSAR DEM. The general zonation was generated from the mean annual air temperature (MAAT) obtained from CR2met data, which was resampled by cubic interpolation into a 0.5 km pixel grid. Mapping and outlining of relevant geoforms using the satellite imagery was done in order to correlate geomorphology with the temperature zonation. CR2met 5 km grid for surface temperatures was compared with data from automatic weather station (AWS) deployed in Juncal Norte's proglacial foreland (−32.978°S; −70.115°W). Their comparison was based on 2013–2015 daily measurements. Time series were highly correlated (r = 0.874, p < 2e-09). Monthly and annual sub-sets of data were analysed by One-Way ANOVA in order to determine the statistical significance of their apparent differences.

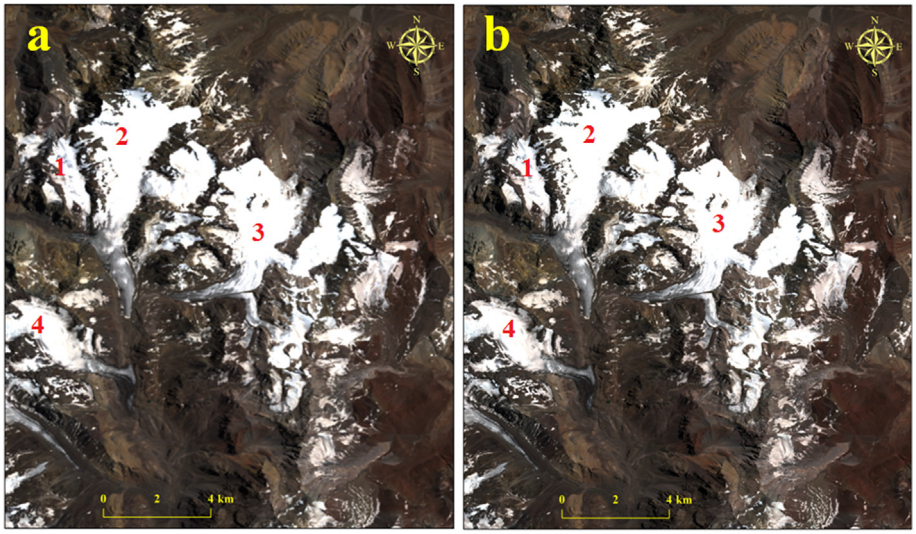

Fig. 2. Comparison of satellite images from selected glaciers: (a) Landsat OLI and (b) Sentinel-2A images.

4. Results

4.1. Overall changes in glacier surface and the suitability of Sentinel-2A for glacier mapping

The overall estimated reduction in selected glaciers in the Juncal sub-basin was 46% and estimated areas in 1956, 1986, 2000, and 2015 were 232 ± 11 km^2, 187.4 ± 5.4 km^2, 156.6 ± 4.4 km^2 and 124.9 ± 3.2 km^2, respectively (Table 2). The overall decline in ice covered areas between 1956 and 2015 was 107.1 km^2. The corresponding error margins in 1986, 2000 and 2015 were ± 2.9%, ± 2.8% and ± 2.6%, respectively. Error margins less than 5% fall within the acceptable limits.

NDSI and two band ratios applied to Landsat-8 OLI and Sentinel-2A MSI data acquired on the same day are shown in Fig. 3. The resulting glacier polygons from these three methods were comparable. NDSI-based polygons gave similar results with OLI and MSI and the area estimated from OLI images using NDSI image was only 0.5% higher compared to the area from MSI and this small difference can be due to mixed pixels (arising from lower spatial resolution of OLI). However, MSI-based glacier maps misclassified a few areas under cast shadows as glaciers and manual editing was needed.

Glacier maps based on OLI4/OLI6 and MSI4/MSI11 band ratios gave slightly different results: OLI-based glacier polygons were 4.1% larger then MSI-based one. Glacier polygons using OLI5/OLI6 were 4.07% larger compared with the ones using MSI8/MSI11. These differences can also be due to mixed pixels arising from relatively lower spatial resolution of the Landsat image. Band ratio methods also resulted in the misclassification of some areas under cast shadows as glaciers while using MSI data. It has been observed that the misclassification of frozen lakes as ice/snow occurred equally with both OLI and MSI data in all the three methods used.

Table 2
Estimated glacier areas in 1955 from historical maps and between 1986 and 2015 from satellite data using NDSI method.

Date of acquisition	Data/Sensor	Area (km^2)
1956	Historical maps	232.7 ± 11
1986 March 01	Landsat TM	187.4 ± 5.4
2000 March 31	Landsat ETM+	156.6 ± 4.4
2015 February 13	Landsat-8 OLI	124.9 ± 3.2
Images used for comparison (Monos de Agua)		
2017 January 26	Landsat-8 OLI	2.38 ± 0.06
2017 January 26	Sentinel-2A MSI	2.39 ± 0.06

4.2. Time series analysis of meteorological data

Time series analysis of CR2met reanalysis data (Fig. 4) showed a decreasing trend in annual accumulated precipitation of about 100 mm ($p > 0.01$) (Fig. 4a) and an increase of about 0.5 °C (1979–2016) in the average surface temperature (Fig. 4b). Fig. 4c shows an increase in the minimum temperature (blue) with only a slight decrease in the maximum (red) annual temperature explaining the increase in the mean temperature throughout the period (black). Additionally, a compression of the (annual surface) thermal amplitude was attested by a 3 °C increase of the minimal mean temperature ($p > 0.01$), while summer temperatures changed only 0.5 °C.

Table 1
Characteristics of remote sensing data used in this study.

Date of acquisition	Data/Sensor	Spatial resolution (m)/Uncertainty (%)	Scene/Product ID/Reference
1955	Aerial photograph	1 m	Hycon aerial photographs
1956	Historical maps	3%	Lliboutry (1956)
1986 March 01	Landsat TM	30 m	LT05_L1TP_233083_19860301_20170218_01_T1
2000 March 31	Landsat ETM+	30 m	LE07_L1TP_233083_20000331_20170212_01_T1
2015 February 13	Landsat-8 OLI	30 m	LC08_L1TP_233083_20150213_20170413_01_T1
2017 January 26	Landsat-8 OLI	30 m	LC08_L1TP_232083_20170126_20170214_01_T1
2017 January 26	Sentinel-2A MSI	10 m, 20 m	L1C_T19HDD_A008344_20170126T144125

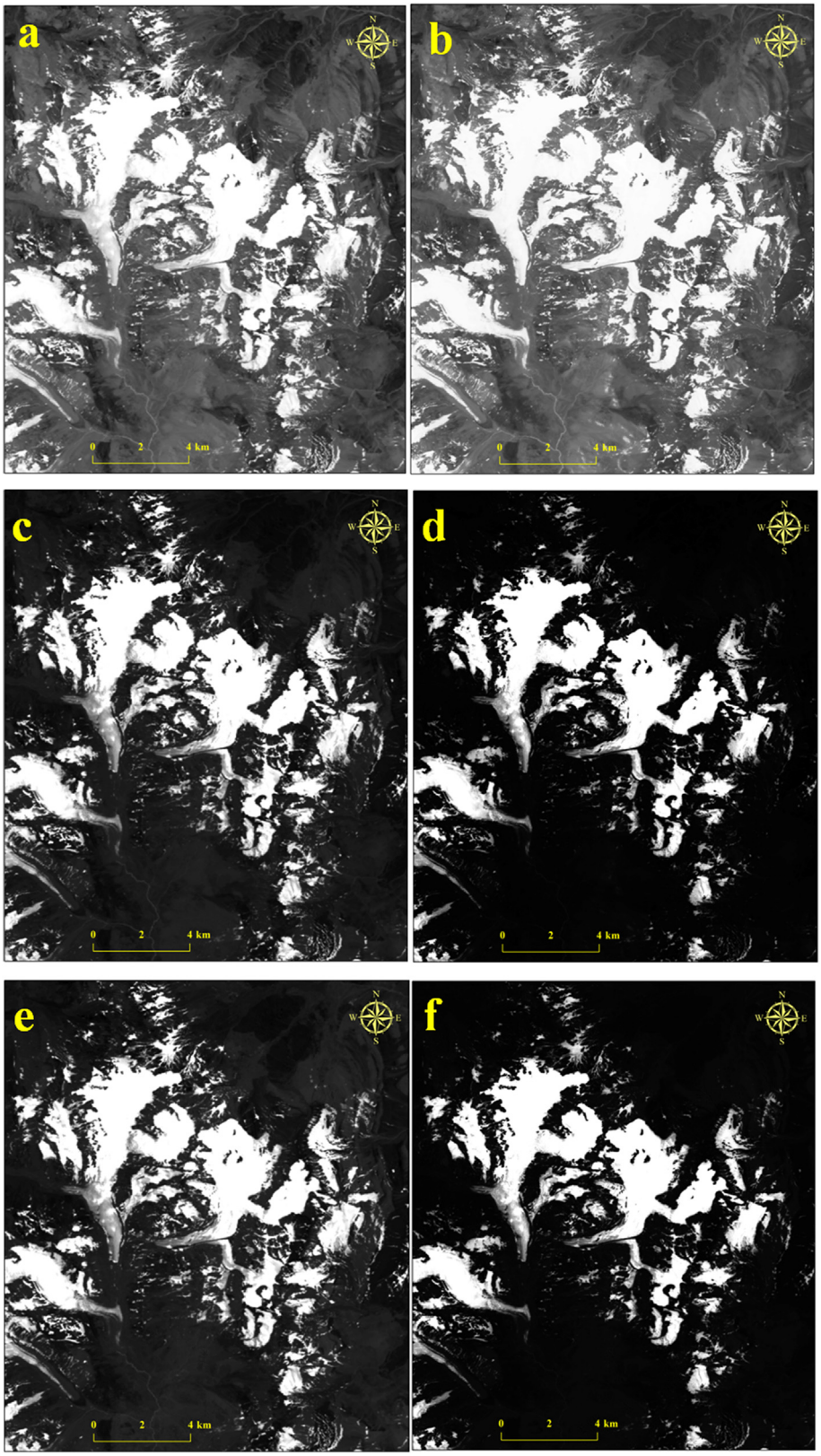

Fig. 3. (a–b) NDSI applied to OLI and MSI; (c–d) OLI4/OLI6 and MSI4/MSI11 (e–f) OLI5/OLI5 and MSI8/MSI11 (images on the left and the right have comparable wavelengths).

4.3. Altitudinal zonation of Monos de Agua and Alto del Plomo sub-catchments

The general zonation of Monos de Agua and Alto del Plomo sub-catchments are given in Table 3. Three distinct zones, which are differentiated attitudinally, were shown in the table. Briefly, sub-catchment zonation at Monos de Agua/Alto del Plomo sub-catchment (Table 3): (I) periglacial conditions categorized by secondary sediment

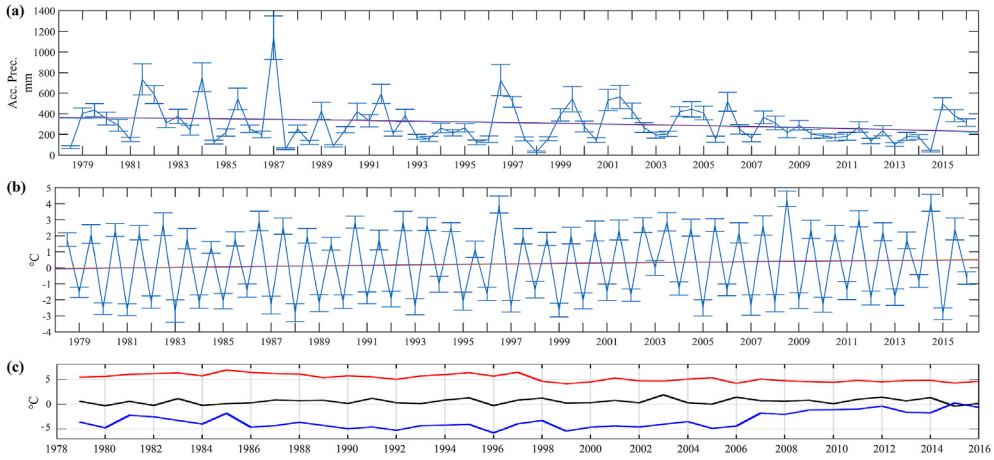

Fig. 4. Surface temperature and precipitation time-series (1979–2016) for Juncal Basin (3200 m a.s.l.) location. (a) Data from CR2met reanalysis shows a decreasing trend for precipitation > 100 mm and a surface temperature increase of about 0.5 °C (b). (c) shows an increase of minimal temperature (blue) but a slight decrease of the maximal (red) annual temperature explaining a steady mean throughout the period (black). A compression of the surface thermal amplitude is hence attested as product of an increasing winter temperature. (For interpretation of the references to color in this figure legend, the reader is referred to the Web version of this article.)

Table 3
General zonation of Monos de Agua/Alto del Plomo sub-catchments.

Basin Segment (m a.s.l.)	Relevant feature	Area	Area/total (%)	Air temperature (1979–2016) range (CR2met)	Morphogenic paraglacial transition	Sediment cohesive deposit
I	*Sub-basin total*	13.7		1.4 to (−4.7)		Fans/Slopes and
2775–3200	Sandur	0.51	3.7		Lower Paraglacial sequence.	Outwash plains
	Alluvial Fans & Slopes	4.48	**32.7**		Mature landscape	
	Rock Glacier associated landform	0.14	1.0		Periglacial conditions	
II	*Sub-basin total*	11		−1.6 to (−4.7)		Rock glaciers (both
3200–3600	Sandur	–	–		Paraglacial condition with secondary	active/inactive)
	Alluvial Fans & Slopes	0.84	7.6		sediment reworking	Moraines & relict ice in
	Glacier	0.88	8.0			slopes.
	Rock Glacier associated landform	1.48	**13.5**			
III	*Sub-basin total*	16.7		−3.1 to (−4.7)	Glacial:	Moraines and Taluses
3600–4000	Sandur	–	–		A proglacial condition with higher	
	Alluvial Fans & Slopes	0.78	4.7		paraglacial sequence	
	Glacier	3.62	**21.7**			
	Rock Glacier associated landform	0.45	2.7			
	Ice Cored Moraine	0.58	3.5			
	Hummocky Terrain – Solifluction	0.36	2.2			

rework and mature features like outwash plain and wetland, (II) transitional paraglacial conditions with dead ice bodies and relict moraines subject to secondary reworking, (III) proglacial environment with clear glacier effects on the sedimentary geoforms.

4.4. Different contexts of glacial landscape evolution at 33°S in the Andes: deglacierization at Monos de Agua/Alto del Plomo sub-catchment, Juncal Basin

Shapefile for Alto del Plomo Glacier obtained from the topographic map (Lliboutry, 1956) describes an eastward terminus retreat until the current limit of 1 km. In 1956, Monos de Agua and Alto del Plomo glaciers were connected (Figs. 5 and 6). A rock-glacier type flow from Mono Verde mountain also contacted Alto del Plomo, being buttressed by its (southern) lateral moraine.

Later, this 1 km retreat left a consistent lateral moraine with southward exposition as seen in Fig. 5 (right), contacted by several solifluction lobes present. Alto del Plomo terminus retreated 500 m from 1956 to 1979 (Landsat 1), until forming an apparent frontal contact there. So, a rough retreat rate (1956–1979) of 22 m/year for Alto del Plomo implies that it was higher than for the remaining period (1979–2016) with 13.5 m/year; the average 1956–2016 was around 18 m/year. Mono Verde is currently depleted from massive ice content at least in appearance (Fig. 6).

Present day topography (Fig. 6) shows that the first 0.5 km (1956–1979) has a maximum slope of 30.8 ± 6.7% (three measurements median absolute deviation) and remnant 500 m (1979–2016) with 41.5 + -7.7%. Both north and south facing moraines show strong gullying from 1956 terminus. Yet, this feature does exist 400 m ahead and progressively fades away with the lateral moraine ridge. The westward segment might correspond to a previous retreat.

On these lateral moraine ridges, clear progradation is visible; south-facing moraine presents apparent sediment overspilling from gelifluction lobes and north-facing ridge shows progradation from flows coming down from Mono Verde Mountain.

From previous statements, it is possible to establish that Alto del Plomo Glacier contained and buttressed the 'rock glacier' flowing downward Mono Verde Mountain (avg. slope 29.5% and max. slope 50%) (Fig. 6 - bottom). Hence, it is possible that, between 1956 and 1979, there was a loss of cohesion at that lateral moraine ridge with subsequent gullying, finally accomplishing an overspilling of sediment (Cossart and Fort, 2008) generating a fan in between gullies.

Since the south-facing lateral moraine is evidently less exposed to direct solar radiation, this side doesn't show such an overspilling likely due to a fast-rate loss of cohesion upon glacier damming retreat, yet they do have a clear streamflow incision from Mono Blanco outflow. Nevertheless, cryoform related elements such as gelifluxion lobes are present along the south-facing moraine ridge, which is surpassed by

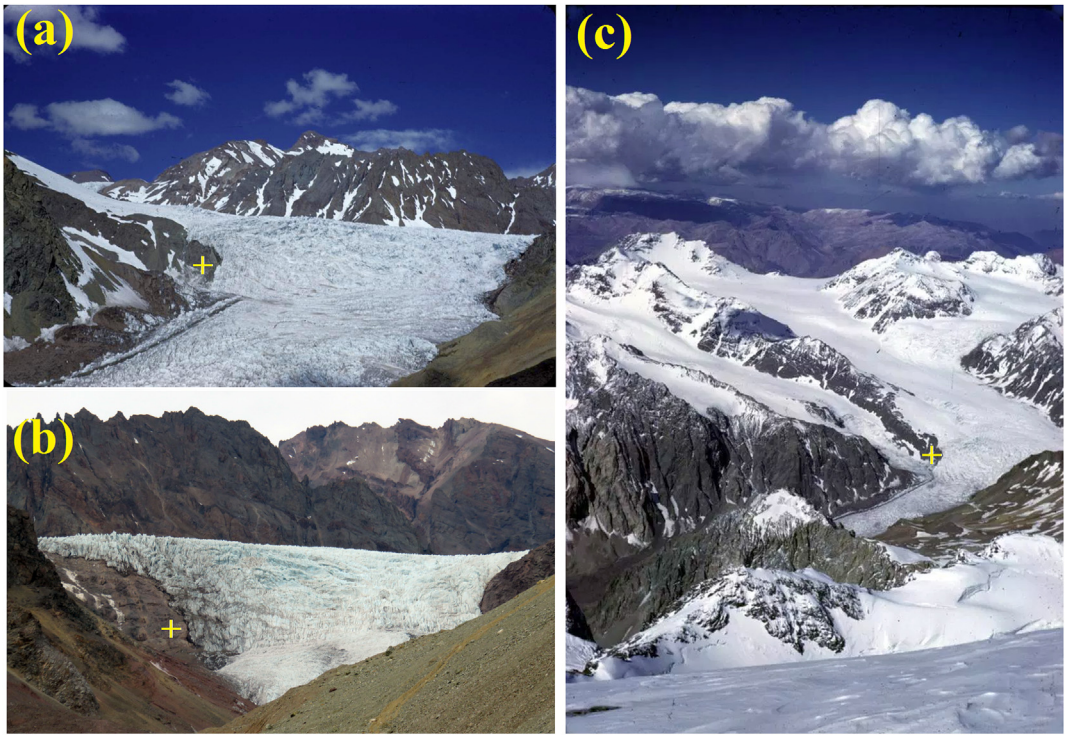

Fig. 5. Monos de Agua/Alto del Plomo sub-catchment. North at 9pm in all photos. (a) Alto-Del-Plomo Glacier in 1951 (Photo: Eberhard Meier Bornet). (b) Alto-Del-Plomo Glacier in 2017 (Photo: SF Ruiz Pereira.). (c) Monos de Agua (N-S orientation) and Alto-Del-Plomo (curved westwards) Glaciers (Photo: Eberhard Meier Bornet).

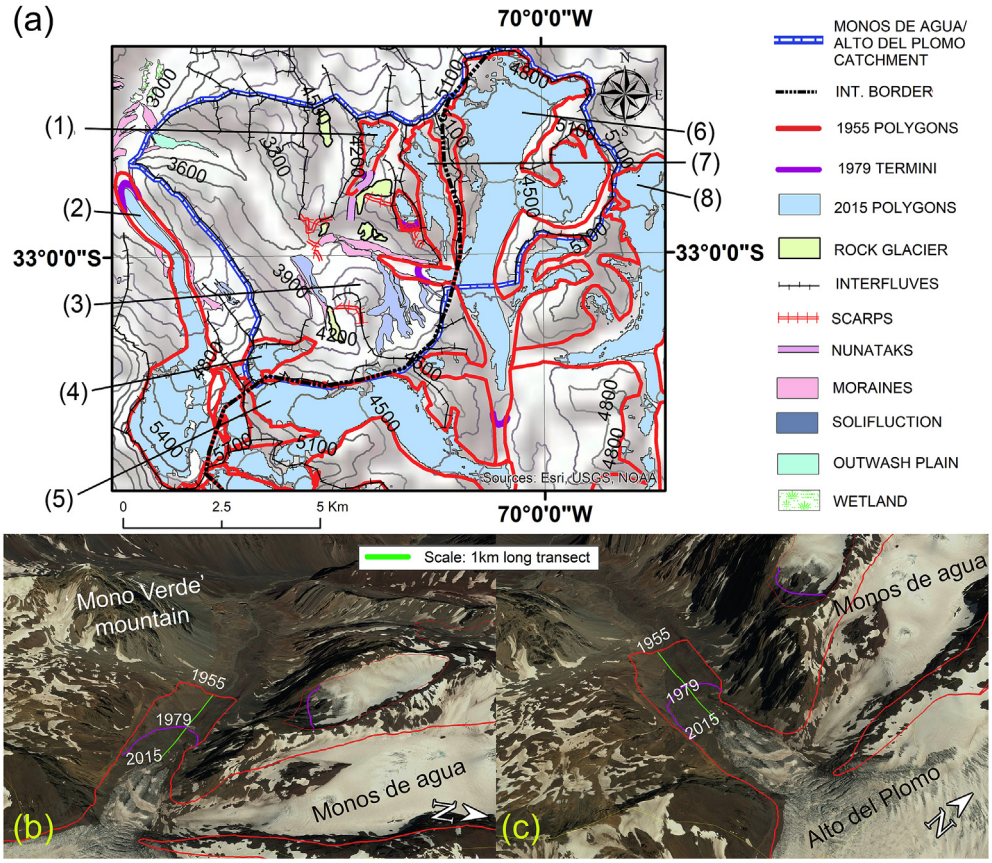

Fig. 6. (a) Glacier changes in the study area between 1955 and 2015; (b–c) Monos de Agua and Alto del Plomo Glacier from different angles showing the glacier retreat between 1955 and 2015 at Argentina/Chile border between 1955 and 2015 (Source: Google Earth, 2017).

lobes with a steep slope (74%) from the ridge onwards their roots. The importance of this south-facing border is hence related to cryoforms present, also consistent with the presence of thermokarst lakes.

As seen in Fig. 6 (top), leftward edge shows the end of the upper segment of the sub-catchment which coincides with a tectonic knick-point (200 m cliff). This edge (Fig. 6, middle at bottom), presents an interesting geoform, a mound, possibly related to a relict frontal-deposit likely to be left out after the Little Ice Age (LIA).

Considering an overall retreat of 18 m/year of the Alto del Plomo (westward) tongue, this means that sedimentary mounds 1.15 km ahead could be related to glacier's position by the end of the XIX, which would explain the presence ice-cored moraine until that point. l.

5. Discussion

Andean basins at 33°S latitude are water-scarce regions and will endure even more drastic hydric shortages in the next decades. Studied glaciers in the Central Andes of Chile underwent a considerable shrinkage (more than 45% or more than 18 km^2/decade) in their ice-covered areas between 1956 and 2015. Historical maps and time-series analysis of satellite imagery made it possible to analyse the 60-year changes in glacierized areas in this region.

Our findings were larger than ice-surface lost estimated for the Olivares sub-basin by Malmros et al. (2016) (30 ± 3% from total) between 1956 and 2013. The present study included neighbouring sub-basins which differ in their overall ice-loss percentage over a six-decade span, hence becoming a regional estimate. The decreasing trend in glacier loss was observed in the south of the study area by Farias-Barahona et al. (2019); the authors observed highly negative mass balance (-1.2 ± 0.09 m w.e.a^{-1}) conditions since 2010 and a 65% total area loss for Echaurren Norte Glacier in Central Andes (of Chile). In addition, Le Quesne et al. (2009) also observed that the glaciers in the Central Andes (of Chile and Argentina) experienced reduction in the ice thickness and mean area since 1955.

As a consequence of deglacierization, around $107 \pm 5\,km^2$ of mountain surfaces are now subject to new ground thermal conditions that may elicit either; permafrost occurrence, persistence or degradation. The catchment studied at 33°S in Argentina/Chile, shows that, above 3200 m a.s.l., there are very young areas left by recent deglacierization, which remain in a current paraglacial transition (secondary sedimentary reworking and further, considering their surface thermal regime endure periglacial environment type conditions (frost events).

Andean basins at 33°S latitude are water-scarce regions and will endure even more drastic hydric shortages in the next decades. We attested a causality exerting effects on glacierized catchments due to natural forcing and the magnitude of deglacierization was exemplified by a representative case at Monos de Agua/Alto del Plomo catchment ice retreat. In order to quantify the reduction in stored ice, volume changes using ice-thickness data is necessary.

Considering an overall retreat of 18m/year of the Alto del Plomo (westward) tongue, this means that sedimentary mounds 1.15 km ahead could be related to glacier's position by the end of the XIX, which would explain the presence of ice-cored moraine until that point. There, a tectonic uplift is present, which aids a differential sedimentary accumulation (Fig. 6). By 1956, Monos de Agua and Alto del Plomo glaciers were connected (Figs. 5 and 6) and, possibly, Monos Verdes had a direct contact with Alto del Plomo terminus if not sufficiently buttressed by the lateral moraine.

Alto del Plomo (westward tongue) retreated and lost cohesion of lateral moraines, in this case, incision happened when streams were before buttressed by it (South Facing Moraine), but where rock-glacier like flows were present (North facing slope from Mono Verde Mountain), a general glacier overspilling happened. On the other hand, Alto del Plomo (southernmost terminus in Argentina) has a different setting, and just covered up and no signs of the two mechanisms mentioned above is there present.

Considering deglacierization context, water from glacial input at warm season is the sole source during dry years, the issue hasn't yet been approached by Chilean authorities; since more than twelve years have already passed since first attempts to implement a specific legislation for glaciers, rock glaciers and permafrost. Since the last official attempt to legislate such elements of the cryosphere has failed in 2018, the question remains unanswered whether permafrost will be legislated, since it is neglected by the only protection measure - Law Water Code (*Código de Aguas*) - which only interprets glaciers as hydrological assets (Chilean Gov. Water Code, Art. 5)..

As explained, landscape transition from glacial to paraglacial environments has interesting considerations regarding water-resources. A first stage of ice-retreat in Central Andes implies sediment deposition at glacier snout (exemplified by Infiernillo, Colgante del Juncal and Juncal Norte) hence segmenting the whole unit which renders interpretation issues in hydrological terms. As presented in the sub-catchment scale deglacierization example at Monos de Agua/Alto del Plomo sub-catchment (subsidiary of Juncal within Aconcagua basin), much centennial scale ice-loss processes were permafrost-related; nowadays mean annual air temperature remains at -2 °C at 3,600 m a.s.l. (33°S) and terminus retreat leaves no homogeneous topography but occasional ice-rich deposits instead. For example, an apparent 0.68 km^2 ice-cored moraine is nowadays present at Monos de Agua sub-catchment and one of 0.41 km^2 at Juncal Norte, the latter with massive metric ice therein.

Considering numerical projections estimating a snowpack decrease around 40% by 2050's and an atmospheric warming rate of at least 1 °C at 30–40°S (Bozkurt et al., 2018), the area is acknowledged as very important to investigate since the glacierized catchments like Juncal, which have at least half their freshwater input from glacial source (Rodriguez et al., 2016). This way a likely regional water deficit downstream from Juncal Basin may directly affect water quality and amount, past events such as the last mega-drought period (2010–2015) (Garreaud et al., 2017) and current expansion of mountain mining industry may further recrudesce an already urgent situation.

These ambiguities are a clear signal that; either the current environmental legislation body is not up to the task of correctly assesses a mega-project as such, in such environments, and/or, the lack of a specific expert-developed legislation plan is mandatory to fulfil such gap yet absent. Both examples - a natural ice-loss process and constant intervention on water resources by private entities, portrait challenges of glacierized basin assessment in officially-declared water scarce regions. Two sides of one problem which is the concern and need for water resources in current and future times.

6. Conclusions

Using the latest Sentinel-2A MSI and Landsat images and historical photographs, we estimated the changes in glacier area of selected glaciers in the semi-arid region of Central Andes in the Chile-Argentina border and compared the performance of these data for glacier mapping using three different methods.

There was more than 45% regional reduction in glacierized areas in the Juncal basin between 1956 and 2015. The error margins were below ± 5% while estimating glacier surface areas. Nevertheless, glacierized asymmetries between Chile and Argentina weren't relevant since during 1956–2015, regional retreat was 47.7% and 47.3% for Chile and Argentina respectively. Since snow-covered mountains in the Central Andes are the major freshwater resource for the highly populated cities of Santiago (Chile) and Mendoza (Argentina), a continuing reduction in the glacierized areas may have negative consequences on the regional communities.

Methods using remote-sensing determined that NDSI-based glacier areas were similar in area for both OLI and MSI data and band ratio methods resulted in glacier areas were 4% larger from OLI compared with MSI. Even though problems related to mixed pixels in MSI data is less compared with OLI dat. a while using NDSI method, MSI data

misclassified a few areas under cast shadows as snow/ice even with a high threshold value and manual editing was needed. Being (relatively) superior in spatial resolution and spectral characteristics, Sentinel 2A data can be used as a good substitute for Landsat 8 images for glacier observation in the semi-arid Andes, except when thermal channels are necessary.

Main processes initiated by deglacierization are basically cohesion loss upon ice-retreat, which may cause a) incision of lateral moraine, b) overspilling and fan development in case of solifluction and c) detritus cover-up. The study has presented the relevance of assessing ice-containing geoforms in deglacierized catchments, which is an object absent in the asset dimension of the Water Code of Law from the Chilean Government.

Last but not the least, there are ongoing mining operations located at high altitude (> 3600 m a.s.l.) in the study region, highlighting legislation gaps in water-scarce regions and industrial negligence as it will be displayed. Glaciers in the Central Andes can be affected by natural as well as anthropogenic (e.g. mining) activities. Both perspectives (natural and anthropogenic) rely on the same object, hydric resources at high altitudes. Future studies may focus on the impacts of such anthropogenic activities in this water scarce region.

Conflicts of interest

Authors declare no conflict of interest.

Acknowledgements

First author acknowledges FONDAP 1511009 (Fund for Research Centers in Priority Areas, Ministerio de Educación, Gobierno de Chile).

Appendix 1. List of glaciers analysed in Argentina and Chile

Local name	GLIMS ID	Location		Country	Basin	Sub-basin
		Latitude	Longitude			
Alto del Plomo	G289993E32989S	−32.9834	−70.0073	Argentina	Mendoza river	Tupungato river
Bajo del Plomo	G290034E33011S	−33.0108	−69.9638	Argentina	Mendoza river	Tupungato river
unnamed	G290041E33060S	−33.0499	−69.9604	Argentina	Mendoza river	Tupungato river
Oriental del Juncal	G289959E33033S	−33.0382	−70.0461	Argentina	Mendoza river	Tupungato river
unnamed	G290037E33056S	−33.0558	−69.9558	Argentina	Mendoza river	Tupungato river
unnamed	G290073E33026S	−33.0362	−69.9414	Argentina	Mendoza river	Tupungato river
Grande del Juncal	G289940E33061S	−33.0583	−70.0658	Argentina	Mendoza river	Tupungato river
Alfa	G289935E33076S	−33.0769	−70.065	Argentina	Mendoza river	Tupungato river
Beta	G289943E33087S	−33.0875	−70.0568	Argentina	Mendoza river	Tupungato river
Gamma	G289954E33100S	−33.1002	−70.0467	Argentina	Mendoza river	Tupungato river
Grande del Nevado	G289966E33120S	−33.1172	−70.0641	Argentina	Mendoza river	Tupungato river
unnamed	G289966E33166S	−33.1608	−70.0477	Argentina	Mendoza river	Tupungato river
Gl. Pequeño del Nevado	G289966E33139S	−33.138	−70.028	Argentina	Mendoza river	Tupungato river
unnamed	G289943E33199S	−33.1996	−70.0578	Argentina	Mendoza river	Tupungato river
unnamed	G289966E33166S	−33.1741	−70.0524	Argentina	Mendoza river	Tupungato river
Monos de Agua	G289975E33004S	−32.985	−70.031	Chile	Aconcagua River	Juncal river
unnamed	G289963E32990S	−32.99	−70.038	Chile	Aconcagua River	Juncal river
unnamed	G289956E32973S	−32.972	−70.045	Chile	Aconcagua River	Juncal river
Colgante del Juncal Norte	G289926E33023S	−33.024	−70.074	Chile	Aconcagua River	Juncal river
Juncal Norte	G289902E33030S	−33.039	−70.105	Chile	Aconcagua River	Juncal river
unnamed	G289865E32973S	−32.973	−70.137	Chile	Aconcagua River	Juncal river
unnamed	G289851E32983S	−32.974	−70.149	Chile	Aconcagua River	Juncal river
unnamed	G289864E33019S	−33.012	−70.13	Chile	Aconcagua River	Juncal river
Río Blanco	G289879E33050S	−33.067	−70.134	Chile	Aconcagua River	Blanco river
Río Blanco	G289848E33070S	−33.065	−70.155	Chile	Aconcagua River	Blanco river
Río Blanco	G289865E33068S	−33.049	−70.12	Chile	Aconcagua River	Blanco river
Juncal Sur	G289884E33094S	−33.097	−70.114	Chile	Maipo river	Olivares river
unnamed	G289864E33133S	−33.134	−70.135	Chile	Maipo river	Olivares river
unnamed	G289854E33132S	−33.135	−70.148	Chile	Maipo river	Olivares river
Olivares Gamma	G289815E33129S	−33.123	−70.168	Chile	Maipo river	Olivares river
Olivares Beta	G289815E33129S	−33.137	−70.198	Chile	Maipo river	Olivares river
Olivares Alfa	G289777E33194S	−33.169	−70.239	Chile	Maipo river	Olivares river
Olivares Alfa	G289767E33184S	−33.175	−70.233	Chile	Maipo river	Olivares river
Olivares Alfa	G289761E33173S	−33.19	−70.222	Chile	Maipo river	Olivares river
La Paloma	G289731E33188S	−33.189	−70.267	Chile	Maipo river	San Francisco river
Del Rincón	G289718E33183S	−33.182	−70.282	Chile	Maipo river	San Francisco river
Esmeralda	G289794E33222S	−33.216	−70.209	Chile	Maipo river	Olivares river
De los Castaños	G289803E33242S	−33.241	−70.204	Chile	Maipo river	Olivares river
Iver	G289782E33246S	−33.238	−70.222	Chile	Maipo river	Molina river

Appendix A. Supplementary data

Supplementary data to this article can be found online at https://doi.org/10.1016/j.jsames.2019.102249.

References

Azócar, G.F., Brenning, A., 2010. Hydrological and geomorphological significance of rock glaciers in the dry Andes, Chile (27°-33°s). Permafr. Periglac. Process. 21, 42–53. https://doi.org/10.1002/ppp.669.

Boisier, J.P., Alvarez-Garretón, C., Cepeda, J., Osses, A., Vásquez, N., Rondanelli, R., 2018. CR2MET: a high-resolution precipitation and temperature dataset for hydroclimatic research in Chile. Geophys. Res. Abstr. 20, EGU2018–19739.

Bolch, T., Menounos, B., Wheate, R., 2010. Landsat-based inventory of glaciers in western Canada, 1985-2005. Rem. Sens. Environ. 114, 127–137. https://doi.org/10.1016/j.rse.2009.08.015.

Bown, F., Rivera, A., Acuña, C., 2008. Recent glacier variations at the Aconcagua basin, central Chilean Andes. Ann. Glaciol. 48, 43–48. https://doi.org/10.3189/172756408784700572.

Bozkurt, D., Rojas, M., Boisier, J.P., Valdivieso, J., 2018. Projected hydroclimate changes over Andean basins in central Chile from downscaled CMIP5 models under the low and high emission scenarios. Clim. Change 150, 131–147. https://doi.org/10.1007/s10584-018-2246-7.

Carrasco, J.F., Casassa, G., Quintana, J., 2005. Changes of the 0°C isotherm and the equilibrium line altitude in central Chile during the last quarter of the 20th century. Hydrol. Sci. J. 50, 3741. https://doi.org/10.1623/hysj.2005.50.6.933.

Cossart, E., Fort, M., 2008. Sediment release and storage in early deglaciated areas: towards an application of the exhaustion model from the case of Massif des Écrins (French Alps) since the Little Ice Age. Norsk Geogr. Tidsskr.-Norwegian J. Geogr. 62 (2), 115–131. https://doi.org/10.1080/00291950802095145.

Davies, B.J., Glasser, N.F., 2012. Accelerating shrinkage of Patagonian glaciers from the Little ice Age (~AD 1870) to 2011. J. Glaciol. 58, 1063–1084. https://doi.org/10.3189/2012JoG12J026.

Espizua, L.E., 1993. Quaternary Glaciations in the Rio Mendoza valley, Argentine Andes. Quat. Res. 40, 150–162. https://doi.org/10.1006/qres.1993.1067.

Farias-Barahana, D., Vivero, S., Casassa, G., Schaeferm, M., Burgerm, F., Seehaus, T., Anacona, P.I., Escobar, F., Braun, M.H., 2019. Geodetic mass balances and area changes of Echaurren Norte Glacier (central Andes, Chile) between 1955 and 2015. Rem. Sens. 11 (3), 260. https://doi.org/10.3390/rs11030260.

Frey, H., Paul, F., Strozzi, T., 2012. Compilation of a glacier inventory for the western Himalayas from satellite data: methods, challenges, and results. Rem. Sens. Environ. 124, 832–843. https://doi.org/10.1016/j.rse.2012.06.020.

García, A., Ulloa, C., Amigo, G., Milana, J.P., Medina, C., 2017. An inventory of cryospheric landforms in the arid diagonal of South America (high Central Andes, Atacama region, Chile). Quat. Int. 438, 4–19. https://doi.org/10.1016/j.quaint.2017.04.033.

Garreaud, R.D., Alvarez-Garreton, C., Barichivich, J., Boisier, J.P., Christie, D., Galleguillos, M., LeQuesne, C., McPhee, J., Zambrano-Bigiarini, M., 2017. The 2010-2015 megadrought in central Chile: impacts on regional hydroclimate and vegetation. Hydrol. Earth Syst. Sci. 21, 6307–6327. https://doi.org/10.5194/hess-21-6307-2017.

Garreaud, R.D., Vuille, M., Compagnucci, R., Marengo, J., 2009. Present-day south American climate. Palaeogeogr. Palaeoclimatol. Palaeoecol. 281, 180–195. https://doi.org/10.1016/j.palaeo.2007.10.032.

Janke, J.R., Bellisario, A.C., Ferrando, F.A., 2015. Classification of debris-covered glaciers and rock glaciers in the Andes of central Chile. Geomorphology 241, 98–121. https://doi.org/10.1016/j.geomorph.2015.03.034.

Kääb, A., Winsvold, S.H., Altena, B., Nuth, C., Nagler, T., Wuite, J., 2016. Glacier remote sensing using sentinel-2. part I: radiometric and geometric performance, and application to ice velocity. Rem. Sens. 8, 598. https://doi.org/10.3390/rs8070598.

Kamp, U., Pan, C.G., 2015. Inventory of glaciers in Mongolia, derived from Landsat imagery from 1989 to 2011. Geogr. Ann. Ser. A Phys. Geogr. 97, 653–669. https://doi.org/10.1111/geoa.12105.

Le Quesne, C., Acuña, C., Boninsegna, J.A., Rivera, A., Barichivich, J., 2009. Long- term glacier variations in the Central Andes of Argentina and Chile, inferred from historical records and tree-ring reconstructed precipitation. Palaeogeogr. Palaeoclimatol. Palaeoecol. 281 (3–4), 334–344. https://doi.org/10.1016/j.palaeo.2008.01.039.

Lliboutry, L., 1956. Nieves y glaciares de Chile, vol. 1957. Fundamentos de Glaciología. Ediciones de la Universidad de Chile, Santiago, pp. 18–25.

Lliboutry, L., Corte, A.E., 1998. Glaciers of South America: Glaciers of Chile and Argentina. US Geological Survey Professional Paper 1386I.

Malmros, J.K., Mernild, S.H., Wilson, R., Yde, J.C., Fensholt, R., 2016. Glacier area changes in the central Chilean and Argentinean Andes 1955–2013/14. J. Glaciol. 62 (232), 391–401. https://doi.org/10.1017/jog.2016.43.

Naegeli, K., Damm, A., Huss, M., Wulf, H., Schaepman, M., Hoelzle, M., 2017. Cross-comparison of albedo products for glacier surfaces derived from airborne and satellite (Sentinel-2 and Landsat 8) optical data. Rem. Sens. 9 (2), 110. https://doi.org/10.3390/rs90201010.

Nogami, M., 1972. The snowline and climate during the last glacial period in the Andes Mountains. Quat. Res. (Jpn.) 11, 71–80.

Paul, F., Barry, R.G., Cogley, J.G., Frey, H., Haeberli, W., Ohmura, A., Ommanney, C.S.L., Raup, B., Rivera, A., Zemp, M., 2009. Recommendations for the compilation of glacier inventory data from digital sources. Ann. Glaciol. 50, 119–126. https://doi.org/10.3189/172756410790595778.

Paul, F., Winsvold, S.H., Kääb, A., Nagler, T., Schwaizer, G., 2016. Glacier remote sensing using Sentinel-2. part II: mapping glacier extents and surface facies, and comparison to Landsat 8. Rem. Sens. 8, 575. https://doi.org/10.3390/rs8070575.

Pellicciotti, F., Ragettli, R., Carenzo, M., McPhee, J., 2014. Changes of glaciers in the Andes of Chile and priorities for future work. Sci. Total Environ. 493, 1197–1210. https://doi.org/10.1016/j.scitotenv.2013.10.055.

Racoviteanu, A.E., Arnaud, Y., Williams, M.W., Ordoñez, J., 2008. Decadal changes in glacier parameters in the Cordillera Blanca, Peru, derived from remote sensing. J. Glaciol. 54, 499–510. https://doi.org/10.3189/002214308785836922.

Rodriguez, M., Ohlanders, N., Pellicciotti, F., Williams, M.W., McPhee, J., 2016. Estimating runoff from a glacierized catchment using natural tracers in the semi-arid Andes cordillera. Hydrol. Process. 30 (20), 3609–3626. https://doi.org/10.1002/hyp.10973.

Sagredo, E.A., Lowell, T.V., 2012. Climatology of Andean glaciers: a framework to understand glacier response to climate change. Glob. Planet. Chang. 86–87, 101–109. https://doi.org/10.1016/j.gloplacha.2012.02.010.

Sagredo, E.A., Rupper, S., Lowell, T.V., 2014. Sensitivities of the equilibrium line altitude to temperature and precipitation changes along the Andes. Quat. Res. (United States) 81, 355–366. https://doi.org/10.1016/j.yqres.2014.01.008.

Silverio, W., Jaquet, J.M., 2005. Glacial cover mapping (1987-1996) of the Cordillera Blanca (Peru) using satellite imagery. Rem. Sens. Environ. 95, 342–350. https://doi.org/10.1016/j.rse.2004.12.012.

United Nations, 1983. The convention on wetlands of international importance especially as waterfowl habitat. Environ. Policy Law 10, 70–71. https://doi.org/10.1016/S0378-777X(83)80165-6.

Veettil, B.K., Kamp, U., 2017. Remote sensing of glaciers in the tropical Andes: a review. Int. J. Remote Sens. 38 (23), 7101–7137. https://doi.org/10.1080/01431161.2017.1371868.

Veettil, B., de Souza, S.F., 2017. Study of 40-year glacier retreat in the northern region of the Cordillera Vilcanota, Peru, using satellite images: preliminary results. Rem. Sens. Lett. 8 (1), 78–85. https://doi.org/10.1080/2150704X.2016.1235811.

Veettil, B.K., Wang, S., de Souza, S.F., Bremer, U.F., Simões, J.C., 2017a. Glacier monitoring and glacier-climate interactions in the tropical Andes: a review. J. South Am. Earth Sci. 77, 218–246. https://doi.org/10.1016/j.jsames.2017.04.009.

Veettil, B.K., Wang, S., Bremer, U.F., de Souza, S.F., Simões, J.C., 2017b. Recent trends in annual snowline variations in the northern wet outer tropics: case studies from southern Cordillera Blanca, Peru. Theor. Appl. Climatol. 129 (1–2), 213–227. https://doi.org/10.1007/s00704-016-1775-0.

Waylen, P.R., Caviedes, C.N., 1990. Annual and seasonal fluctuations of precipitation and streamflow in the Aconcagua River basin, Chile. J. Hydrol. 120, 79–102. https://doi.org/10.1016/0022-1694(90)90143-L.

Zemp, M., Frey, H., Gartner-Roer, I., Nussbaumer, U., Hoelzle, M., Paul, F., Haeberli, W., Denzinger, F., Ahlstrom, A.P., Anderson, B., Bajracharya, S., Baroni, C., Braun, L.N., Cáceres, B.E., Casassa, G., Cobos, G., Dávila, L.R., Granados, H.D., Demuth, M.N., Espizua, L., Fischer, A., Fujita, K., Gadek, B., Ghazanfar, A., Hagen, J.O., Holmlund, P., Karimi, N., Li, Z., Pelto, M., Pitte, P., Popovnin, V.V., Portocarrero, C.A., Prinz, R., Sangewar, C.V., Severskiy, I., Sigurdsson, O., Soruco, A., Usubaliev, R., Vincent, C., 2015. Historically unprecedented global glacier decline in the early 21st century. J. Glaciol. 61, 745–762. https://doi.org/10.3189/2015JoG15J017.

Journal of South American Earth Sciences 109 (2021) 103293

Contents lists available at ScienceDirect

Journal of South American Earth Sciences

journal homepage: www.elsevier.com/locate/jsames

Permafrost evolution in a mountain catchment near Santiago de Chile

S. Ruiz Pereira [a,b], C. Marquardt [c], E. Beriain [d], F. Lambert [a,b,*]

[a] Instituto de Geografía, Pontificia Universidad Católica de Chile, Chile
[b] Center for Climate and Resilience Research, Universidad de Chile, Chile
[c] DIEG/DIM, Engineering School, Pontificia Universidad Católica de Chile, Chile
[d] GeoNomadic, Santiago de Chile, Chile

ARTICLE INFO

Keywords:
Central andes
Aconcagua basin
Permafrost
Degradation
Aggradation

ABSTRACT

The Chilean Central Andes near Santiago are a semi-arid region with substantial frozen water reserves in their high altitude cryosphere. Millions of people depend on the Andean cryosphere for freshwater supply. Over the last sixty years, global warming has altered the mountains' water balance, as the temperature rose, precipitation decreased, and deglacierization exposed hundreds of square kilometers. The distribution of solid water stored in soil permafrost and the potential effects of climate change on it are unknown.

Here, we map favorable spots for permafrost occurrence at the "Monos de Agua" catchment, Aconcagua basin at 33°S, between 3600 and 5100 m a.s.l.. We identify these "cold spots" based on ground surface temperature and incoming solar radiation between 2017 and 2019. We suggest that these locations currently present permafrost and frozen water might actually be there. We confirmed a body of frozen water at one of these cold spots using an electrical resistivity survey.

Our mapping suggests that at least 15 ± 7% of the catchment's surface is underlain by permafrost. Permafrost occurrence begins around 3600 m a.s.l. with low probability and only at locations with favorable conditions of low exposure and isolation. Permafrost occurrence probability increases with altitude, with the largest fraction present above 4200 m a.s.l.

Our results suggest that the permafrost area in this region will decrease between 13 and 87% by the end of the century under the future global warming RCP scenarios. This event represents new challenges for the hydrological memory and water security planning in the Chilean Central Andes.

1. Introduction

Along with the Andes mountain range in South America, millions of people depend on the mountain cryosphere for freshwater supply (Barnett et al., 2005). However, climate change-induced surface warming will reduce snow cover and accelerate glacier and permafrost retreat (Baraer et al., 2012). Consequently, these changes may modulate the hydrogeology of such areas affected by permafrost regions (Cheng and Jin, 2013; Oliva and Fritz, 2018), bringing a series of ecological and environmental impacts.

In high mountain catchments, climate feedbacks between land ecosystems and the atmosphere may influence ecosystem services (Field et al., 2007; Schuur et al., 2008; Jansson and Taş, 2014). Permafrost dynamics affect groundwater recharge and runoff generation (Kuchment et al., 2000), as permafrost thaw may also contribute to summertime discharge (Gascoin et al., 2011).

Permafrost degradation could also potentially impact surface and subsurface hydrologic conditions by affecting soil strength properties (Kurylyk et al., 2014) and consequently surface water quality in high-mountain areas (Szopińska et al., 2016; Toohey et al., 2016) by enhancing chemical weathering (Colombo et al., 2019). Hence, current research and ecosystem management gaps in mountain environments could constrain cryospheric science, as has been proposed for regions in China (Xu et al., 2019).

The distribution of permafrost in the South American Andes Cordillera is diverse. For example, ground temperature measurements at 27°S showed no permafrost between 4200–4550 m and no clear evidence for permafrost even at 5260 m (Nagy et al., 2020).

Further south, the (high) Andes Cordillera (30–38°S) in central Chile is assumed to be permafrost affected region. It features a Mediterranean climate (Miller, 1976) with annual mean precipitation between 100 and 1000 mm (Garreaud et al., 2017). Nevertheless, this region has had a

* Corresponding author. Instituto de Geografía, Pontificia Universidad Católica de Chile, Chile.
E-mail address: lambert@uc.cl (F. Lambert).

https://doi.org/10.1016/j.jsames.2021.103293
Received 6 January 2021; Received in revised form 23 March 2021; Accepted 23 March 2021
Available online 1 April 2021
0895-9811/© 2021 Elsevier Ltd. All rights reserved.

declining precipitation trend over recent decades (1960–2016) (Boisier et al., 2018), and also up to 75–85% snowpack loss is expected by the year 2100 (Bozkurt et al., 2018). Such a decrease in mountain snowpack cover may induce water scarcity for local ecosystems, population centers, agriculture, and industry since snow (Cornwell et al., 2016) and glacial melt (Dussaillant et al., 2019) are central Chile's primary freshwater sources after the rain season.

In the (western) Central Andes, the Aconcagua river runs along 32°40′-32°56′S from watersheds between 3000 and 5000 m A.S.L. down to the Eastern South Pacific Ocean. Snow cover in the Aconcagua basin has been steadily shrinking (Stehr and Aguayo, 2017). Also, several watersheds in the Central Andes ("Juncal River", "Olivares" and "Tupungato") experienced regional glacier shrinkage of over 30% between 1955 and 2016, equivalent to tens of square kilometers (Bodin et al., 2010; Monnier and Kinnard, 2017; Ruiz and Veettil, 2019).

Because of the combination of reduced precipitation, snowpack loss, and glacier retreat, the Chilean Public Works Ministry passed decrees nos. 99 and 126 in 2018 and 2019 respectively, officially declaring the Aconcagua basin a water-scarce region. Permafrost quantification as a freshwater source is of utmost importance for a regional water budget and future adaptation plans.

Several permafrost maps for the Central Andes exist. For example, using global elevation data and air temperatures from reanalysis at 1 km resolution, Gruber (2012) suggested "favorable" conditions for permafrost in the Aconcagua basin above 4200 m. Later, Saito et al. (2016) used downscaled models (1 arc-minute resolution) and showed the "Juncal River" sub-basin to be affected by discontinuous and continuous permafrost above 3000 m a.s.l. and 4000m a.s.l., respectively.

Similarly, Bartsch et al. (2016), estimated a high probability for permafrost occurrence above 3600 m a.s.l. They considered Mean Annual Ground Temperatures (MAGT) inputs between −2 and −4 °C (Gisnås et al., 2013; Westermann et al., 2015; Obu et al., 2019). Later, Tapia-Baldis and Trombotto-Liaudat (2020) estimated mid and high-probability above 3400 m and 4200 m a.s.l., respectively. However, although these studies are well-suited for estimating large-scale permafrost distribution, they lack the resolution for catchment-sized investigation.

In the central Andes, drastic changes in glacier coverage are observed from catchment to catchment. One possibility is that slope aspect constrains sunlight and hence cryoform occurrence. Here, we propose a straightforward method to generate permafrost distribution grids with an adequate resolution for a rugged terrain within a Central Andes sub-basin at 33°S, the "Monos de Agua" catchment at the border between Argentina and Chile (Juncal River/Tupungato sub-basin).

We estimated the minimal conditions for permafrost occurrence and distribution in high-mountain areas of the "Monos de Agua" catchment. Additionally, we estimated magnitudes for permafrost aggradation and future degradation, emphasizing solar radiation heterogeneity given the extremely rugged terrain.

2. Methods

2.1. Study site and geomorphology

The "Juncal River" sub-basin (Aconcagua basin) spans over an area of 342 km^2. It is 75 km north-east of Santiago de Chile and had an approximate mean air temperature between 1979 and 2016 of −3.1 °C at 3600 m a.s.l. (Boisier et al., 2018) and median annual precipitation of 581 mm at the outlet (32°52′5″ S; 70°9′3″ W)(CAMELS-CL database, Alvarez-Garreton et al., 2018). Here, the dominant input (>50% of peak) to the main channel during melt season (mid-October until April) is glacial melt rather than snowmelt (Ohlanders et al., 2013), while snowmelt is the dominant input only during spring (mid-October to mid-November).

Fig. 1 shows a 1955 aerial photograph of the "Juncal River" sub-basin with two main valleys, the "Juncal River" catchment in the south-west and the "Monos de Agua" to the north-east. The easternmost areas in Argentina belong to the Tupungato sub-basin, Mendoza River basin, and consist of mostly glacierized surfaces. Our study-site lies within the "Monos de Agua" catchment (red frame and insert in Fig. 1), a branch that crosses the border between Argentina and Chile. The "Monos de Agua" catchment is technically part of the "Alto del Plomo" (in Argentina) sub-basin, starting at high peaks over 5000m a.s.l. and ending at the outwash plains in Chile at around 2700m a.s.l..

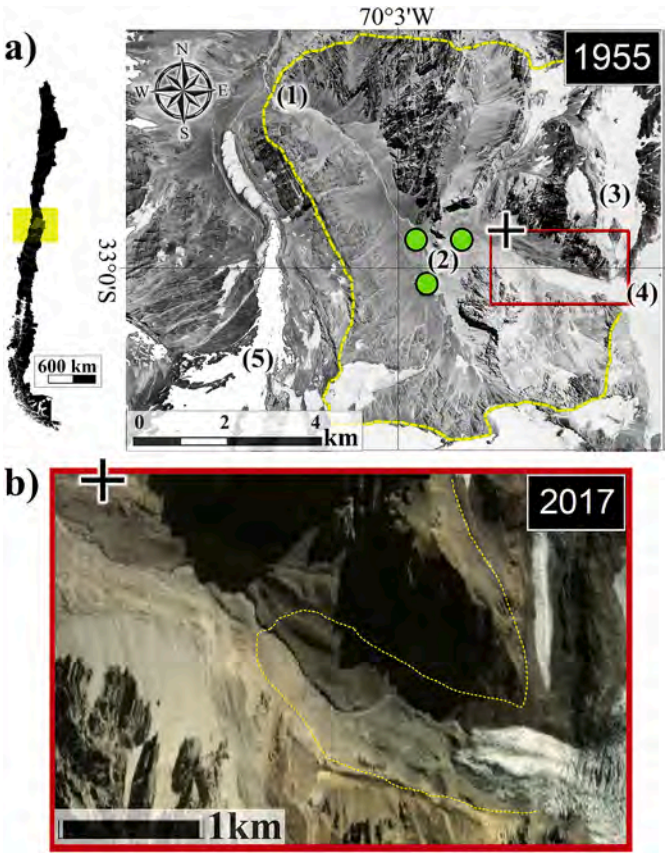

Fig. 1. Glacierized catchments North East from Santiago de Chile. (a) Shows "Río Juncal Alto" sub-basin (Aconcagua basin) with the "Monos de Agua" catchment in the segmented yellow line. (b) is the "Upper Monos de Agua" (red rectangle in a) showing the frontal retreat of the central valley glacier between 1955 and 2017. (1) is the outlet, and (2) the Weather Station. The thermal loggers are green circles and glaciers are; "Monos de Agua" (3), "Alto del Plomo" (4), and "Juncal Norte" (5). The (+) represents the position of the rock glacier analyzed in this study.

In 1955 the "Monos de Agua" catchment featured one glacier now divided into "Monos de Agua" (formerly "León Negro") and the "Alto del Plomo" glaciers (Fig. 1), a sign of a kilometric scale deglacierization in the area. The "Monos de Agua" name appears in recent scientific literature instead of "León Negro", therefore our preference.

The south-facing slopes of the "Monos de Agua" catchment are highly glacierized above 3900 m A.S.L.. In contrast, north-facing slopes predominantly feature surface flows mapped as rock-glacier type features (Rodriguez et al., 2016). However, an older study by Bown et al. (2008) did not map any rock glacier unit in the "Monos de Agua" catchment.

The mapping of Rodriguez et al. (2016) does show several units as debris-covered rock glaciers, coinciding with Lliboutry (1956). The Inventory from the *General Directory of Waters* (Unidad de Glaciología, 2015) shows several rock glaciers in the catchment.

In Fig. 2, we show the geomorphological mapping of the region. It used aerial and satellite imagery from HYCON (1955) and LANDSAT (1–8). Some of the features mapped (scarps, moraines, rock glaciers)

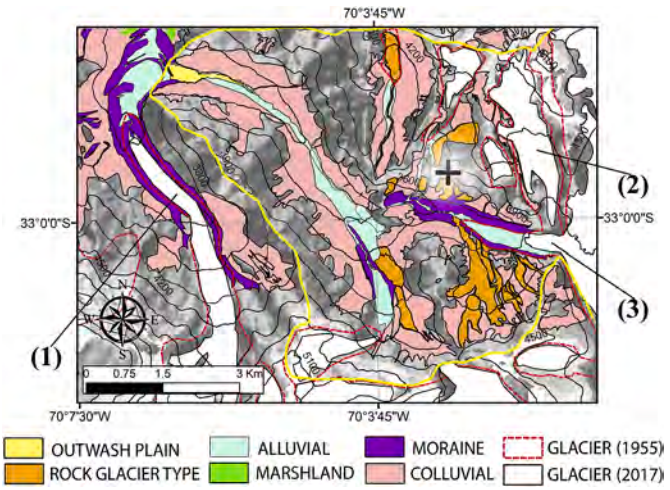

Fig. 2. Geomorphology at the "Monos de Agua" catchment (thick yellow line). Rock glaciers are present above 3600 m A.S.L.; the one analyzed is marked with a (+). Glaciers with recent deglacierization in the catchment: "Juncal Norte" (1), "Monos de Agua" (formerly "León Negro") (2), and "Alto del Plomo" (3).

were field checked between summer 2017 and summer 2019. In general, the area has coarse sediment material on the surface.

2.2. Electrical Resistivity Tomography

Previous mappings (Bartsch et al., 2016; Gruber, 2012; Saito et al., 2016) described a fringe area (0.5 probability) for permafrost between 3600 and 3900 m A.S.L.. Finding frozen ground during summer at fringe areas implies favorable conditions for permafrost. To confirm an active cryoform in this altitudinal range we used Electrical Resistivity Tomography (ERT). Electrical resistivity increases at the freezing point due to the phase change from electrically conductive water to electrically nonconductive ice (Kneisel et al., 2008).

We chose a location at 3600 m A.S.L. identified as a rock glacier in the geomorphological map (Fig. 2). The rock glacier topography was determined by using UAV on 7-April 2019 at 6 p.m. The drone flew 150m above surface level and took pictures at 1-m resolution. It utilized no ground control points.

The ERT fieldwork was conducted the same day and measured one transect in search of the frozen ground below the sediment. The yellow line in Fig. 3-b shows the transect (133m long). The ERT used a *Lippman* 4-point light resistivity-meter with 20 electrodes (Fig. 3-c). The distance between the electrodes was 7 m, and the arrangement employed for the resistivity lecture was dipole-dipole. The total measuring transect was 133m from 3680 to 3710 m A.S.L. at an average slope of 3% on a very irregular surface. The sampling error remained <1%, and the apparent resistivity uncertainty was 36%. The inverse model resistivity section

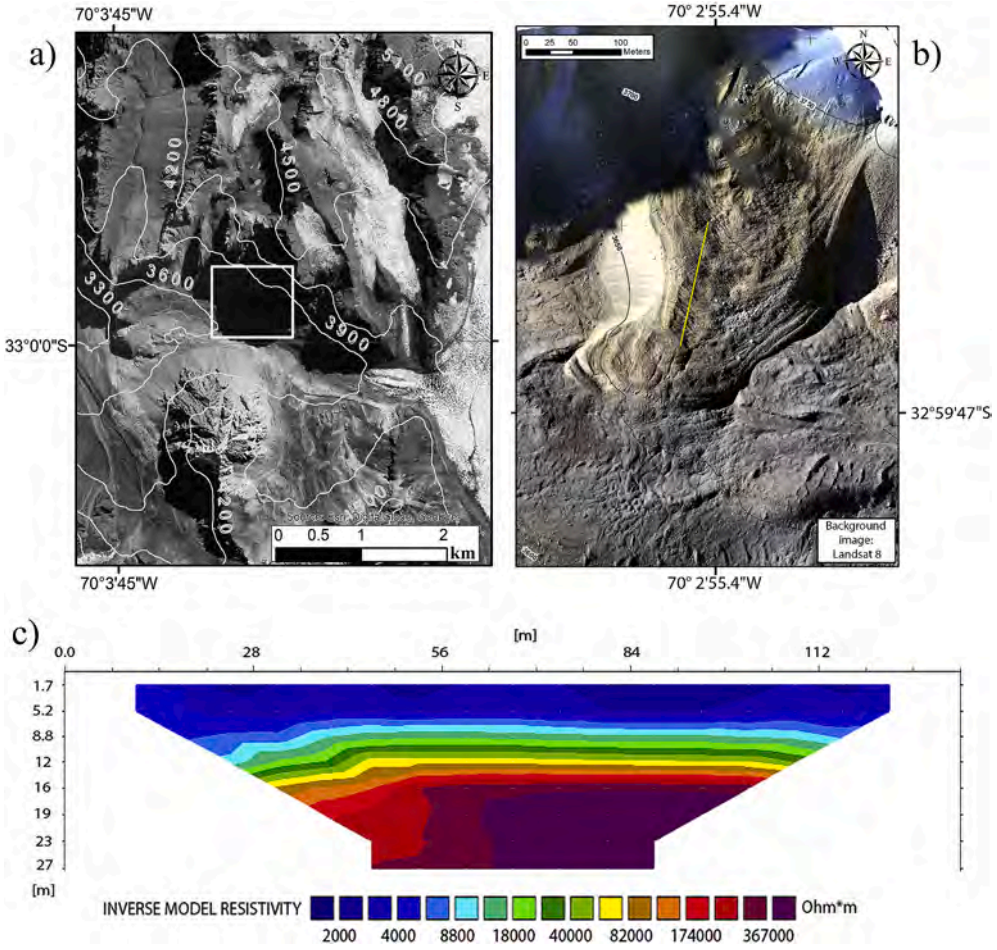

Fig. 3. Rock glacier Electrical Resistivity Tomography (ERT). (a) Upper "Monos de Agua" catchment (Landsat-8 image, 2017) with the studied rock-glacier within the white square. (b) Shows the rock-glacier with the transect (yellow line) of the ERT survey. (c) ERT output with X and Y axes show electrode transect and depth respectively.

was generated by ZOND RES 2D software using *smoothness constrained* inversion type.

2.3. Ground surface temperatures

Ground surface temperatures (Fig. 4) were measured using thermistor triplicates (*Geoprecision* Mlog-5W-US) installed around the knickpoint (abrupt thalweg slope change) in Fig. 1 (green circles) at 3200, 3600, and 3700 m A.S.L.. The measuring period lasted from 24-April-2018 to 04-April- 2019, recording data every 20 min with ±0.01 °C precision. Freeze-thaw cycles consisted of counting the number of times sub-zero temperatures turned positive.

We used an ALOS-PALSAR (Rosenqvist et al., 2007) DEM with a 12.5m resolution (Dataset: © JAXA/METI ALOS PALSAR L1.0 2007. Accessed ASF DAAC March 2020). We then produced a surface temperature grid of the catchment by calculating the temperature at each grid point from the point's altitude and the catchment's mean Altitudinal Lapse Rate (ALR) (Fig. 5-a).

The ALR estimation used point measurements (as mentioned in Petersen and Pellicciotti, 2011) of ground surface temperature (Table 1) and also the standard moist adiabatic lapse rate of (−0.65)°/100m. It resulted in a 0.80 ± 0.15°/100m value used to extrapolate the temperatures onto the grid. The result is the ground surface temperature grid presented in Fig. 5-a.

2.4. Solar radiation

We estimated potential incoming solar radiation in the catchment by using the catchment ALOS-PALSAR DEM as input for the "Area Solar Radiation" tool (ArcGIS 10.5, ESRI, 2009) following the procedure done by Niu et al. (2018).

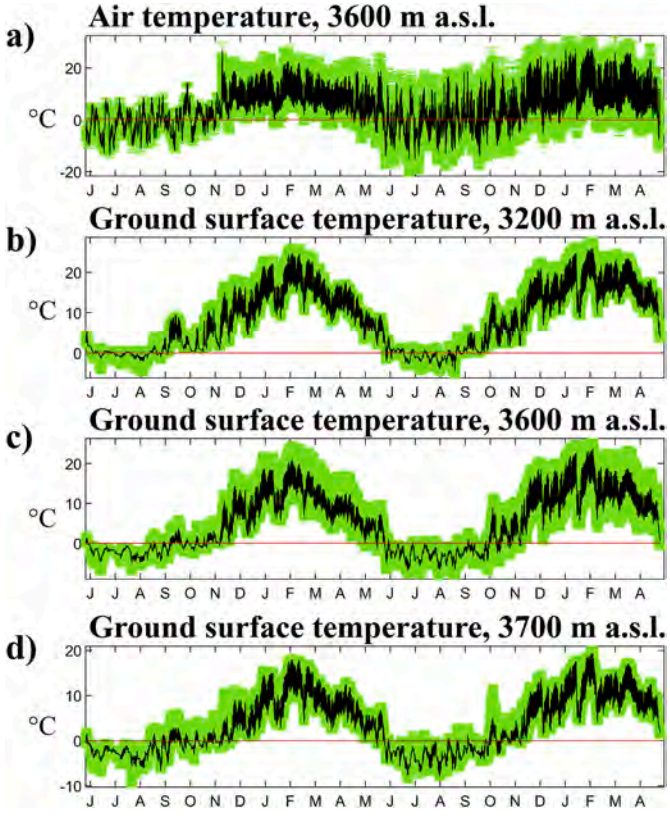

Fig. 4. Air temperature and ground surface temperatures between May-2018 and April-2020 in "Monos de Agua" catchment. Green is the standard deviation, and the red line is 0 °C reference. The number of freeze-thaw cycles is 254, 40, 48, and 69 for (a), (b), (c), and (d), respectively.

We calibrated this output with local incoming radiation values measured throughout 2019 using a *Davis Vantage Plus* station (location in Fig. 1(2)). The measurements have a radiation range of 0–1100 W/m^2 with a 5% measuring error, used to calibrate the "Area Solar Radiation" matrix (Fig. 5-b).

2.5. Estimation of permafrost occurrence

Our estimates used the ratio between ground surface temperature and incoming solar radiation. Their ratio is a magnitude of their correlation and a measure of surface energy budget conditioned by aspect (Duguay et al., 2005; Smith, 1975). Hence, by dividing the Mean Annual Ground Surface Temperature (MAGST) grid by the *Area Solar Radiation* grid (Fig. 5-c), we produced a "ratio" grid. On this new ratio grid, we can identify cold spots that may be due to combinations of cold temperatures or low insolation at specific locations in the catchment.

We analyzed the ratio grid using partitional (*k-means*) and hierarchical (agglomerative) clustering methods. The *k-means* uses a heuristic algorithm finding centroid seeds (Arthur and Vassilvitskii, 2007) and has been used in temperature analysis (Azócar et al., 2017; Carvalho et al., 2016; Zeng et al., 2020).

K-means clustering is an unsupervised technique used to separate spatial datasets (Gulbrandsen et al., 2016) into a predefined number of clusters (*k*) and segment abundance in permafrost regions (Nitze et al., 2018). We also used an agglomerative algorithm that clusters data points using a bottom-up approach from individual data points (Sembiring et al., 2011). The optimum number of clusters was determined using the *Calinski-Harabasz* criterion (Caliński and Harabasz, 1974), the *Silhouette* approach (Rousseeuw, 1987), and the *Davis-Bouldin* index (Casteleiro-Roca et al., 2020).

We assessed the cluster validity of our temperature/radiation ratio data using the *Silhouette* index, a ratio-type index measuring the mean distance between intra-cluster points (cohesion), and mean inter-cluster distances (separation). The *Silhouette* index is considered one of the more reliable indexes for the case of multidimensional and noisy data (Arbelaitz et al., 2013), mainly because it is not a diameter-based index optimized for Gaussian context (Lamirel et al., 2016).

Other indices like *Davies-Bouldin* measure the ratio between "within-cluster" distances and average distances to the centroid (Davies and Bouldin, 1979) but present less accurate results than using *Silhouette* index (Petrovic, 2006). Another tool, the *Dunn* index, identifies cluster cohesion and separation (Dunn, 1974; Ilc, 2012) but is not suited for overlapping data (Arbelaitz et al., 2013). The *Silhouette* index also outperformed *Dunn* in relative errors (De Amorim and Hennig, 2015) and is less affected by noisy data (Saitta et al., 2007).

We additionally checked consistency between clustering approaches by performing a *Rand* index (Santos, 2007). We also conducted a one-way ANOVA per cluster data, looking to differentiate if clustering methods disagree between clusters.

2.6. Past aggradation and future degradation

We considered that only deglacierized areas (the area between the glacier limits of 1955 and 2017) with favorable conditions for permafrost occurrence, currently are potential surfaces for permafrost aggradation. These areas are now without ice insulation and potentially subject to colder conditions.

Additionally, to estimate the future evolution of permafrost in the catchment, we increased the surface temperature calculated in our MAGST grids according to RCP2.6 and RCP8.5 climate change projections (Stocker et al., 2013) and then clustered again. The increase in catchment surface temperature (the whole grid) for the RCP2.6 and RCP8.5 projections are + 1.2 °C and + 3.5 °C, respectively (Bozkurt et al., 2018).

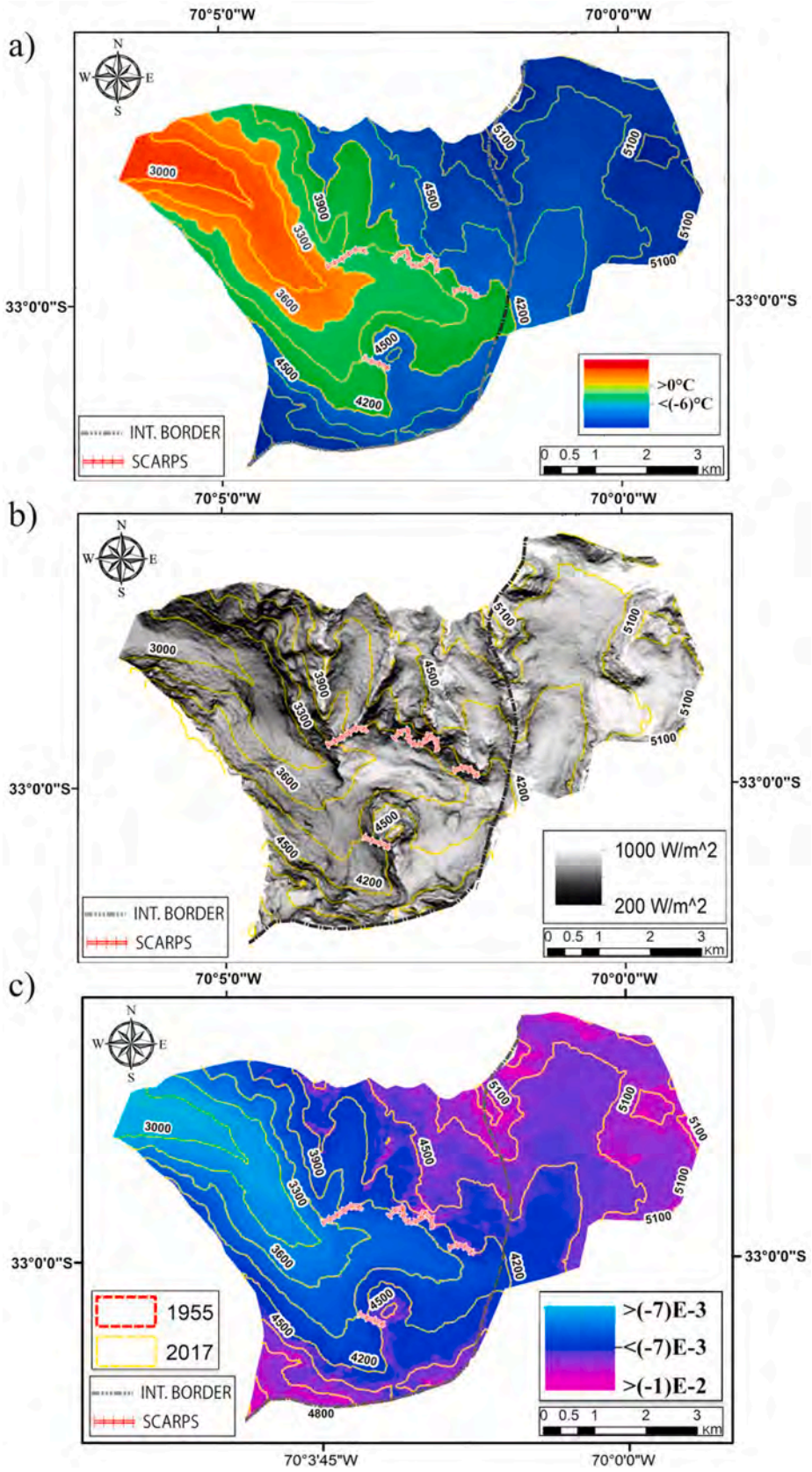

Fig. 5. Inputs for permafrost mapping at 33°S, Central Andes. (a) Ground Surface Temperature grid resampled from ground surface temperature loggers. (b) Incoming solar radiation grid resampled from the automatic weather station (3600m ASL). (c) Shows the temperature/radiation ratio grid.

Table 1
Ground surface temperature measurements (2018–2020). Freeze-thaw cycles constitute thermal weathering conditions of a periglacial environment.

	Mean Temperature (°C)	Freeze-thaw cycles	Clear sky %
3700 m a.s.l.	2.23 ± 1.0	69	51 ± 13
3600 m a.s.l.	3.98 ± 2.14	48	50 ± 11
3200 m a.s.l.	7.78 ± 0.77	40	48 ± 10

2.7. Uncertainty estimation

We determined the uncertainty for the temperature/radiation ratio grids considering error propagation for temperatures between our site measurements at 3600 m A.S.L. and all the remaining values calculated for the rest of the catchment up to the highest mountain tops over 5000 m A.S.L..

The error propagation considered an ALR deviation of ±0.15°/100m. The uncertainty accounts for altitudinal change, instrumental error (logger accuracy and pyranometer error), and statistical deviation for each input variable.

In brief, each ratio grid point was randomly resampled within its normal distribution range, generating a new vector for clustering. The re-clustering process repeats a thousand times, and finally, the mean and standard deviation account for the clustering uncertainty.

3. Results

3.1. Geomorphology

Over the last 60 years, large areas of the upper "Monos de Agua" catchment have become ice-free in the "Juncal River sub-basin". The "Alto del Plomo" glacier retreated 1 km (Figs. 1 and 2) at roughly 18 m/yr over a slope of 35 ± 7.2%. In contrast, the further south "Juncal Norte" glacier (front at 2900 m A.S.L.) retreated about 0.3 km at 5.5 m/yr through an average slope of 17 ± 1.3% considering previous maps (Ruiz Pereira and Veetil, 2019).

Between 2750 and 3000 m A.S.L., the "Monos de Agua" catchment presents a mature landscape with outwash plains, wetlands, and colluvial/alluvial slopes with vegetal patches. The most extensive terrain incisions are products of fluvial processes.

The catchment becomes a paraglacial environment between 3200 and 3900 m A.S.L., showing features of secondary sedimentary reworking and coalescing cryoforms (rock-glaciers in Fig. 2). Most of the Quaternary units in this section represent colluvial and alluvial fans/slopes. Apparent rock-glacier type features appear only above the moraine ridge above 3900 m A.S.L. (Fig. 2).

Overall, areas between 3600 and 3900 m a.s.l. in the whole "Monos de Agua" catchment show visible expressions of cumulative deformation (as rock glacier types). These features on the left-lateral (south-facing) moraine (Fig. 2) are likely influenced by long-term creep of ice/debris mixtures under permafrost conditions.

We analyzed the largest cryoforms coincident with a rock glacier (cross in Fig. 2). Its toe lies at 3650 m A.S.L., while the root starts at 3750m a.s.l.. The toe has a low frontal thickness of about 6–7m. Its width ranges from a minimal 110m at its center to almost double that value at the root level, coinciding with slope increase. At its root level, several protalus-ramparts are present. The toe-root length is 340m, with an average slope of 24.1%.

This cryoform (rectangle in Fig. 3-a) lies at 3600m a.s.l.,within the permafrost fringe altitude mapped by previous studies. It is detailed in Fig. 3-b and is also present in the 1955 imagery (Fig. 1, red square), showing it is coalescent with other surface flows and moraine edges (Fig. 2).

It shows defined furrow-and-ridge topography on its surface and lacks vegetation. Additionally, there were no thaw-lakes on the surface. The feature has a clear ridge on its westward margin, then a steep lateral slope of finer material. In contrast, the eastward margin does not have a clear ridge, and several furrows appear to result from the buttressing of the coalescing moraine and talus cones. These general features were also present in the HYCON imagery (1955), with no significant differences evident in 2017 Landsat imagery.

3.2. Rock glacier ERT

ERT (Fig. 3-c) measurements evidence horizontal layers running longitudinally, covering the full extension of the array's length. The topmost is a "low-resistivity" layer (~2000–8800 Ωm) located between the surface and 12 m depth and decreasing in thickness from the toe to root by about 30%.

Below exists an intermediate layer between 12 and 16 m depth with an apparent resistivity between 18,600 Ωm and 82,600 Ωm. The deepest layer is located below 16 m depth, with apparent resistivity from 80 kΩm to 174 kΩm.

The highest resistivities (360 kΩm) were found from 19 m depth to the bottom of the ERT's detection limit at 27 m over a length of 63 m. These results suggest that this rock glacier is an active cryoform with ice content under a debris cover.

Based on this finding, we posit that permafrost is present in the catchment and may occur in very favorable conditions within the 3600–3900 m a.s.l. fringe region. Hence our assumption that permafrost exists under more favorable conditions.

3.3. Ground surface temperature and solar radiation

We measured ground surface and air temperature over 22 months using individual temperature loggers and the monitoring station, respectively (Fig. 4). Seasonal variability is apparent with a low-temperature period between June–August. Starting August, temperatures gradually increase until mid-February. The ground surface temperature data, freeze-thaw cycles, and sky exposure are in Table 1.

The site at 3600m presented some zero curtain like periods (latent heat in maintaining temperatures near 0 °C) from mid-September to early November. However, this site has the highest number of freeze-thaw cycles. The less (sun) exposed loggers registered the coldest temperatures at 3600m, with 50% of clear sky exposition.

Fig. 5-b shows incoming solar radiation throughout the "Monos de Agua" catchment (2750–5000m a.s.l.). Between 3000 and 3600 m A.S.L., several regions with "low" incoming solar radiation (<500 W/m^2) are present due to the very abrupt topography in these locations. Above 3600 m a.s.l., low radiation levels associate with (topographic) scarps (red lines in Fig. 5 a-b).

Above 4200 m a.s.l., the overall catchment area is considerably less steep, partially because of the glacierized surfaces. Radiation at these high-altitude areas is generally above 1000 W/m^2. The radiation monitoring station (Fig. 5(2)) at 3600 m a.s.l. registered a summer maximum (February) of 900 ± 200 W/m^2.

Fig. 5-c shows the ratio between ground surface temperatures and incoming solar radiation. Favorable ratios (magenta) associated with probable permafrost occurrence occupy vast areas (>2.5 km transects) within the catchment, especially at locations above 3900 m A.S.L.. Surfaces with a stronger magenta start from 3900 m A.S.L. and reach the mountain tops. These favorable surfaces are nonetheless very heterogeneous.

3.4. Permafrost distribution

Our mapping procedure clustered the temperature/radiation ratio grid (Fig. 5-c). The ratio data population rejected the null-hypothesis for the normal distribution after a *Kolmogorov-Smirnov* test at a 5% significance level. The *Calinski-Harabasz*, *Silhouette,* and *Davis-Bouldin* indexes suggested an optimum number of five clusters (Additional Table 1).

Additionally, the partitional *k-means* and agglomerative *Ward*

methods delivered a *Rand* index of (0.76), implying a good agreement between both clustering processes considering a 6% average difference between clustering methods.

The clusters represent subsets of data neighboring centroids, positioned depending on the clustering approach. Therefore, it is necessary to validate the clustering method using different indices (Table 2) accounting for inter-cluster cohesion. The three clustering methods had a good agreement between them.

In brief, the *Silhouette* score ranges between −1 and 1 (Petrovic, 2006). The decision boundary of 0.0 implies that samples are are outliers. Our result was +0.56, well above the decision boundary. Next, for a *Davies-Bouldin* analysis, the range is between 0 and 1; the lower, the better (Halkidi et al., 2001).

Our result was 0.52 ± 0.01, suggesting a non-conclusive estimate. Finally, the *Dunn* index ranges between 0 and +∞, the worst and best classification respectively (Luna-Romera et al., 2018). It delivered a very low result, implying a "bad clustering".

We also compared clustering methods for all cluster data subsets using one-way ANOVA (Additional Figure Additional Fig. 1). The analysis showed significant differences between methods (Additional Figure Additional Fig. 2). Considering all indices and ANOVA analysis, the *k-means* analysis was shown to be the most consistent method. The more dissimilar was the *Agglomerative* (Centroid distance, UPGMC) clustering approach, which we discarded because results were significantly different to the other two methods.

In general, the five clusters represent different combinations of temperatures and incoming radiation levels (Additional Table Additional 1), often overlapping between themselves. Additional Figure Additional Fig. 3 shows cluster values. Two clusters coincided with areas within the catchment located above fringe areas from the five resulting clusters, meaning >3900m a.s.l..

The *k-means* method uncertainty resulted in ±7%, explained from error propagation and clustering deviation (histograms per cluster in Additional Figure Additional Fig. 4). The main driver for errors in our methodology is the ALR for *Ground Surface Temperature*. Nevertheless, the importance of the *Incoming Solar Radiation* grid was to capture the topography, increasing mapping resolution. The clustering in Additional Figure Additional Figs. 1 and 2 show clusters coincident with mountain tops in the topography.

Consequently, *k-means* clustering suggests that about 22.18 ± 7% of the catchment's area is under favorable permafrost conditions, with vast areas above 4200m a.s.l. likely affected (Fig. 6). These clusters in most favorable conditions corresponded to 22.18% of the catchment. The total area is 10.37 ± 3.45 km^2 from a 57.61 km^2 catchment.

Favorable areas for permafrost (clusters 4–5 in Additional Table Additional 1) are almost exclusively above 3900m a.s.l. (Fig. 6). Between 3900 and 4500 m a.s.l., there is isolated permafrost distribution and >4500m a.s.l. discontinuous distribution up to the mountain tops.

The permafrost affected areas have an orientation consistently facing south, with patches on north-facing slopes appearing only above 4500m a.s.l.. Large favorable areas lie within the glacial foreland (red contour, Fig. 6), which opens the question for the likelihood of permafrost aggradation therein.

In summary, our catchment scale mapping examined the clustering of a temperature/incoming-radiation ratio grid. The permafrost confirmation by ERT coincided with areas previously mapped as having a 0.5 probability for permafrost occurrence. Therefore, clusters with more favorable conditions (overall higher in the catchment) retained >0.5 probability for permafrost occurrence. Among these these clusters, one covered mostly glacierized areas and was unsuitable as indicative for permafrost. Consequently, only clusters with the most favorable conditions were considered to have a probability equal to one.

Table 2
Clustering method analyses.

Clustering Method	Dunn index	Davies Bouldin score	Silhouette score
k-means	0.007	0.51	0.57
Ward	0.007	0.53	0.56
Agglomerative	0.001	0.53	0.56

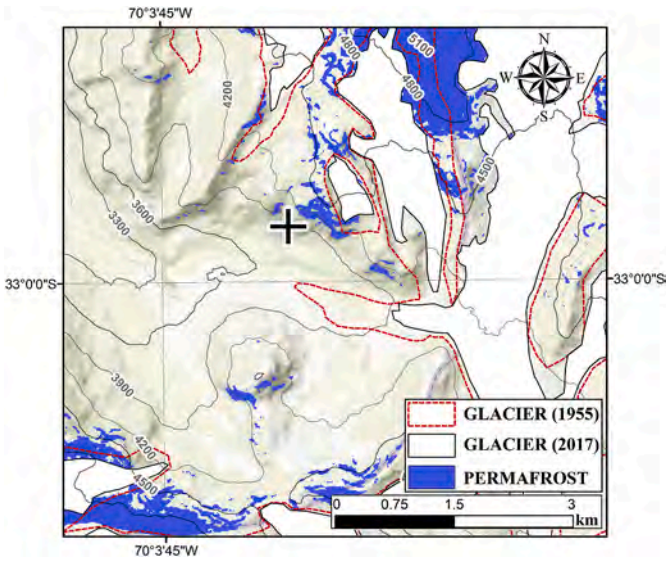

Fig. 6. Permafrost affected areas present at the "Monos de Agua" catchment. Areas subject to current permafrost condition (in blue) exclude glacial areas. Glacier contours for 1955 are red, and glacier polygons for 2017 are white with dark margins. The black cross (+) represents the ERT site.

3.5. Permafrost evolution

Overall, our mapping showed that the "Monos de Agua" catchment has 22.18 ± 7% of its area at the most favorable conditions for permafrost occurrence. Most of these areas are within the recently deglacierized foreland margins, where colder conditions might elicit potential permafrost aggradation.

Deglacierization (since 1955) has made available several square kilometers for potential permafrost aggradation above 3900 m A.S.L. within the catchment. This magnitude represents a permafrost aggradation proportion and relates to a positive permafrost/glacier feedback.

Projected warmings over Andean basins in Central Chile (~ 30–40° S) under RCP 2.6 and RCP8.5 delivered permafrost estimation in Fig. 7 covering 57.61 km^2. These surface warmings represent a potential decrease of permafrost affected areas of at least 13 and 87% for RCP 2.6 and RCP 8.5, respectively, suggesting extensive permafrost affected areas below 5000 m a.s.l. disappearing throughout the catchment.

4. Discussion

The current work mapped the most favorable spots for permafrost occurrence within a catchment undergoing active deglacierization. Previous studies in the Central Andes (Saito et al., 2015; Bartsch et al., 2016) mapped permafrost using air temperature as an input variable, delivering far colder mean annual surface conditions than our estimates and suggested a discontinuous permafrost boundary starting as low as 3600m a.s.l..

In our case, areas mapped for permafrost were only isolated patches as low as 3900m a.s.l.. These locations fell within the fringe areas for permafrost occurrence determined by previous studies (Gruber, 2012; Obu et al., 2019; Tapia-Baldis and Trombotto-Liaudat, 2019) who allocated them a 0.5 probability for permafrost occurrence.

A brief comparison with recent mappings shows that between 3600 and 5100m a.s.l., our results matched 70% of pixels with a permafrost probability close to one in Obu et al. (2019) and 37% with the results

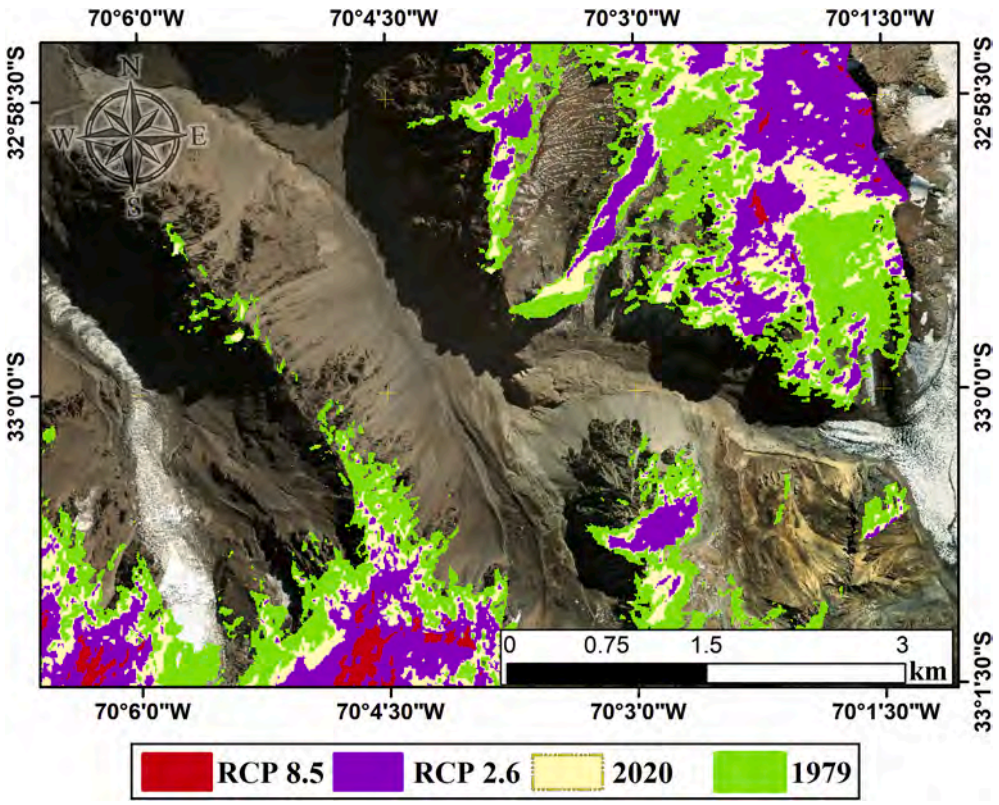

Fig. 7. Permafrost evolution at 33°S, Central Andes. Projections of permafrost degradation for RCP 2.6 and RCP 8.5 scenarios. Inputs for ground surface temperature from 1979 considered ERA-5, *Soil Temperature Level 1* (Hersbach et al., 2020). The current permafrost extent within the "Monos de Agua" catchment is 22.18 ± 7%.

from Tapia Baldis and Trombotto Liaudat, 2019. Between 4200 and 5100m a.s.l., our results coincided with 86% and 74% for the same references respectively. These comparisons are displayed in Additional Figs. 5 and 6.

Areas between 3600 and 3900m a.s.l. in the "Monos de Agua" catchment present several rock glaciers and coalescent cryoforms, which could be interpreted as *rock glacier complexes*. Most of these cryoforms have been mapped for decades (Lliboutry, 1956; Unidad de Glaciología, DGA, 2015). We found a highly resistive body at 3600m a.s.l. Under 7–12m of debris cover (Fig. 3-c). A similar result at "Muragl" rock-glacier (Hauck et al., 2011) had resistivities above 100 kΩm, implying ice-cemented and supersaturated permafrost from buried snowbanks and groundwater freezing (Onaca et al., 2013). For such magnitudes, Kneisel et al. (2008) pointed out that unless dealing with massive granite, 10^5 Ωm apparent resistivity measurements should relate to frozen sediments. Considering the porous nature of the sediment cover, we suggest it corresponds to interstitial ice.

Nevertheless, this cryoform lies within a "low probability" fringe for permafrost occurrence (Additional Figure Additional Fig. 5). Therefore, we advise caution when using rock glaciers as a proxy for permafrost occurrence at the Central Andes; as it might be misleading as pointed out by Arenson and Jakob (2010). The differentiation between active/-inactive rock glaciers should include subsurface investigations and not only visible expressions of cumulative deformation by the long-term creep of ice/debris mixtures under permafrost conditions (Berthling, 2011).

Additionally, rock glaciers at 33°S in the Andes only reach altitudes up to 4500m a.s.l. (García et al., 2017), hence they cannot by a direct proxy for higher altitude conditions, for example, in watersheds up to 5100m a.s.l.. Current deglacierization and permafrost aggradation (Kneisel, 1998; Kneisel and Kääb, 2007) can occur at higher altitudes. Consequently, assuming that areas with rock glaciers are under permafrost condition (P = 1) neglects the importance of longitudinal/altitudinal offset and exposition to incoming solar radiation for extremely rugged terrain. Using rock glaciers as a response variable for areal extrapolation may bear a high uncertainty if they have frozen ground at low altitudes (e.g., 3200 m a.s.l.) and under positive MAGST.

Our mapping (Fig. 6) used both *k-means* and *agglomerative* ('Ward') clustering methods, delivering two clusters coincident with high altitudes and associated with either lower incoming radiations, temperatures, or their combination (Additional Table Additional 1 and Additional Figure Additional Fig. 3). The *agglomerative* approach presented a +12.4% (7 km^2) of permafrost surface than the *k-means* method.

We used different indices to evaluate the clustering methods. The *Rand* index between Partitional (*k-means*) and Hierarchical (*Ward* and *Centroid* distance) clustering was (0.76) from a maximum of (1), meaning that the algorithm makes the correct distinction between classes, as elements are well separated (Santos and Embrechts, 2009). The evaluation of cluster cohesion utilized other tools like the *Dunn* index, which presents difficulties when dealing with noisy data. It is more useful for identifying clean clusters in data containing no more than hundreds of points (Saitta et al., 2007).

The *Davies-Bouldin* index resulted in a value implying that clusters are very similar and not compact and well-separated (Legány et al., 2006). Only the *Silhouette* index resulted in a value above the non-conclusiveness boundary 0.0, meaning that clusters were separated enough for a decision based on the index. In our opinion, this evaluation tells us that some clustering indices are highly sensitive to spatial data with a fixed distribution set by the altitudinal condition, hence presenting "islets" of restricted data coincident to scarps and peaks/ridges. These islets are within larger clusters and might consequently affect the ratio between distances.

For this reason, we analyzed intra-cluster distances by one-way ANOVA (Additional Figure Additional Fig. 1). This analysis showed

that only (temperature/radiation ratio) value differences beyond [3.0E-06] are sufficient to discretize *k-means* and *Ward* methods for permafrost associated clusters significantly.

Therefore, our evaluation is that *k-means* is a consistent clustering method, even though *Rand* and *Davis-Bouldin* indices show non-conclusive scores. For this reason, when clustering data with a fixed distribution and spatial significance, we deem *Silhouette* scores appropriate for evaluating *k-means* clustering results and ANOVA against other options.

In summary, our permafrost distribution maps coincide with the outputs presented by GIS GlobPermafrost Andes (Bartsch et al., 2016) and other works (Additional Figure Additional Fig. 5 and Additional Fig. 6), suggesting that permafrost affected areas exist above 3900m a.s.l. in the upper section of the "Monos de Agua" catchment. The Permafrost Zonation maps (Gruber, 2012) also establish favorable conditions as low as 4000m a.s.l. in the same area of the "Monos de Agua" catchment. The lower boundary for permafrost occurrence in both simulations is around 4000 m a.s.l..

In our case, the lowest boundary is currently around 3900 m A.S.L., increasing to 4100 and 4600, considering RCP 2.6 and 8.5 scenarios, respectively (Additional Figure Additional Fig. 7). Additionally, when considering projected warmings from RCP 2.6 and RCP 8.5 scenarios, drastic changes in permafrost affected areas are expected (Fig. 7) to impact the aquifer's overall residence time, speeding up the transit time of transit pathways at high altitude.

Finally, considering permafrost affected areas within the 1955 glacier limits (Fig. 6), they account for 3 km^2, implying that deglacierization (since 1955) made several square kilometers available for permafrost aggradation conditions above 3900 m a.s.l.. Consequently, the catchment's permafrost area has theoretically increased by at least 0.2 km^2 per square kilometer of ice lost over the last six decades (Fig. 6). The latter represents a permafrost aggradation proportion and relates to a negative glacier/permafrost feedback.

5. Conclusions

The current work mapped the most favorable spots for permafrost occurrence within a catchment undergoing active deglacierization and under current conditions of permafrost variability considering 21st-century climate projections.

Our results suggest that at least 15% of the "Monos de Agua" catchment area is currently under permafrost conditions, predominantly above 4200 m A.S.L.. The lower boundary for permafrost occurrence is at 3900 m A.S.L., with a patchy distribution. These cold spots are consistent with negative mean annual ground surface temperatures below −2.25 °C even with incoming radiations above 700 W/m^2 during summer months.

Glaciers in the catchment retreated significantly in the period 1955–2015 and a 40% of the total favorable areas mapped for permafrost are now ice-free surfaces. About a fifth of every square kilometer of ice lost in these areas is above 4200 m a.s.l.. Nevertheless, surfaces with conditions for permafrost occurrence will decrease by −37% and −87% considering RCP 2.6 and 8.5 respectively, with a consequent rise of the lowest permafrost boundary to 4100 and 4600 m a.s.l. for each case.

Understanding permafrost distribution at 33°S, an officially declared water scarce region over the last fifteen years, is crucial for interpreting subsurface hydrology, and groundwater flows in its high mountain catchments, the head of the mountain tower. Hence, understanding the future evolution of the mountain cryosphere is vital for resource baselines, planning, and future water security policies.

Author statement

The authors thank the peer reviewers and Editor for their careful consideration of our study. We state that Ruiz Pereira, S. designed the methodology, oversaw fieldworks, and wrote the original manuscript. Marquardt, C. supervised the methodology and fieldworks. Beriain, E. contributed to the fieldworks and ERT survey. Lambert, F. provided research supervision, manuscript edition and Project Administration. All authors contributed to the writing process and approved the final version of the manuscript.

Funding

This study has been partially funded by the Geography Institute (Pontificia Universidad Católica de Chile), ANID/FONDAP 1511009, and ANID/FONDECYT 1191223.

Declaration of competing interest

The authors declare that they have no known competing financial interests or personal relationships that could have appeared to influence the work reported in this paper.

Acknowledgments

The authors acknowledge the General Direction of Water (Ministry of Public Works, Chile), Parque Andino Juncal, Municipalidad de Putaendo, S. Gruber (Carleton University), Cristóbal Cvitanic, Hans Fernández, Einer Sepúlveda, Rodrigo Soteres, Jorge Palominos and César Benavidez.

Appendix

Additional Table 1
Ranges of ground surface temperature and incoming radiation per cluster.

Cluster number (k-means)		1	2	3	4	5
Incoming radiation (W/m^2)	Min	390	683	427	392	409
	Max	980	995	990	996	996
	median	546.4	877.9	703.8	763.1	726.9
	m.a.d.	93.2	96.7	125.0	130.4	117.5
Ground surface temperature (°C)	min	−4.471	−3.441	−4.101	−4.120	−4.400
	max	−0.567	−1.495	−1.371	−1.400	−1.438
	median	−1.48	−2.21	−2.14	−2.25	−2.10
	m.a.d.	0.32	0.33	0.38	0.38	0.34

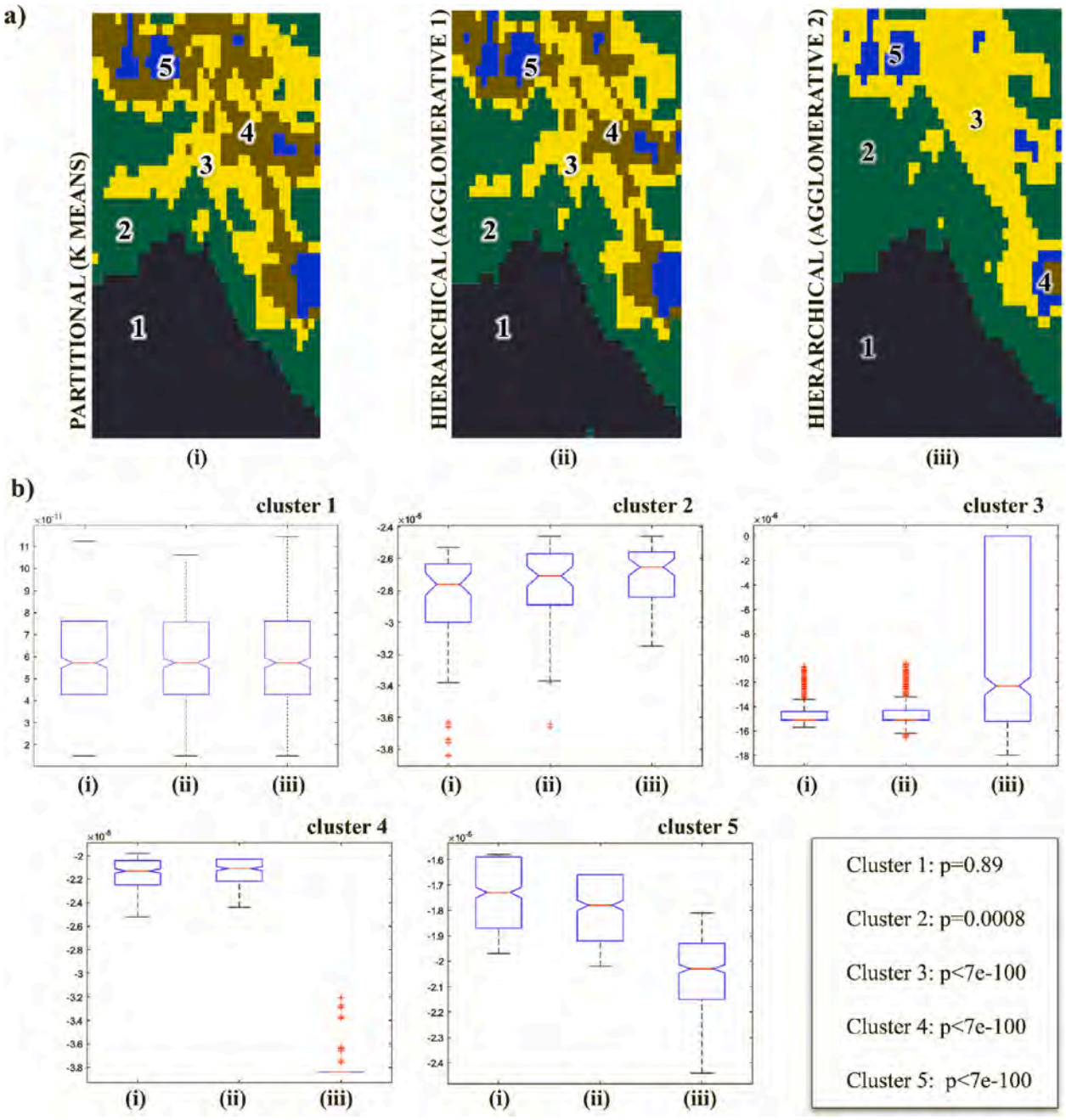

Additional Fig. 1. Comparison of clustering methods. In (a), temperature/radiation ratio values clustered by partitional (i), and hierarchical (ii-iii) approaches delivering five clusters (numbers 1–5). In (b), one-way ANOVA for each cluster values depending on the clustering method (i, ii, iii).

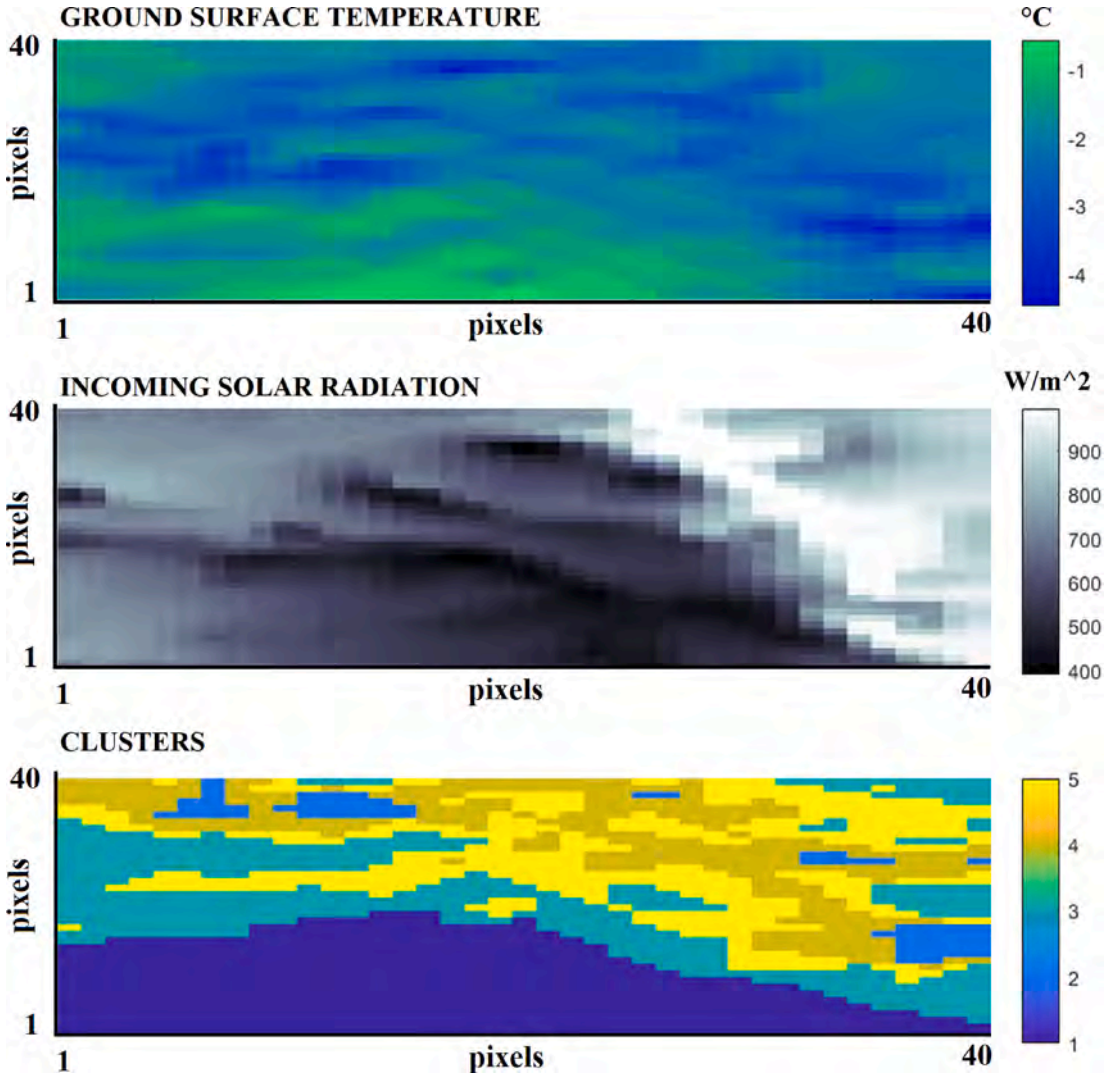

Additional Fig. 2. Clustering subset. Inputs for the clustering process are a 40 × 40 subset of the whole catchment grid. The subset is located between 3900 and 4200 m A.S.L..

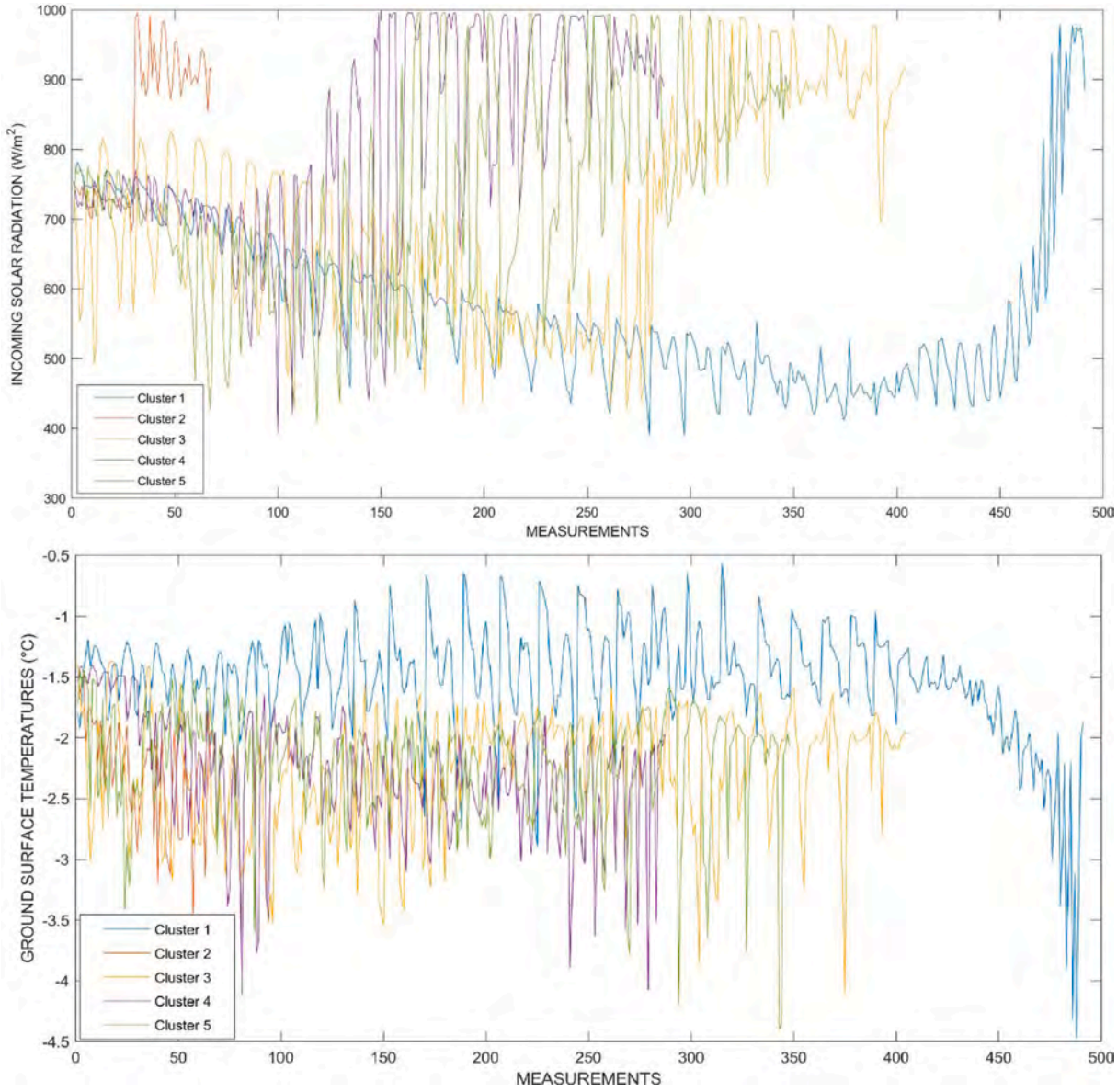

Additional Fig. 3. Ranges of input data for clustering. Top, incoming solar radiation for all clusters. Bottom, ground surface temperature for all clusters.

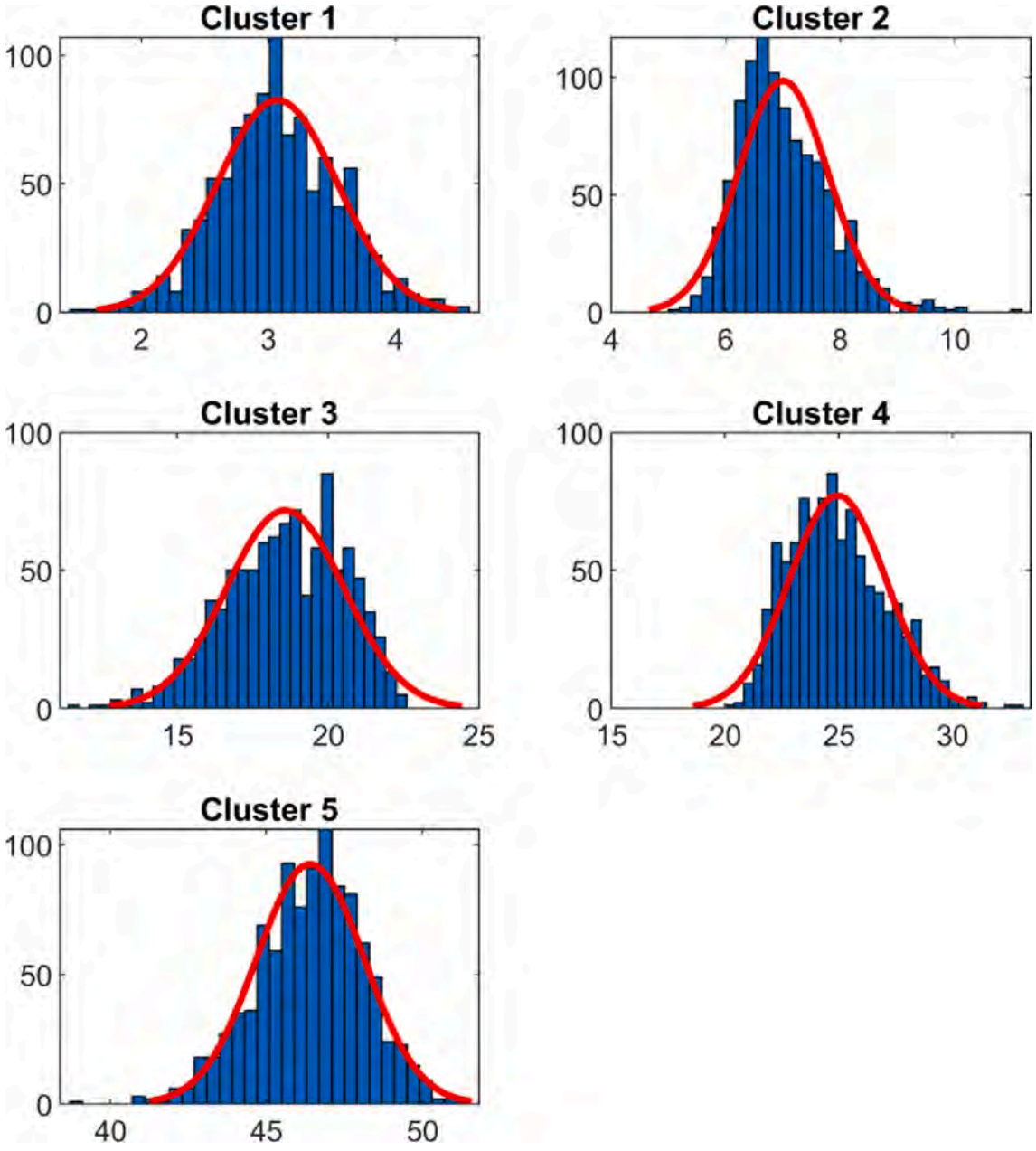

Additional Fig. 4. Histogram of cluster deviations. The cluster analysis was repeated a thousand times throughout the deviation for each ratio grid value.

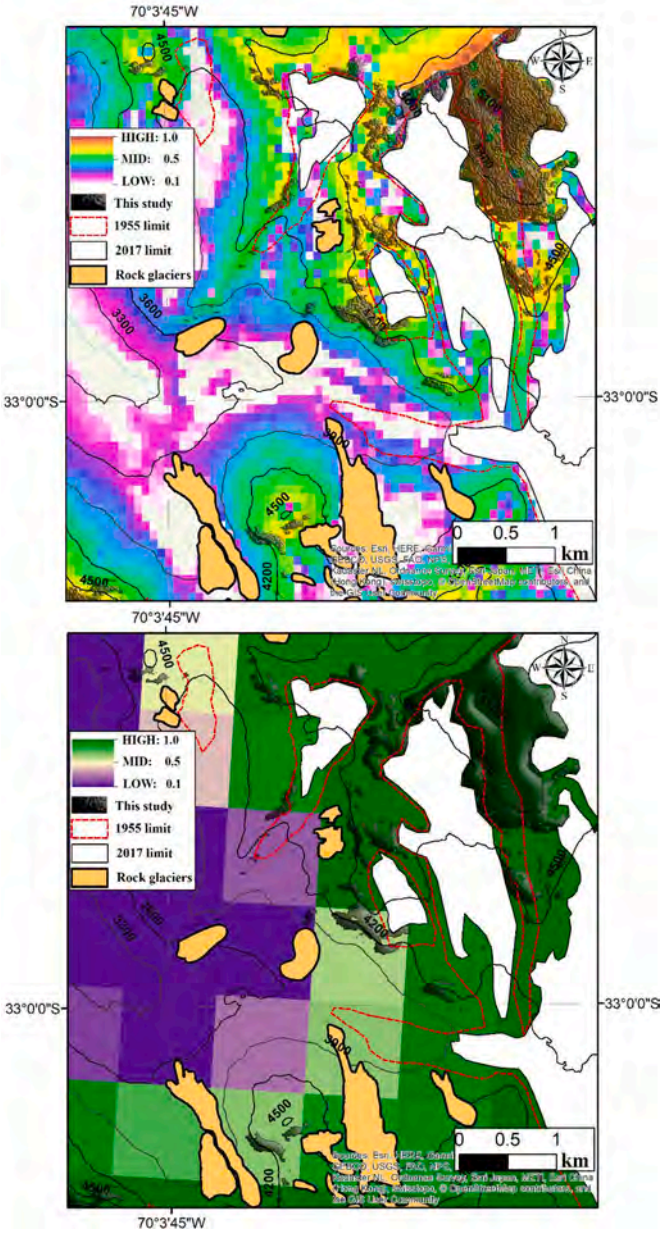

Additional Fig. 5. Permafrost distribution map comparison. Map from Tapia-Baldis and Trombotto-Liaudat (2019) (top) and Obu et al. (2019) (bottom). The present study shows alignement of the permafrost occurrence output within mid and high probability for both studies. Rock glaciers from local (DGA) inventory displayed in light orange.

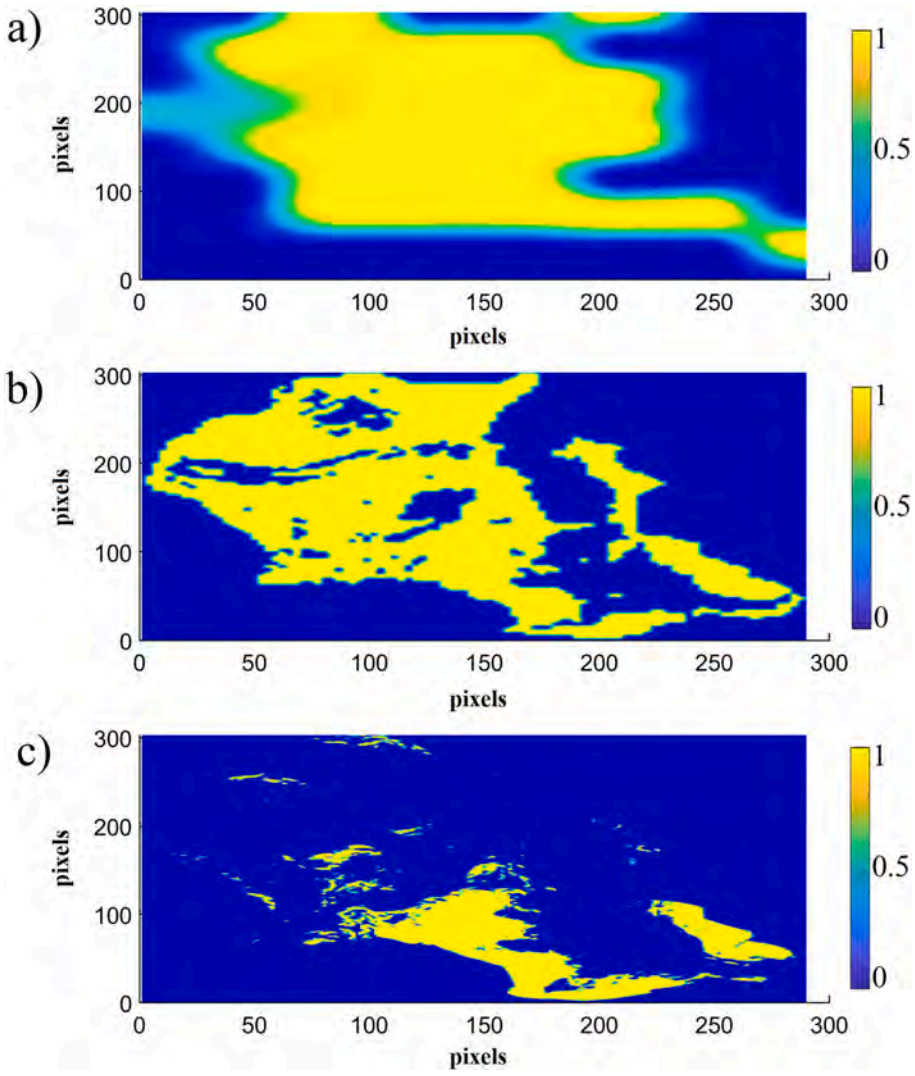

Additional Fig. 6. Comparison of permafrost occurrence map in the upper section of the "Monos de Agua" catchment (3600–5100 m A.S.L.). Raw pixels and heatmap describe the probability for permafrost occurrence in the different approaches. Surface plots (a), (b), and (c) are Obu et al., (2019), Tapia-Baldis and Trombotto-Liaudat (2019), and the present study, respectively.

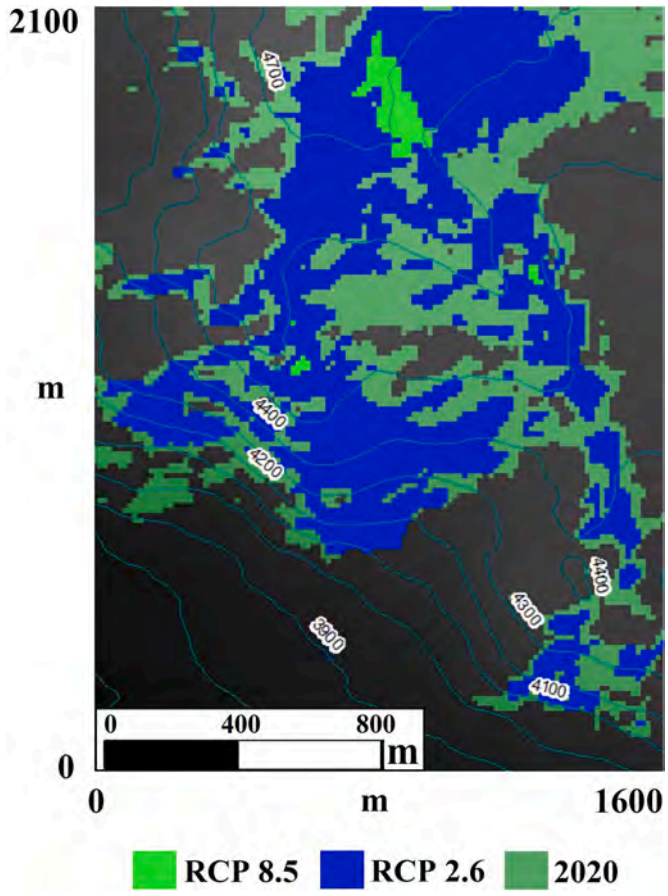

Additional Fig. 7. Change in the minimal altitude for permafrost occurrence within the "Monos de Agua" catchment, 33°S.

References

Alvarez-Garreton, C., Mendoza, P.A., Boisier, J.P., Addor, N., Galleguillos, M., Zambrano-Bigiarini, M., Lara, A., Cortes, G., Garreaud, R., McPhee, J., 2018. The CAMELS-CL dataset: catchment attributes and meteorology for large sample studies-Chile dataset. Hydrol. Earth Syst. Sci. 22, 5817–5846.

Arbelaitz, O., Gurrutxaga, I., Muguerza, J., PéRez, J.M., Perona, I., 2013. An extensive comparative study of cluster validity indices. Pattern Recogn. 46, 243–256.

Arenson, L.U., Jakob, M., 2010. The significance of rock glaciers in the dry Andes–a discussion of Azócar and Brenning (2010) and Brenning and Azócar (2010). Permafr. Periglac. Process. 21, 282–285.

Arthur, D., Vassilvitskii, S., 2007. k-means++: the advantages of careful seeding. In: Proceedings of the Eighteenth Annual ACM-SIAM Symposium on Discrete Algorithms. Society for Industrial and Applied Mathematics, pp. 1027–1035.

Azócar, G.F., Brenning, A., Bodin, X., 2017. Permafrost distribution modelling in the semi-arid Chilean Andes. Cryosphere 11, 877–890.

Baraer, M., Mark, B.G., McKENZIE, J.M., Condom, T., Bury, J., Huh, K.-I., Portocarrero, C., Gómez, J., Rathay, S., 2012. Glacier recession and water resources in Peru's Cordillera Blanca. J. Glaciol. 58, 134–150.

Barnett, T.P., Adam, J.C., Lettenmaier, D.P., 2005. Potential impacts of a warming climate on water availability in snow-dominated regions. Nature 438, 303–309.

Bartsch, A., Grosse, G., Kääb, A., Westermann, S., Strozzi, T., Wiesmann, A., Duguay, C., Seifert, F.M., Obu, J., Goler, R., 2016. GlobPermafrost—how space-BasedEarth observation supports understanding of permafrost. In: Living Planet Symp, p. 332.

Berthling, I., 2011. Beyond confusion: rock glaciers as cryo-conditioned landforms. Geomorphology 131, 98–106. https://doi.org/10.1016/j.geomorph.2011.05.002.

Bodin, X., Rojas, F., Brenning, A., 2010. Status and evolution of the cryosphere in the Andes of Santiago (Chile, 33.5 S.). Geomorphology 118, 453–464.

Boisier, J.P., Alvarez-Garretón, C., Cordero, R.R., Damiani, A., Gallardo, L., Garreaud, R. D., Lambert, F., Ramallo, C., Rojas, M., Rondanelli, R., 2018. Anthropogenic drying in central-southern Chile evidenced by long-term observations and climate model simulations. Elem Sci Anth 6.

Bown, F., Rivera, A., Acuña, C., 2008. Recent glacier variations at the Aconcagua basin, central Chilean Andes. In: Annals of Glaciology. https://doi.org/10.3189/172756408784700572.

Bozkurt, D., Rojas, M., Boisier, J.P., Valdivieso, J., 2018. Projected hydroclimate changes over Andean basins in central Chile from downscaled CMIP5 models under the low and high emission scenarios. Climatic Change 150, 131–147. https://doi.org/10.1007/s10584-018-2246-7.

Caliński, T., Harabasz, J., 1974. A dendrite method for cluster analysis. Commun. Stat. Methods 3, 1–27.

Carvalho, M.J., Melo-Gonçalves, P., Teixeira, J.C., Rocha, A., 2016. Regionalization of Europe based on a K-Means Cluster Analysis of the climate change of temperatures and precipitation. Phys. Chem. Earth, Parts A/B/C 94, 22–28. https://doi.org/10.1016/j.pce.2016.05.001.

Casteleiro-Roca, J.-L., García-Ordás, M.T., Jove, E., Zayas-Gato, F., Quintián, H., Alaiz-Moretón, H., Calvo-Rolle, J.L., 2020. A solar thermal system temperature prediction of a smart building for data recovery and security purposes. In: International Conference on Intelligent Data Engineering and Automated Learning. Springer, pp. 468–476.

Cheng, G.D., Jin, H.J., 2013. Groundwater in the permafrost regions on the Qinghai-Tibet Plateau and it changes. Hydrogeol. Eng. Geol. 40, 1–10.

Colombo, N., Salerno, F., Martin, M., Malandrino, M., Giardino, M., Serra, E., Godone, D., Said-Pullicino, D., Fratianni, S., Paro, L., Tartari, G., Freppaz, M., 2019. Influence of permafrost, rock and ice glaciers on chemistry of high-elevation ponds (NW Italian Alps). Sci. Total Environ. 685, 886–901. https://doi.org/10.1016/j.scitotenv.2019.06.233.

Cornwell, E., Molotch, N.P., McPhee, J., 2016. Spatio-temporal variability of snow water equivalent in the extra-tropical Andes Cordillera from distributed energy balance modeling and remotely sensed snow cover. Hydrol. Earth Syst. Sci. 20.

Davies, D.L., Bouldin, D.W., 1979. A cluster separation measure. IEEE Trans. Pattern Anal. Mach. Intell. 224–227.

De Amorim, R.C., Hennig, C., 2015. Recovering the number of clusters in data sets with noise features using feature rescaling factors. Inf. Sci. (Ny) 324, 126–145.

Duguay, C.R., Zhang, T., Leverington, D.W., Romanovsky, V.E., 2005. Satellite remote sensing of permafrost and seasonally frozen ground. Geophys. Monogr. Geophys. UNION 163, 91.

Dunn, J.C., 1974. Well-separated clusters and optimal fuzzy partitions. J. Cybern. 4, 95–104.

Dussaillant, I., Berthier, E., Brun, F., Masiokas, M., Hugonnet, R., Favier, V., Rabatel, A., Pitte, P., Ruiz, L., 2019. Two decades of glacier mass loss along the Andes. Nat. Geosci. 1–7.

Field, C.B., Lobell, D.B., Peters, H.A., Chiariello, N.R., 2007. Feedbacks of terrestrial ecosystems to climate change. Annu. Rev. Environ. Resour. 32, 1–29.

García, A., Ulloa, C., Amigo, G., Milana, J.P., Medina, C., 2017. An inventory of cryospheric landforms in the arid diagonal of South America (high Central Andes, Atacama region, Chile). Quat. Int. 438 (Part A), 4–19. https://doi.org/10.1016/j.quaint.2017.04.033.

Garreaud, R.D., Alvarez-Garreton, C., Barichivich, J., Boisier, J.P., Christie, D., Galleguillos, M., LeQuesne, C., McPhee, J., Zambrano-Bigiarini, M., 2017. The 2010-2015 megadrought in central Chile: impacts on regional hydroclimate and vegetation. Hydrol. Earth Syst. Sci. 21.

Gascoin, S., Kinnard, C., Ponce, R., Macdonell, S., Lhermitte, S., Rabatel, A., 2011. Glacier contribution to streamflow in two headwaters of the huasco river, dry Andes of Chile. Cryosphere 1099–1113.

Gisnås, K., Etzelmüller, B., Farbrot, H., Schuler, T.V., Westermann, S., 2013. CryoGRID 1.0: permafrost distribution in Norway estimated by a spatial numerical model. Permafr. Periglac. Process. 24, 2–19.

Gruber, S., 2012. Derivation and analysis of a high-resolution estimate of global permafrost zonation. The Cryosphere 6 (1), 221–233. https://doi.org/10.5194/tc-6-221-2012.

Gulbrandsen, M.L., Minsley, B.J., Ball, L.B., Hansen, T.M., 2016. Semiautomatic mapping of permafrost in the Yukon flats, Alaska. Geophys. Res. Lett. 43, 12–131.

Halkidi, M., Batistakis, Y., Vazirgiannis, M., 2001. On clustering validation techniques. J. Intell. Inf. Syst. 17, 107–145.

Hauck, C., Böttcher, M., Maurer, H., 2011. A new model for estimating subsurface ice content based on combined electrical and seismic data sets. Cryosphere 5, 453–468.

Hersbach, H., Bell, B., Berrisford, P., Hirahara, S., Horányi, A., Muñoz-Sabater, J., Nicolas, J., Peubey, C., Radu, R., Schepers, D., 2020. The ERA5 global reanalysis. Q. J. R. Meteorol. Soc. 146, 1999–2049.

Ilc, N., 2012. Modified Dunn's cluster validity index based on graph theory. Przeglad Elektrotechniczny 88, 126–131.

Jansson, J.K., Taş, N., 2014. The microbial ecology of permafrost. Nat. Rev. Microbiol. 12, 414–425.

Kneisel, C., 1998. Occurrence of surface ice and ground ice/permafrost in recently deglaciated glacier forefields, St. Moritz area, eastern Swiss Alps. In: Proceedings of the Seventh International Conference on Permafrost, Yellowknife, Canada. University of Laval Press Nordicana, pp. 575–581.

Kneisel, C., Hauck, C., Fortier, R., Moorman, B., 2008. Advances in geophysical methods for permafrost investigations. Permafr. Periglac. Process. 19, 157–178.

Kneisel, C., Kääb, A., 2007. Mountain permafrost dynamics within a recently exposed glacier forefield inferred by a combined geomorphological, geophysical and photogrammetrical approach. Earth Surf. Process. Landforms J. Br. Geomorphol. Res. Gr. 32, 1797–1810.

Kurylyk, B.L., MacQuarrie, K.T.B., McKenzie, J.M., 2014. Climate change impacts on groundwater and soil temperatures in cold and temperate regions: implications, mathematical theory, and emerging simulation tools. Earth Sci. Rev. 138, 313–334.

Lamirel, J.-C., Dugué, N., Cuxac, P., 2016. New efficient clustering quality indexes. In: 2016 International Joint Conference on Neural Networks (IJCNN). IEEE, pp. 3649–3657.

Legány, C., Juhász, S., Babos, A., 2006. Cluster validity measurement techniques. In: Proceedings of the 5th WSEAS International Conference on Artificial Intelligence, Knowledge Engineering and Data Bases. World Scientific and Engineering Academy and Society (WSEAS) Stevens Point, pp. 388–393.

Lliboutry, L., 1956. Nieves y glaciares de Chile. Fundamentos de Glaciología. Ediciones de la Universidad de Chile, Santiago, pp. 18–25, 1957.

Luna-Romera, J.M., García-Gutiérrez, J., Martínez-Ballesteros, M., Santos, J.C.R., 2018. An approach to validity indices for clustering techniques in big data. Prog. Artif. Intell. 7, 81–94.

Miller, A., 1976. The climate of Chile. World Surv. Climatol. 12, 113–145.

Monnier, S., Kinnard, C., 2017. Pluri-decadal (1955-2014) evolution of glacier-rock glacier transitional landforms in the central Andes of Chile (30-33° S). Earth Surf. Dyn. 5.

Nagy, B., Kovács, J., Ignéczi, Á., Beleznai, S., Mari, L., Kereszturi, Á., Szalai, Z., 2020. The thermal behavior of ice-bearing ground: the highest cold, dry desert on Earth as an analog for conditions on Mars, at Ojos del Salado, Puna de Atacama-Altiplano region. Astrobiology 20, 701–722.

Nitze, I., Grosse, G., Jones, B.M., Romanovsky, V.E., Boike, J., 2018. Remote sensing quantifies widespread abundance of permafrost region disturbances across the Arctic and Subarctic. Nat. Commun. 9, 5423. https://doi.org/10.1038/s41467-018-07663-3.

Niu, F., Yin, G., Luo, J., Lin, Z., Liu, M., 2018. Permafrost distribution along the Qinghai-Tibet Engineering Corridor, China using high-resolution statistical mapping and modeling integrated with remote sensing and GIS. Rem. Sens. 10, 215.

Obu, J., Westermann, S., Kaab, A., Bartsch, A., 2019. Ground Temperature Map, 2000-2016, Andes, New Zealand and East African Plateau Permafrost. Univ. Oslo. https://doi.org/10.1594/PANGAEA.905512.

Ohlanders, N., Rodriguez, M., Mc Phee Torres, J., 2013. Stable Water Isotope Variation in a Central Andean Watershed Dominated by Glacier and Snowmelt.

Oliva, M., Fritz, M., 2018. Permafrost degradation on a warmer Earth: challenges and perspectives. Curr. Opin. Environ. Sci. Heal. 5, 14–18.

Onaca, A., Urdea, P., Ardelean, A., Şerban, R., 2013. Assessement of internal structure of periglacial landforms from southern Carpathians (Romania) using DC resistivity tomography. Carpathian J. Earth Environ. Sci. 8, 113–122.

Petersen, L., Pellicciotti, F., 2011. Spatial and temporal variability of air temperature on a melting glacier: atmospheric controls, extrapolation methods and their effect on melt modeling, Juncal Norte Glacier, Chile. J. Geophys. Res. Atmos. 116.

Petrovic, S., 2006. A comparison between the silhouette index and the davies-bouldin index in labelling ids clusters. In: Proceedings of the 11th Nordic Workshop of Secure IT Systems. Citeseer, pp. 53–64.

Rodriguez, M., Ohlanders, N., Pellicciotti, F., Williams, M.W., McPhee, J., 2016. Estimating runoff from a glacierized catchment using natural tracers in the semi-arid Andes cordillera. Hydrol. Process. 30, 3609–3626. https://doi.org/10.1002/hyp.10973.

Rosenqvist, A., Shimada, M., Ito, N., Watanabe, M., 2007. Alos PALSAR: a pathfinder mission for global-scale monitoring of the environment. IEEE Trans. Geosci. Rem. Sens. 45, 3307–3316.

Rousseeuw, P.J., 1987. Silhouettes: a graphical aid to the interpretation and validation of cluster analysis. J. Comput. Appl. Math. 20, 53–65.

Ruiz Pereira, S., Veettil, B.K., 2019. Glacier decline in the Central Andes (33° S): context and magnitude from satellite and historical data. J. South Am. Earth Sci. 102249.

Saito, K., Trombotto Liaudat, D., Yoshikawa, K., Mori, J., Sone, T., Marchenko, S., Romanovsky, V., Walsh, J., Hendricks, A., Bottegal, E., 2016. Late quaternary permafrost distributions downscaled for south America: examinations of GCM-based maps with observations. Permafr. Periglac. Process. 27, 43–55.

Saitta, S., Raphael, B., Smith, I.F.C., 2007. A bounded index for cluster validity. In: International Workshop on Machine Learning and Data Mining in Pattern Recognition. Springer, pp. 174–187.

Santos, J.M., Embrechts, M., 2009. On the use of the adjusted rand index as a metric for evaluating supervised classification. In: International Conference on Artificial Neural Networks. Springer, pp. 175–184.

Santos, J.M.L., 2007. Transferring landscape values: how and how accurately?. In: Environmental Value Transfer: Issues and Methods. Springer, Dordrecht, pp. 45–75. https://doi.org/10.1007/1-4020-5405-x_4.

Schuur, E.A.G., Bockheim, J., Canadell, J.G., Euskirchen, E., Field, C.B., Goryachkin, S. V., Hagemann, S., Kuhry, P., Lafleur, P.M., Lee, H., 2008. Vulnerability of permafrost carbon to climate change: implications for the global carbon cycle. Bioscience 58, 701–714.

Sembiring, R.W., Zain, J.M., Embong, A., 2011. A Comparative Agglomerative Hierarchical Clustering Method to Cluster Implemented Course. arXiv Prepr. arXiv1101.4270.

Smith, M.W., 1975. Microclimatic influences on ground temperatures and permafrost distribution, Mackenzie Delta, Northwest Territories. Can. J. Earth Sci. 12, 1421–1438.

Stehr, A., Aguayo, M., 2017. Snow cover dynamics in Andean watersheds of Chile (32.0–39.5 S) during the years 2000–2016. Hydrol. Earth Syst. Sci. 21, 5111–5126.

Stocker, T.F., Qin, D., Plattner, G.-K., Tignor, M., Allen, S.K., Boschung, J., Nauels, A., Xia, Y., Bex, V., Midgley, P.M., 2013. Climate Change 2013. The Physical Science Basis. Working Group I Contribution to the Fifth Assessment Report of the Intergovernmental Panel on Climate Change-Abstract for Decision-Makers; Changements Climatiques 2013. Les Elements Scientifiques. Contribut.

Szopińska, M., Szumińska, D., Polkowska, Ż., Machowiak, K., Lehmann, S., Chmiel, S., 2016. The chemistry of river–lake systems in the context of permafrost occurrence (Mongolia, Valley of the Lakes). Part I. Analysis of ion and trace metal concentrations. Sediment. Geol. 340, 74–83.

Tapia Baldis, C., Trombotto Liaudat, D., 2019. Rockslides and rock avalanches in the Central Andes of Argentina and their possible association with permafrost degradation. Permafr. Periglac. Process. 30, 330–347.

Tapia-Baldis, C., Trombotto-Liaudat, D., 2020. Permafrost model in coarse-blocky deposits for the Dry Andes, Argentina (28°-33° S). Cuadernos Investigación Geográfica 46 (1), 33–58.

Toohey, R.C., Herman-Mercer, N.M., Schuster, P.F., Mutter, E.A., Koch, J.C., 2016. Multidecadal increases in the Yukon River Basin of chemical fluxes as indicators of changing flowpaths, groundwater, and permafrost. Geophys. Res. Lett. 43.

Unidad de Glaciología, D., 2015. Inventario de Glaciares DGA v2015 [WWW Document].

Westermann, S., Østby, T.I., Gisnås, K., Schuler, T.V., Etzelmüller, B., 2015. A ground temperature map of the North Atlantic permafrost region based on remote sensing and reanalysis data. Cryosphere 9, 1303–1319.

Xu, L.-X., Yang, D.-W., Wu, T.-H., Yi, S.-H., Fang, Y.-P., Xiao, C.-D., Lin, H.-X., Huang, J.-C., Simbi, C.H., 2019. An ecosystem services zoning framework for the permafrost regions of China. Adv. Clim. Change Res. 10, 92–98.

Zeng, W., Jiang, Y., Huo, Z., Hu, K., 2020. Clustering analysis of extreme temperature based on K-means algorithm. In: International Conference on Artificial Intelligence and Security. Springer, pp. 523–533.